

**Towards the Synthesis of *N*-Acetyl-2-amino-2-deoxy-D-mannopyranose uronic acid  
(D-ManNAcA) and Derivatives**

by

G. Adam Cox

Submitted in Partial Fulfillment of the Requirements

for the Degree of

Master of Science

in the

Chemistry

Program

YOUNGSTOWN STATE UNIVERSITY

August, 2007

**Towards the Synthesis of *N*-acetyl-2-amino-2-deoxy-D-mannopyranose uronic acid  
(D-ManNAcA) and Derivates**

G. Adam Cox

I hereby release this thesis to the public. I understand that this thesis will be made available from the OhioLINK ETD Center and the Maag Library Circulation Desk for public access. I also authorize the University or other individuals to make copies of this thesis as needed for scholarly research.

Signature:

---

G. Adam Cox

Date

Approvals:

---

Dr. Peter Norris  
Thesis Advisor

Date

---

Dr. John A. Jackson  
Committee Member

Date

---

Dr. Tim R. Wagner  
Committee Member

Date

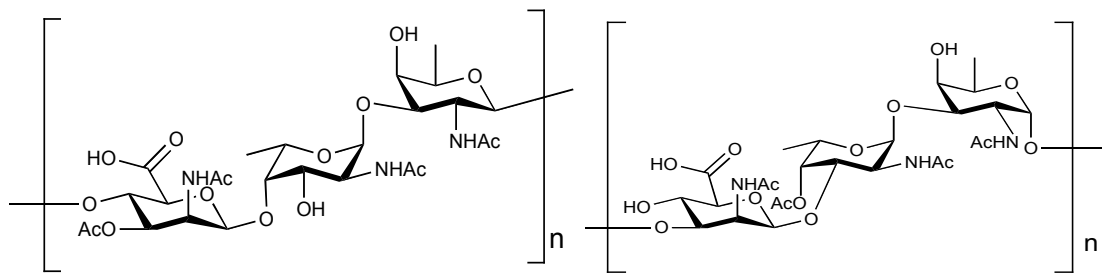
---

Dr. Peter J. Kasvinsky  
Dean of Graduate Studies and Research

Date

## Thesis Abstract

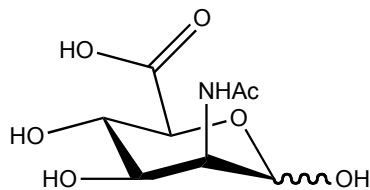
The following details attempts at a stereoselective synthesis of deoxygenated D-mannose uronic acid derivatives from D-glucurono-6,3-lactone. These derivatives will be tested as potential inhibitors of enzymes used by *Staphylococcus aureus* to form its polysaccharide microcapsule, which functions as a protective barrier against destruction by the host. Two serotypes (types 5 and 8) comprise the majority of *S. aureus* bacteria and also the most virulent strains of this bacterium.



**Serotype 5**

**Serotype 8**

The goal of this research project is to synthesize glycomimetics of D-ManNAcA (below) that may act as potential inhibitors of the enzymes such as UDP-GlcNAc 2-epimerase.



Since infections caused by *S. aureus* are an increasing threat in hospitals and the general community, it is of considerable interest within the biological community to find new treatments to combat these drug-resistant bacteria.

## Acknowledgements

I would like to thank the Youngstown State University Department of Chemistry and the School of Graduate Studies for allowing me the opportunity to pursue the Master's of Science degree. I would also like to thank my thesis committee members, Dr. John Jackson and Dr. Tim Wagner, for their help and suggestions throughout the writing process. Dr. Roland Reisen, Dr. Matthias Zeller, and Ray Hoff have been tremendously helpful in dealing with the use and repair of instrumentation during the research process.

I would especially like to thank Dr. Peter Norris for the opportunity to work on such an interesting research project and also to work with an extraordinary group of people. I would also like to thank Dr. Peter Norris for his guidance, not only in chemistry, but also in choosing a career path and discussing the many opportunities that exist for a chemist.

A special thanks to my parents and family for their continued love, support, and understanding which means so much to me, especially during difficult times. Finally, I would like to thank my fiancé Gina, who has always been supportive and encouraging. I am fortunate to have her by my side as we begin this new part of our lives.

## **Table of Contents**

Title Page .....	i
Signature Page .....	ii
Thesis Abstract .....	iii
Acknowledgements .....	iv
Table of Contents .....	v
List of Schemes .....	vi
List of Equations .....	vi
List of Figures .....	vii
Introduction .....	1
Statement of Problem .....	21
Results and Discussion .....	22
Experimental .....	51
References .....	72
Appendix A .....	80
Appendix B .....	137

## List of Schemes

<b>Scheme 1:</b> Oxidation and glycosyl transfer to form glycosyl linkage.....	6
<b>Scheme 2:</b> Reaction pathway of modified Staudinger reaction.....	18
<b>Scheme 3:</b> Preparation of $\alpha/\beta$ methyl D-glucopyranuronate.....	22
<b>Scheme 4:</b> Acetylation and crystallization of methyl 1,2,3,4-tetra- <i>O</i> -acetyl- $\beta$ -D-glucopyranuronate.....	23
<b>Scheme 5:</b> Preparation of precursors ( <b>9</b> and <b>10</b> ) to key reduction step.....	30
<b>Scheme 6:</b> Lichtenthaler's synthesis of precursor to the key reduction step.....	33
<b>Scheme 7:</b> Proposed mechanism for the catalytic cycle with $Cp_2TiCl_2$ .....	36
<b>Scheme 8:</b> Selective protection of C-3 hydroxyl.....	39
<b>Scheme 9:</b> Protection of <b>19</b> using silyl protecting groups.....	43
<b>Scheme 10:</b> Synthetic strategy to perform an $S_N2$ reaction on C-2.....	49

## List of Equations

<b>Equation 1:</b> Epimerization of UDP-GlcNAc to UDP-ManNAc.....	5
<b>Equation 2:</b> Mechanism of nucleophilic displacement ( $S_N2$ ) on a glycosyl bromide to form a glycosyl azide.....	18
<b>Equation 3:</b> Azidonitration of glycals <i>via</i> azide radical.....	19
<b>Equation 4:</b> Azidophenylselenation of glycals <i>via</i> azide ion.....	19
<b>Equation 5:</b> Preparation of methyl 2,3,4-tri- <i>O</i> -acetyl- $\alpha$ -D-glucopyranuronosyl bromide ( <b>6</b> ).....	24
<b>Equation 6:</b> Preparation of glycal <b>7</b> <i>via</i> elimination reaction.....	25
<b>Equation 7:</b> Formation of methyl 3,4-di- <i>O</i> -acetyl-2-deoxy-2-(hydroxyimino)-D- <i>arabino</i> -hex-2-enopyranuronate.....	28
<b>Equation 8:</b> Formation of methyl 3,4-di- <i>O</i> -acetyl-2- <i>N</i> -acetyl-2-deoxy-D-glucopyranuronate.....	34

<b>Equation 9:</b> Reduction of 4-nitrobenzoyloxime <b>10</b> with sodium borohydride in methanol.....	35
<b>Equation 10:</b> Synthesis of methyl 3,4-di- <i>O</i> -acetyl-1,5-anhydro-2-deoxy-D- <i>arabino</i> -hex-1-enopyranuronate ( <b>15</b> ).....	36
<b>Equation 11:</b> Deacetylation of compound <b>15</b> .....	38
<b>Equation 12:</b> Protection of O-4 with silyl group.....	40
<b>Equation 13:</b> Isolation of C-5 hydroxyl with an isopropylidene group.....	41
<b>Equation 14:</b> Pivaloylation of compound <b>19</b> .....	42
<b>Equation 15:</b> Removal of isopropylidene group from <b>20</b> .....	46
<b>Equation 16:</b> Activation of hydroxyl at C-2 with a triflate group.....	47
<b>Equation 17:</b> Attempted S <sub>N</sub> 2 reaction on compound <b>24</b> .....	48

## List of Figures

<b>Figure 1:</b> Genome map of MSRA strain representing antibiotic resistance genes, located on the outermost circle.....	3
<b>Figure 2:</b> The repeating amino sugar units associated with serotypes 5 and 8 capsular polysaccharides of <i>S. aureus</i> .....	4
<b>Figure 3:</b> Components of the capsular polysaccharide of <i>S. aureus</i> .....	5
<b>Figure 4:</b> Proposed pathway of CP5 biosynthesis involving UDP-D-GlcNAc as the precursor compound.....	6
<b>Figure 5:</b> Fischer projection of D-(+)-glyceraldehyde.....	10
<b>Figure 6:</b> General structure of aldose and ketose sugars.....	11
<b>Figure 7:</b> Possible forms of D-glucose in solution.....	11
<b>Figure 8:</b> $\alpha$ and $\beta$ anomers in pyranose form.....	12
<b>Figure 9:</b> Resonance forms representing the anomeric effect.....	13

<b>Figure 10:</b> Newman projection illustrating repulsive forces between substituents at C-1 and the unshared pair of electrons from the oxygen in the ring.....	13
<b>Figure 11:</b> Nomenclature used to describe the two chair conformations of pyranoses.....	14
<b>Figure 12:</b> Three common representations of a typical glycal.....	15
<b>Figure 13:</b> Depiction of dipole-dipole interactions of axial and equatorial substituents adjacent to an sp <sup>2</sup> hybridized carbon.....	16
<b>Figure 14:</b> Typical examples of amino sugars.....	17
<b>Figure 15:</b> X-Ray structure of methyl 2,3,4-tri-O-acetyl- $\alpha$ -D-glucopyranuronosyl bromide ( <b>6</b> ).....	25
<b>Figure 16:</b> X-Ray structure of methyl 2,3,4-tri-O-acetyl-1,5-anhydro-D-arabino-hex-1-enopyranuronate ( <b>7</b> ).....	27
<b>Figure 17:</b> X-Ray structure of methyl 3,4-di-O-acetyl-2-deoxy-2-(hydroxyimino)-D-arabino-hex-2-enopyranuronate ( <b>8</b> ).....	29
<b>Figure 18:</b> X-Ray structure of methyl 3,4-di-O-acetyl-2-deoxy-2-(benzoyloxyimino)-D-arabino-hex-2-enopyranuronate ( <b>9</b> ).....	31
<b>Figure 19:</b> X-Ray structure of methyl 3,4-di-O-acetyl-2-deoxy-2-(4-nitro benzoyloxyimino)-D-arabino-hex-2-enopyranuronate ( <b>10</b> ).....	32
<b>Figure 20:</b> X-Ray structure of methyl 3,4-di-O-acetyl-1,5-anhydro-2-deoxy-D-arabino-hex-1-enopyranuronate ( <b>15</b> ).....	37
<b>Figure 21:</b> X-Ray structure of 1,2-O-isopropylidene- $\alpha$ -D-glucofuranosiduronono-6,3-lactone ( <b>19</b> ).....	42
<b>Figure 22:</b> X-Ray structure of 1,2-O-isopropylidene-6-O-tert-butyldiphenylsilyl- $\alpha$ -D-glucurono-6,3-lactone ( <b>21</b> ).....	44
<b>Figure 23:</b> X-Ray structure of 1,2-O-isopropylidene-6-O-tert-butyldimethylsilyl- $\alpha$ -D-glucurono-6,3-lactone ( <b>22</b> ).....	45
<b>Figure 24:</b> X-Ray crystal structure of methyl 6-O-pivaloyl-2-O-trifluoromethylsulfonyl- $\beta$ -D-glucurono-6,3-lactone ( <b>24</b> ).....	48
<b>Figure 25:</b> 400 MHz <sup>1</sup> H NMR spectrum of methyl 1,2,3,4-tetra-O-acetyl- $\beta$ -D-glucopyranuronate ( <b>5<math>\beta</math></b> ).....	81

<b>Figure 26:</b> 100 MHz $^{13}\text{C}$ NMR spectrum of methyl 1,2,3,4-tetra- <i>O</i> -acetyl- $\beta$ -D-glucopyranuronate ( <b>5<math>\beta</math></b> ).....	82
<b>Figure 27:</b> 400 MHz $^1\text{H}$ NMR spectrum of methyl 1,2,3,4-tetra- <i>O</i> -acetyl- $\alpha$ -D-glucopyranuronate ( <b>5<math>\alpha</math></b> ).....	83
<b>Figure 28:</b> 100 MHz $^{13}\text{C}$ NMR spectrum of methyl 1,2,3,4-tetra- <i>O</i> -acetyl- $\beta$ -D-glucopyranuronate ( <b>5<math>\alpha</math></b> ).....	84
<b>Figure 29:</b> ESI mass spectrum of methyl 1,2,3,4-tetra- <i>O</i> -acetyl- $\alpha,\beta$ -D-glucopyranuronate ( <b>5<math>\alpha/\beta</math></b> ).....	85
<b>Figure 30:</b> 400 MHz $^1\text{H}$ NMR spectrum of methyl 2,3,4-tri- <i>O</i> -acetyl- $\alpha$ -D-glucopyranosyl bromide ( <b>6</b> ).....	86
<b>Figure 31:</b> 100 MHz $^{13}\text{C}$ NMR spectrum of methyl 2,3,4-tri- <i>O</i> -acetyl- $\alpha$ -D-glucopyranosyl bromide ( <b>6</b> ).....	87
<b>Figure 32:</b> APCI mass spectrum of methyl 2,3,4-tri- <i>O</i> -acetyl- $\alpha$ -D-glucopyranosyl bromide ( <b>6</b> ).....	88
<b>Figure 33:</b> 400 MHz $^1\text{H}$ NMR spectrum of methyl 2,3,4-tri- <i>O</i> -acetyl-1,5-anhydro-D- <i>arabino</i> -hex-1-enopyranuronate ( <b>7</b> ).....	89
<b>Figure 34:</b> 100 MHz $^{13}\text{C}$ NMR spectrum of methyl 2,3,4-tri- <i>O</i> -acetyl-1,5-anhydro-D- <i>arabino</i> -hex-1-enopyranuronate ( <b>7</b> ).....	90
<b>Figure 35:</b> APCI mass spectrum of methyl 2,3,4-tri- <i>O</i> -acetyl-1,5-anhydro-D- <i>arabino</i> -hex-1-enopyranuronate ( <b>7</b> ).....	91
<b>Figure 36:</b> 400 MHz $^1\text{H}$ NMR ( $\text{CDCl}_3$ ) spectrum of methyl 3,4-di- <i>O</i> -acetyl-2-deoxy-2-(hydroxyimino)-D- <i>arabino</i> -hex-2-enopyranuronate ( <b>8</b> ).....	92
<b>Figure 37:</b> 400 MHz $^1\text{H}$ NMR ( $\text{THF}-d_6$ ) spectrum of methyl 3,4-di- <i>O</i> -acetyl-2-deoxy-2-(hydroxyimino)-D- <i>arabino</i> -hex-2-enopyranuronate ( <b>8</b> ).....	93
<b>Figure 38:</b> 100 MHz $^{13}\text{C}$ NMR ( $\text{CDCl}_3$ ) spectrum of methyl 3,4-di- <i>O</i> -acetyl-2-deoxy-2-(hydroxyimino)-D- <i>arabino</i> -hex-2-enopyranuronate ( <b>8</b> ).....	94
<b>Figure 39:</b> ESI mass spectrum of methyl 3,4-di- <i>O</i> -acetyl-1,2-dideoxy-2-(hydroxyimino)-D- <i>arabino</i> -hex-2-enopyranuronate ( <b>8</b> ).....	95
<b>Figure 40:</b> 400 MHz $^1\text{H}$ NMR spectrum of methyl 3,4-di- <i>O</i> -acetyl-1,2-dideoxy-2-(benzoyloxyimino)-D- <i>arabino</i> -hex-2-enopyranuronate ( <b>9</b> ).....	96

<b>Figure 41:</b> 100 MHz $^{13}\text{C}$ NMR spectrum of methyl 3,4-di- <i>O</i> -acetyl-1,2-dideoxy-2-(benzoyloxyimino)-D- <i>arabino</i> -hex-2-enopyranuronate ( <b>9</b> ).....	97
<b>Figure 42:</b> ESI mass spectrum of methyl 3,4-di- <i>O</i> -acetyl-1,2-dideoxy-2-(benzoyloxyimino)-D- <i>arabino</i> -hex-2-enopyranuronate ( <b>9</b> ).....	98
<b>Figure 43:</b> 400 MHZ $^1\text{H}$ NMR spectrum of methyl 3,4-di- <i>O</i> -acetyl-1,2-dideoxy-2-(4-nitrobenzoyloxyimino)-D- <i>arabino</i> -hex-2-enopyranuronate ( <b>10</b> ).....	99
<b>Figure 44:</b> 100 MHZ $^{13}\text{C}$ NMR spectrum of methyl 3,4-di- <i>O</i> -acetyl-1,2-dideoxy-2-(4-nitrobenzoyloxyimino)-D- <i>arabino</i> -hex-2-enopyranuronate ( <b>10</b> ).....	100
<b>Figure 45:</b> ESI mass spectrum of methyl 3,4-di- <i>O</i> -acetyl-1,2-dideoxy-2-(4-nitrobenzoyloxyimino)-D- <i>arabino</i> -hex-2-enopyranuronate ( <b>10</b> ).....	101
<b>Figure 46:</b> 400 MHz $^1\text{H}$ NMR spectrum of methyl 3,4-di- <i>O</i> -acetyl-1,2-dideoxy-2-acetamido-D-glucopyranuronate ( <b>13</b> ).....	102
<b>Figure 47:</b> 400 MHz $^1\text{H}$ NMR of methyl 3,4,6-tri- <i>O</i> -acetyl-1,2-dideoxy-2-(acetoxyimino)-D- <i>arabino</i> -hex-2-enopyranuronate ( <b>14</b> ).....	103
<b>Figure 48:</b> ESI mass spectrum of methyl 3,4,6-tri- <i>O</i> -acetyl-1,2-dideoxy-2-(acetoxyimino)-D- <i>arabino</i> -hex-2-enopyranuronate ( <b>14</b> ).....	104
<b>Figure 49:</b> 400 MHz $^1\text{H}$ NMR spectrum of methyl 3,4-di- <i>O</i> -acetyl-1,5-anhydro-2-deoxy-D- <i>arabino</i> -hex-1-enopyranuronate ( <b>15</b> ).....	105
<b>Figure 50:</b> 100 MHz $^{13}\text{C}$ NMR spectrum of methyl 3,4-di- <i>O</i> -acetyl-1,5-anhydro-1,2-dideoxy-D- <i>arabino</i> -hex-1-enopyranuronate ( <b>15</b> ).....	106
<b>Figure 51:</b> ESI mass spectrum of methyl 3,4-di- <i>O</i> -acetyl-1,5-anhydro-2-deoxy-D- <i>arabino</i> -hex-1-enopyranuronate ( <b>15</b> ).....	107
<b>Figure 52:</b> 400 MHz $^1\text{H}$ NMR spectrum of methyl 1,5-anhydro-2-deoxy-D- <i>arabino</i> -hex-1-enopyranuronate ( <b>16</b> ).....	108
<b>Figure 53:</b> 400 MHz $^1\text{H}$ NMR spectrum of methyl 1,5-anhydro-2-deoxy-D- <i>arabino</i> -hex-1-enopyranuronate ( <b>16</b> ) treated with D <sub>2</sub> O.....	109
<b>Figure 54:</b> 100 MHz $^{13}\text{C}$ NMR spectrum of methyl 1,5-anhydro-2-deoxy-D- <i>arabino</i> -hex-1-enopyranuronate ( <b>16</b> ).....	110
<b>Figure 55:</b> ESI mass spectrum of methyl 1,5-anhydro-2-deoxy-D- <i>arabino</i> -hex-1-enopyranuronate ( <b>16</b> ).....	111

<b>Figure 56:</b> 400 MHz $^1\text{H}$ NMR spectrum of methyl 1,5-anhydro-2-deoxy-3- <i>O</i> -pivaloyl-D- <i>arabino</i> -hex-1-enopyranuronate ( <b>17</b> ).....	112
<b>Figure 57:</b> 100 MHz $^{13}\text{C}$ NMR spectrum of methyl 1,5-anhydro-2-deoxy-3- <i>O</i> -pivaloyl-D- <i>arabino</i> -hex-1-enopyranuronate ( <b>17</b> ).....	113
<b>Figure 58:</b> ESI mass spectrum of methyl 1,5-anhydro-2-deoxy-3- <i>O</i> -pivaloyl-D- <i>arabino</i> -hex-1-enopyranuronate ( <b>17</b> ).....	114
<b>Figure 59:</b> 400 MHz $^1\text{H}$ NMR spectrum of 1,2- <i>O</i> -isopropylidene- $\alpha$ -D-glucofuranosiduron-6,3-lactone ( <b>19</b> ).....	115
<b>Figure 60:</b> 100 MHz $^{13}\text{C}$ NMR spectrum of 1,2- <i>O</i> -isopropylidene- $\alpha$ -D-glucofuranosiduron-6,3-lactone ( <b>19</b> ).....	116
<b>Figure 61:</b> ESI mass spectrum of 1,2- <i>O</i> -isopropylidene- $\alpha$ -D-glucofuranosiduron-6,3-lactone ( <b>19</b> ).....	117
<b>Figure 62:</b> 400 MHz $^1\text{H}$ NMR spectrum of 1,2- <i>O</i> -isopropylidene-6- <i>O</i> -pivaloyl- $\alpha$ -D-glucurono-6,3-lactone ( <b>20</b> ).....	118
<b>Figure 63:</b> 100 MHz $^{13}\text{C}$ NMR spectrum of 1,2- <i>O</i> -isopropylidene-6- <i>O</i> -pivaloyl- $\alpha$ -D-glucurono-6,3-lactone ( <b>20</b> ).....	119
<b>Figure 64:</b> ESI mass spectrum of 1,2- <i>O</i> -isopropylidene-6- <i>O</i> -pivaloyl- $\alpha$ -D-glucurono-6,3-lactone ( <b>20</b> ).....	120
<b>Figure 65:</b> 400 MHz $^1\text{H}$ NMR spectrum of 1,2- <i>O</i> -isopropylidene-6- <i>O</i> - <i>tert</i> -butyldiphenylsilyl- $\alpha$ -D-glucurono-6,3-lactone ( <b>21</b> ).....	121
<b>Figure 66:</b> 100 MHz $^{13}\text{C}$ NMR spectrum of 1,2- <i>O</i> -isopropylidene-6- <i>O</i> - <i>tert</i> -butyldiphenylsilyl- $\alpha$ -D-glucurono-6,3-lactone ( <b>21</b> ).....	122
<b>Figure 67:</b> ESI mass spectrum of 1,2- <i>O</i> -isopropylidene-6- <i>O</i> - <i>tert</i> -butyldiphenylsilyl- $\alpha$ -D-glucurono-6,3-lactone ( <b>21</b> ).....	123
<b>Figure 68:</b> 400 MHz $^1\text{H}$ NMR spectrum of 1,2- <i>O</i> -isopropylidene-6- <i>O</i> - <i>tert</i> -butyldimethylsilyl- $\alpha$ -D-glucurono-6,3-lactone ( <b>22</b> ).....	124
<b>Figure 69:</b> 100 MHz $^{13}\text{C}$ NMR spectrum of 1,2- <i>O</i> -isopropylidene-6- <i>O</i> - <i>tert</i> -butyldimethylsilyl- $\alpha$ -D-glucurono-6,3-lactone ( <b>22</b> ).....	125
<b>Figure 70:</b> ESI mass spectrum of 1,2- <i>O</i> -isopropylidene-6- <i>O</i> - <i>tert</i> -butyldimethylsilyl- $\alpha$ -D-glucurono-6,3-lactone ( <b>22</b> ).....	126

<b>Figure 71:</b> 400 MHz $^1\text{H}$ NMR spectrum of methyl 6- <i>O</i> -pivaloyl- $\beta$ -D-glucurono-6,3-lactone ( <b>23</b> ).....	127
<b>Figure 72:</b> 400 MHz $^1\text{H}$ NMR spectrum of methyl 6- <i>O</i> -pivaloyl- $\beta$ -D-glucurono-6,3-lactone ( <b>23</b> ) treated with $\text{D}_2\text{O}$ .....	128
<b>Figure 73:</b> 100 MHz $^{13}\text{C}$ NMR spectrum of methyl 6- <i>O</i> -pivaloyl- $\beta$ -D-glucurono-6,3-lactone ( <b>23</b> ).....	129
<b>Figure 74:</b> ESI mass spectrum of methyl 6- <i>O</i> -pivaloyl- $\beta$ -D-glucurono-6,3-lactone ( <b>23</b> ).....	130
<b>Figure 75:</b> 400 MHz $^1\text{H}$ NMR spectrum of methyl 6- <i>O</i> -pivaloyl-2- <i>O</i> -trifluoromethylsulfonyl- $\beta$ -D-glucurono-6,3-lactone ( <b>24</b> ).....	131
<b>Figure 76:</b> 100 MHz $^{13}\text{C}$ NMR spectrum of methyl 6- <i>O</i> -pivaloyl-2- <i>O</i> -trifluoromethylsulfonyl- $\beta$ -D-glucurono-6,3-lactone ( <b>24</b> ).....	132
<b>Figure 77:</b> ESI mass spectrum of methyl 6- <i>O</i> -pivaloyl-2- <i>O</i> -trifluoromethylsulfonyl- $\beta$ -D-glucurono-6,3-lactone ( <b>26</b> ).....	133
<b>Figure 78:</b> 400 MHz $^1\text{H}$ NMR spectrum of methyl 6- <i>O</i> -pivaloyl-2- <i>O</i> -( <i>p</i> -methylphenylsulfonyl)- $\beta$ -D-glucurono-6,3-lactone ( <b>26</b> ).....	134
<b>Figure 79:</b> 100 MHz $^{13}\text{C}$ NMR spectrum of methyl 6- <i>O</i> -pivaloyl-2- <i>O</i> -( <i>p</i> -methylphenylsulfonyl)- $\beta$ -D-glucurono-6,3-lactone ( <b>26</b> ).....	135
<b>Figure 80:</b> ESI mass spectrum of methyl 6- <i>O</i> -pivaloyl-2- <i>O</i> -( <i>p</i> -methylphenylsulfonyl)- $\beta$ -D-glucurono-6,3-lactone ( <b>26</b> ).....	136
<b>Figure 81:</b> X-Ray crystal structure of methyl 2,3,4-tri- <i>O</i> -acetyl- $\alpha$ -D-glucopyranosyluronosyl bromide ( <b>6</b> ) .....	138
<b>Figure 82:</b> X-Ray crystal structure of methyl 2,3,4-tri- <i>O</i> -acetyl-1,5-anhydro-D- <i>arabino</i> -hex-1-enopyranuronate ( <b>7</b> ) .....	146
<b>Figure 83:</b> X-Ray crystal structure of methyl 3,4-di- <i>O</i> -acetyl-2-deoxy-2-(4-nitrobenzoyloxyimino)-D- <i>arabino</i> -hex-2-enopyranuronate ( <b>10</b> ).....	153
<b>Figure 84:</b> X-Ray crystal structure of methyl 3,4-di- <i>O</i> -acetyl-1,5-anhydro-2-deoxy-D- <i>arabino</i> -hex-1-enopyranuronate ( <b>15</b> ) .....	162
<b>Figure 85:</b> X-Ray crystal structure of 1,2- <i>O</i> -isopropylidene- $\alpha$ -D-glucurono-6,3-lactone ( <b>19</b> ).....	168

<b>Figure 86:</b> X-Ray crystal structure of 1,2- <i>O</i> -isopropylidene-6- <i>O-tert</i> -butyldiphenylsilyl- $\alpha$ -D-glucurono-6,3-lactone ( <b>21</b> ).....	175
<b>Figure 87:</b> X-Ray crystal structure of 1,2- <i>O</i> -isopropylidene-6- <i>O-tert</i> -butyldimethylsilyl- $\alpha$ -D-glucurono-6,3-lactone ( <b>22</b> ).....	185
<b>Figure 88:</b> X-Ray crystal structure of methyl 6- <i>O</i> -pivaloyl-2- <i>O</i> -trifluoromethylsulfonyl- $\beta$ -D-glucurono-6,3-lactone ( <b>24</b> ).....	193

## Introduction

### *Staphylococcus aureus*

Staphylococci are spherical, Gram-positive bacteria that assemble in microscopic clusters resembling bunches of grapes. In 1884, Rosenbach distinguished between two pigmented colony types of staphylococci and proposed the nomenclature: *Staphylococcus aureus* (yellow) and *Staphylococcus albus* (white).<sup>1</sup> However, the name *Staphylococcus albus* has since been changed to *Staphylococcus epidermidis*. Staphylococci are inevitably found in the mucous membranes and on the skin of humans. Staphylococci generally have a benign, symbiotic relationship with the host, but are considered to be opportunistic pathogens. This can arise from the breach of the cutaneous organ system by trauma, inoculation needles, or direct implantation of medical devices, which enables the staphylococci to gain entry into the host and assume the role of pathogen.<sup>2</sup> Of the two types of colonies: *S. aureus* and *S. epidermidis*, *S. aureus* is a more aggressive pathogen, causing a range of acute and pyrogenic infections, including abscesses, bacteremia, central nervous system infections, endocarditis, osteomyelitis, pneumonia, urinary tract infections, chronic lung infections associated with cystic fibrosis, and several syndromes caused by exotoxins and enterotoxins, including food poisoning, scalded skin and toxic shock syndromes.<sup>2,3</sup> *S. aureus* is a major cause of community-acquired and health-care related infections in the United States and around the world. Approximately 20% of community-acquired and nosocomial bacteremias in the United States are caused by *S. aureus*.<sup>4</sup> Studies show that nearly 500,000 patients in American hospitals contract staphylococcal infections each year.<sup>5</sup> These studies demonstrate that *S. aureus* poses a significant threat to the health of the general public.

Therefore, an effective strategy needs to be developed to prevent and/or treat staphylococcal infections successfully.

### **Antibiotic Resistance of *S. aureus***

In 1944, penicillin was introduced to treat infections caused by sulphonamide resistant *S. aureus*. By 1950, nearly 50% of all clinical isolates of *S. aureus* contained plasmids with penicillin-resistant genes, and by 1990, it was estimated that 90% of *S. aureus* were penicillin resistant.<sup>6</sup> However, shortly after the introduction of penicillin, other antibiotics including chloramphenicol, streptomycin, erythromycin, and tetracycline were used as effective treatments of staphylococcal infections. Again, resistance emerged rapidly and these treatments gradually lost their effectiveness. This resistance prompted the use of more powerful antibiotics such as methicillin and vancomycin. Notable percentages of methicillin-resistant *S. aureus* (MRSA) are currently emerging in hospital settings and in the general community. The first MRSA was observed the very first year of the drug's launch in 1961.<sup>6</sup> MRSA bears a striking resemblance to the emergence of penicillinase-mediated resistance in *S. aureus* fifty years ago.<sup>7</sup> Another recent development emerged with the discovery of vancomycin-resistant *enterococci* (VRE), which significantly contributes to hospital-acquired infections worldwide. Studies by Gemmel show that the vancomycin-resistance of *Enterococcus faecalis* can be transferred to *S. aureus* through a plasmid.<sup>8</sup> The genome of a MRSA strain was sequenced in 2001, and confirmed that the genome coded for a staggering number of antibiotic resistance genes (Figure 1).<sup>9</sup>

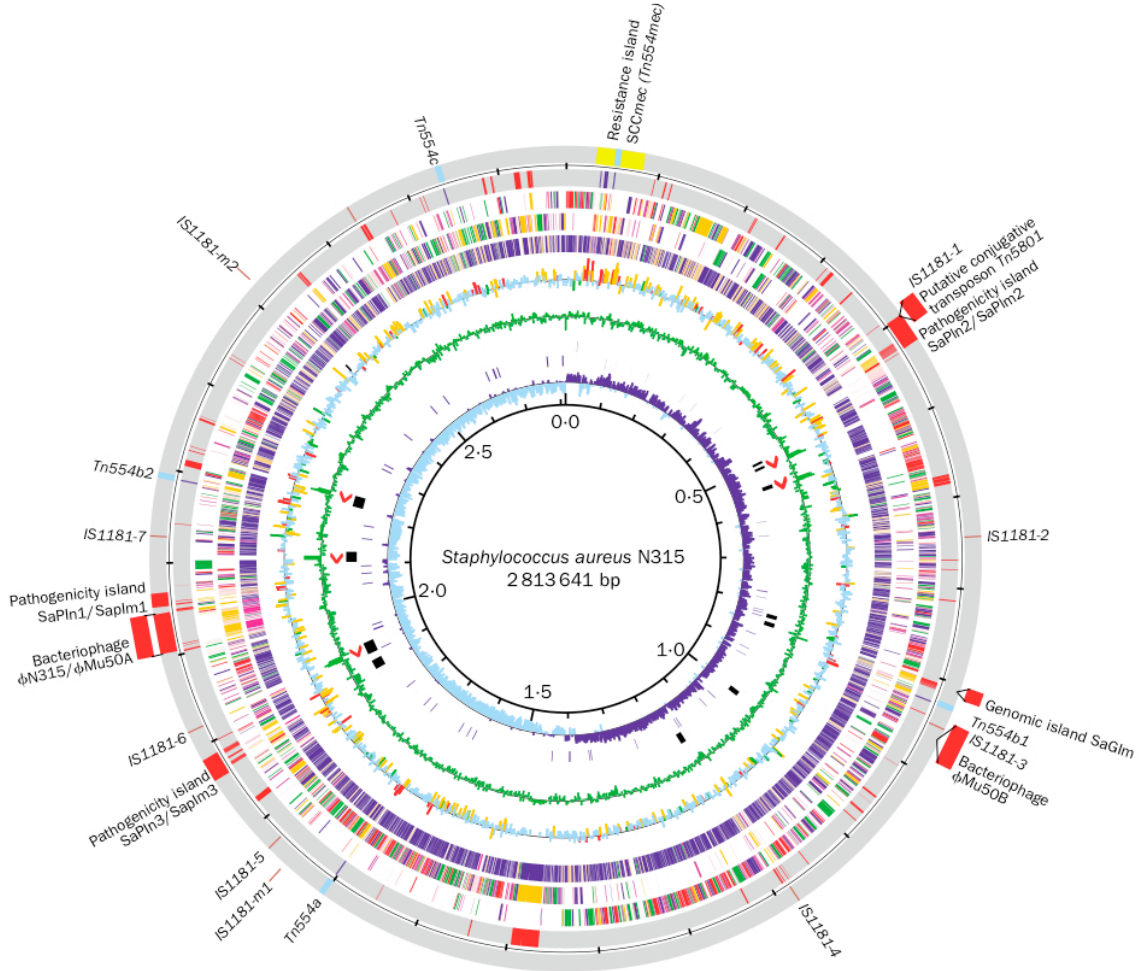


**Figure 1:** Genome map of MRSA strain representing antibiotic resistance genes, located on the outermost circle.

Infections caused by multi-drug resistant *S. aureus* strains are currently treated with a combination of two oral antibiotics, usually rifampicin and fusidic acid.<sup>10</sup> However, according to Courvalin, “evolution of bacteria towards resistance to antimicrobial drugs, including multi-drug resistance, is unavoidable because it represents a particular aspect of the general evolution of bacteria that is unstoppable.”<sup>11</sup> This particular aspect of bacterial evolution is that the selective pressure of antibiotic exposure favors the selection of resistant strains. Therefore, minimizing the antibiotic pressure is essential for

controlling the emergence of multi-resistant strains in both hospitals and the community.<sup>7</sup>

As a result, alternative methods have been implemented to inhibit the biosynthesis of the capsular polysaccharide of *S. aureus*, which functions as a protective barrier against host defense mechanisms.

### Capsular Polysaccharide of *S. aureus*

*S. aureus* surrounds itself with a capsule composed of three repeating amino sugar units called the capsular polysaccharide. Capsular polysaccharides are common in microorganisms that cause invasive diseases because the capsule enhances the microbial virulence by rendering the bacterium resistant to phagocytosis.<sup>12</sup> Most of all the virulent strains of *S. aureus* contain serotypes five and eight (Figure 2). These two serotypes contain the three monomer amino sugars: *N*-acetyl-2-amino-2-deoxy-D-mannopyranose uronic acid (D-ManNAcA), *N*-acetyl-2-amino-2-deoxy-D-fucopyranose (D-FucNAc), and *N*-acetyl-2-amino-2-deoxy-L-fucopyranose (L-FucNAc) (Figure 3).

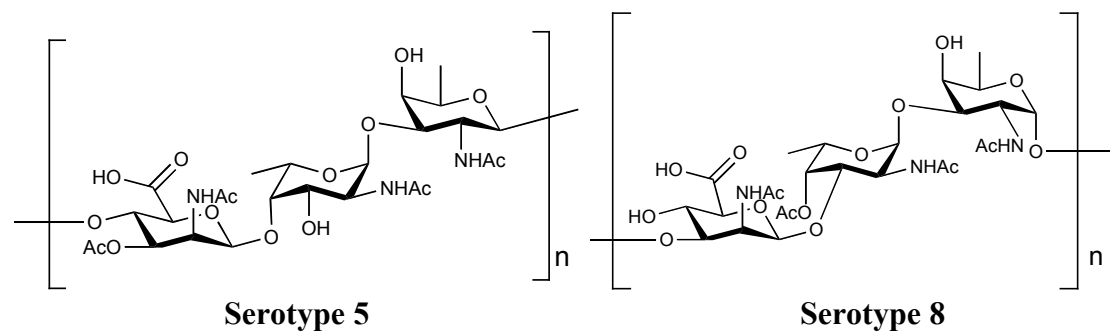


**Figure 2:** The repeating amino sugar units associated with serotypes 5 and 8 capsular polysaccharides of *S. aureus*.

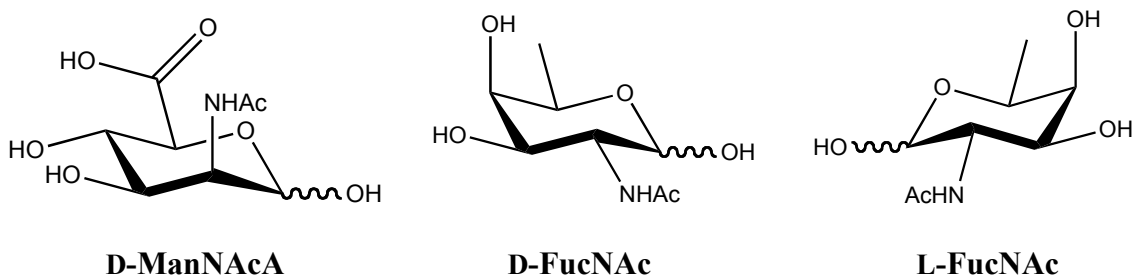
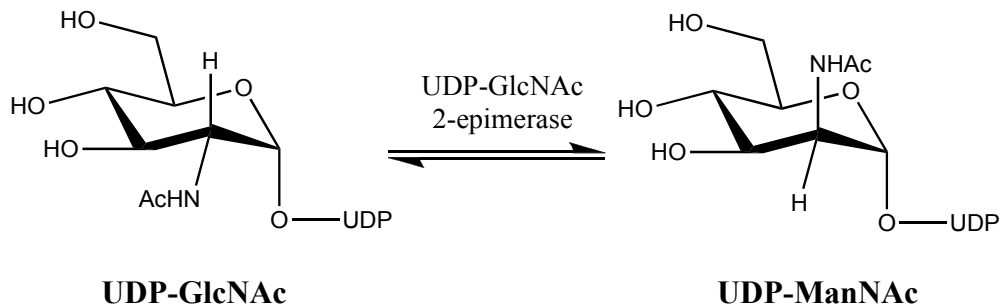


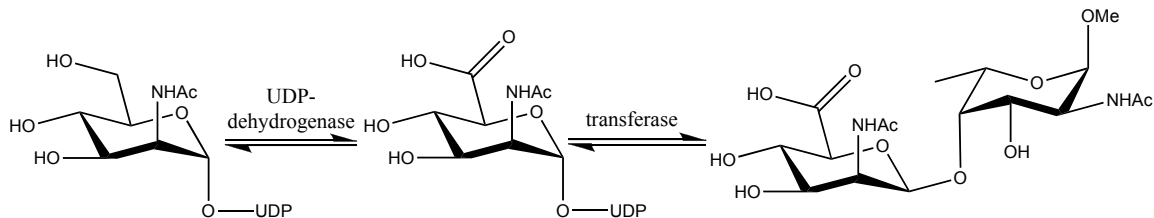
**Figure 3:** Components of the capsular polysaccharide of *S. aureus*.

A series of specific enzyme-catalyzed reactions are responsible for the biosynthesis of the capsular polysaccharide. Studies by Kiser et al. show that sixteen genes (*cap5A* through *cap5P*) are involved in the biosynthesis of Serotype 5 capsular polysaccharide (CP5) and that UDP-GlcNAc is the precursor compound for the entire CP5 synthesis.<sup>13</sup> The *cap5P* gene in *S. aureus* encodes a UDP-*N*-acetylglucosamine 2-epimerase which is responsible for the formation of the precursor compound UDP-ManNAc (Equation 1).<sup>14</sup>



**Equation 1:** Epimerization of UDP-GlcNAc to UDP-ManNAc.

UDP-ManNAc is then oxidized by the enzyme D-ManNAc dehydrogenase to give UDP-ManNAcA which is transferred to an L-FucNAc residue, thus completing the linkage between D-ManNAc and L-FucNAc (Scheme 1).



**Scheme 1:** Oxidation and glycosyl transfer to form glycosyl linkage.

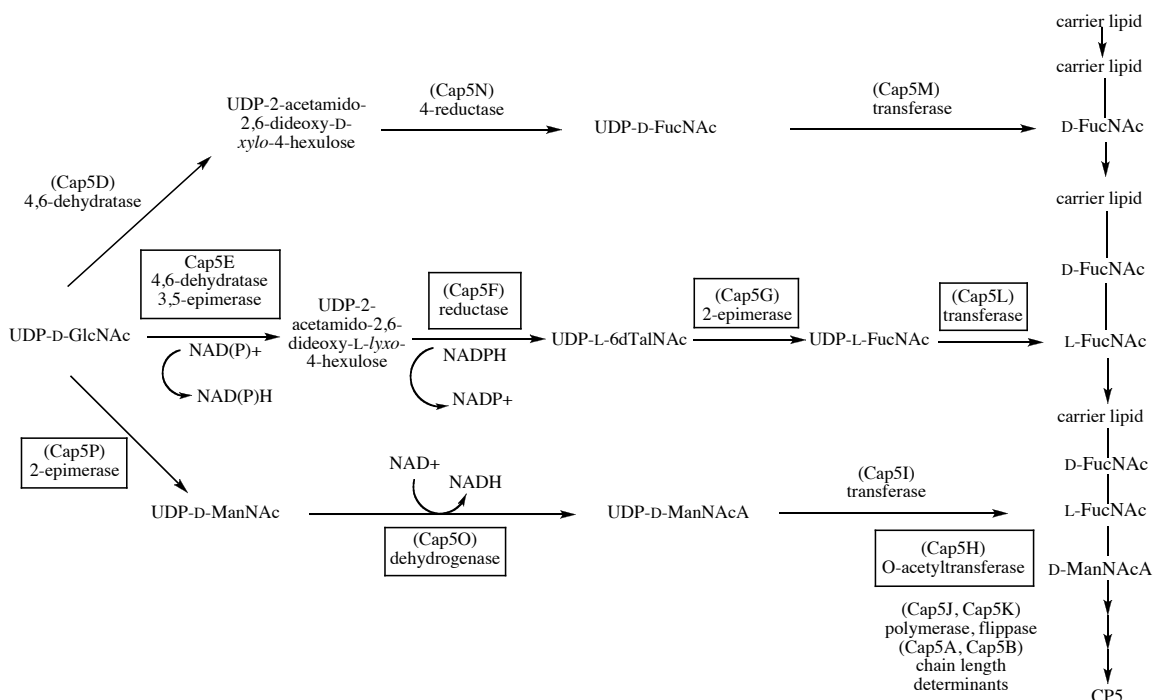


**Figure 4:** Proposed pathway of CP5 biosynthesis involving UDP-D-GlcNAc as the precursor compound.<sup>12</sup>

The proposed pathway of CP5 biosynthesis involves a sequence of enzymatic reactions, each of which uses carbohydrates as the substrate. There is tremendous potential to inhibit any of these enzymes involved in the CP5 biosynthesis. Glycomimetics can be synthesized with the ability to act as competitive inhibitors of the enzymes involved, and inhibition of enzymes involved in CP5 biosynthesis can be achieved in several different ways. Glycomimetics that resemble the natural substrates

but, for instance, lack an essential functional group for glycosyl linkage, could inhibit particular transferase enzymes. Glycomimetics can also resemble an intermediate of the enzymatic process, which can inhibit the enzyme activity. Finally, inhibitors that mimic the transition state of a particular enzymatic reaction are often the most potent inhibitors; if a glycomimetic can be synthesized to resemble the transition state of an enzymatic process, then it will most likely be very effective in binding tightly in the enzyme pocket. Although these approaches have distinct differences, one unifying characteristic is they all employ the use of a modified carbohydrate to modulate the enzymatic machinery of a biological system. The study of these types of events is called *glycobiology*.

## Glycobiology

Glycobiology investigates the roles of carbohydrates in biological events, specifically: (1) what influence do carbohydrates have on the proteins to which they are bound? (2) how are carbohydrates involved in recognition events?<sup>15</sup> Research carried out mainly in the last 40 years has attested to the fact that carbohydrates play a fundamental role in important biological events. Apart from being the primary source of energy in biological systems and being involved in molecular recognition processes for cells, carbohydrates also play a fundamental role in many other important biological processes including fertilization, embryogenesis, immune defense, viral replication, parasitic infection, cellular proliferation, apoptosis, cell-cell adhesion, blood-type antigens, degradation of blood clots, and inflammation.<sup>15-19</sup> Carbohydrates can be present in the cell without being attached to other molecules, however, the majority are attached to either proteins (glycoproteins) or lipids (glycolipids). Additionally, the attached

carbohydrate is often referred to as an oligosaccharide or glycan. Oligosaccharides or a set of oligosaccharides can be attached to different glycosylation sites on macromolecules *via* enzymatic processes to yield glycoconjugates.

The biosynthesis of glycoconjugates is mediated by multiple factors such as amino acid sequence, overall protein conformation, and available carbohydrates and transferases. The number of possible glycosylation sites is determined by the primary amino acid sequence and estimates based on the SwissProt database suggest that more than half of all proteins are glycosylated.<sup>20</sup> There are three major types of glycan linkages found in Nature: O-linked (linkage to the hydroxyl group of serine, threonine, or hydroxylysine), N-linked (linkage to the amide group of asparagine), and C-linked (linkage to a carboxyl group of tryptophan).<sup>21</sup> The possible variations in sequence or position of the attached oligosaccharides have led to the concept of a glycoprotein being defined as a set of glycoforms. Varying conditions in the cell can lead to the predominance of one glycoform over the others. This has been shown during cell development, where specific sets of oligosaccharides are expressed at distinct stages of differentiation and tumorigenesis.<sup>22</sup> Alterations in the glycosylations of glycoconjugates can drastically modify their structure and function, and these alterations are believed to act in a manner similar to a point mutation in DNA.<sup>23</sup> Specifically, alterations in certain cell-surface oligosaccharides are associated with various pathological conditions including malignant transformation.<sup>15</sup> In short, glycosylation is a highly sensitive process and abnormal glycosylation is characteristic of cells in a diseased state and are collectively referred to as congenital disorders of glycosylation (CDG).<sup>24</sup> However, the key benefit of glycosylation is it allows the cell to put the same recognition markers on

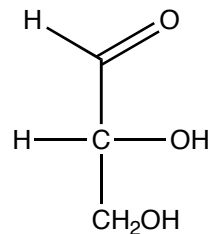
quite different proteins without having to code the information into the DNA of that protein. This gives the cell tremendous versatility and exemplifies the uniqueness and importance of carbohydrates in Nature.

## Carbohydrate Structure

Carbohydrates are the most abundant class of macromolecules and differ from DNA, protein, and lipids in that they can be highly branched molecules and many different types of linkages can connect their monomeric units. Furthermore, due to the number of stereogenic centers, functional groups, and linkage possibilities, the number of structural variations is essentially limitless.<sup>25</sup> For this reason, research focused toward carbohydrate systems has emerged more slowly than research geared towards other important biomolecules. However, due to the growing interest in the influence of carbohydrates on biological systems, an increased appreciation of the roles of carbohydrates in biological processes has evolved. Elucidation of the structure of carbohydrates was initially investigated by Emil Fischer.

In the late 1800's, Fischer began his seminal studies on the structures of carbohydrates. His work was influenced by a novel theory proposed by Le Bel and van't Hoff in 1874, which stated a carbon atom with four different groups should be tetrahedral in shape and able to exist in two separate forms (isomers), as non-superimposable mirror images.<sup>26</sup> Fischer adopted these revolutionary ideas which formed the cornerstone of his arguments on the structure of carbohydrates.<sup>26</sup> For every stereogenic center ( $n$ ) in a compound, there are  $2^n$  possible isomers of that compound. In the case of glucose (Fischer's most famous configuration determination), there are four stereogenic centers

that lead to a total of 16 possible isomers. In order to determine the relative configuration of all four of these centers, Fischer used the dextrorotatory form of glyceraldehyde, now designated D-(+)-glyceraldehyde (**1**), as a reference compound. Fischer arbitrarily proposed that the hydroxyl attached to C-2 is to the right when represented by a Fischer projection (Figure 5) and labeled this compound as (+)-glyceraldehyde, which was later described the small capital letter D.<sup>25</sup> Fortunately, this configuration was confirmed with the emergence of X-ray techniques in the mid twentieth century.



**1**

**Figure 5:** Fischer projection of D-(+)-glyceraldehyde.

The Rosanoff convention, introduced in 1906, uses D and L to denote the absolute configuration of the bottom-most stereogenic center as depicted in a Fischer projection.

The term “carbohydrate” literally means hydrates of carbon and describes a family of compounds possessing the empirical formula  $C_n(H_2O)_n$ .<sup>27</sup> However, the term has been expanded to encompass many other materials derived from monosaccharides. In general, carbohydrates can be classified into two main types: polyhydroxylated aldehydes (aldoses) and polyhydroxylated ketones (ketoses) (Figure 6).

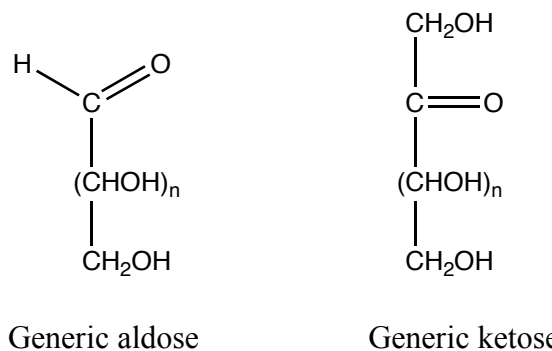


**Figure 6:** General structure of aldose and ketose sugars.

These compounds can be further classified according to the number of carbon atoms in their chains (trioses, tetroses, pentoses, hexoses, etc.), and according to the type of ring they form (furanoses and pyranoses).<sup>25</sup> In solution, carbohydrates can assume many different forms. They generally exist as acyclic (**2a**), furanose (**2d**, **2e**), and pyranose (**2b**, **2c**) forms. Figure 7 illustrates the possible forms of D-glucose in solution.

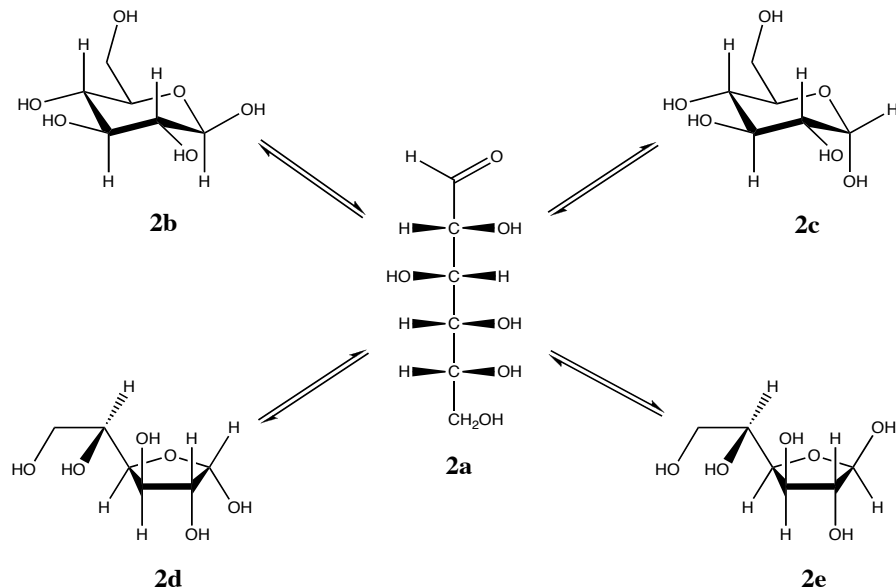


**Figure 7:** Possible forms of D-glucose in solution.

Most commonly, synthetic procedures involve the more stable pyranose form of carbohydrates. Pyranoses can be further classified by the use of  $\alpha$  and  $\beta$  based on the orientation of the substituent on C-1. The prefix  $\alpha$  refers to the substituent at C-1 being in the axial position and  $\beta$  refers to the substituent at C-1 being in the equatorial position (Figure 8).

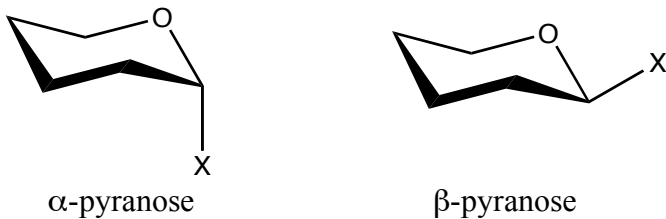


**Figure 8:**  $\alpha$  and  $\beta$  anomers in pyranose form.

The introduction of oxygen to a six-membered ring (pyranose) does not change its fundamental conformational characteristics: the chair conformation is preferred and substituents prefer to be equatorial. However, an important difference is that electronegative groups attached to the carbon atoms adjacent to the oxygen atom in the ring prefer to be in the axial orientation. This phenomenon, known as the anomeric effect, is significant in carbohydrate chemistry because it contributes to the free energies of pyranoses, their preferred conformations and reactivities, and the compositions of anomeric mixtures at equilibrium.<sup>28</sup> The anomeric effect, coined by Lemieux, is caused by the interaction between the axial lone pair of the oxygen in the ring and the antibonding  $\sigma^*$ -orbitals of the bond between C-1 and X (Figure 9).<sup>29</sup>

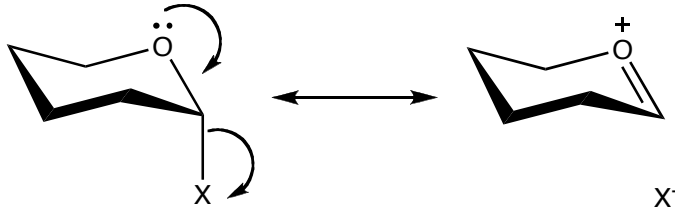


**Figure 9:** Resonance forms representing the anomeric effect.

This interaction leads to the shortening of the bond between the oxygen in the ring and C-1, while lengthening the bond between C-1 and X, which leads to a stabilizing effect by increasing the distance from the dipole of the C-1—X bond to the lone pair of the oxygen in the ring.<sup>28</sup> Correspondingly, electronegative groups in the  $\beta$  conformation ( $-X_e$ ) endure stronger repulsive forces with the unshared pair of electrons of the oxygen in the ring than the  $\alpha$  conformation ( $-X_a$ ) (Figure 10).

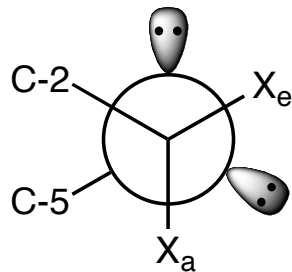


**Figure 10:** Newman projection illustrating repulsive forces between substituents at C-1 and the unshared pair of electrons from the oxygen in the ring.

The introduction of oxygen to a six-membered ring significantly changes the characteristics of the ring during the process of a ring flip. The two chair forms of cyclohexane are indistinguishable, however, the same does not apply for pyranoses because a ring flip results in the formation of non-equivalent chair forms (Figure 10).<sup>28</sup>



**Figure 11:** Nomenclature used to describe the two chair conformations of pyranoses.

Therefore, an adequate nomenclature system must be established to distinguish between the different conformations of not only chairs, but also boats, skews, envelopes, and five-membered rings. This is accomplished by symbolizing the general shape of the ring by the first letter of that shape: chair, *C*; boat, *B*; half-chair, *H*; skew, *S*; and envelope, *E*. A reference plane is selected which contains the maximum number of ring atoms in the same plane. Superscript and subscript are used to describe the out-of-plane atoms. The superscript refers to the exoplanar atom projecting up through the plane of the ring when the ring is orientated so that the numbering of the ring proceeds in a clockwise fashion. Conversely, the subscript refers to the atom that projects down through the plane of the ring as represented in Figure 11. The conformation that a particular pyranose will adopt is primarily influenced by energetics. This was demonstrated by Rao, Sundararajan, et al. who calculated the free energy of the  $^4C_1$  and  $^1C_4$  conformations of the 16 D-aldohexoses using the valence force field approach, and their calculations closely agree with the experimentally observed conformations.<sup>18</sup> Therefore, the preferred conformation has the lowest free energy, thus, more favorable electronic and steric interactions. Consequently, altering substituents on a pyranose ring may change the electronic interactions resulting in a change of conformation.

In addition to the effects of introducing oxygen to a six-membered ring, the introduction of unsaturation into a six-membered ring has a profound effect on the conformational properties. There are two types of unsaturation in pyranoses: endocyclic and exocyclic. An endocyclic double bond can be formed between adjacent carbon atoms in the ring and changes the fundamental conformational family from a chair to half-chair. Many reactive pyranose intermediates contain a double bond between C-1 and C-2, and are commonly referred to as glycals (Figure 12).

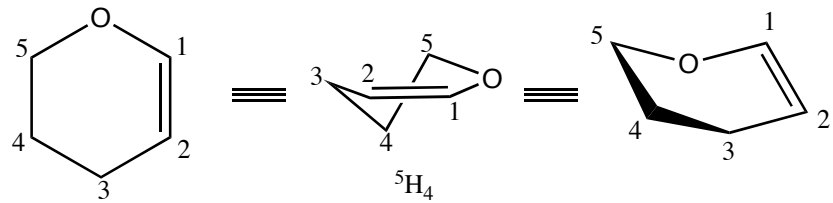


**Figure 12:** Three common representations of a typical glycal.

Exocyclic double bonds can also influence the conformation of a pyranose. By introducing an  $sp^2$  hybridized carbon to the ring in the form of a carbonyl or imine, the ring will become more flattened which lowers the activation barrier of a ring flip.<sup>30</sup> Furthermore, substituents adjacent to the  $sp^2$  hybridized carbon may have electronic interactions with the double bond. When an equatorial, electronegative substituent is adjacent to a carbonyl or imine, the dipole of the substituent is nearly parallel to that of the carbonyl or imine, which results in a repulsive interaction, whereas the dipole of an axial, electronegative substituent is orthogonal which results in little interaction (Figure 13).<sup>31</sup>



**Figure 13:** Depiction of dipole-dipole interactions of axial and equatorial substituents adjacent to an  $sp^2$  hybridized carbon ( $R = O$  or  $NR$ ).

There are also orbital interactions between the substituent and the exocyclic double bond that are similar to the anomeric effect. In the axial conformation, an electronegative substituent is better aligned to donate electrons from the C-X  $\sigma$  bond to the  $\pi^*$  orbital of the double bond, whereas an equatorial substituent is not aligned for any donation to take place. Lastly, the polarity of the solvent also influences the orientation of the substituent. A polar solvent will nullify the above-mentioned interactions by decreasing the dipole-dipole and orbital interactions, thus favoring the equatorial orientation.<sup>31</sup> Likewise, a non-polar solvent will have little effect on the dipole-dipole and orbital interactions. Since the activation barrier of a ring flip is lowered because of the introduction of an  $sp^2$  hybridized carbon to the ring, these electronic interactions can influence a change in conformation.

### Amino Sugars

In terms of biological significance, carbohydrates can be divided into three major categories: amino sugars, glycols, and glycosides. Amino sugars are characterized by the replacement of one or more alcoholic hydroxy groups with an amino or acetamido group (Figure 14).

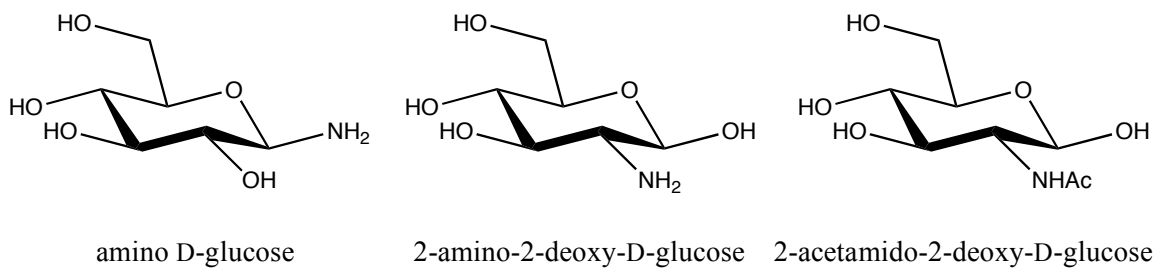
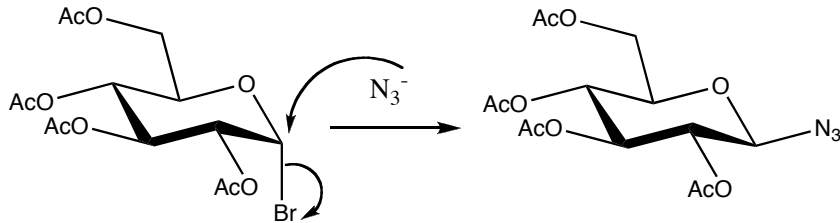


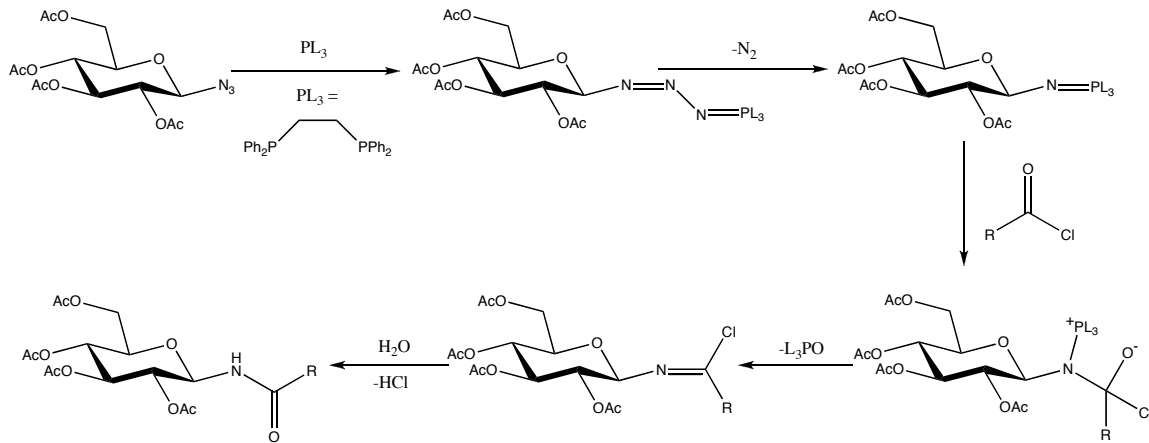
**Figure 14:** Typical examples of amino sugars.

Amino sugars are present in the most important classes of glycoconjugates and naturally occurring oligosaccharides.<sup>31</sup> Most commonly, amino or acetamido functionality is introduced at either C-1 or C-2. Amino sugars in which the nitrogen group replaces the hemiacetal hydroxy group at C-1 are referred to as *N*-glycosides; more specifically, glycosylamines and glycosylamides. *N*-Glycosides are involved in important biological activities like the linkage of nucleotides with deoxyribose or ribose in DNA and RNA, respectively. Interests in synthesizing *N*-glycosides have been increasing because of their natural occurrence in macromolecules such as DNA, and their interesting biological activities in compounds such as the glycoprotein vancomycin.<sup>32</sup> Most commonly, the synthesis of amino sugars involves the use of an azide as a protected amine group. Azide serves as an excellent source of nitrogen to be introduced to a sugar and employing azides gives several advantages in terms of general synthetic applications such as low steric hinderance, greater solubility, lack of rotamer formation, and the absence of hydrogen and carbon nuclei to complicate NMR spectra.<sup>33</sup> Azides are generally introduced at C-1 *via* nucleophilic displacement ( $S_N2$ ), often involving a bromide as the leaving group (Equation 2).



**Equation 2:** Mechanism of nucleophilic displacement ( $S_N2$ ) on a glycosyl bromide to form a glycosyl azide.

The synthesis of glycosylamides formerly involved the reduction of an azide to a glycosylamine. However, more recent methods developed by Boullanger et al. use a modified Staudinger reaction which produces high yields of product in a stereospecific way through a series of reactive intermediates (Scheme 2).<sup>34</sup>

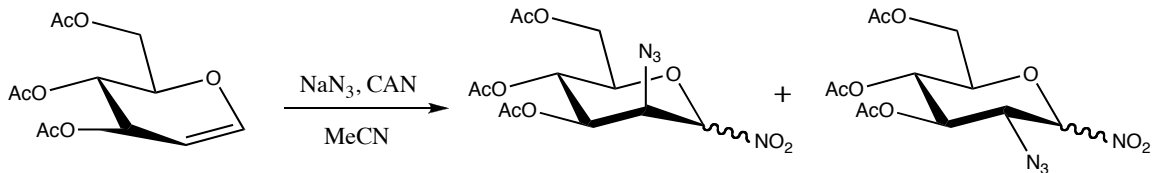


**Scheme 2:** Reaction pathway of modified Staudinger reaction.

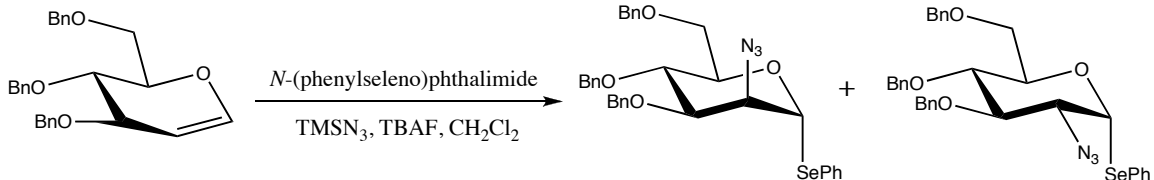
The modified Staudinger reaction provides an efficient method to convert an azide to a variety of different amides, which is not only important in carbohydrate synthesis, but also in the synthesis of pharmaceuticals and peptidomimetic compounds.<sup>35</sup>

Apart from  $N$ -glycosides, the synthesis of 2-amino-2-deoxy sugars is of significant interest because these are the types of sugars incorporated into the capsular polysaccharide of *S. aureus*. Several methods for the stereoselective synthesis of 2-

amino-2-deoxy sugars have emerged during the past two decades. The synthesis of 2-amino-2-deoxy sugars can be achieved by the introduction of a 2-azido moiety to glycals *via* azide radical<sup>36</sup> (Equation 3) or *via* azide ion<sup>37</sup> (Equation 4).



**Equation 3:** Azidonitration of glycals *via* azide radical.



**Equation 4:** Azidophenylselenation of glycals *via* azide ion.

Synthesis of 2-amino-2-deoxy sugars can also be achieved *via* nucleophilic displacement ( $S_N2$ ) at C-2. The  $S_N2$  reaction is an essential tool for introducing substituents to the sugar, resulting in an inversion of configuration. However, it can be difficult to perform the  $S_N2$  reaction on furanoses and equatorial substituents because the site of displacement is crowded, usually resulting in an elimination reaction or no reaction at all. The efficiency of the displacement is determined by several factors such as steric hinderance, nature of the nucleophile and the leaving group, and polarity of the solvent. These factors must be taken into account when developing synthetic approaches toward 2-amino-2-deoxy sugars.

Recently, the trend in the synthesis of 2-amino-2-deoxy sugars is not only to introduce a nitrogen group to the sugar, but also specific functionality at C-1 to be used for a subsequent glycosylation reaction. These methods involve: cycloaddition reactions *via* pyrano-oxadiazines and triazolines; amidation of glycals *via* phosphoramidation, sulfonamidoglycosylation, transition metal-mediated amidation, and 2-acetamido glycosylation; and S<sub>N</sub>2 reactions *via* O-sulfonyl derivatives and epoxides.<sup>38</sup>

There are several approaches to the synthesis of 2-amino-2-deoxy sugars and the objective is to develop a synthetic strategy that is both efficient and inexpensive. Many difficulties can arise due to the complexity of the physical structure and unique chemistry of each sugar; however, due to the significant role carbohydrates play in biological systems, contributions to the field of carbohydrate chemistry must continue to be made.

### Statement of Problem

*S. aureus* is responsible for several types of infectious diseases in the community and, particularly, in hospital settings. Treatments involving antibiotics are becoming less effective due to the emergence of resistant strains of the bacteria. The growing resistance is facilitated by a staggering number of antibiotic resistance genes coded in the DNA and the formation of a capsular polysaccharide. The capsular polysaccharide functions as a protective barrier, which prevents the host from destroying the bacteria *via* phagocytosis. The goal of this research project is to develop glycomimetics of the aminosugars found in the capsular polysaccharide of *S. aureus* in an attempt to inhibit the enzymes responsible for its formation.

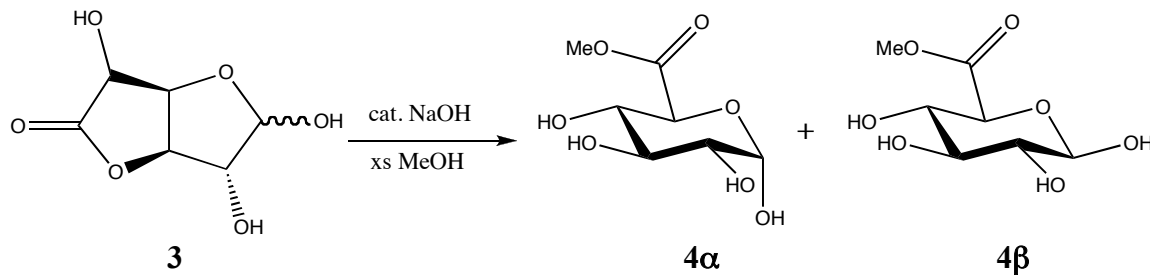
The following work describes stereoselective synthetic pathways toward D-ManNAcA from D-glucurono-6,3-lactone, an inexpensive, readily-available starting material. Two main approaches were employed to introduce nitrogen and invert the stereochemistry at C-2. The first approach removes the chirality at C-2 by introducing unsaturation through the formation of an imine or a glycal, and the second approach utilizes the S<sub>N</sub>2 reaction to epimerize and introduce nitrogen at C-2 through the use of an azide. Key intermediates in these pathways are to be tested for possible inhibition of the formation of the capsular polysaccharide of *S. aureus*.

## Results and Discussion

### 1. Synthesis of precursors to D-ManNAcA *via* oxime intermediate.

Lichtenthaler et al. developed a method for the facile preparation of a novel  $\beta$ -D-ManNAcA donor. The method is advantageous because many of the intermediates are securable in crystalline form and it involves many high-yielding steps.<sup>39</sup> The key step in this pathway involves the reduction of an imine derivative and subsequent acetylation at C-2. The synthesis of the intermediates in the Lichtenthaler pathway is described in detail below.

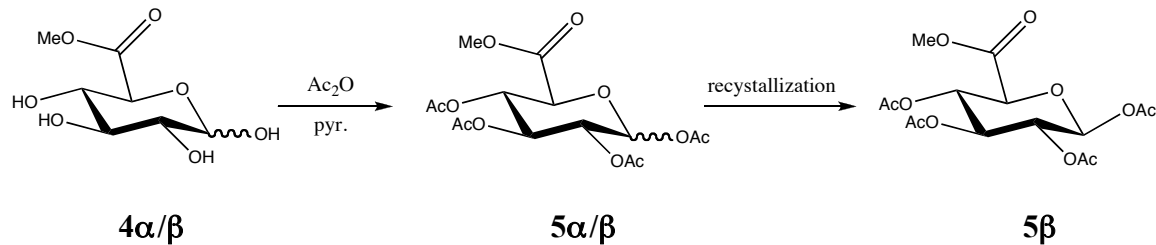
The synthetic pathway utilizes D-glucurono-6,3-lactone (**3**) as the starting material, which can be obtained inexpensively from Aldrich. The initial step involves the treatment of **3** with a catalytic amount of sodium hydroxide in an excess of methanol to convert the lactone into a mixture of  $\alpha/\beta$  methyl D-glucopyranuronate (**4**) (Scheme 3).



**Scheme 3:** Preparation of  $\alpha/\beta$  methyl D-glucopyranuronate.

The resulting mixture of **4 $\alpha/\beta$**  was evaporated and the free hydroxyl groups were protected *via* acetylation with acetic anhydride in pyridine. The reaction was stopped when TLC showed consumption of starting material and the appearance of a spot with a higher  $R_f$  value. The crude product was purified by extraction followed by an aqueous

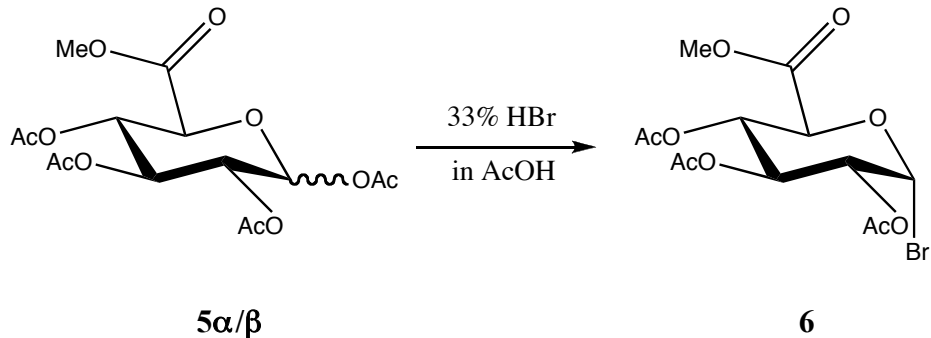
workup to provide a mixture of isomers, which were separated by crystallization to afford **5 $\beta$**  as colorless crystals (Scheme 4). The mother liquor was concentrated under reduced pressure to give **5 $\alpha$**  as a brown syrup.



**Scheme 4:** Acetylation and subsequent recrystallization of methyl 1,2,3,4-tetra-*O*-acetyl- $\beta$ -D-glucopyranuronate.

<sup>1</sup>H NMR is crucial in determining the identity of the isomers because the coupling constant between H-1 and H-2 in the  $\alpha$  isomer should be smaller than the  $\beta$  isomer. Indeed, the crystalline product has an H-1–H-2 coupling constant of 7.69 Hz while the syrup has a coupling of 3.66 Hz. <sup>13</sup>C NMR shows five signals in the ester range at 166.5, 168.5, 168.9, 169.2, and 169.6 ppm corresponding to four acetyl protecting groups and the methyl ester at C-6. Electrospray ionization (ESI) mass spectrometry shows a mass at 399.1 for both isomers, which corresponds to the molecular weight of **5 $\alpha$**  and **5 $\beta$**  plus a sodium atom. Further, single crystal X-ray data for both the  $\alpha$  and  $\beta$  anomers have previously been reported.<sup>40, 41</sup>

Bromide (**6**) was readily obtained by the treatment of **5 $\alpha/\beta$**  with 33% HBr in acetic acid to give a single stereoisomer in quantitative yield (Equation 5).



**Equation 5:** Preparation of methyl 2,3,4-tri-*O*-acetyl- $\alpha$ -D-glucopyranuronosyl bromide (**6**).

TLC indicated the consumption of starting material and the appearance of a spot with a lower  $R_f$  value.  $^1\text{H}$  NMR shows a shift of the H-1 proton signal downfield from 5.79 to 6.67 ppm with a coupling constant of 4.03 Hz, which indicates a gauche alignment with H-2. The preference of the bromine atom to be in the axial position is due to the anomeric effect described earlier.  $^{13}\text{C}$  NMR shows the disappearance of one of the acetyl protecting groups, which is consistent with the substitution of Br at C-1. Atmospheric pressure chemical ionization (APCI) mass spectrometry shows a mass of 397.0 that agrees with the calculated mass of 396.01 with the addition of a hydrogen atom. Single crystal X-ray data was obtained for the bromide and confirms the configuration of the  $\alpha$ -isomer (Figure 15).

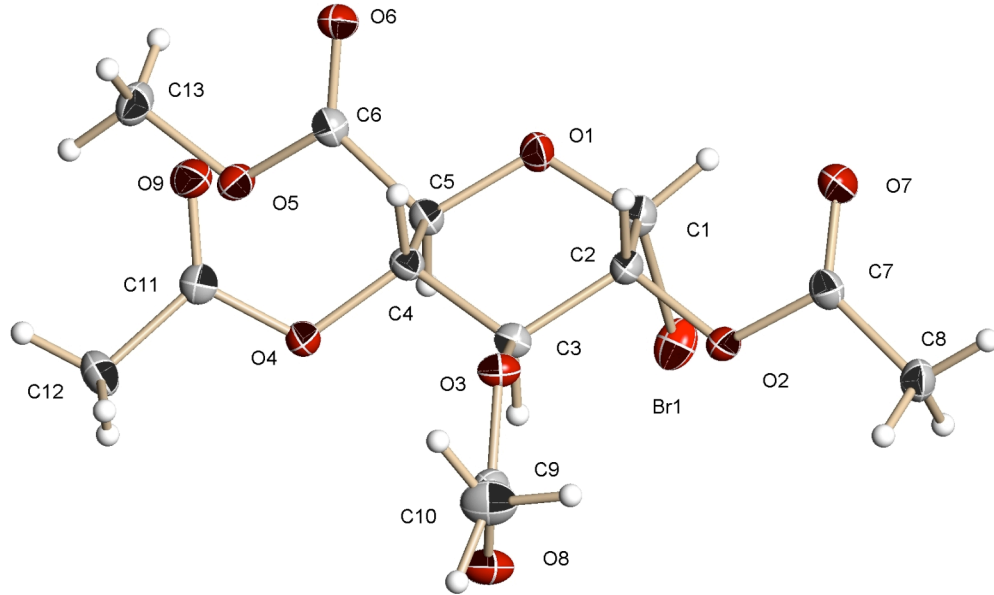
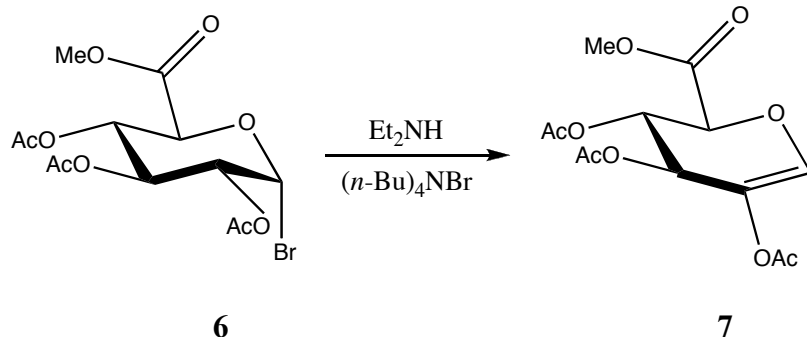


**Figure 15:** X-Ray structure of methyl 2,3,4-tri-O-acetyl- $\alpha$ -D-glucopyranuronosyl bromide (**6**).

Having the Br in the axial position helps facilitate the subsequent elimination reaction. Since the H-2 proton is also in the axial position, the elimination reaction should be facile because of the *anti* relationship between the bromine and the proton at C-2.



**Equation 6:** Preparation of glycal **7** *via* elimination reaction.

Utilizing bromine's ability to be a good leaving group, the treatment of **6** with diethylamine and tetrabutylammonium bromide in DMF gave glycal **7** *via* E2 reaction (Equation 6). TLC showed consumption of starting material and the appearance of a UV-active spot with a lower  $R_f$  value.  $^1\text{H}$  NMR shows the H-1 proton shifted slightly downfield from 6.67 ppm to 6.84 ppm due to the introduction of a double bond between C-1 and C-2. The splitting pattern of H-1 also changed from a doublet to a singlet because of the absence of a proton neighbor on C-2. Interestingly, the splitting patterns of H-3, H-4, and H-5 are unpredicted. H-3 is a triplet with a coupling constant of 2.56 Hz, H-4 is a doublet of doublets with coupling constants of 1.47 and 2.56 Hz, and H-5 is a doublet of doublets with coupling constants of 1.47 and 2.20 Hz. This could be due to the fact that **7** exists in two different conformations,  $^5H_4$  and  $^4H_5$ .  $^{13}\text{C}$  NMR shows a downfield shift of carbon signals for C-1 and C-2 from 85.3 to 127.2 ppm and 70.1 to 139.2 ppm, respectively. Again, this is due to the introduction of a double bond between C-1 and C-2. APCI mass spectrometry provided a mass of 317.1, which corresponds to the calculated mass of 316.08 with the addition of a proton. Single crystal X-ray data was obtained for glycal **7** (Figure 16), which confirms the structure of **7** and also illustrates the  $^5H_4$  conformation of **7** in the solid-state.

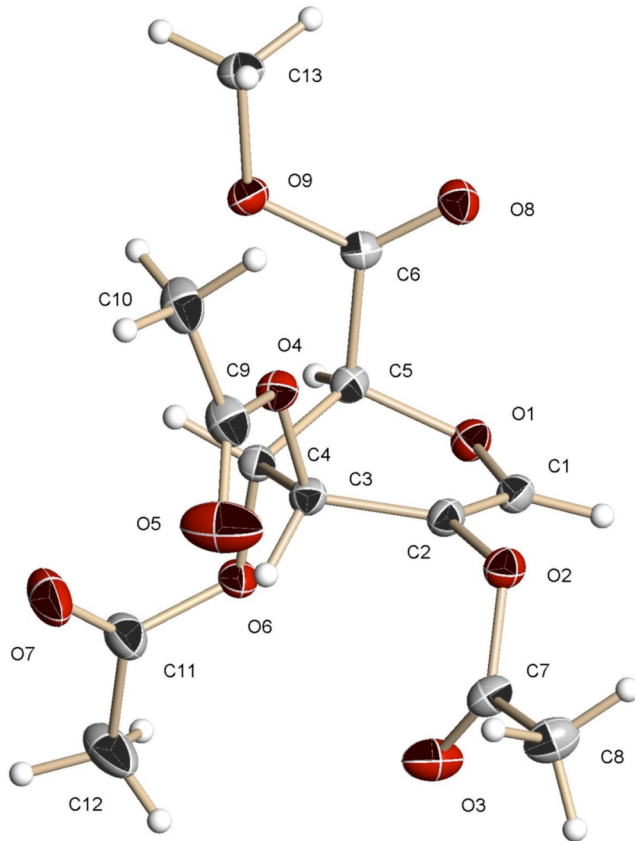
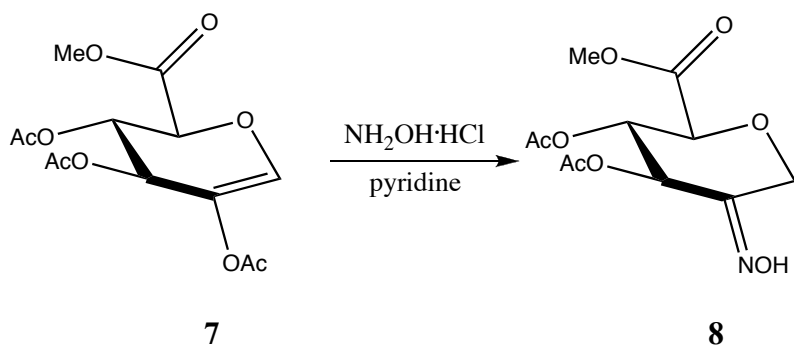


**Figure 16:** X-Ray structure of methyl 2,3,4-tri-O-acetyl-1,5-anhydro-D-arabino-hex-1-enopyranuronate (**7**).

Glycal **7** is an important precursor that is used to introduce nitrogen to the sugar framework in the form of an oxime. The reaction of glycal **7** with hydroxylamine hydrochloride in pyridine produced oxime **8** as a pale yellow solid, which was crystallized using isopropanol to give colorless crystals in 80% yield (Equation 7).



**Equation 7:** Formation of methyl 3,4-di-*O*-acetyl-2-deoxy-2-(hydroxyimino)-D-arabino-hex-2-enopyranuronate (**8**).

TLC showed consumption of starting material and the appearance of a UV-active spot with a lower  $R_f$  value.  $^1\text{H}$  NMR shows the disappearance of one acetyl protecting group and the appearance of another proton signal for the hydrogen attached to C-1. The H-1<sub>A</sub> and H-1<sub>B</sub> signals are doublets with a coupling constant of 15.75 Hz. The splitting patterns for H-3, H-4, and H-5 in  $\text{CDCl}_3$  are more consistent with what is expected for this compound. H-3 is a doublet with a coupling of 4.76 Hz. H-4 is a doublet of doublets with couplings of 4.39 and 4.76 Hz. H-5 is a doublet with a coupling of 4.39 Hz. Therefore, there are not two visible conformations of **8** in the  $^1\text{H}$  NMR, but rather the observed couplings are an average representing the equilibrium of conformations. This is evident when the NMR solvent is changed to  $\text{THF}-d_6$ , when the observed couplings for H-3, H-4, and H-5 range from 2.20-4.03 Hz. Additional evidence for the formation of oxime **8** is the appearance of a signal at 8.51 ppm, which corresponds to the proton of the hydroxyimine.  $^{13}\text{C}$  NMR reveals the upfield shift of C-1 from 127.2 to 58.9 ppm caused by the change in hybridization of C-1 from  $\text{sp}^2$  to  $\text{sp}^3$ . The signal for C-2 remained downfield at 149.2 ppm because it is still involved in a double bond with the nitrogen of the hydroxyimine. Both signals corresponding to the acetyl protecting group at C-2 are

no longer present and all other signals did not undergo significant change. ESI mass spectrometry shows an  $M^+$  of 312.1, which agrees with the calculated mass of 289.08 with the addition of a sodium atom. Single crystal X-ray data confirming formation and stereochemistry of oxime **8** has previously been reported (Figure 17).<sup>41</sup>

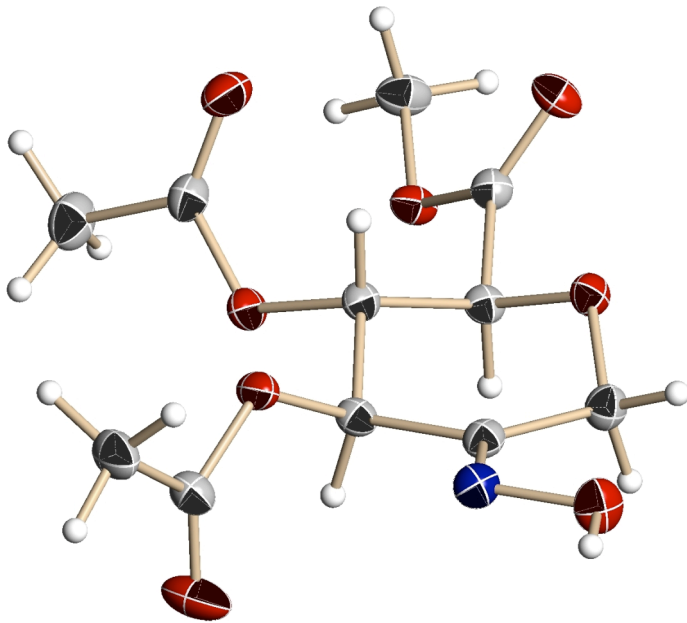
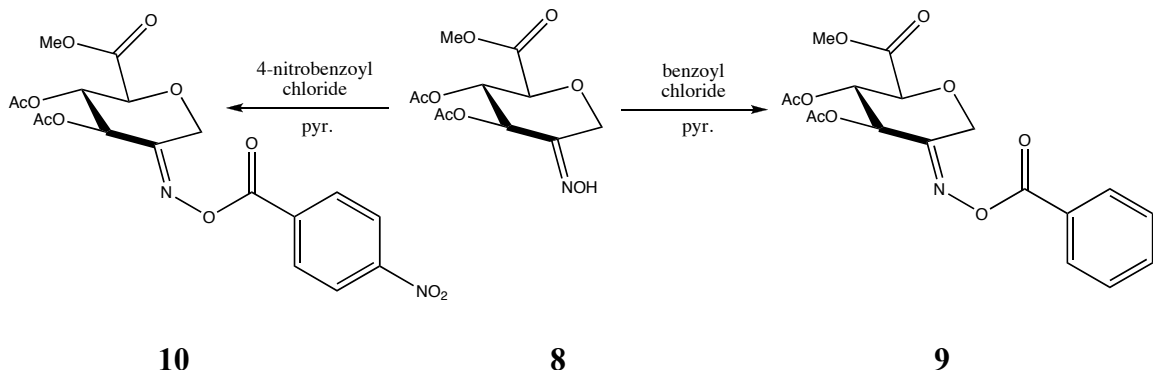


**Figure 17:** X-Ray structure of methyl 3,4-di-O-acetyl-2-deoxy-2-(hydroxyimino)-D-arabino-hex-2-enopyranuronate (**8**).<sup>41</sup>

The X-ray structure shows oxime **8** assumes the  ${}^4C_1$  conformation in crystalline form. However, based on  $^1H$  NMR coupling constants, the  ${}^4C_1$  conformation is not favored in solution. The  ${}^4C_1$  conformation is favored in the crystalline form because of the added stability of hydrogen bonding between the hydrogen of the hydroxyimine in one molecule and the ethereal oxygen and acyl oxygen of the methyl ester of another molecule. Therefore, the hydrogen bonding interactions in the  ${}^1C_4$  conformation are either not present or are not as strong.

Protection of the hydroxyimine will not only protect the oxime from unwanted reactions, but also activate the oxime to facilitate the subsequent reduction reaction. The hydroxyimine is protected by using either a benzoyl group or a 4-nitrobenzoyl group (Scheme 5).



**Scheme 5:** Preparation of precursors to the key reduction step.

Benzoylation of oxime **8** using benzoyl chloride in pyridine gave benzoyloxime **9** in 46% yield as a white solid, which was recrystallized using isopropanol to give colorless crystals. TLC showed the appearance of a UV-active spot with a slightly higher  $R_f$  value than the starting material. Analysis of the  $^1\text{H}$  NMR spectrum confirms the addition of a benzoyl group by the appearance of signals at 7.50, 7.64, and 8.04 ppm that integrate to a total of five protons. Furthermore, the signal at 8.51 ppm corresponding to the hydroxyimine proton is no longer present. Coupling constants for H-3, H-4, and H-5 are between 3.66 and 4.76 Hz, which suggests the preference of the  $^1\text{C}_4$  conformation in solution ( $\text{CDCl}_3$ ).  $^{13}\text{C}$  NMR also confirms the addition of a benzoyl group with the appearance of four signals between 127.7 and 133.7 ppm, corresponding to the aryl carbons, and the addition of a signal at 162.5 ppm, corresponding to carbonyl of the benzoyl group. ESI mass spectrometry indicates an  $M^+$  of 416.2, which agrees with the

calculated mass of 393.11 with the addition of sodium. The X-ray structure of benzoyloxime **9** has also been reported<sup>41</sup> and confirms the  $^1C_4$  conformation in the solid-state, which agrees with the conformation in solution as determined by  $^1H$  NMR (Figure 18).

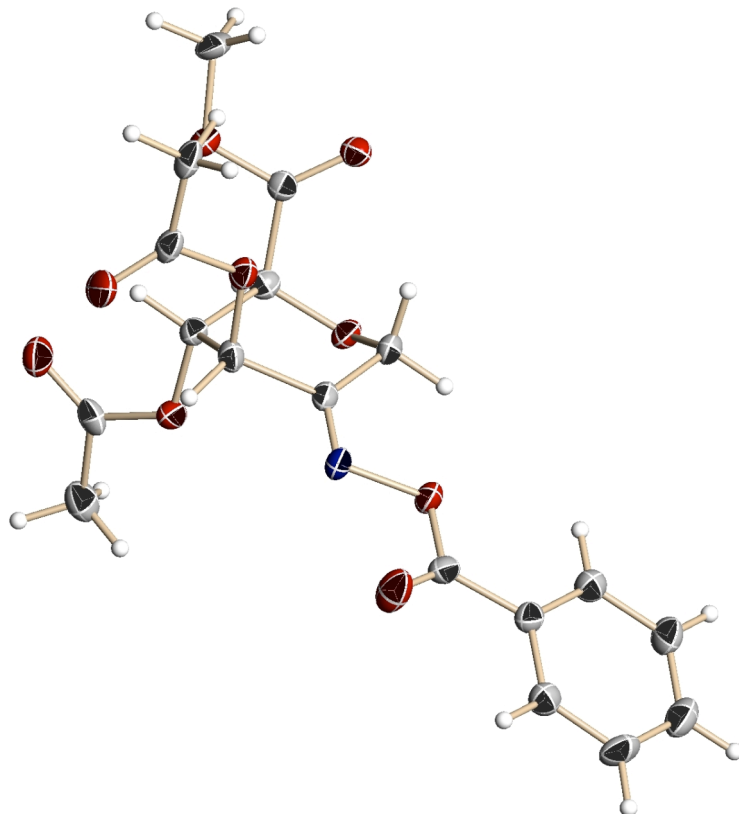


**Figure 18:** X-Ray structure of methyl 3,4-di-O-acetyl-2-deoxy-2-(benzoyloxyimino)-D-arabino-hex-2-enopyranuronate (**9**).<sup>41</sup>

The reaction of oxime **8** with 4-nitrobenzoyl chloride in pyridine afforded *p*-nitrobenzoyloxime **10** in quantitative yield as a yellow solid, which was crystallized using isopropanol to give pale yellow crystals. TLC showed consumption of starting material and the appearance of a UV-active spot with a slightly higher  $R_f$  value.  $^1H$  NMR indicated the presence of the 4-nitrobenzoyl group with the appearance of signals at 8.23

and 8.36 ppm, which integrate to a total of four protons. The signal corresponding to the proton on the hydroxyimine at 8.51 ppm is no longer present. Coupling constants for H-3, H-4, and H-5 are between 3.66 and 4.76 Hz, which suggest a preference for the  ${}^1C_4$  conformation in solution ( $CDCl_3$ ). Analysis of the  ${}^{13}C$  NMR spectrum indicates the appearance of four signals corresponding to the 4-nitrobenzoyl group. Signals at 123.7 (2 x C), 130.6 (2 x C), 133.2, and 158.4 ppm correspond to the carbon atoms in the aromatic ring and a signal at 160.7 ppm corresponding to the carbonyl of the 4-nitrobenzoyl group. ESI mass spectrometry shows a mass of 461.2 for compound **10**, which is consistent with the calculated mass of 438.09 plus a sodium atom. Single crystal X-ray data was obtained for compound **10** (Figure 19).

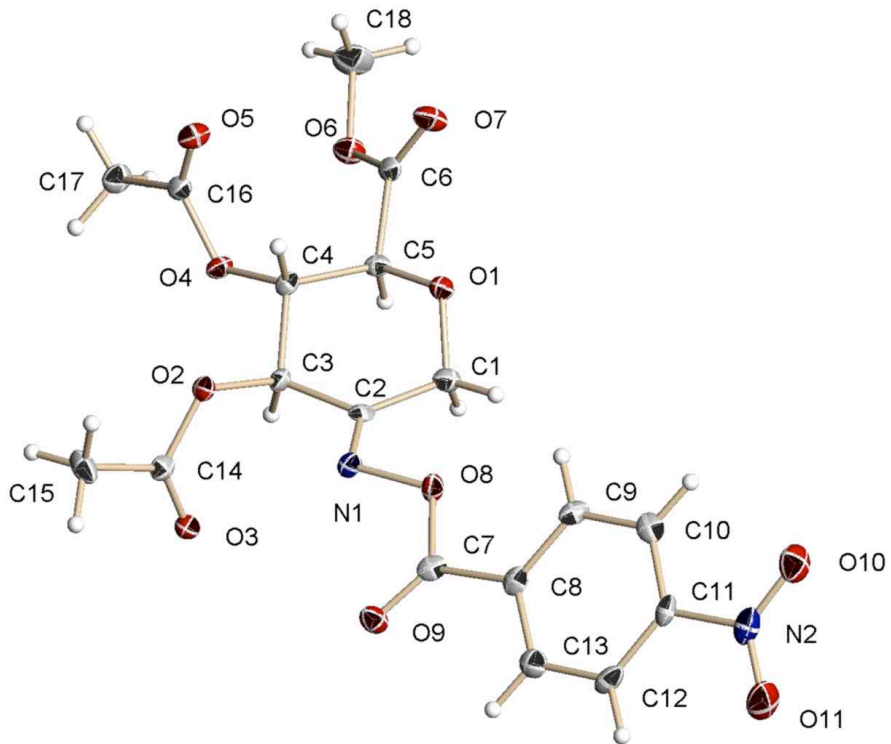
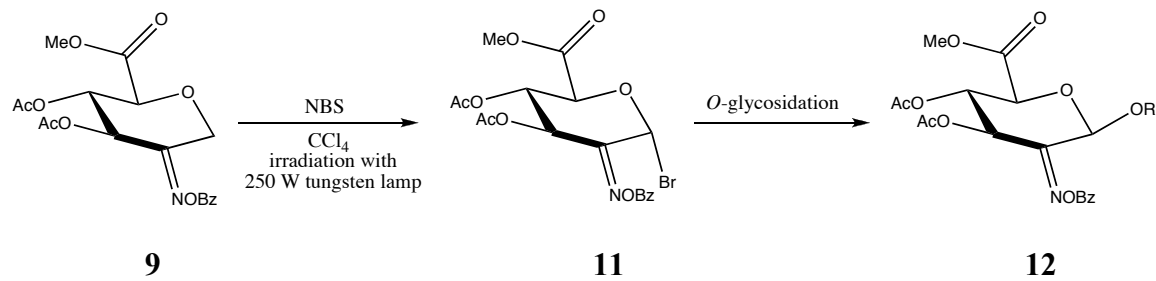


**Figure 19:** X-Ray structure of methyl 3,4-di-*O*-acetyl-2-deoxy-2-(4-nitrobenzoyloxyimino)-D-*arabino*-hex-2-enopyranuronate (**10**).

The X-ray structure of 4-nitrobenzoyloxime **10** confirms the  $^4C_1$  conformation in the solid state, which is in contrast to the observed  $^1C_4$  conformation in solution based on coupling constants determined by  $^1H$  NMR.

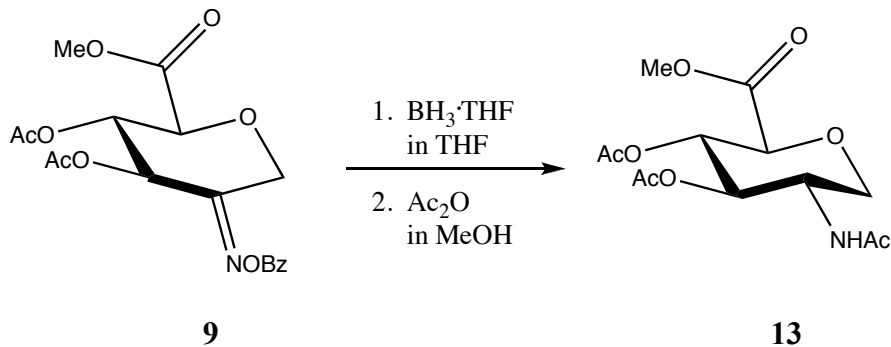
The reduction of compounds **9** and **10** with 1.0 M solution of  $BH_3\cdot THF$  complex in THF diverges from Lichtenthaler's synthetic pathway, in which, prior to the reduction reaction, Lichtenthaler used a photobromination reaction to form bromide **11** followed by *O*-glycosylation to provide *O*-glycoside **12** (Scheme 6).



**Scheme 6:** Lichtenthaler's synthesis of precursor to the key reduction step.

The subsequent reduction of compound **12** with borane results in the stereoselective formation of the *manno*-configuration. The stereoselectivity of this reduction is evidence for the preference of the  $^1C_4$  conformation of **12** in solution. In the  $^1C_4$  conformation, the groups at C-1, C-3, and C-5 are all in a pseudo-axial position, which severely hinders the attack of the hydride from the top face of the molecule. Therefore, reduction occurs by the attack of the hydride from underneath the molecule, resulting in the *manno* isomer. Similar results were not seen in the reductions of compounds **9** and **10**.

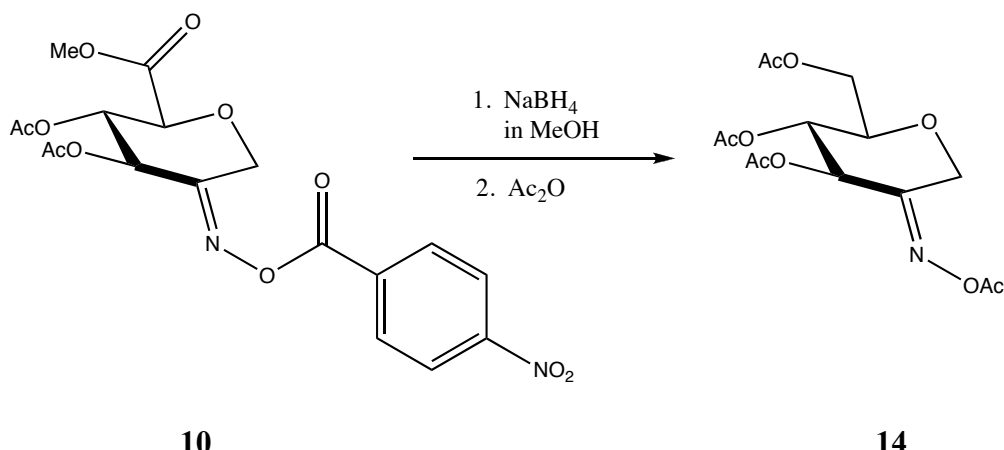
Treatment of benzoyloxime **9** with 1.0 M  $\text{BH}_3\text{-THF}$  complex in THF, followed by acetylation with acetic anhydride in methanol resulted in the formation of **13** in 22% yield (Equation 8).



**Equation 8:** Formation of methyl 3,4-di-*O*-acetyl-2-*N*-acetyl-2-deoxy-D-glucopyranuronate.

The only isolated product is the undesired *gluco* isomer. Since the reduction does not proceed in a reversible fashion, thermodynamics does not play a significant role in the stereochemical outcome. Therefore, the borane must coordinate with the pseudo-axial substituents on the top-face of the molecule, thus delivering the hydride from above.

The reduction of 4-nitrobenzoyloxime **10** was modified from the conditions above. The reduction was carried out with sodium borohydride in the polar solvent methanol (Equation 9) in an effort to shift the preference of the  ${}^1\text{C}_4$  conformation to the  ${}^4\text{C}_1$  conformation, which should make C-2 more accessible for a hydride attack from the top and bottom face of the molecule.

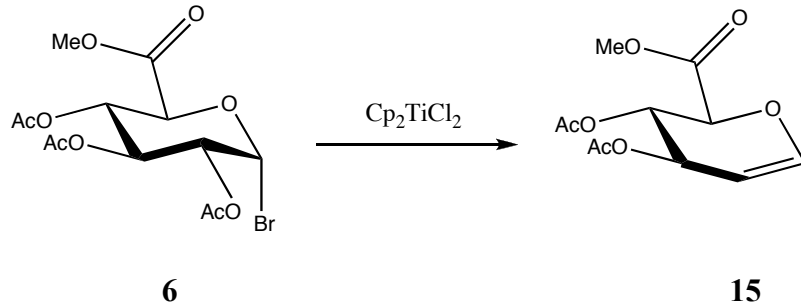


**Equation 9:** Reduction of 4-nitrobenzoyloxime **10** with sodium borohydride in methanol

However, this reduction method resulted in the reduction of the 4-nitrobenzoyl group on the oxime and the methyl ester at C-6, followed by the acetylation of the newly formed hydroxyl groups to give **14**. Analysis of  $^1\text{H}$  NMR shows the presence of four acetyl groups from 2.09 to 2.20 ppm. Also, signals for the aromatic ring and methyl ester are no longer present. ESI mass spectrometry shows an  $\text{M}^+$  of 368.1, which corresponds to the calculated mass of 345.11 with the addition of sodium.

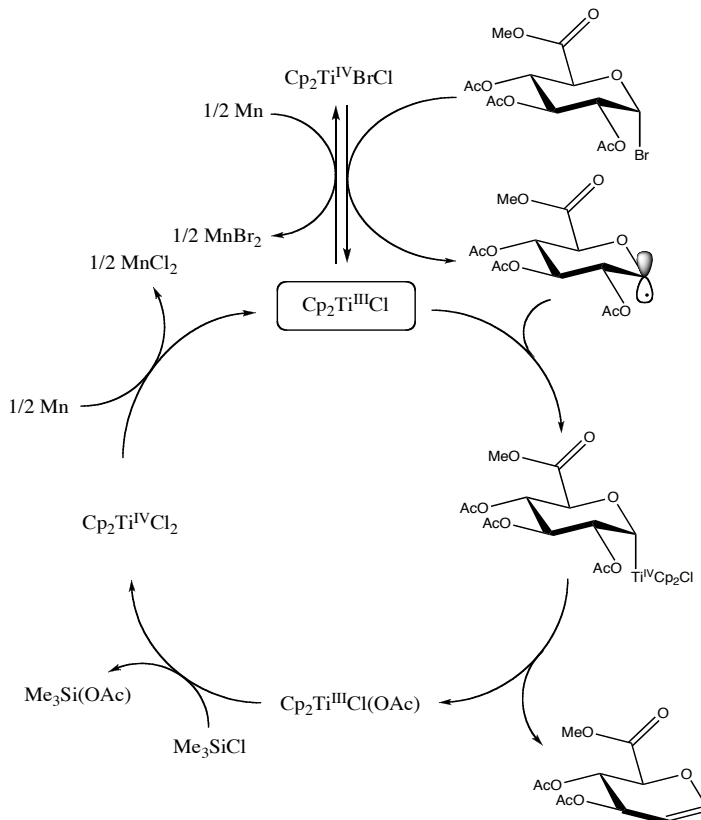
## 2. Synthesis of precursors suitable for azidonitration via azide radical.

The treatment of glycals with ceric ammonium nitrate and sodium azide results in the formation of a 1-nitro-2-azido-pyranose.<sup>42</sup> Azidonitration of glycals is an efficient method for introducing nitrogen at C-2 in the form of an azide. The synthesis of glycals can be achieved by treating a glycosyl halide with bis(cyclopentadienyl)titanium chloride (Equation 10).



**Equation 10:** Synthesis of methyl 3,4-di-*O*-acetyl-1,5-anhydro-2-deoxy-D-*arabino*-hex-1-enopyranuronate (**15**).

Recently developed methods involve the use of a catalytic amount of  $\text{Cp}_2\text{TiCl}_2$ , which is in contrast to the 2 equivalents previously employed.<sup>43</sup> The catalytic cycle is achieved by using a reductant such as manganese and a trialkylsilyl chloride such as trimethylsilyl chloride (Scheme 7).



**Scheme 7:** Proposed mechanism for the catalytic cycle with  $\text{Cp}_2\text{TiCl}_2$ .<sup>43</sup>

The reaction of bromide **6** with  $\text{Cp}_2\text{TiCl}_2$ , manganese, and TMSCl in dry THF afforded glycal **15** in 88% yield (Scheme 7). TLC showed consumption of starting material and the appearance of a spot with a slightly lower  $R_f$  value.  $^1\text{H}$  NMR indicated a slight downfield shift of the H-1 and H-2 signals from 6.67 to 6.69 ppm and 4.89 to 5.02 ppm, respectively. There are only two signals corresponding to the acetyl groups, which is consistent with the loss of the C-2 substituent.  $^{13}\text{C}$  NMR also showed the loss of an acetyl group with the absence of two signals around 20-21 ppm and 169-170 ppm. Due to the introduction of a double bond, signals for C-1 and C-2 shifted downfield from 85.3 to 146.6 ppm and 70.1 to 97.1, respectively. ESI mass spectrometry shows an  $\text{M}^+$  of 281.1 which corresponds to the calculated mass of 258.1 with the addition of sodium. Single crystal X-ray data was obtained for compound **15** (Figure 20).

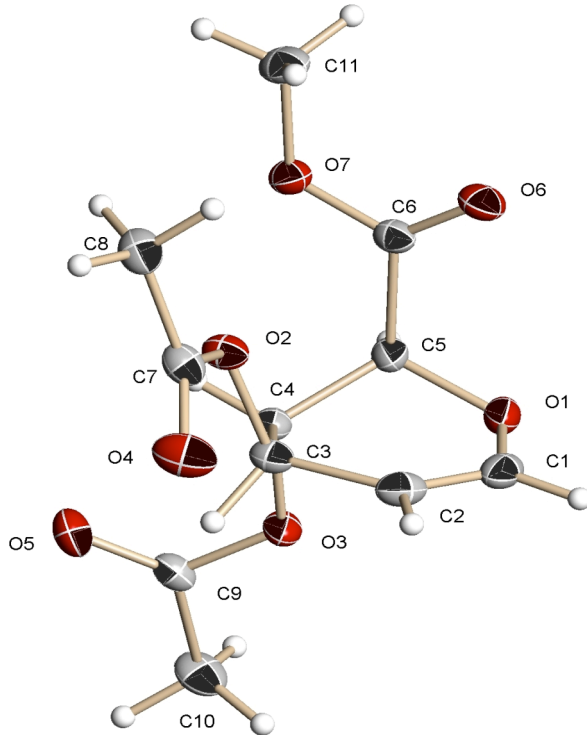
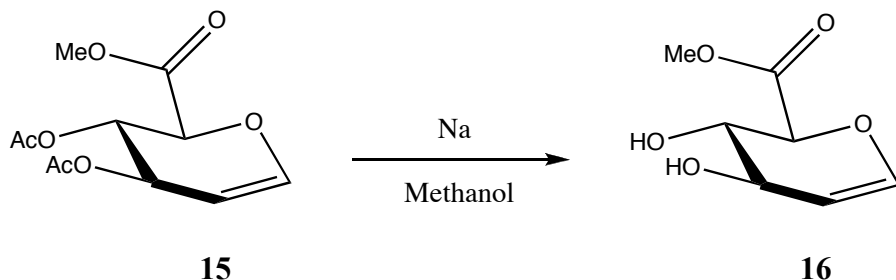


**Figure 20:** X-Ray structure of methyl 3,4-di-*O*-acetyl-1,5-anhydro-2-deoxy-D-*arabinohex-1-enopyranuronate* (**15**).

However, stereoselectivity is an issue with this azidation technique since there is the possibility of forming different isomers. Previous attempts at the azidonitration of compound **15** have proceeded with poor yields (6%) of the desired *manno*-isomer.<sup>44</sup> The stereoselectivity of the azidonitration reaction depends heavily upon the steric hindrance about C-2, and the position and size of substituents at C-3 and C-4 can dramatically influence the stereochemical outcome of this reaction.<sup>43</sup> Therefore, methods were studied to selectively block the addition of the azide radical from underneath the ring (*gluco* isomer).

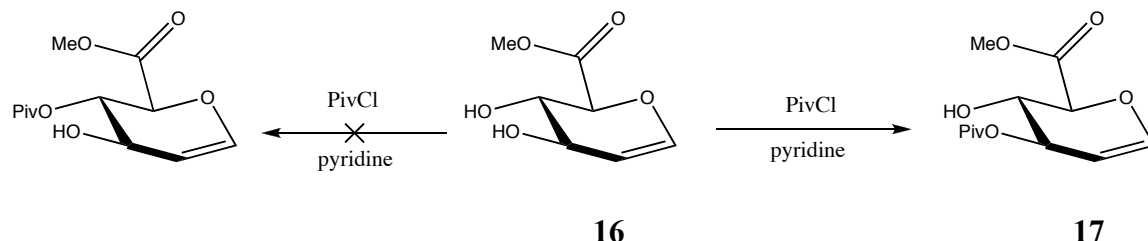


**Equation 11:** Deacetylation of compound **15**.

The deacetylation of compound **15** under Zemplén conditions<sup>45</sup> afforded **16** in 88% yield as a pale orange syrup (Equation 11). TLC showed consumption of starting material and the appearance of a spot with a lower  $R_f$  value.  $^1\text{H}$  NMR confirmed the loss of two acetyl groups at 2.01 and 2.13 ppm. Signals for the hydroxyl groups appeared at 4.97 and 5.41 ppm, which later disappeared upon addition of  $\text{D}_2\text{O}$ . Analysis of the  $^{13}\text{C}$  NMR spectrum confirmed the loss of four signals corresponding to the acetyl groups at 20.9, 20.9, 169.0, and 169.2 ppm for a total seven signals in the spectrum. ESI mass

spectrometry shows an  $M^+$  of 337.7, which corresponds to twice the calculated mass of 174.05 with the loss of a molecule of  $H_2O$ .

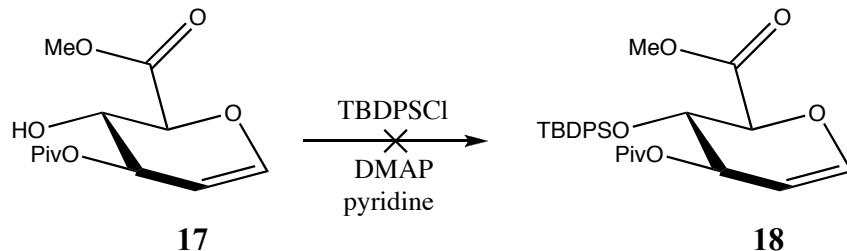
The selective protection of C-4 was attempted with the treatment of **16** with trimethylacetyl chloride in pyridine at -10 °C (acetone: ice bath). However, the reaction resulted in the protection of C-3 instead (Scheme 8).



**Scheme 8:** Selective protection of C-3 hydroxyl.

Compound **17** was prepared by the treatment of **16** with trimethylacetyl chloride in pyridine in 78% yield as a yellow syrup. TLC showed consumption of starting material and the appearance of a spot with a higher  $R_f$  value.  $^1H$  NMR showed the presence of the pivaloyl group with the appearance of a singlet at 1.16 ppm, which integrates to nine hydrogens. Further, the signal for the proton attached to C-3 shifted downfield from 3.75 to 5.04 ppm, indicating the C-3 hydroxyl was protected and not the C-4 hydroxyl.  $^{13}C$  NMR shows the appearance of three signals at 26.9 (3 x C), 38.6, and 178.0 ppm, corresponding to the pivaloyl group. ESI mass spectrometry shows an  $M^+$  of 325.9 which corresponds to the calculated mass of 258.11 with the addition of two molecules of methanol.

Indirectly, the C-4 hydroxyl is now isolated and can be protected with a bulky protecting group. *Tert*-butyldiphenylsilyl chloride was used for the protection because it is not only bulky, but can also withstand Zemplén conditions in the subsequent step.



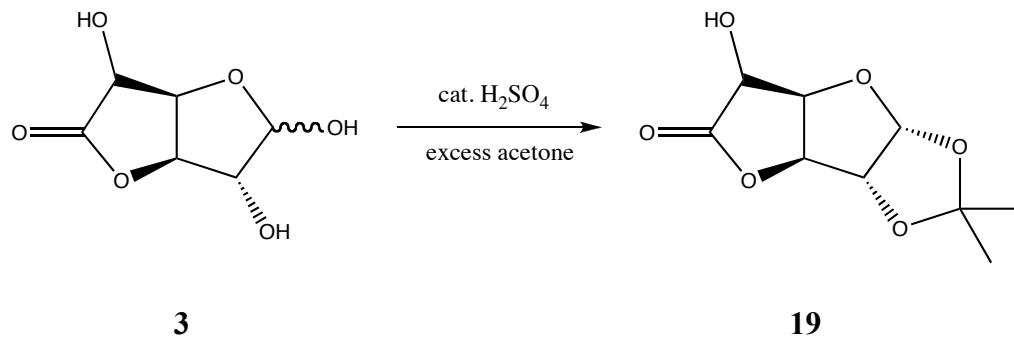
**Equation 12:** Attempted protection of C-4 with silyl group.

However, the treatment of **17** with *tert*-butyldiphenylsilyl chloride and DMAP in pyridine did not result in the formation of **18**. The massive size of the *tert*-butyldiphenylsilyl group hinders its ability to behave as a protecting group in a sterically hindered compound such as **17**. The use of a slightly smaller silyl protecting group should be employed not only to facilitate the protection of the C-4 hydroxyl, but also to withstand the subsequent deprotection of the C-3 hydroxyl under Zemplén conditions.

### 3. Synthesis of suitable precursors for nucleophilic displacement on C-2.

Nucleophilic displacement *via S<sub>N</sub>2* is an indispensable tool that can be used to introduce an azide while simultaneously inverting the stereochemistry. However, factors such as the nature of the leaving group and steric hinderance must be taken into account in order to avoid unwanted reactions, including eliminations. The following describes, in detail, progress toward the preparation of suitable precursors for nucleophilic displacement on C-2 by an azide. Using D-glucurono-6,3-lactone (**3**) as a starting

material, the hydroxyl group at C-5 must be protected in order to subsequently isolate the C-2 hydroxyl group. This is accomplished by the protection of the hydroxyl groups on C-1 and C-2 (Equation 13) with an isopropylidene group.



**Equation 13:** Isolation of C-5 hydroxyl with an isopropylidene group.

The reaction of **3** with a catalytic amount of concentrated sulfuric acid in an excess of acetone afforded **19** in 83% yield as a clear syrup, which is crystallized in hot isopropanol to give colorless crystals. TLC showed the appearance of a spot with a higher  $R_f$  value than the starting material. Analysis of the  $^1\text{H}$  NMR spectrum shows the presence of the isopropylidene group with signals at 1.35 and 1.53 ppm, which integrate for a total of six hydrogens.  $^{13}\text{C}$  NMR indicates the appearance of three signals at 26.5, 26.8, and 113.3 ppm, which correspond to the isopropylidene group. A total of nine signals are observed in the  $^{13}\text{C}$  spectrum, which is consistent with the predicted spectrum of **19**. Also, the signal at 174.0 ppm indicates that the lactone ring is still intact. ESI mass spectrometry shows an  $\text{M}^+$  of 239.1 corresponding to the calculated mass of 216.06 with the addition of a sodium atom. Single crystal X-ray data was obtained, confirming the formation of **19** (Figure 21).

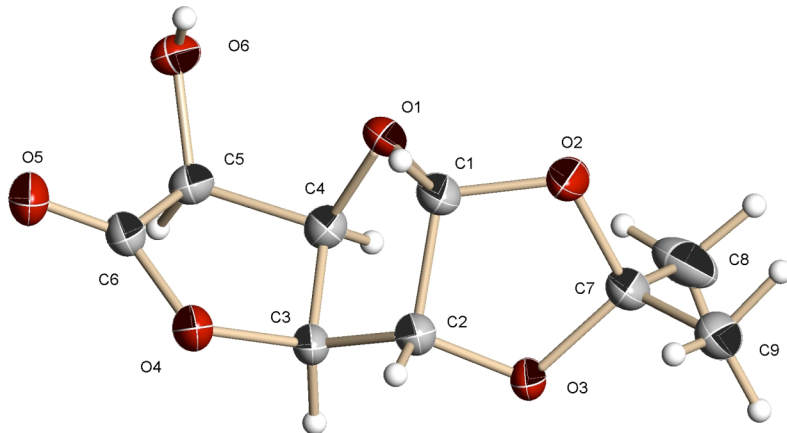
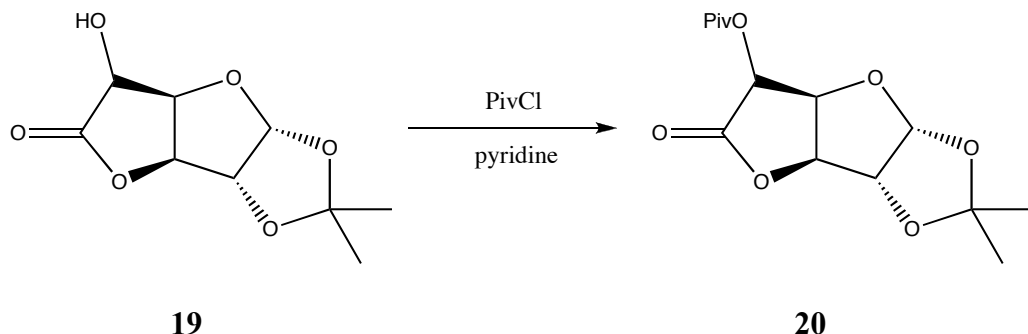


**Figure 21:** X-Ray structure of 1,2-*O*-isopropylidene- $\alpha$ -D-glucofuranosiduron-6,3-lactone (**19**).

The hydroxyl at C-5 is available for protection with a variety of groups. Two basic types of groups were used for protection, an ester and a silyl protecting group. The treatment of **19** with trimethylacetyl chloride in pyridine afforded **20** as a clear syrup in quantitative yield (Equation 14).

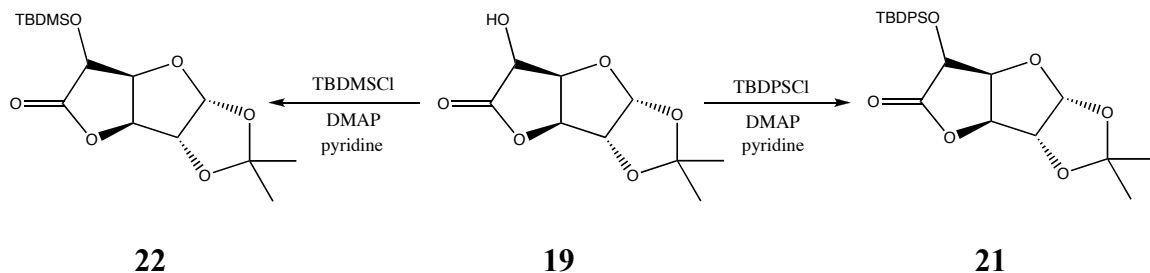


**Equation 14:** Pivaloylation of compound **19**.

TLC showed consumption of starting material and the appearance of a spot with a higher  $R_f$  value.  $^1\text{H}$  NMR shows the appearance of a singlet at 1.28 ppm that integrates for a

total of 9 hydrogens, which corresponds to the methyl protons of the pivaloyl group. Also, the signal for H-5 shifted downfield from 4.83 to 5.50 ppm, and the broad singlet at 3.77 ppm corresponding to the hydroxyl proton is no longer present. Analysis of the  $^{13}\text{C}$  NMR spectrum indicates the addition of three signals at 26.9 (triple intensity), 38.8, and 169.9 ppm corresponding to the pivaloyl group. ESI mass spectrometry shows an  $\text{M}^+$  of 321.9, which corresponds to the calculated mass of 300.12 with the addition of a sodium atom.

Two silyl protecting groups were employed in the protection of the hydroxyl at C-5; *tert*-butyldiphenylsilyl and *tert*-butyldimethylsilyl (Scheme 9).



**Scheme 9:** Protection of **19** using silyl protecting groups.

The reaction of **19** with *tert*-butyldiphenylsilyl chloride and DMAP in pyridine afforded **20** as colorless crystals in 81% yield. TLC showed the appearance of a UV-active spot with a higher  $R_f$  value than the starting material. Analysis of the  $^1\text{H}$  NMR spectrum indicated the addition of the *tert*-butyldiphenylsilyl group with the appearance of signals between 7.42 and 7.81 ppm, corresponding to the aryl protons of the protective group. The appearance of a singlet at 1.11 ppm, which integrates to nine hydrogens, corresponds

to the *tert*-butyl portion of the *tert*-butyldiphenylsilyl group. The broad singlet at 3.77 ppm, corresponding to the hydroxyl proton at C-5, is no longer present. ESI mass spectrometry shows an  $M^+$  of 475.8, which corresponds to the calculated mass of 454.18 with the addition of a sodium atom. Single crystal X-ray data was obtained, confirming the formation of compound **21** (Figure 22).

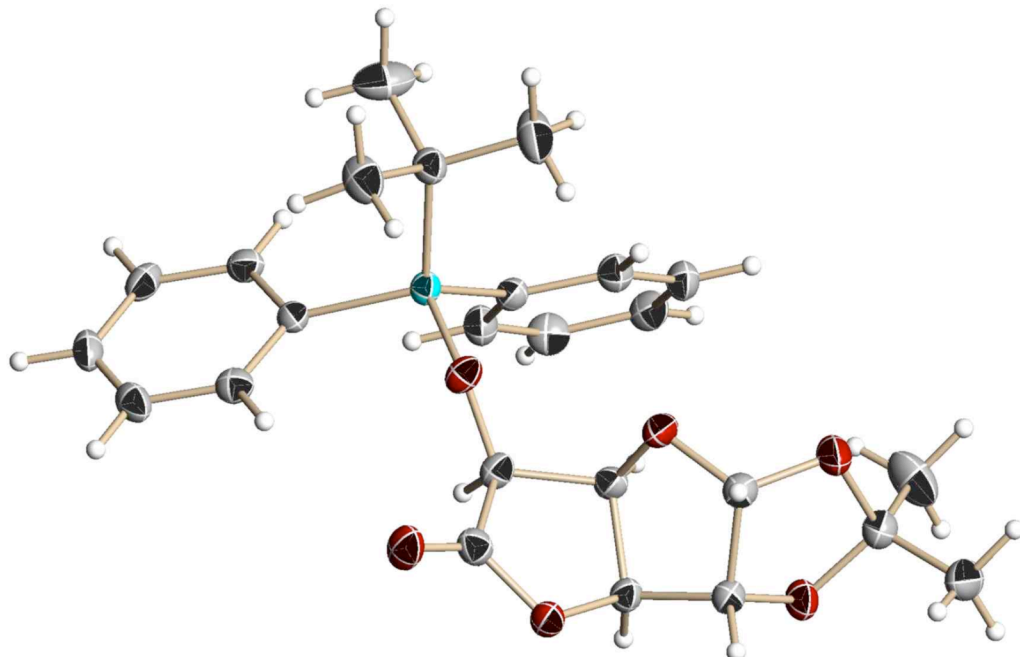


**Figure 22:** X-Ray structure of 1,2-O-isopropylidene-6-O-*tert*-butyldiphenylsilyl- $\alpha$ -D-glucurono-6,3-lactone (**21**).

The treatment of **19** with *tert*-butyldimethylsilyl chloride and DMAP in pyridine gave **22** as colorless crystals in 96% yield. TLC showed the consumption of starting material and the appearance of a spot with a higher  $R_f$  value.  $^1\text{H}$  NMR showed the appearance of signals at 0.18, 0.22, and 0.95 ppm corresponding to the two methyl and *tert*-butyl groups. Also, the broad singlet at 3.77 ppm is no longer present. Analysis of the  $^{13}\text{C}$  NMR spectrum indicated the addition of the *tert*-butyldimethylsilyl group with the

appearance of four signals at -5.2, -4.7, 18.4, and 25.6 (triple intensity). ESI mass spectrometry shows an  $M^+$  of 351.8, which corresponds to the calculated mass of 330.15 with the addition of a sodium atom. Single crystal X-ray data was obtained, confirming the formation of compound **22** (Figure 23).

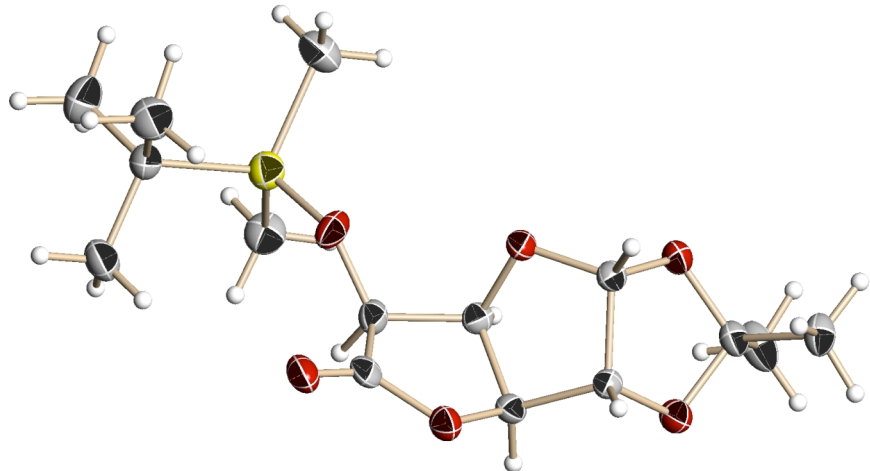
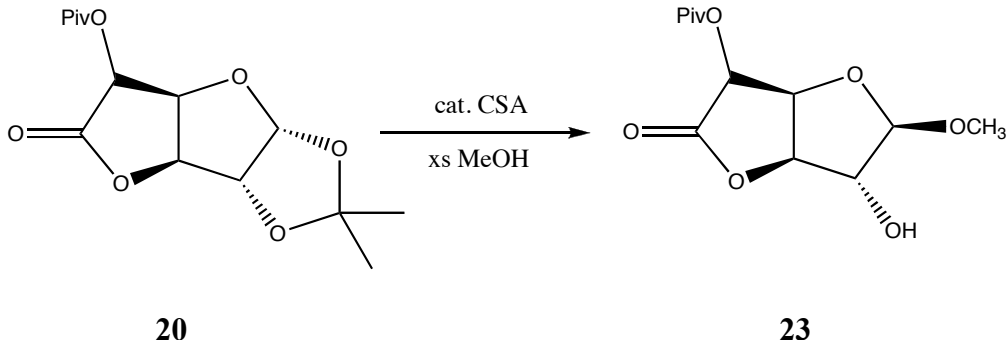


**Figure 23:** X-Ray structure of 1,2-*O*-isopropylidene-6-*O*-*tert*-butyldimethylsilyl- $\alpha$ -D-glucurono-6,3-lactone (**22**).

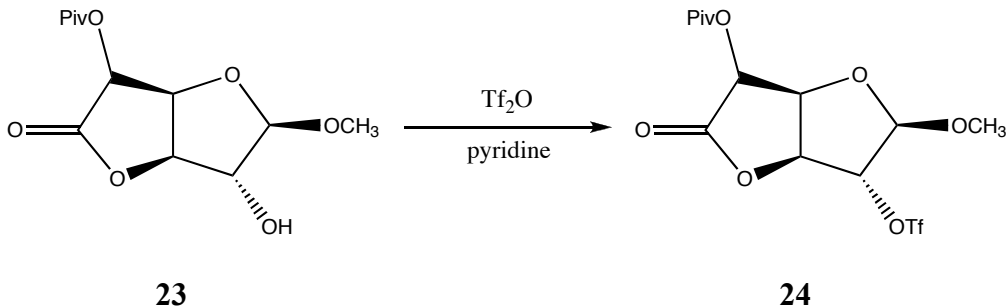
The deprotection of the isopropylidene group is an important step that involves glycosylation at C-1 and the isolation of the hydroxyl at C-2. However, the deprotection of compounds **21** and **22** resulted in the decomposition of starting material. Therefore, the deprotection proceeded with compound **20** (Equation 15).



**Equation 15:** Removal of isopropylidene group from **20**.

The treatment of **20** with a catalytic amount of camphor sulfonic acid in an excess of methanol afforded **23** as a clear syrup in 74% yield. TLC showed consumption of starting material and the appearance of a spot with a lower  $R_f$  value. Analysis of the  $^1\text{H}$  NMR spectrum shows the disappearance of signals at 1.35 and 1.52 ppm, corresponding to the loss of the isopropylidene group. A signal at 3.37 ppm that integrates to three hydrogens, indicates the methoxy group at C-1 and a broad singlet at 4.38 ppm corresponds to the hydroxyl at C-2, which disappears with the addition of  $\text{D}_2\text{O}$ .  $^{13}\text{C}$  NMR shows the absence of signals at 26.4, 26.8, and 113.0 ppm, corresponding to the loss of the isopropylidene group and the appearance of a signal at 55.3 ppm, corresponding to the methoxy group at C-1. ESI mass spectrometry shows an  $\text{M}^+$  of 295.8, which corresponds to the calculated mass of 274.11 with the addition of a sodium atom and the absence of a hydrogen.

The hydroxyl attached to C-2 is now available for modification. The hydroxyl was activated with a triflate group, which is an excellent leaving group (Equation 16).



**Equation 16:** Activation of hydroxyl at C-2 with a triflate group.

The treatment of **23** with triflic anhydride in pyridine and methylene chloride at -78 °C afforded **24** in 82% yield as orange crystals. TLC showed the consumption of starting material and the appearance of a spot with a higher  $R_f$  value.  $^1\text{H}$  NMR shows the downfield shift of H-2 from 4.38 to 5.30 ppm, indicating the presence of the triflate group.  $^{13}\text{C}$  NMR indicates the presence of the triflate group with the appearance of a signal at 119.8 ppm. Further, the signal for C-2 shifted downfield from 76.8 to 86.6 ppm, corresponding to the presence of the triflate group. ESI mass spectrometry shows an M<sup>+</sup> of 379.6, which corresponds to the calculated mass of 406.05 with the absence of a methoxy group. Single crystal x-ray data was obtained, confirming the formation of compound **24** (Figure 24).

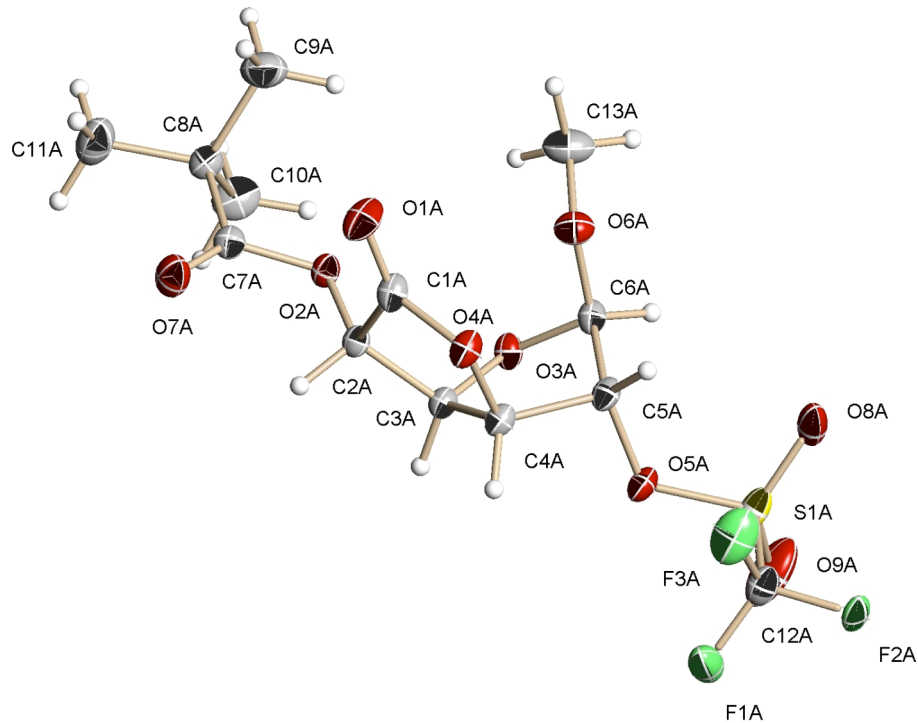
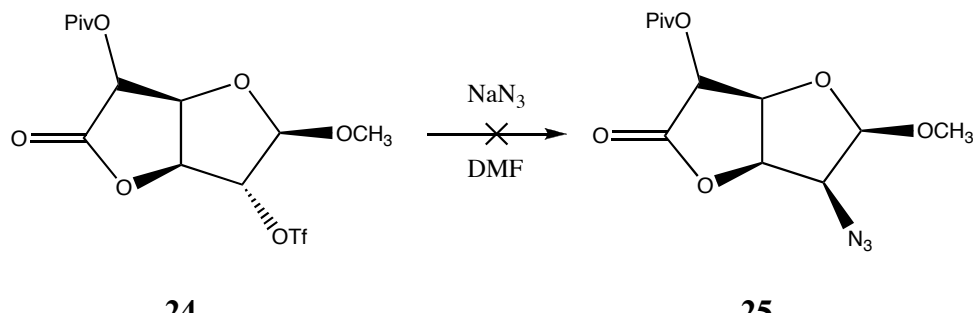


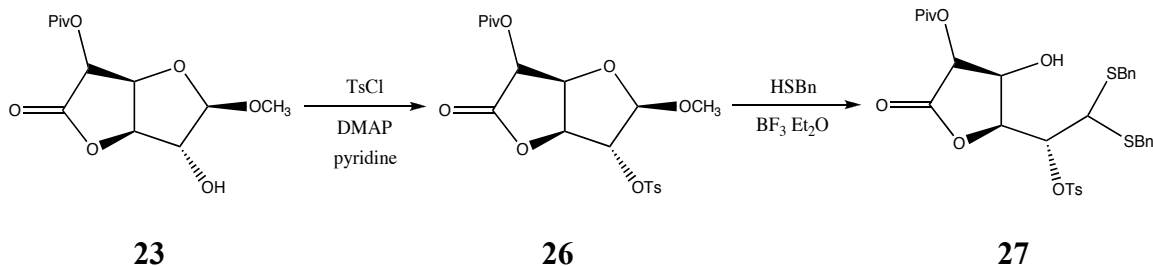
**Figure 24:** X-Ray crystal structure of methyl 6-*O*-pivaloyl-2-*O*-trifluoromethylsulfonyl- $\beta$ -D-glucurono-6,3-lactone (**24**).

Compound **24** was synthesized in an effort to perform an S<sub>N</sub>2 reaction on C-2. However, the X-ray structure of **24** indicates C-2 is extremely hindered and an S<sub>N</sub>2 reaction is not likely, which is supported by experimental evidence. The reaction of **24** with sodium azide in DMF did not result in the formation of an azide (Equation 17).



**Equation 17:** Attempted S<sub>N</sub>2 reaction on compound **24**.

Since an S<sub>N</sub>2 reaction did not occur on the furanose ring, alternative methods were studied to utilize the S<sub>N</sub>2 reaction by first opening the furanose ring, resulting in less hindrance at C-2 (Scheme 10).



**Scheme 10:** Synthetic strategy to perform an S<sub>N</sub>2 reaction on C-2.

The treatment of **23** with tosyl chloride and DMAP in pyridine afforded **26** in 87% yield as a clear syrup. TLC showed consumption of starting material and the appearance of a UV-active spot with a higher R<sub>f</sub> value. Analysis of the <sup>1</sup>H NMR spectrum confirms the addition of the tosyl group with signals at 2.46, 7.41, and 7.82 ppm. <sup>1</sup>H NMR also shows the absence of the broad singlet at 4.38 ppm, corresponding to the hydroxyl group attached to C-2. <sup>13</sup>C NMR shows the appearance of signals at 21.6, 127.8 (2 x C), 130.1 (2 x C), 131.7, and 145.9 ppm corresponding to the tosyl group. ESI mass spectrometry shows an M<sup>+</sup> 397.7, which corresponds to the calculated mass of 428.11 with the loss of the methoxy group.

The subsequent ring-opening reaction involved the treatment of **26** with benzyl mercaptan and boron trifluoride etherate in THF. However, the reaction did not result in the formation of **27**. Alternative methods involving the use of titanium(IV) chloride as a

lewis acid have been successful with compounds similar to **26**,<sup>46</sup> which suggests the prospect of an S<sub>N</sub>2 reaction using an azide still remains.

There exists the potential of several of these compounds to be precursors to the target compound D-ManNAcA. The ability to transform an abundant and inexpensive compound into a biologically useful compound is the theme of this research project. Due to the increasing knowledge and understanding of the role of carbohydrates in Nature, efforts must continue to be made to synthesize unique carbohydrates from readily available materials.

## Experimental

### General Procedures

Reaction progress was monitored by thin layer chromatography (TLC). Ultraviolet light detection was used for reaction materials containing UV-active functionality. TLC plates were then treated with a solution of 5% sulfuric acid/methanol and burned to detect carbohydrate reaction materials. Purification was accomplished by either recrystallization or flash column chromatography, the latter performed with 32-63  $\mu\text{m}$ , 60- $\text{\AA}$  silica gel. A Bruker Esquire-HP 1100 mass spectrometer was used for low-resolution MS. A Varian Gemini 2000 NMR system was used for  $^1\text{H}$  and  $^{13}\text{C}$  spectroscopy at 400 MHz and 100 MHz respectively. Proton and carbon chemical shifts ( $\delta$ ) are recorded in parts per million (ppm). Splitting patterns of multiplets are labeled in the following manner: s (singlet), d (doublet), dd (doublet of doublets), ddd (doublet of doublet of doublets), t (triplet), q (quartet), m (multiplet) with coupling constants measured in Hertz (Hz). Optical rotation data was obtained using a Perkin Elmer 343 polarimeter at a wavelength of 589 nm. X-Ray diffraction was also used to determine the solid-state crystal structure of some of the compounds.

### Preparation of methyl $\alpha,\beta$ -D-glucopyranuronate from $\alpha,\beta$ -D-glucurono-6,3-lactone.

In a 3000 mL round-bottom flask equipped with a magnetic stir bar, a catalytic amount of NaOH (0.1 g, 2.5 mmol) was dissolved in methanol (2000 mL) at room temperature. D-Glucurono-6,3-lactone (60.0 g, 340.68 mmol) was added in 5.0 g

portions to the reaction mixture and the solution was allowed to stir at room temperature for 4 hours to convert the furanose into the pyranose.

**Preparation of methyl 1,2,3,4-tetra-O-acetyl- $\alpha,\beta$ -D-glucopyranuronate (**5 $\alpha/\beta$** ) from methyl-D-glucopyranuronate.**

After concentration of the mixture from the previous experiment under reduced pressure, the syrup **4 $\alpha/\beta$**  was dissolved in dry pyridine (150 mL) and cooled to 0 °C using an ice-water bath. Acetic anhydride (150 mL) was added slowly to the reaction mixture, and the reaction was stirred at room temperature for 6 hours until TLC (1:1 hexanes: ethyl acetate, product  $R_f$  = 0.60) showed consumption of starting material. The reaction mixture was then poured over ice/water (100 mL) and extracted with dichloromethane (100 mL). The organics were washed with 5% H<sub>2</sub>SO<sub>4</sub> (3 x 50 mL) and water (3 x 50 mL). The organics were then dried over MgSO<sub>4</sub>, filtered, and evaporated under reduced pressure to give **5** as a mixture of anomers. The mixture was recrystallized using hot ethanol to give **5 $\beta$**  (83.42 g, 221.7 mmol, 65%) as clear crystals. The mother liquor was concentrated to give **5 $\alpha$**  (42.31 g, 112.4 mmol, 33%) as a brown syrup.

**$\beta$ -anomer:**

<sup>1</sup>H NMR (CDCl<sub>3</sub>):  $\delta$  2.04, 2.051, 2.053, 2.13 (4s, 12H total, 4 x COCH<sub>3</sub>), 3.75 (s, 3H, OCH<sub>3</sub>), 4.22 (d, 1H, H-5,  $J$  = 9.52 Hz), 5.15 (dd, 1H, H-2,  $J$  = 7.69, 9.15 Hz), 5.24 (t, 1H, H-4,  $J$  = 9.52 Hz), 5.34 (t, 1H, H-3,  $J$  = 9.15 Hz), 5.79 (d, 1H, H-1,  $J$  = 7.69 Hz).

<sup>13</sup>C NMR (CDCl<sub>3</sub>): δ 20.4, 20.51, 20.54, 20.7, 52.9, 68.7, 69.9, 71.6, 72.7, 91.1, 166.5, 168.5, 168.9, 169.2, 169.6.

*m/z* calculated: 376.10

*m/z* found (ESI): 397.8 (+Na)

M.P. = 176-178 °C

R<sub>f</sub> = 0.60 (1:1 hexanes: ethyl acetate)

[α]<sub>D</sub> = +25.9 (*c* = 1.0, CH<sub>2</sub>Cl<sub>2</sub>)

**α-anomer:**

<sup>1</sup>H NMR (CDCl<sub>3</sub>): δ 2.02, 2.05, 2.06, 2.20 (4s, 12H total, 4 x COCH<sub>3</sub>), 3.76 (s, 3H, OCH<sub>3</sub>), 4.42 (d, 1H, H-5, *J* = 10.25 Hz), 5.12 (dd, 1H, H-2, *J* = 3.66, 10.25 Hz), 5.23 (t, 1H, H-3, *J* = 10.25 Hz), 5.53 (t, 1H, H-4, *J* = 9.89 Hz), 6.40 (d, 1H, H-1, *J* = 3.66 Hz).

<sup>13</sup>C NMR (CDCl<sub>3</sub>): δ 20.4, 20.5, 20.6, 20.8, 53.0, 68.7, 68.8, 69.0, 70.2, 88.6, 167.9, 168.2, 169.1, 169.3, 169.7.

*m/z* calculated: 376.10

*m/z* found (ESI): 397.8 (+Na)

M.P. = N/A (syrup)

R<sub>f</sub> = 0.60 (1:1 hexanes: ethyl acetate)

[α]<sub>D</sub> = + 146.2 (*c* = 1.0, CH<sub>2</sub>Cl<sub>2</sub>)

**Preparation of methyl 2,3,4-tri-*O*-acetyl- $\alpha$ -D-glucopyranosyluronosyl bromide (6) from methyl 1,2,3,4-tetra-*O*-acetyl- $\beta$ -D-glucopyranuronate (5 $\beta$ ).**

In a 100 mL round-bottom flask equipped with a septum, vent, and magnetic stir bar, methyl 1,2,3,4-tetra-*O*-acetyl- $\beta$ -D-glucopyranuronate (5.00 g, 12.59 mmol) was dissolved in 33% HBr in acetic acid (20 mL). The reaction mixture was stirred at room temperature for 4 hours until TLC (1:1 hexanes: ethyl acetate, product  $R_f$  = 0.56) showed complete consumption of the starting material. The mixture was diluted with 30 mL of CH<sub>2</sub>Cl<sub>2</sub> and then cooled to 0 °C. The mixture was then neutralized using 10% *w/v* NaOH until the pH of the mixture approached 7. The neutralization was completed using saturated NaHCO<sub>3</sub>. The organics were separated and washed with ice-water (3 x 30 mL), dried over MgSO<sub>4</sub>, and concentrated under reduced pressure to afford **6** in quantitative yield as a clear syrup, which then crystallized upon cooling in the freezer.

<sup>1</sup>H NMR (CDCl<sub>3</sub>):  $\delta$  2.063, 2.066, 2.11 (3s, 9H total, 3 x COCH<sub>3</sub>), 3.76 (s, 3H, OCH<sub>3</sub>), 4.57 (d, 1H, H-5,  $J$  = 10.25 Hz), 4.89 (dd, 1H, H-2,  $J$  = 4.03, 9.89 Hz), 5.24 (dd, 1H, H-4,  $J$  = 9.52, 10.25 Hz), 5.60 (dd, 1H, H-3,  $J$  = 9.52, 9.89 Hz), 6.67 (d, 1H, H-1,  $J$  = 4.03 Hz).

<sup>13</sup>C NMR (CDCl<sub>3</sub>):  $\delta$  20.4, 20.6 (2 x C), 53.1, 68.3, 69.1, 70.1, 71.8, 85.3, 166.4, 169.2, 169.3, 169.4.

*m/z* calculated: 396.01

*m/z* found (APCI): 397.0 (+H)

M.P. = 0-4 °C

$R_f = 0.56$  (1:1 hexanes: ethyl acetate)

$[\alpha]_D = +115.6$  ( $c = 1.0$ ,  $\text{CH}_2\text{Cl}_2$ )

**Formation of methyl 2,3,4-tri-*O*-acetyl-1,5-anhydro-D-arabino-hex-1-enopyranuronate (7) from methyl 2,3,4-tri-*O*-acetyl- $\alpha$ -D-glucopyranuronosyl bromide (6).**

Methyl 2,3,4-tri-*O*-acetyl- $\alpha$ -D-glucopyranuronosyl bromide (10.39 g, 26.16 mmol) and tetrabutylammonium bromide (8.43 g, 26.16 mmol) were dissolved in DMF (105 mL) in a 250 mL round-bottom flask equipped with a septum and magnetic stir bar, under a  $\text{N}_2$  atmosphere. The reaction mixture was cooled to 0 °C in an ice-water bath and diethyl amine (2.99 mL, 28.78 mmol, 1.1 equiv.) was added dropwise *via* syringe. The mixture was allowed to warm to room temperature over 24 hours, until TLC (1:1 hexanes: ethyl acetate, product  $R_f = 0.38$ ) showed consumption of starting material. The mixture was diluted with 50 mL of  $\text{CH}_2\text{Cl}_2$  and then poured over 50 mL of ice. The organics were extracted and washed with 5% *v/v*  $\text{H}_2\text{SO}_4$  (3 x 30 mL) and ice-water (3 x 30 mL). The organics were then dried over  $\text{MgSO}_4$  and concentrated under reduced pressure. The resulting residue was purified *via* flash column (3:2 hexanes: ethyl acetate) and the major fraction was collected and concentrated to afford glycal 7 (6.38 g, 20.17 mmol, 77%) as pale yellow crystals.

$^1\text{H}$  NMR ( $\text{CDCl}_3$ ):  $\delta$  2.02, 2.12, 2.16 (3s, 9H total, 3 x  $\text{COCH}_3$ ), 3.82 (s, 3H,  $\text{OCH}_3$ ), 4.85 (dd, 1H, H-5,  $J = 1.47, 2.20$  Hz), 5.40 (dd, 1H, H-4,  $J = 1.47, 2.56$  Hz), 5.48 (dd, 1H, H-3,  $J = 2.56$  Hz), 6.84 (s, 1H, H-1).

<sup>13</sup>C NMR (CDCl<sub>3</sub>): δ 20.6, 20.8 (2 x C), 52.5, 63.4, 67.8, 72.2, 127.2, 139.2, 166.4, 169.0, 169.2, 169.3.

*m/z* calculated: 316.26

*m/z* found (APCI): 317.1 (+H)

M.P. = 108-110 °C

R<sub>f</sub> = 0.38 (1:1 hexanes: ethyl acetate)

[α]<sub>D</sub> = -38.1 (*c* = 1.0, CH<sub>2</sub>Cl<sub>2</sub>)

**Formation of methyl 3,4-di-*O*-acetyl-2-deoxy-2-(hydroxyimino)-D-*arabino*-hex-2-enopyranuronate (8) from methyl 2,3,4-tri-*O*-acetyl-1,5-anhydro-D-*arabino*-hex-1-enopyranuronate (7).**

To a 250 mL round-bottom flask equipped with a septum and magnetic stir bar, methyl 2,3,4-tri-*O*-acetyl-1,5-anhydro-D-*arabino*-hex-1-enopyranuronate (4.00 g, 12.64 mmol) and hydroxylamine hydrochloride (4.39 g, 63.2 mmol, 5 equiv.) was dissolved in dry pyridine (80 mL) under a N<sub>2</sub> atmosphere. The solution was stirred at room temperature for 24 hours until TLC (2:1 ethyl acetate: hexanes, product R<sub>f</sub> = 0.31) showed consumption of starting material. The solution was diluted with 100 mL of CH<sub>2</sub>Cl<sub>2</sub> and then washed with 5% v/v H<sub>2</sub>SO<sub>4</sub> (3 x 50 mL), saturated Na<sub>2</sub>SO<sub>4</sub> (3 x 50 mL), and water (3 x 50 mL). The organics were dried over MgSO<sub>4</sub>, filtered, and concentrated under reduced pressure to give a pale yellow solid, which was crystallized using isopropanol to afford oxime **8** (2.92 g, 10.09 mmol, 80%) as white crystals.

<sup>1</sup>H NMR (CDCl<sub>3</sub>): δ 2.08, 2.13 (2s, 6H total, 2 x COCH<sub>3</sub>), 3.82 (s, 3H, OCH<sub>3</sub>), 4.35 (d, 1H, H-5, *J* = 4.39 Hz), 4.70 (d, 1H, H-1<sub>A</sub>, *J* = 15.75 Hz), 4.87 (d, 1H, H-1<sub>B</sub>, *J* = 15.75 Hz), 5.44 (dd, 1H, H-4, *J* = 4.39, 4.76 Hz), 5.48 (d, 1H, H-3, *J* = 4.76 Hz), 8.51 (s, 1H, NOH).

<sup>13</sup>C NMR (CDCl<sub>3</sub>): δ 20.6, 20.7, 52.5, 58.9, 68.0, 69.6, 74.0, 149.2, 168.2, 168.7, 169.2.

*m/z* calculated: 289.1

*m/z* found (ESI): 312.1 (+Na)

M.P. = 144-146 °C

R<sub>f</sub> = 0.31 (1:1 hexanes: ethyl acetate)

[α]<sub>D</sub> = +19.3 (*c* = 1.0, CH<sub>2</sub>Cl<sub>2</sub>)

**Formation of methyl 3,4-di-*O*-acetyl-2-deoxy-2-(benzoyloxyimino)-D-*arabino*-hex-2-enopyranuronate (9) from methyl 3,4-di-*O*-acetyl-2-deoxy-2-(hydroxyimino)-D-*arabino*-hex-2-enopyranuronate (8).**

To a 100 mL round-bottom flask equipped with a septum and magnetic stir bar, methyl 3,4-di-*O*-acetyl-2-deoxy-2-(hydroxyimino)-D-*arabino*-hex-2-enopyranuronate (0.324 g, 1.12 mmol) was dissolved in dry pyridine (15 mL) under a N<sub>2</sub> atmosphere. Benzoyl chloride (0.14 mL, 1.20 mmol, 1.1 equiv.) was added dropwise *via* syringe. The solution was stirred at room temperature for 48 hours until TLC (1:1 hexanes: ethyl acetate, product R<sub>f</sub> = 0.37) showed consumption of starting material. The solution was diluted with 25 mL of CH<sub>2</sub>Cl<sub>2</sub> and then washed with 5% *v/v* H<sub>2</sub>SO<sub>4</sub> (3 x 15 mL),

saturated NaHCO<sub>3</sub> (3 x 15 mL), and water (3 x 15 mL). The organics were dried over MgSO<sub>4</sub>, filtered, and concentrated under reduced pressure to give a white solid, which was crystallized using isopropanol to afford benzoyloxime **9** (0.203 g, 0.52 mmol, 46%) as colorless crystals.

<sup>1</sup>H NMR (CDCl<sub>3</sub>): δ 2.11, 2.15 (2s, 6H total, 2 x COCH<sub>3</sub>), 3.84 (s, 3H, OCH<sub>3</sub>), 4.48 (d, 1H, H-5, *J* = 3.66 Hz), 4.96 (d, 1H, H-1<sub>A</sub>, *J* = 15.74 Hz), 5.04 (d, 1H, H-1<sub>B</sub>, *J* = 15.74 Hz), 5.58 (dd, 1H, H-4, *J* = 3.66, 4.76 Hz), 5.70 (d, 1H, H-3, *J* = 4.76 Hz), 7.50 (m, 2H, 2 x Ar-H), 7.64 (m, 1H, Ar-H), 8.04 (m, 2H, 2 x Ar-H).

<sup>13</sup>C NMR (CDCl<sub>3</sub>): δ 20.5, 20.8, 52.6, 59.4, 67.6, 69.0, 73.6, 127.7, 128.5 (2 x C), 129.5 (2 x C), 133.7, 157.2, 162.4, 167.98, 168.02, 168.9.

*m/z* calculated: 393.11

*m/z* found (ESI): 416.2 (+Na)

M.P. = 124-126 °C

R<sub>f</sub> = 0.37 (1:1 hexanes: ethyl acetate)

[α]<sub>D</sub> = -1.8 (*c* = 1.0, CH<sub>2</sub>Cl<sub>2</sub>)

**Formation of methyl 3,4-di-*O*-acetyl-2-deoxy-2-(4-nitrobenzoyloxyimino)-D-arabino-hex-2-enopyranuronate (10) from methyl 3,4-di-*O*-acetyl-2-deoxy-2-(hydroxyimino)-D-arabino-hex-2-enopyranuronate (8).**

To a 100 mL round-bottom flask equipped with a septum and magnetic stir bar, methyl 3,4-di-*O*-acetyl-2-deoxy-2-(hydroxyimino)-D-arabino-hex-2-enopyranuronate (0.500 g, 1.73 mmol) and 4-nitrobenzoyl chloride (0.353 g, 1.90 mmol, 1.1 equiv.) were

dissolved in dry pyridine (25 mL) under a N<sub>2</sub> atmosphere. The solution was stirred at room temperature for 24 hours until TLC (1:1 hexanes: ethyl acetate, product R<sub>f</sub> = 0.35) showed consumption of starting material. The solution was diluted with 25 mL of CH<sub>2</sub>Cl<sub>2</sub> and then washed with 5% v/v H<sub>2</sub>SO<sub>4</sub> (3 x 15 mL), saturated NaHCO<sub>3</sub> (3 x 15 mL), and water (3 x 15 mL). The organics were dried over MgSO<sub>4</sub>, filtered, and concentrated under reduced pressure to give a yellow solid, which was crystallized using isopropanol to afford 4-nitrobenzoyloxime **10** (0.757 g, 1.73 mmol, 100%) as pale yellow crystals.

<sup>1</sup>H NMR (CDCl<sub>3</sub>): δ 2.12, 2.16 (2s, 6H total, 2 x COCH<sub>3</sub>), 3.85 (s, 3H, OCH<sub>3</sub>), 4.49 (d, 1H, H-5, J = 3.66 Hz), 4.94 (d, 1H, H-1<sub>A</sub>, J = 15.74 Hz), 5.06 (d, 1H, H-1<sub>B</sub>, J = 15.74 Hz), 5.59 (dd, 1H, H-4, J = 3.66, 4.76 Hz), 5.72 (d, 1H, H-3, J = 4.76 Hz), 8.23 (d, 2H, 2 x Ar-H, J = 8.42 Hz), 8.36 (d, 2H, 2 x Ar-H, J = 8.42 Hz).

<sup>13</sup>C NMR (CDCl<sub>3</sub>): δ 20.5, 20.7, 52.6, 59.2, 67.4, 69.0, 73.6, 123.7 (2 x C), 130.6 (2 x C), 133.2, 150.6, 158.4, 160.7, 167.8, 168.0, 168.9.

m/z calculated: 438.09

m/z found (ESI): 461.2 (+Na)

M.P. = 164-166 °C

R<sub>f</sub> = 0.35 (1:1 hexanes: ethyl acetate)

[α]<sub>D</sub> = -11.8 (c = 1.0, CH<sub>2</sub>Cl<sub>2</sub>)

**Formation of methyl 3,4-di-*O*-acetyl-1,5-anhydro-2-deoxy-D-arabino-hex-1-enopyranuronate (15) from methyl 2,3,4-tri-*O*-acetyl- $\alpha$ -D-glucopyranuronosyl bromide (6).**

Methyl 2,3,4-tri-*O*-acetyl- $\alpha$ -D-glucopyranuronosyl bromide (5.45 g, 13.72 mmol), bis(cyclopentadienyl)titanium chloride (2.73 g, 10.98 mmol, 0.8 equiv.), and manganese (3.02 g, 54.88 mmol, 4 equiv.) were dissolved in dry THF (80 mL) in a 250 mL round-bottom flask equipped with a septum and magnetic stir bar, under a N<sub>2</sub> atmosphere. Trimethylsilyl chloride (2.1 mL, 16.46 mmol, 1.2 equiv.) was added dropwise *via* syringe and the reaction was allowed to stir at room temperature until TLC (1:1 hexanes: ethyl acetate, product R<sub>f</sub> = 0.44) showed consumption of starting material. The reaction mixture was filtered through a bed of silica and then concentrated under reduced pressure. The resulting residue was purified by flash column (2:1 hexanes: ethyl acetate) and the major fraction was collected to give glycal **15** (2.85 g, 11.04 mmol, 88%) as colorless crystals.

<sup>1</sup>H NMR (CDCl<sub>3</sub>): δ 2.01, 2.13 (s, 6H total, 2 x COCH<sub>3</sub>), 3.81 (s, 3H, OCH<sub>3</sub>), 4.85 (dd, 1H, H-5, J = 1.47, 2.56 Hz), 5.00 (m, 1H, H-3), 5.02 (m, 1H, H-2), 5.43 (dd, 1H, H-4, J = 2.56, 4.03 Hz), 6.69 (d, 1H, H-1, J = 5.86 Hz).

<sup>13</sup>C NMR (CDCl<sub>3</sub>): δ 20.86, 20.91, 52.3, 62.4, 67.2, 72.1, 97.1, 146.2, 166.9, 169.0, 169.2.

*m/z* calculated: 258.07

*m/z* found (ESI): 281.1 (+Na)

M.P. = 88-90 °C

$R_f$  = 0.44 (1:1 hexanes: ethyl acetate)

$[\alpha]_D$  = -65.6 ( $c$  = 1.0, CH<sub>2</sub>Cl<sub>2</sub>)

**Formation of methyl 1,5-anhydro-2-deoxy- $\beta$ -D-*arabino*-hex-1-enopyranuronate (16)  
from methyl 3,4-di-*O*-acetyl-1,5-anhydro-2-deoxy-D-*arabino*-hex-1-enopyranuronate  
(15).**

Methyl 3,4-di-*O*-acetyl-1,5-anhydro-2-deoxy-D-*arabino*-hex-1-enopyranuronate (1.80 g, 6.97 mmol) was dissolved in methanol (25 mL) in a 100 mL round-bottom flask equipped with a septum and magnetic stir bar, under a N<sub>2</sub> atmosphere. A solution containing sodium (0.20 g) in methanol (10 mL) was added dropwise *via* syringe and the reaction was allowed to stir at room temperature until TLC (100% ethyl acetate, product  $R_f$  = 0.29) showed consumption of starting material. The reaction mixture was concentrated under reduced pressure and the resulting residue was purified by flash column (10:1 ethyl acetate: hexanes) and the major fraction was collected to give unprotected glycal **16** (1.07 g, 6.14 mmol, 88%) as a pale orange syrup..

<sup>1</sup>H NMR (DMSO-*d*<sub>6</sub>):  $\delta$  3.61 (s, 3H, OCH<sub>3</sub>), 3.75 (m, 1H, H-3), 3.83 (m, 1H, H-4), 4.42 (d, 1H, H-5, *J* = 5.13 Hz), 4.72 (m, 1H, H-2), 4.97 (d, 1H, OH, *J* = 4.03 Hz), 5.41 (d, 1H, OH, *J* = 4.76 Hz), 6.39 (d, 1H, H-1, *J* = 6.22 Hz).

<sup>13</sup>C NMR (DMSO-*d*<sub>6</sub>):  $\delta$  51.6, 63.7, 69.1, 75.3, 102.7, 142.5, 168.7.

*m/z* calculated: 174.05

*m/z* found (ESI): 337.7 (2 x **16**)

M.P. = N/A (syrup)

$R_f$  = 0.44 (100% ethyl acetate)

$[\alpha]_D$  = +5.0 (*c* = 1.0, CH<sub>3</sub>OH)

**Formation of methyl 1,5-anhydro-2-deoxy-3-*O*-pivaloyl-D-*arabino*-hex-1-enopyranuronate (**17**) from methyl 1,5-anhydro-2-deoxy-D-*arabino*-hex-1-enopyranuronate (**16**).**

Methyl 1,5-anhydro-2-deoxy-D-*arabino*-hex-1-enopyranuronate (0.55 g, 3.16 mmol) was dissolved in pyridine (5 mL) and methylene chloride (5 mL) in a 100 mL round-bottom flask equipped with a septum and magnetic stir bar, under a N<sub>2</sub> atmosphere. The reaction mixture was cooled to -78 °C in an acetone: dry ice bath and trimethylacetyl chloride (0.39 mL, 3.16 mmol, 1.0 equiv.) was added dropwise *via* syringe. The reaction was allowed to stir at -78 °C until TLC (1:1 hexanes: ethyl acetate, product  $R_f$  = 0.36) showed consumption of starting material. The reaction mixture was diluted with 10 mL of CH<sub>2</sub>Cl<sub>2</sub> and washed with 5% v/v H<sub>2</sub>SO<sub>4</sub> (3 x 15 mL) and water (3 x 15 mL). The reaction mixture was dried over MgSO<sub>4</sub>, filtered, and concentrated under reduced pressure. The resulting residue was purified by flash column (1:1 ethyl acetate: hexanes) and the major fraction was collected to give glycal **17** (0.64 g, 2.48 mmol, 78%) as a pale yellow syrup.

<sup>1</sup>H NMR (CDCl<sub>3</sub>): δ 1.16 (s, 9H total, C(CH<sub>3</sub>)<sub>3</sub>), 3.54 (bs, 1H, OH), 3.82 (s, 3H, OCH<sub>3</sub>), 4.32 (m, 1H, H-4), 4.71 (m, 1H, H-5), 4.94 (m, 1H, H-2), 5.04 (m, 1H, H-3), 6.63 (d, 1H, H-1, *J* = 6.22 Hz).

<sup>13</sup>C NMR (CDCl<sub>3</sub>): δ 26.9 (3 x C), 38.6, 52.5, 66.3, 67.0, 75.2, 97.6, 145.6, 168.0, 178.0.

*m/z* calculated: 258.11

*m/z* found (ESI): 325.9 (+2 x MeOH)

M.P. = N/A (syrup)

R<sub>f</sub> = 0.36 (1:1 hexanes: ethyl acetate)

[α]<sub>D</sub> = -77.5 (*c* = 1.0, CH<sub>3</sub>OH)

**Formation of 1,2-*O*-isopropylidene- $\alpha$ -D-glucofuranosiduron-6,3-lactone (19) from  $\alpha,\beta$ -D-glucurono-6,3-lactone (3).**

In a 1000 mL round-bottom flask equipped with a magnetic stir bar, D-glucurono-6,3-lactone (5.00 g, 28.39 mmol) was dissolve in freshly distilled acetone (500 mL). Concentrated H<sub>2</sub>SO<sub>4</sub> (0.4 mL, 7.2 mmol) was added dropwise to the reaction mixture. The solution was stirred at room temperature for 48 hours until TLC (100% ethyl acetate, product R<sub>f</sub> = 0.57) showed consumption of starting material. The solution was concentrated under reduced pressure to give a yellow residue that was dissolved in 100 mL of CH<sub>2</sub>Cl<sub>2</sub> and cooled to 0 °C. The solution was then neutralized by washing with saturated NaHCO<sub>3</sub> (3 x 25 mL). The organics were dried over MgSO<sub>4</sub>, filtered, and

concentrated under reduced pressure to give a white solid, which was crystallized with isopropanol to afford **19** (5.95 g, 27.52 mmol, 97%) as white crystals.

<sup>1</sup>H NMR (CDCl<sub>3</sub>): δ 1.35 (s, 3H, CH<sub>3</sub>), 1.53 (s, 3H, CH<sub>3</sub>), 3.77 (bs, 1H, OH), 4.61 (d, 1H, H-2, *J* = 3.66 Hz), 4.83 (d, 1H, H-5, *J* = 3.30 Hz), 4.86 (d, 1H, H-3, *J* = 2.93), 4.96 (dd, 1H, H-4, *J* = 2.93, 4.39 Hz), 6.01 (d, 1H, H-1, *J* = 3.66 Hz).

<sup>13</sup>C NMR (CDCl<sub>3</sub>): δ 26.5, 26.8, 70.4, 78.2, 81.3, 82.7, 106.4, 113.3, 174.0.

*m/z* calculated: 216.1

*m/z* found (ESI): 239.1 (+Na)

M.P. = 118-119 °C

R<sub>f</sub> = 0.57 (100% ethyl acetate)

[α]<sub>D</sub> = +51.7 (*c* = 1.0, CH<sub>2</sub>Cl<sub>2</sub>)

### Formation of 1,2-*O*-isopropylidene-6-*O*-pivaloyl- $\alpha$ -D-glucurono-6,3-lactone (20)

#### from 1,2-*O*-isopropylidene- $\alpha$ -D-glucurono-6,3-lactone (19).

In a 250 mL round-bottom flask equipped with a septum and magnetic stir bar, 1,2-*O*-isopropylidene- $\alpha$ -D-glucurono-6,3-lactone (10.00 g, 46.26 mmol) was dissolved in dry pyridine (60 mL) under a N<sub>2</sub> atmosphere. Trimethyl acetyl chloride (6.83 mL, 55.51 mmol, 1.2 equiv.) was added dropwise to the solution *via* syringe. The solution was allowed to stir at room temperature for 1.5 hours until TLC (1:1 hexanes: ethyl acetate, product R<sub>f</sub> = 0.64) showed consumption of starting material. The solution was diluted with 100 mL of CH<sub>2</sub>Cl<sub>2</sub> and washed with 5% *v/v* H<sub>2</sub>SO<sub>4</sub> (3 x 30 mL) and water (3 x 30

mL). The organics were dried over MgSO<sub>4</sub>, filtered, and concentrated under reduced pressure to afford **20** in quantitative yield as a clear syrup.

<sup>1</sup>H NMR (CDCl<sub>3</sub>): δ 1.29 (s, 9H, C(CH<sub>3</sub>)<sub>3</sub>), 1.35 (s, 3H, CH<sub>3</sub>), 1.52 (s, 3H, CH<sub>3</sub>), 4.84 (d, 1H, H-2, *J* = 3.66 Hz), 4.85 (d, 1H, H-3, *J* = 2.93 Hz), 5.06 (dd, 1H, H-4, *J* = 2.93, 4.39 Hz), 5.47 (d, 1H, H-5, *J* = 4.39 Hz), 6.01 (d, 1H, H-1, *J* = 3.66 Hz).

<sup>13</sup>C NMR (CDCl<sub>3</sub>): δ 26.4, 26.8, 26.9 (3 x C), 38.8, 69.5, 77.0, 82.2, 82.4, 106.7, 113.0, 169.6, 177.0.

*m/z* calculated: 300.12

*m/z* found (ESI): 321.9 (+Na)

M.P. = N/A (syrup)

R<sub>f</sub> = 0.64 (1:1 hexanes: ethyl acetate)

[α]<sub>D</sub> = +92.8 (*c* = 1.0, CH<sub>2</sub>Cl<sub>2</sub>)

### Formation of 1,2-*O*-isopropylidene-6-*O*-tert-butyldiphenylsilyl- $\alpha$ -D-glucurono-6,3-lactone (**21**) from 1,2-*O*-isopropylidene- $\alpha$ -D-glucurono-6,3-lactone (**19**).

To a 100 mL round-bottom flask equipped with a septum and magnetic stir bar, 1,2-*O*-isopropylidene- $\alpha$ -D-glucurono-6,3-lactone (2.00 g, 9.25 mmol) and DMAP (0.57 g, 4.62 mmol, 0.5 equiv.) were dissolved in dry pyridine (25 mL) under a N<sub>2</sub> atmosphere. *Tert*-butyldiphenylsilyl chloride (2.65 mL, 10.18 mmol, 1.1 equiv.) was added dropwise to the solution *via* syringe. The solution was allowed to stir at room temperature for 24 hours until TLC (1:1 hexanes: ethyl acetate, product R<sub>f</sub> = 0.57) showed consumption of

starting material. The solution was diluted with 50 mL of CH<sub>2</sub>Cl<sub>2</sub> and washed with 5% v/v H<sub>2</sub>SO<sub>4</sub> (3 x 30 mL) and water (3 x 30 mL). The organics were dried over MgSO<sub>4</sub>, filtered, and concentrated under reduced pressure to afford **21** (3.04 g, 7.48 mmol, 81%) as colorless crystals.

<sup>1</sup>H NMR (CDCl<sub>3</sub>): δ 1.11 (s, 9H, C(CH<sub>3</sub>)<sub>3</sub>), 1.32 (s, 3H, CH<sub>3</sub>), 1.42 (s, 3H, CH<sub>3</sub>), 4.34 (d, 1H, H-3, *J* = 4.39 Hz), 4.38 (dd, 1H, H-4, *J* = 2.93, 4.39 Hz), 4.49 (d, 1H, H-5, *J* = 2.93 Hz), 4.72 (d, 1H, H-2, *J* = 4.03 Hz), 6.03 (d, 1H, H-1, *J* = 4.03 Hz), 7.38-7.46 (m, 6H, Ar-H), 7.77-7.84 (m, 4H, Ar-H).

<sup>13</sup>C NMR (CDCl<sub>3</sub>): δ 1.0, 19.2, 26.4 (3 x C), 26.6, 26.8, 71.5, 78.3, 80.8, 82.4, 106.5, 112.7, 127.6 (2 x C), 127.7 (2 x C), 129.9, 130.0, 131.4, 132.4, 135.5 (2 x C), 135.6 (2 x C), 172.4.

*m/z* calculated: 454.18

*m/z* found (ESI): 475.8 (+Na)

M.P. = 165–168 °C

R<sub>f</sub> = 0.57 (1:1 hexanes: ethyl acetate)

[α]<sub>D</sub> = +46.3 (*c* = 1.0, CH<sub>2</sub>Cl<sub>2</sub>)

**Formation of 1,2-*O*-isopropylidene-6-*O*-*tert*-butyldimethylsilyl- $\alpha$ -D-glucurono-6,3-lactone (22) from 1,2-*O*-isopropylidene- $\alpha$ -D-glucurono-6,3-lactone (19).**

To a 100 mL round-bottom flask equipped with a septum and magnetic stir bar, 1,2-*O*-isopropylidene- $\alpha$ -D-glucurono-6,3-lactone (1.00 g, 4.63 mmol) and DMAP (0.685

g, 5.55 mmol, 1.2 equiv.) were dissolved in dry pyridine (25 mL) under a N<sub>2</sub> atmosphere. *Tert*-butyldimethylsilyl chloride (0.829 g, 5.55 mmol, 1.2 equiv.) was added to the reaction mixture. The solution was allowed to stir at room temperature for 24 hours until TLC (1:1 hexanes: ethyl acetate, product R<sub>f</sub> = 0.57) showed consumption of starting material. The solution was diluted with 25 mL CH<sub>2</sub>Cl<sub>2</sub> and washed with 5% v/v H<sub>2</sub>SO<sub>4</sub> (3 x 15 mL) and water (3 x 15 mL). The organics were dried over MgSO<sub>4</sub>, filtered, and concentrated under reduced pressure to afford **22** (1.47 g, 4.45 mmol, 96%) as colorless crystals.

<sup>1</sup>H NMR (CDCl<sub>3</sub>): δ 0.18, 0.22 (s, 6H total, 2 x SiCH<sub>3</sub>), 0.95 (s, 9H, C(CH<sub>3</sub>)<sub>3</sub>), 1.34 (s, 3H, CH<sub>3</sub>), 1.52 (s, 3H, CH<sub>3</sub>), 4.53 (d, 1H, H-3, J = 4.39 Hz), 4.74 (d, 1H, H-5, J = 2.56 Hz), 4.78 (d, 1H, H-2, J = 3.66 Hz), 4.82 (dd, 1H, H-4, J = 2.56, 4.39 Hz), 6.03 (d, 1H, H-1, J = 3.66 Hz).

<sup>13</sup>C NMR (CDCl<sub>3</sub>): δ -5.2, -4.7, 18.4, 25.6 (3 x C), 26.4, 26.8, 71.4, 78.7, 81.1, 82.4, 106.6, 112.7, 172.6.

m/z calculated: 330.15

m/z found (ESI): 351.8 (+Na)

M.P. = 116-118 °C

R<sub>f</sub> = 0.57 (1:1 hexanes: ethyl acetate)

[α]<sub>D</sub> = +45.0 (c = 1.0, CH<sub>2</sub>Cl<sub>2</sub>)

**Formation of methyl 6-O-pivaloyl- $\beta$ -D-glucurono-6,3-lactone (23) from 1,2-O-isopropylidene-6-O-pivaloyl- $\alpha$ -D-glucurono-6,3-lactone (20).**

To a 1000 mL round-bottom flask equipped with a septum and magnetic stir bar, 1,2-O-isopropylidene-6-O-pivaloyl- $\alpha$ -D-glucurono-6,3-lactone (13.89 g, 46.26 mmol) was dissolved in methanol (500 mL) under a N<sub>2</sub> atmosphere. Camphor sulfonic acid (1.00 g, 4.30 mmol) was added to the reaction mixture and the solution was allowed to stir at room temperature for 48 hours until TLC (1:1 hexanes: ethyl acetate, product R<sub>f</sub> = 0.23) showed consumption of starting material. The solution was concentrated under reduced pressure and the resulting residue was purified by flash column (2:1 ethyl acetate: hexanes) and the major fraction was collected to give **23** (9.38 g, 34.20 mmol, 74%) as a clear syrup.

<sup>1</sup>H NMR (CDCl<sub>3</sub>): δ 1.31 (s, 9H, C(CH<sub>3</sub>)<sub>3</sub>), 3.37 (s, 3H, OCH<sub>3</sub>), 4.09 (bs, 1H, OH), 4.38 (s, 1H, H-2), 4.97 (s, 1H, H-1), 4.98 (d, 1H, H-3, J = 6.59 Hz), 5.15 (dd, 1H, H-4, J = 4.76, 6.59 Hz), 5.37 (d, 1H, H-5, J = 6.59 Hz).

<sup>13</sup>C NMR (CDCl<sub>3</sub>): δ 27.0 (3 x C), 38.8, 55.3, 69.2, 75.7, 76.8, 83.8, 109.4, 171.4, 177.1.

m/z calculated: 274.11

m/z found (ESI): 295.8 (+Na)

M.P. = N/A (syrup)

R<sub>f</sub> = 0.64 (1:1 hexanes: ethyl acetate)

[α]<sub>D</sub> = +2.8 (c = 1.0, CH<sub>2</sub>Cl<sub>2</sub>)

**Formation of methyl 6-O-pivaloyl-2-O-trifluoromethylsulfonyl- $\beta$ -D-glucurono-6,3-lactone (24) from methyl 6-O-pivaloyl- $\beta$ -D-glucurono-6,3-lactone (23).**

To a 100 mL round-bottom flask equipped with a septum and magnetic stir bar, methyl 6-O-pivaloyl- $\beta$ -D-glucurono-6,3-lactone (0.94 g, 3.43 mmol) was dissolved in pyridine (1 mL) and methylene chloride (5 mL) under a N<sub>2</sub> atmosphere. The reaction mixture was cooled to -78 °C using an acetone: dry ice bath and triflic anhydride (0.64 mL, 3.77 mmol, 1.1 equiv.) was added to the reaction mixture dropwise *via* syringe and the solution was allowed to stir at -78 °C until TLC (1:1 hexanes: ethyl acetate, product R<sub>f</sub> = 0.66) showed consumption of starting material. The solution was concentrated under reduced pressure and the resulting residue was purified by flash column (2:1 hexanes: ethyl acetate) to give **24** (1.14 g, 2.81 mmol, 82%) as a pale orange solid.

<sup>1</sup>H NMR (CDCl<sub>3</sub>): δ 1.31 (s, 9H, C(CH<sub>3</sub>)<sub>3</sub>), 3.46 (s, 3H, OCH<sub>3</sub>), 5.19 (d, 1H, H-3, J = 5.13 Hz), 5.22 (s, 1H, H-1), 5.24 (dd, 1H, H-4, J = 5.13, 6.96 Hz), 5.30 (s, 1H, H-2), 5.38 (d, 1H, H-5, J = 6.96 Hz).

<sup>13</sup>C NMR (CDCl<sub>3</sub>): δ 27.1 (3 x C), 38.9, 56.1, 68.1, 75.9, 80.3, 86.6, 106.4, 119.8, 169.0, 176.8.

*m/z* calculated: 406.05

*m/z* found (ESI): 379.6 (-OCH<sub>3</sub>)

M.P. = 88-91 °C

R<sub>f</sub> = 0.66 (1:1 hexanes: ethyl acetate)

$[\alpha]_D = +47.8$  ( $c = 1.0$ , CH<sub>2</sub>Cl<sub>2</sub>)

**Formation of methyl 6-O-pivaloyl-2-O-(*p*-methylphenylsulfonyl)- $\beta$ -D-glucurono-6,3-lactone (26) from methyl 6-O-pivaloyl- $\beta$ -D-glucurono-6,3-lactone (23).**

To a 100 mL round-bottom flask equipped with a septum and magnetic stir bar, methyl 6-O-pivaloyl- $\beta$ -D-glucurono-6,3-lactone (4.63 g, 16.88 mmol) was dissolved in pyridine (30 mL) under a N<sub>2</sub> atmosphere. A solution of *p*-methylphenylsulfonyl chloride (3.86 g, 20.26 mmol, 1.2 equiv.) in 10 mL of pyridine was added to the reaction mixture dropwise *via* syringe and the solution was allowed to stir at room temperature for 48 hours until TLC (1:1 hexanes: ethyl acetate, product R<sub>f</sub> = 0.46) showed consumption of starting material. The solution was concentrated under reduced pressure and the resulting residue was purified by flash column (1:1 ethyl acetate: hexanes) to give **26** (6.29 g, 14.68 mmol, 87%) as a clear syrup.

<sup>1</sup>H NMR (CDCl<sub>3</sub>):  $\delta$  1.28 (s, 9H, C(CH<sub>3</sub>)<sub>3</sub>), 2.46 (s, 3H, Ar-CH<sub>3</sub>), 3.34 (s, 3H, OCH<sub>3</sub>), 4.87 (s, 1H, H-2), 5.00 (s, 1H, H-1), 5.03 (d, 1H, H-3,  $J$  = 4.76 Hz), 5.14 (dd, 1H, H-4,  $J$  = 4.76, 6.59 Hz), 5.37 (d, 1H, H-5,  $J$  = 6.96 Hz), 7.41 (d, 2H, Ar-H,  $J$  = 8.42 Hz), 7.82 (d, 2H, Ar-H, 8.42 Hz).

<sup>13</sup>C NMR (CDCl<sub>3</sub>):  $\delta$  21.6, 27.0 (3 x C), 38.7, 55.6, 68.4, 75.9, 80.9, 82.2, 106.7, 127.8 (2 x C), 130.1 (2 x C), 131.7, 145.9, 169.6, 176.6.

*m/z* calculated: 428.11

*m/z* found (ESI): 397.9 (-OCH<sub>3</sub>)

M.P. = N/A (syrup)

$R_f$  = 0.46 (1:1 hexanes: ethyl acetate)

$[\alpha]_D$  = +79.4 ( $c$  = 1.0, CH<sub>2</sub>Cl<sub>2</sub>)

## References

1. Todar, K. Univ. of Wisconsin-Madison Department of Bacteriology. <http://textbookofbacteriology.net/staph.html>. (Accessed Nov. 2005)
2. Gill, S.; Fraser, C. M. "Insights on Evolution of Virulence and Resistance from the Complete Genome Analysis of an Early Methicillin-Resistant *Staphylococcus aureus* Strain and a Biofilm-Producing Methicillin-Resistant *Staphylococcus epidermidis* Strain," *J. Bacteriol.* **2005**, 187, 2426-2438.
3. Lyczak, J. B.; Cannon, C. L.; Pier, G. B. "Lung Infections Associated with Cystic Fibrosis," *Clin. Microbiol. Rev.* **2002**, 15, 194–222.
4. Tenover, F. C.; Biddle, J. W.; Lancaster, M. V. "Increasing Resistance to Vancomycin and Other Glycopeptides in *Staphylococcus aureus*," *Emerg. Infect. Diseases*, **2001**, 7, 327-332.
5. BioNews Online. [http://www.bionewsonline.com/i/what\\_is\\_staphylococcus-aureus.htm](http://www.bionewsonline.com/i/what_is_staphylococcus-aureus.htm). (Accessed Nov 2005).
6. Livermore, D. M. "Antibiotic Resistance in *Staphylococci*," *Int. J. Antimicro. Ag.* **2000**, 16, S3-S10.

7. Chambers, H. F. "The Changing Epidemiology of *Staphylococcus aureus*?" *Emerg. Infect. Diseases*, **2001**, 7, 178-182.
8. Gemmell, C. G. "Glycopeptide Resistance in *Staphylococcus aureus*: Is it a Real Threat?" *J. Infect. Chemother.* **2004**, 10, 69-75.
9. Kuroda, M.; Ohta, T.; Uchiyama, I.; Baba, T.; Yuzawa, H.; Kobayashi, I.; Cui, L.; Oguchi, A.; Aoki, K.; Nagai, Y.; Lian, J.; Ito, T.; Kanamori, M.; Matsumaru, H.; Maruyama, A.; Murakami, H.; Hosoyama, A.; Mizutani-Ui, Y.; Takahashi, N.; Sawano, T.; Inoue, R.; Kaito, C.; Sekimizu, K.; Hirakawa, H.; Kuhara, S.; Goto, S.; Yabuzaki, J.; Kanehisa, M.; Yamashita, A.; Oshima, K.; Furuya, K.; Yoshino, C.; Shiba, T.; Hattori, M.; Ogasawara, N.; Hayashi, H.; Hiramatsu, K. "Whole Genome Sequencing of Methicillin-resistant *S. aureus*," *Lancet*, **2001**, 357, 1225-1240.
10. Rayner, C.; Munckhof, W. J.; "Antibiotics Currently Used in the Treatment of Infections Caused by *Staphylococcus aureus*," *Intern. Med.* **2005**, 35, S3-S16.
11. Courvalin, P. "Antimicrobial Drug Resistance: 'Prediction Is Very Difficult, Especially about the Future,'" *Emerg. Infect. Diseases*, **2005**, 11, 1503-1506.

12. O'Riordan, K.; Lee, J. C. "S. aureus Capsular Polysaccharides," *Clin. Microbiol. Rev.* **2004**, *17*, 218-234.
13. Kiser, K. B.; Lee, J. C. "S. aureus cap5P Encodes a UDP-N-acetylglucosamine 2-Epimerase with Functional Redundancy," *J. Bacteriol.* **1999**, *181*, 4818-4824.
14. Morgan, P. M.; Sala, R. F.; Tanner, E. "Eliminations in the Reaction Catalyzed by UDP-N-Acetylglucosamine 2-Epimerase," *J. Am. Chem. Soc.* **1997**, *119*, 10269-10277.
15. Dwek, R. A. "Glycobiology: Toward Understanding the Function of Sugars," *Chem. Rev.* **1996**, *96*, 683-720.
16. Boons, G. "Carbohydrate Chemistry," Blackie Academic & Professional: London, England, **1998**, 430-442.
17. Goldstein, I. J. "Carbohydrate-Protein Interaction," American Chemical Society: Washington, D.C. **1979**, 1-10.
18. Aspinall, G. O. "Carbohydrates," University Park Press: Baltimore, Maryland, **1973**, 2-8, 214-216.

19. Huopaniemi, L.; Kolmer, M.; Niittymaki, J.; Pelto-Huikko, M.; Renkonen, R. "Inflammation-induced Transcriptional Regulation of Golgi Transporters Required for the Synthesis of Sulfo sLex Glycan Epitopes," *Glycobiology*, **2004**, *14*, 1285-1294.
20. Apweiler, R.; Hermjakob, H.; Sharon, N. "On the Frequency of Glycosylation, as Deduced from Analysis of the SWISS-PROT Database," *Biochim. Biophys. Acta*, **1999**, *1473*, 4-8.
21. Hofsteenge, J.; Muller, D.; de Beer, T.; Loffler, A.; Richter, W.; Vliegenthart, J. "New Type of Linkage between a Carbohydrate and a Protein: C-Glycosylation of a Specific Tryptophan Residue in Human RNase U<sub>s</sub>," *Biochemistry*, **1994**, *33*, 13524-13530.
22. Brockhausen, I. "Pathways of O-Glycan Biosynthesis in Cancer Cells," *Biochim. Biophys. Acta*, **1999**, *1473*, 67-95.
23. Schachter, H. "The Clinical Relevance of Glycobiology," *J. Clin. Invest.* **2001**, *108*, 1579-1582.
24. Wopereis, S.; Lefeber, D.; Morava, E.; Wevers, R. "Mechanisms in Protein O-Glycan Biosynthesis and Clinical and Molecular Aspects of Protein O-Glycan Biosynthesis Defects: A Review," *Clin. Chem.* **2006**, *52*, 574-600.

25. El Khadem, H. S. "Carbohydrate Chemistry: Monosaccharides and Their Oligomers," Academic Press: San Diego, California, **1988**, 1-26.
26. Stick, R. V. "Carbohydrates: The Sweet Molecules of Life," Academic Press: San Diego, California, **2001**, 9-34.
27. Davis, B. G.; Fairbanks, A. J. "Carbohydrate Chemistry," Oxford University Press: Oxford, England, **2002**, 3-17.
28. Collins, P.; Ferrier, R. "Monosaccharides: Their Chemistry and Their Roles in Natural Products," Wiley: New York, New York, **1995**, 4-26.
29. De Mayo, P. "Molecular Rearrangements: Part 2," Interscience Publishers: New York, New York, **1963**, 6-12.
30. Basso, E.; Kaiser, C.; Rittner, R.; Lambert, J. "Axial/Equatorial Proportions for 2-Substituted Cyclohexanones," *J. Org. Chem.* **1993**, 58, 7865-7869.
31. Grant, L.; Liu, Y.; Walsh, K.; Walter, D.; Gallagher, T. "*Galacto, Gluco, Manno*, and Disaccharide-Based C-Glycosides of 2-Amino-2-deoxy Sugars," *Organic Letters*, **2002**, 4, 4623-4625.

32. Kren, V.; Martinkova, L. "Glycosides in Medicine: The Role of Glycosidic Residue in Biological Activity," *Curr. Med. Chem.* **2001**, 8, 1303-1328.
33. Nyffeler, P.; Chang-Hsing, L.; Koeller, K.; Wong, C-H. "The Chemistry of Amine-Azide Interconversion: Catalytic Diazotransfer and Regioselective Azide Reduction," *J. Am. Chem. Soc.* **2002**, 124, 10773-10778.
34. Boullanger, P.; Maunier, V.; Lafont, D. "Syntheses of amphiphilic glycosylamides from glycosyl azides without transient reduction to glycosylamines," *Carbohydr. Res.* **2000**, 324, 97-106.
35. Thurston, D.; Bose, D. "Synthesis of DNA-Interactive Pyrrolo[2,1-*c*][1,4]benzodiazepines," *Chem. Rev.* **1994**, 94, 433-465.
36. Seeberger, P.; Roehrig, S.; Schell, P.; Wang, Y.; Christ, W. "Selective Formation of C-2 Azidodeoxy-D-glucose Derivatives from D-Glucal Precursors Using the Azidonitration Reaction," *Carbohydr. Res.* **2000**, 328, 61-69.
37. Czernecki, S.; Ayadi, E.; Randriamandimbly, D. "Selenoglycosides. 3. Synthesis of Phenyl 2-(*N*-Acetylamino)- and 2-Azido-2-deoxy-1-seleno- $\alpha$ -D-glycopyranosides via Azido-phenylselenylation of Diversely Protected Glycals," *J. Org. Chem.* **1994**, 59, 8256-8260.

38. Bongat, A.; Demchenko, A. "Recent Trends in the Synthesis of *O*-Glycosides of 2-Amino-2-deoxysugars," *Carbohydr. Res.* **2007**, *342*, 374-406.
39. Kaji, E.; Osa, Y.; Takahashi, K.; Hirooka, M.; Zen, S.; Lichtenthaler, F. "Facile Preparation and Utilization of a Novel  $\beta$ -D-ManNAcA-Donor: Methyl 2-Benzoyloxyimino-1-bromo-2-deoxy- $\alpha$ -D-*arabino*-hexopyranuronate," *Bull. Chem. Soc. Jpn.* **1994**, *67*, 1130-1140.
40. Root, Y.; Wagner, T.; Norris, P. "Crystal Structure of Methyl 1,2,3,4-tetra-*O*-acetyl- $\beta$ -D-glucopyranuronate," *Carbohydr. Res.* **2002**, *337*, 2343-2346.
41. Smith, C. " Facile Preparation of Glycomimetics from Uronic Acids," M.S. Thesis, Youngstown State University, **2005**, 28-33.
42. Abul, K.; Horton, D. "Preparative Synthesis of 2-Acetamido-2,6-dideoxy-L-galactose (*N*-acetyl-L-fucosamine)," *Carbohydr. Res.* **1987**, *169*, 258-262.
43. Hansen, T.; Daasbjerg, K.; Skrydstrup, T. "Development of a Catalytic Cycle for the Generation of C1-Glycosyl Carbanions with  $Cp_2TiCl_2$ : Application to Glycal Synthesis," *Tetrahedron Lett.* **2000**, *41*, 8645-8649.
44. Paulsen, H.; Lorentzen, J.; Kutschker, W. "Attempted Synthesis of 2-Azido-2-deoxy-D-mannose and 2-Azido-2-deoxy-D-mannouronic acid as Synthons for the

- Synthesis of Bacterial Polysaccharide Sequences," *Carbohydr. Res.* **1985**, 136, 153-176.
45. Petrakova, E.; Glaudemans, C. "Anomalous Zemplén Deacylation of Protected Methyl 2-Deoxy- $\alpha$ -D-*arabino*-hexopyranosides and Related Methyl  $\alpha$ -Isomaltosides and  $\alpha$ -Isomaltotriosides," *Carbohydr. Res.* **1995**, 268, 135-141.
46. Birtwistle, I.; Maddocks, P.; O'Callaghan, J.; Warren, J. "Synthesis of Four Ester Protected Thiofuranose Sugars," *Synth. Commun.* **2001**, 31, 3829-3838.

# **Appendix A**

## **NMR and Mass Spectra**

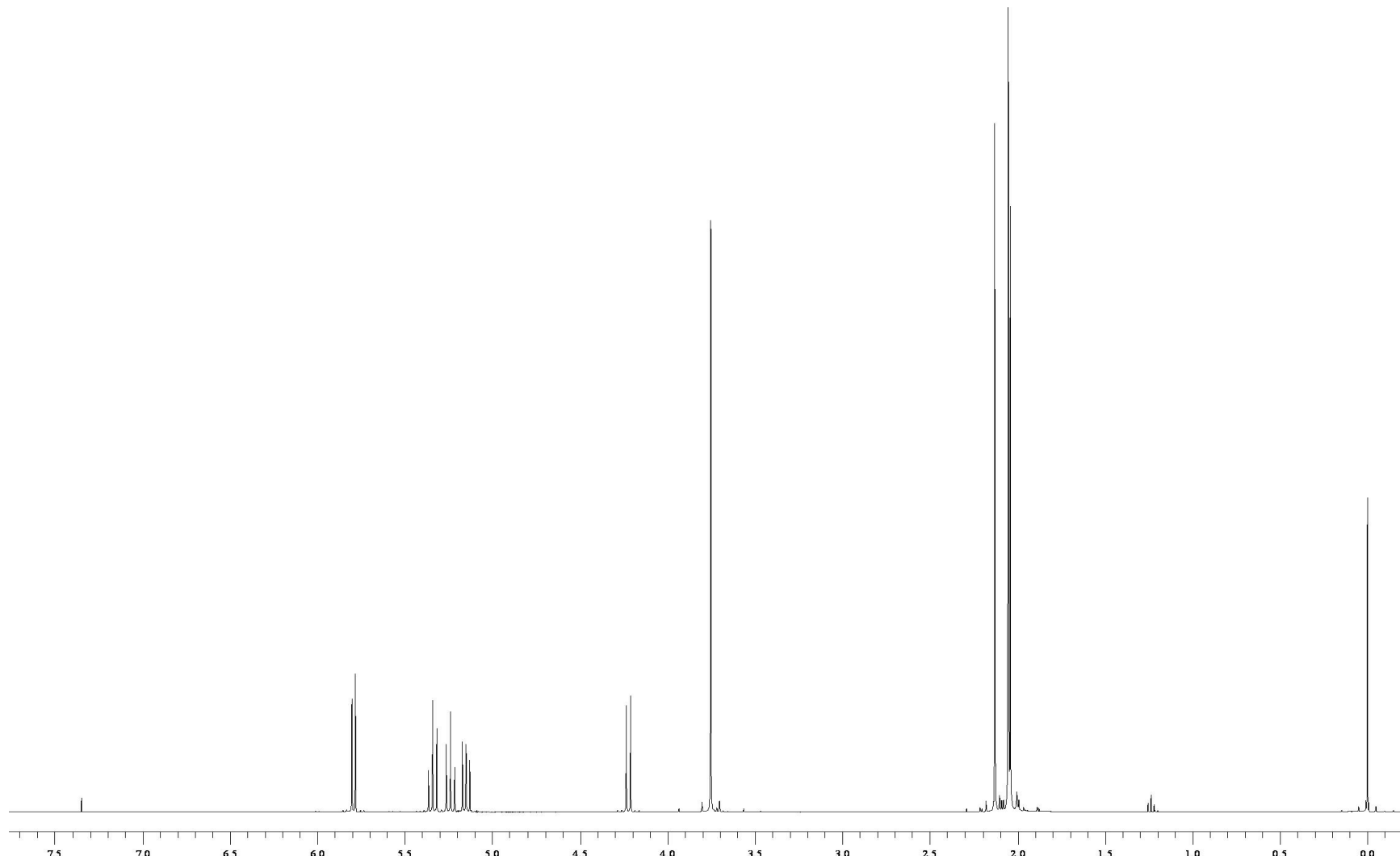


**Figure 25:** 400 MHz  $^1\text{H}$  NMR spectrum of methyl 1,2,3,4-tetra- $O$ -acetyl- $\beta$ -D-glucopyranuronate (**5 $\beta$** ).

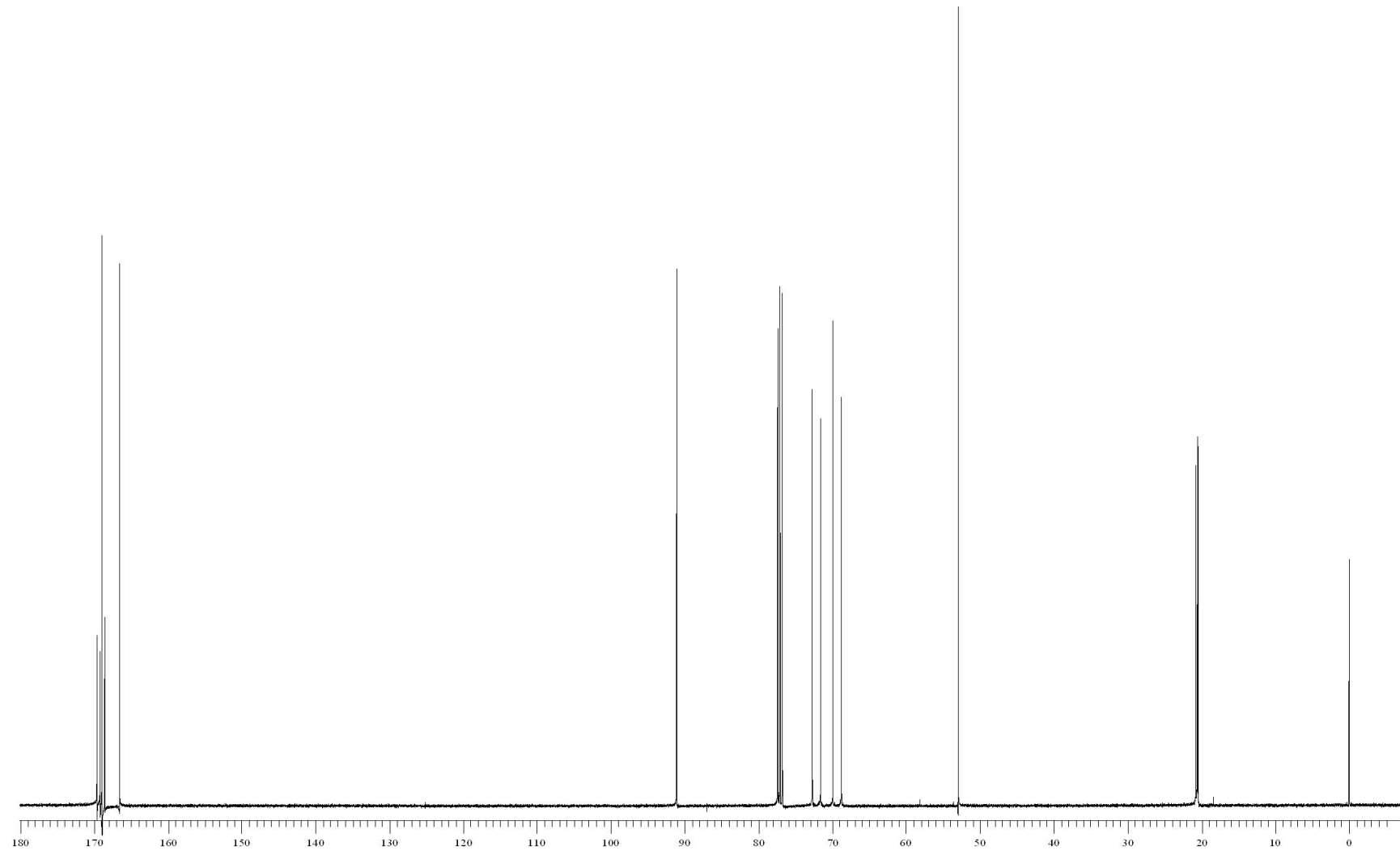


**Figure 26:** 100 MHz  $^{13}\text{C}$  NMR spectrum of methyl 1,2,3,4-tetra-*O*-acetyl- $\beta$ -D-glucopyranuronate (**5 $\beta$** ).

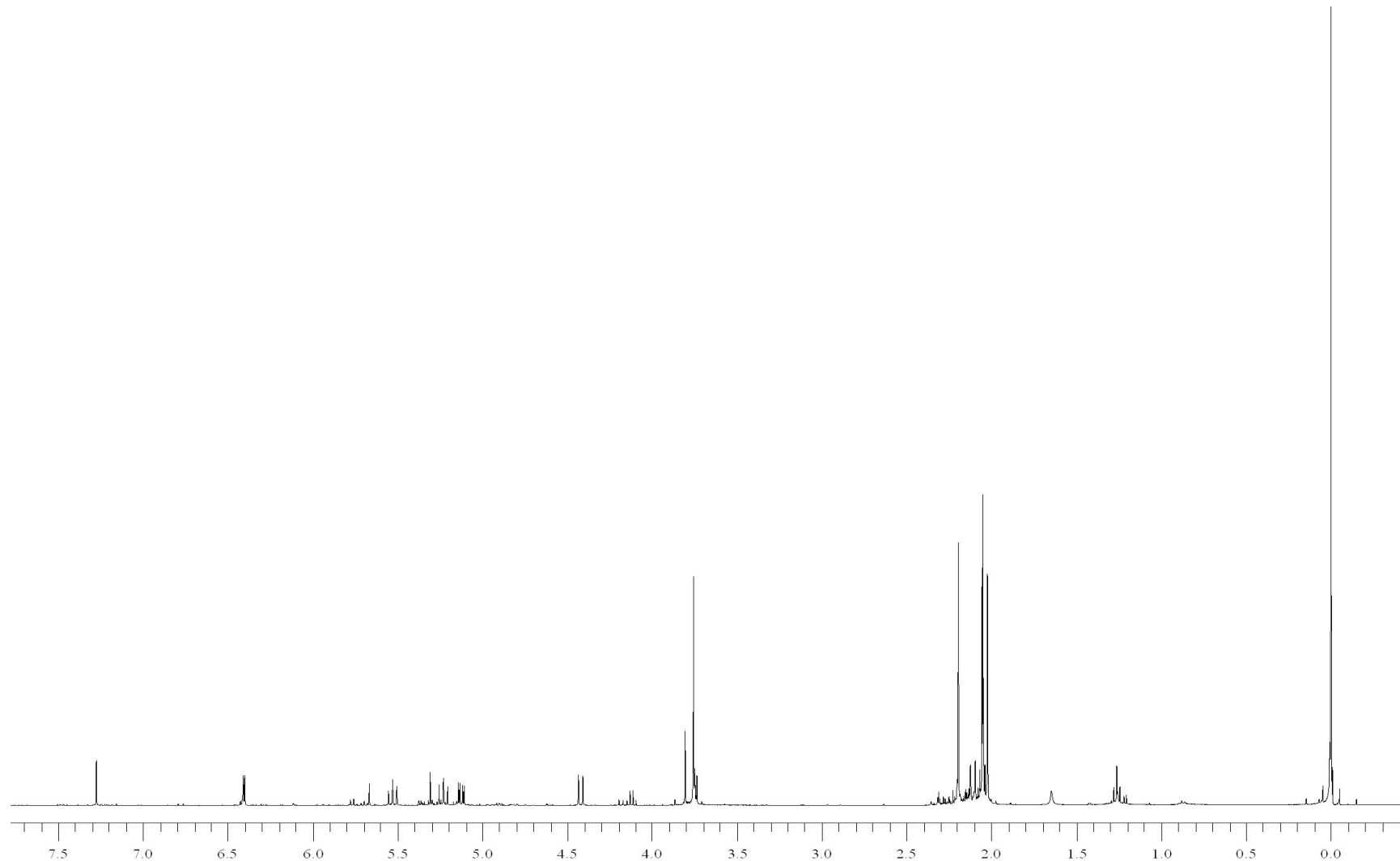


**Figure 27:** 400 MHz  $^1\text{H}$  NMR spectrum of methyl 1,2,3,4-tetra-O-acetyl- $\alpha$ -D-glucopyranuronate (**5a**).

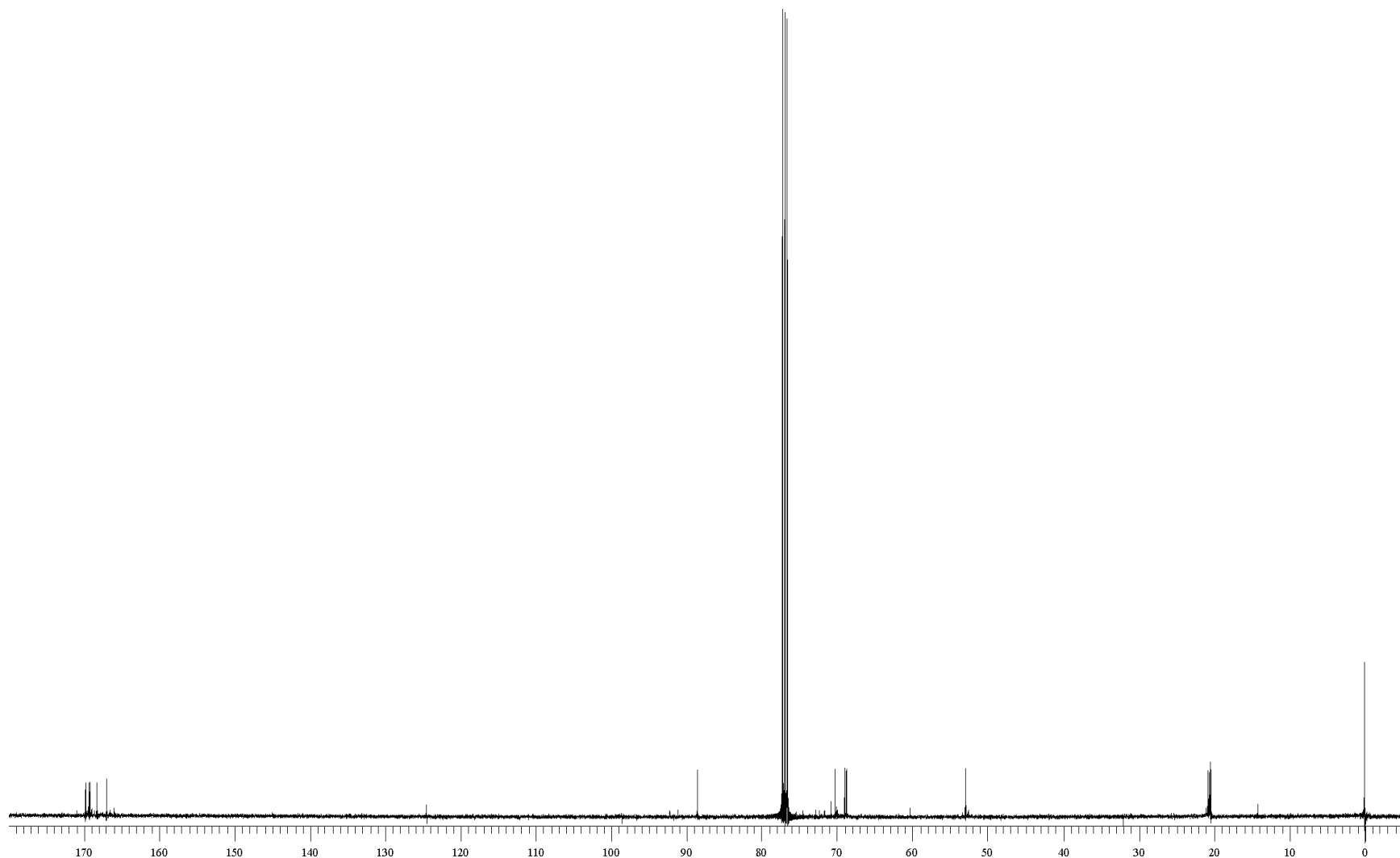


**Figure 28:** 100 MHz  $^{13}\text{C}$  NMR spectrum of methyl 1,2,3,4-tetra-O-acetyl- $\alpha$ -D-glucopyranuronate (**5 $\alpha$** ).

## Display Report

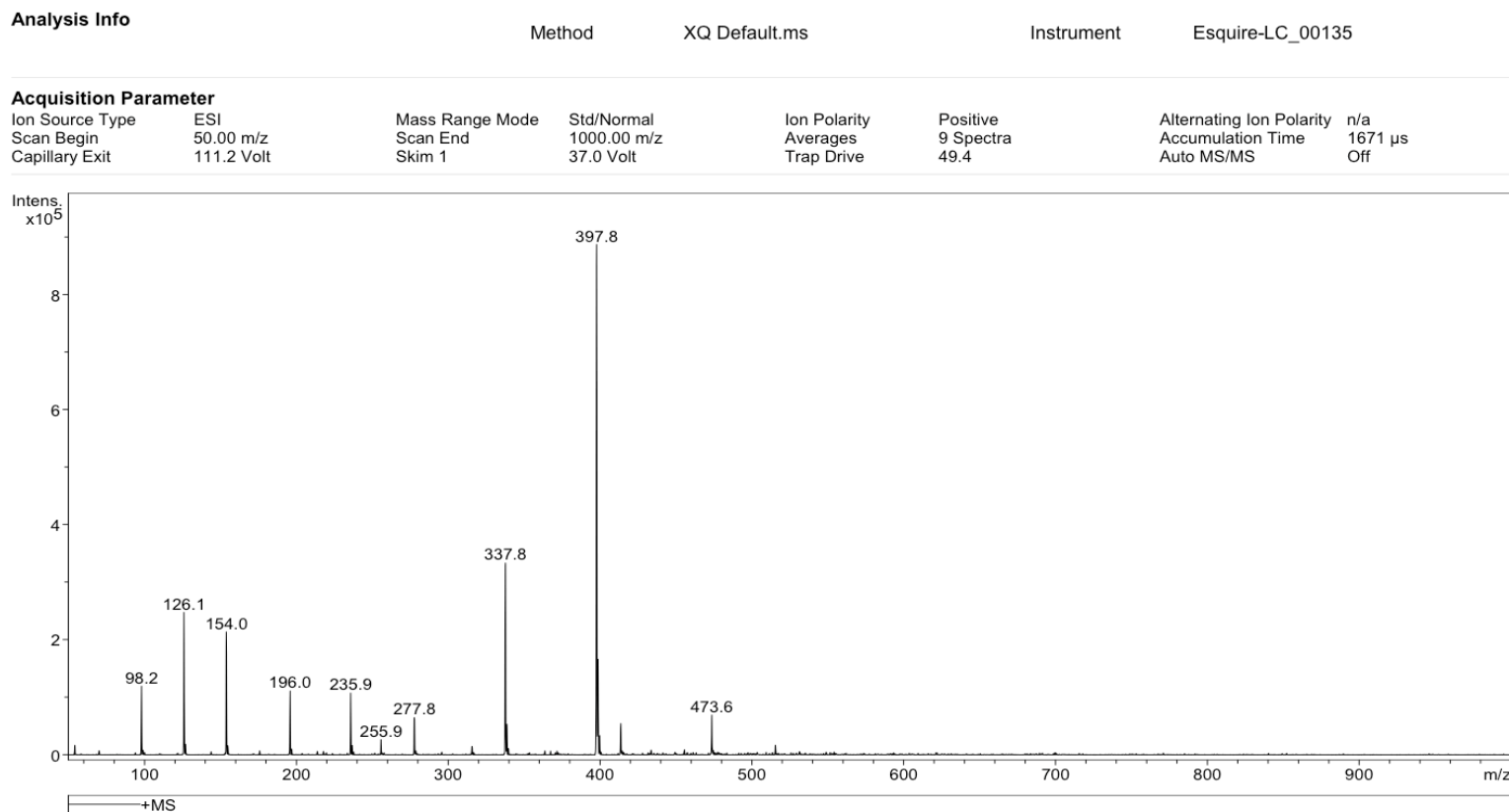


**Figure 29:** ESI mass spectrum of methyl 1,2,3,4-tetra-*O*-acetyl- $\alpha$ / $\beta$ -D-glucopyranuronate (**5 $\alpha$ / $\beta$** ).

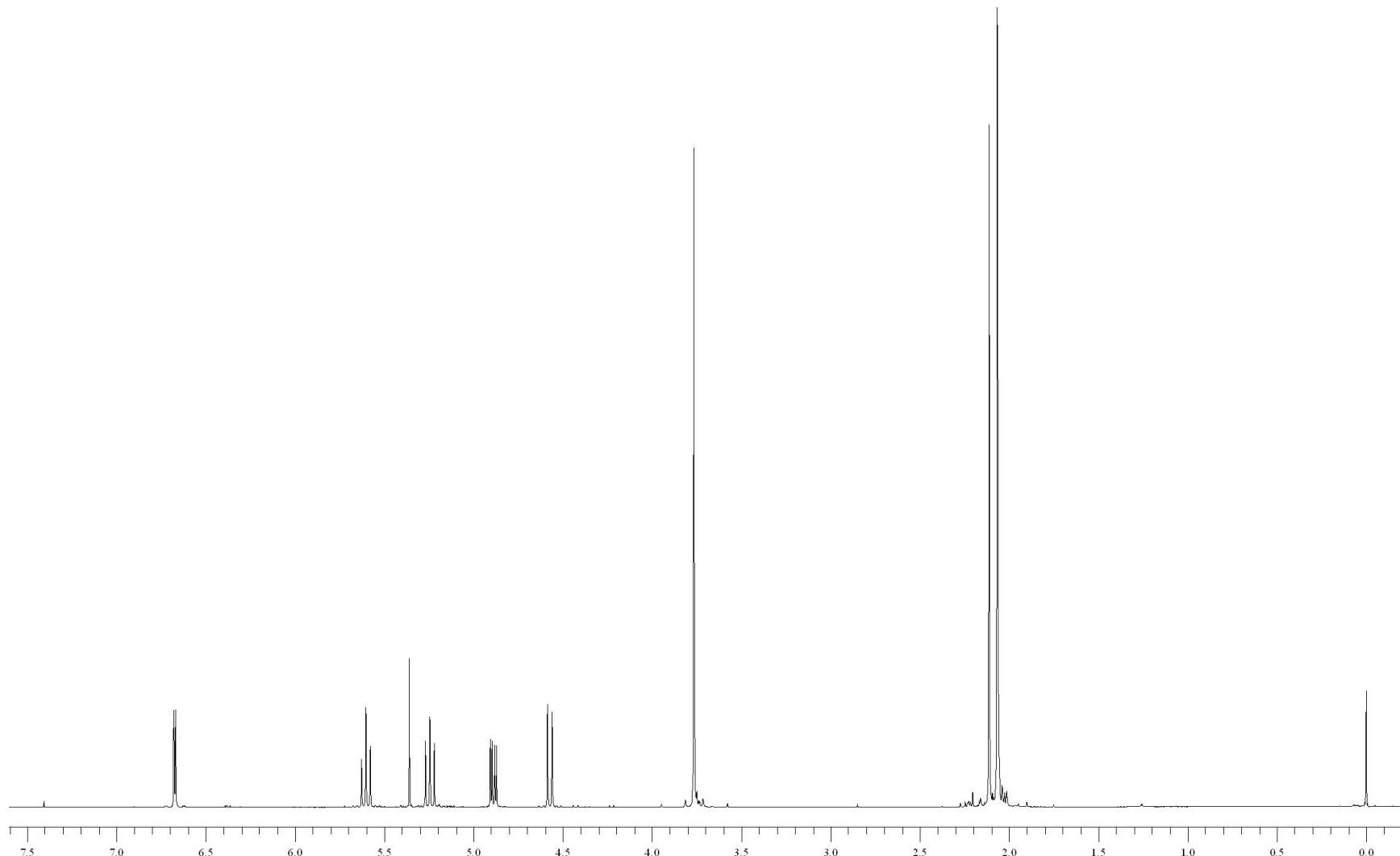


**Figure 30:** 400 MHz  $^1\text{H}$  NMR spectrum of methyl 2,3,4-tri- $O$ -acetyl- $\alpha$ -D-glucopyranuronosyl bromide (6).

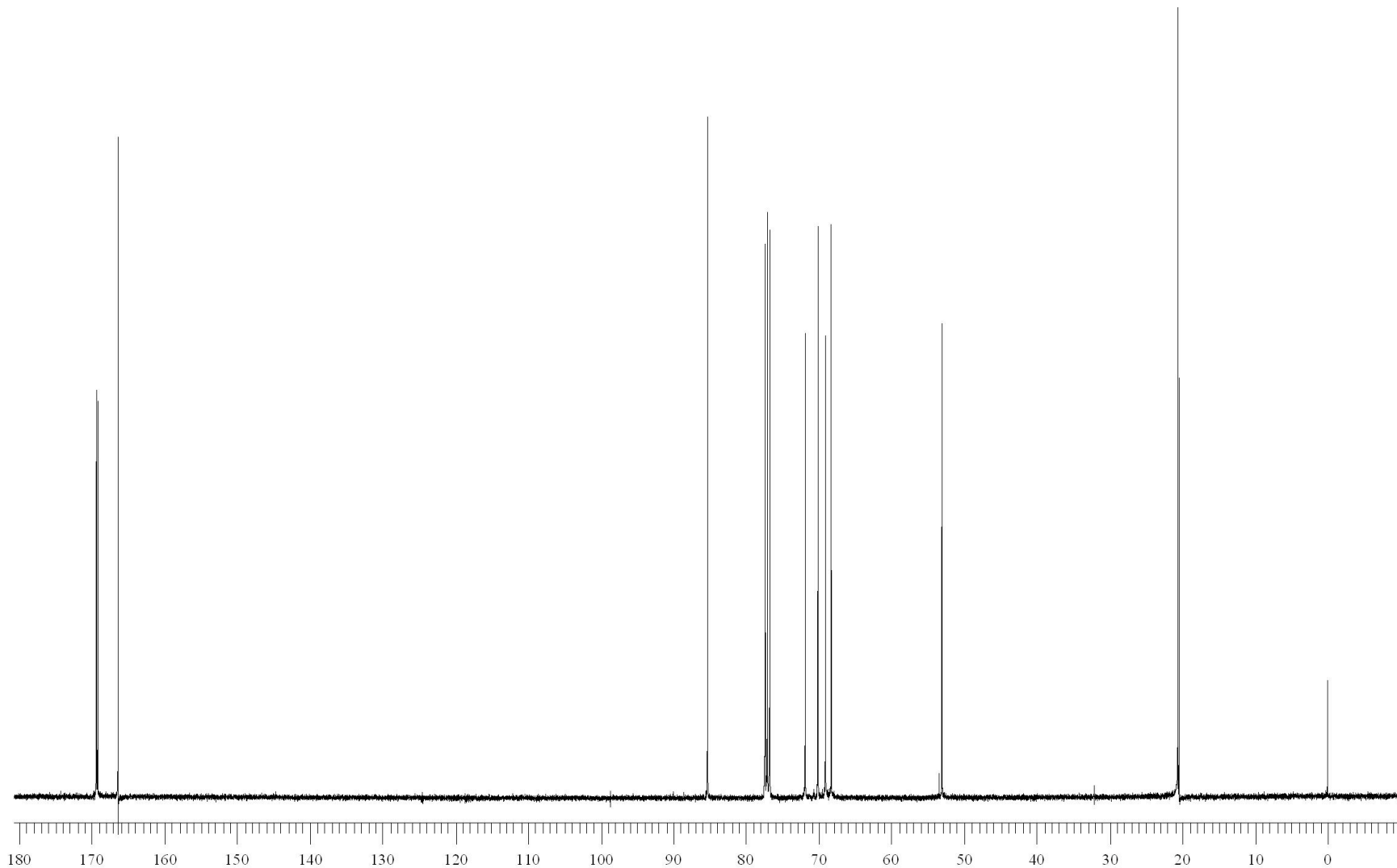


**Figure 31:** 100 MHz  $^{13}\text{C}$  NMR spectrum of methyl 2,3,4-tri- $O$ -acetyl- $\alpha$ -D-glucopyranuronosyl bromide (**6**).

## Display Report

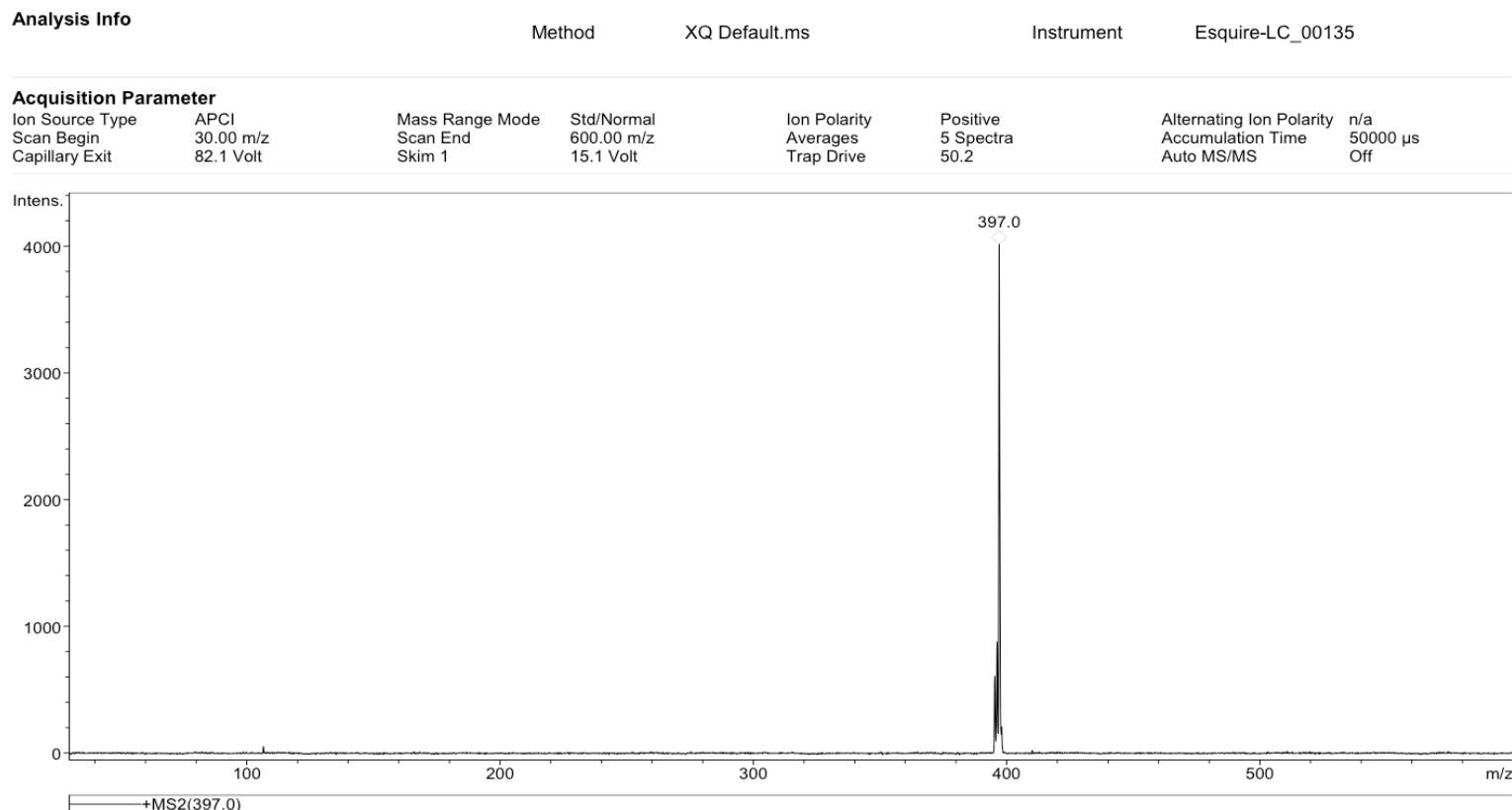


**Figure 32:** APCI mass spectrum of methyl 2,3,4-tri-*O*-acetyl- $\alpha$ -D-glucopyranuronosyl bromide (**6**).

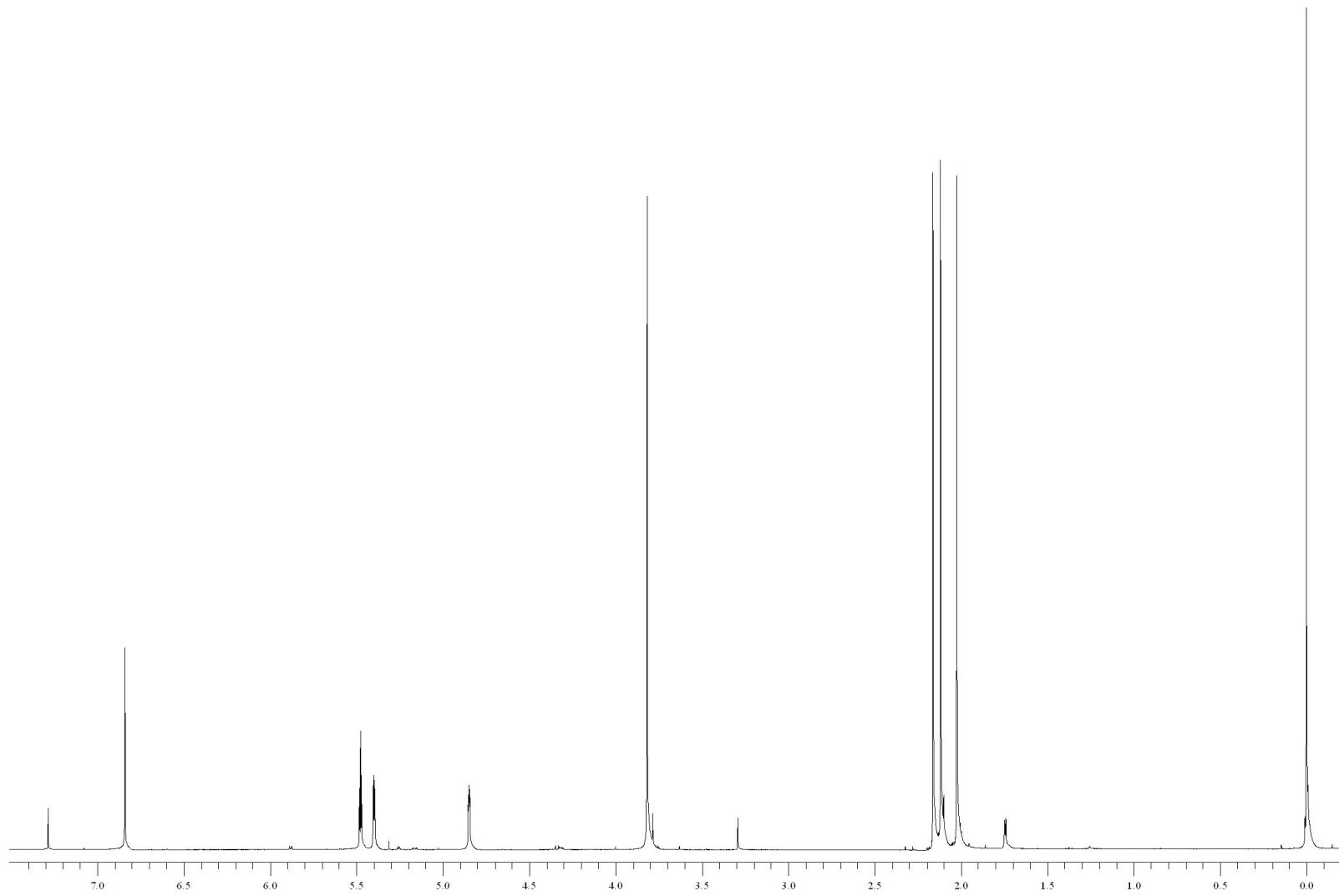


**Figure 33:** 400 MHz  $^1\text{H}$  NMR spectrum of methyl 2,3,4-tri-*O*-acetyl-1,5-anhydro-D-*arabino*-hex-1-enopyranuronate (7).

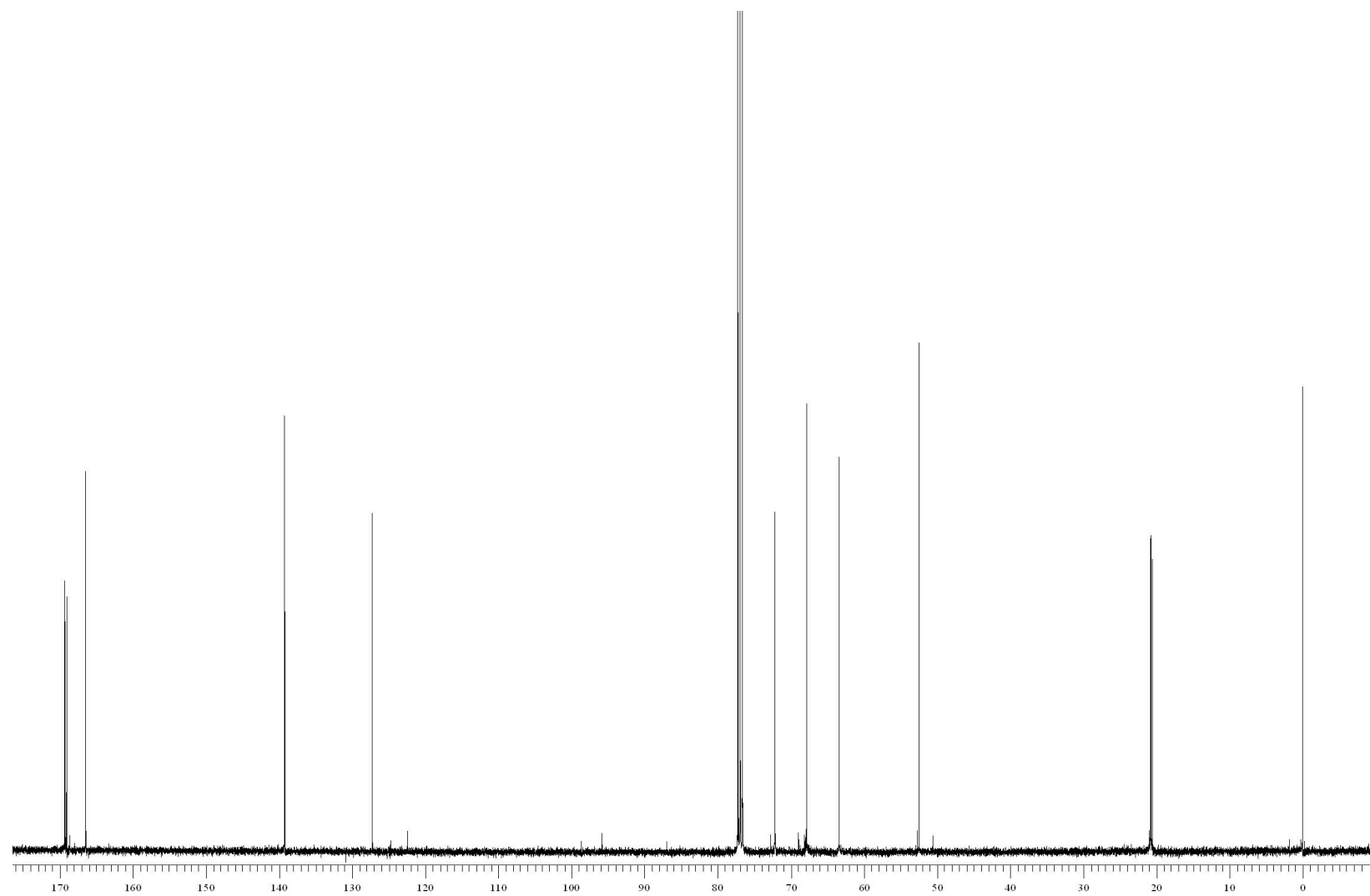


**Figure 34:** 100 MHz  $^{13}\text{C}$  NMR spectrum of methyl 2,3,4-tri-O-acetyl-1,5-anhydro-D-arabino-hex-1-enopyranuronate (7).

## Display Report

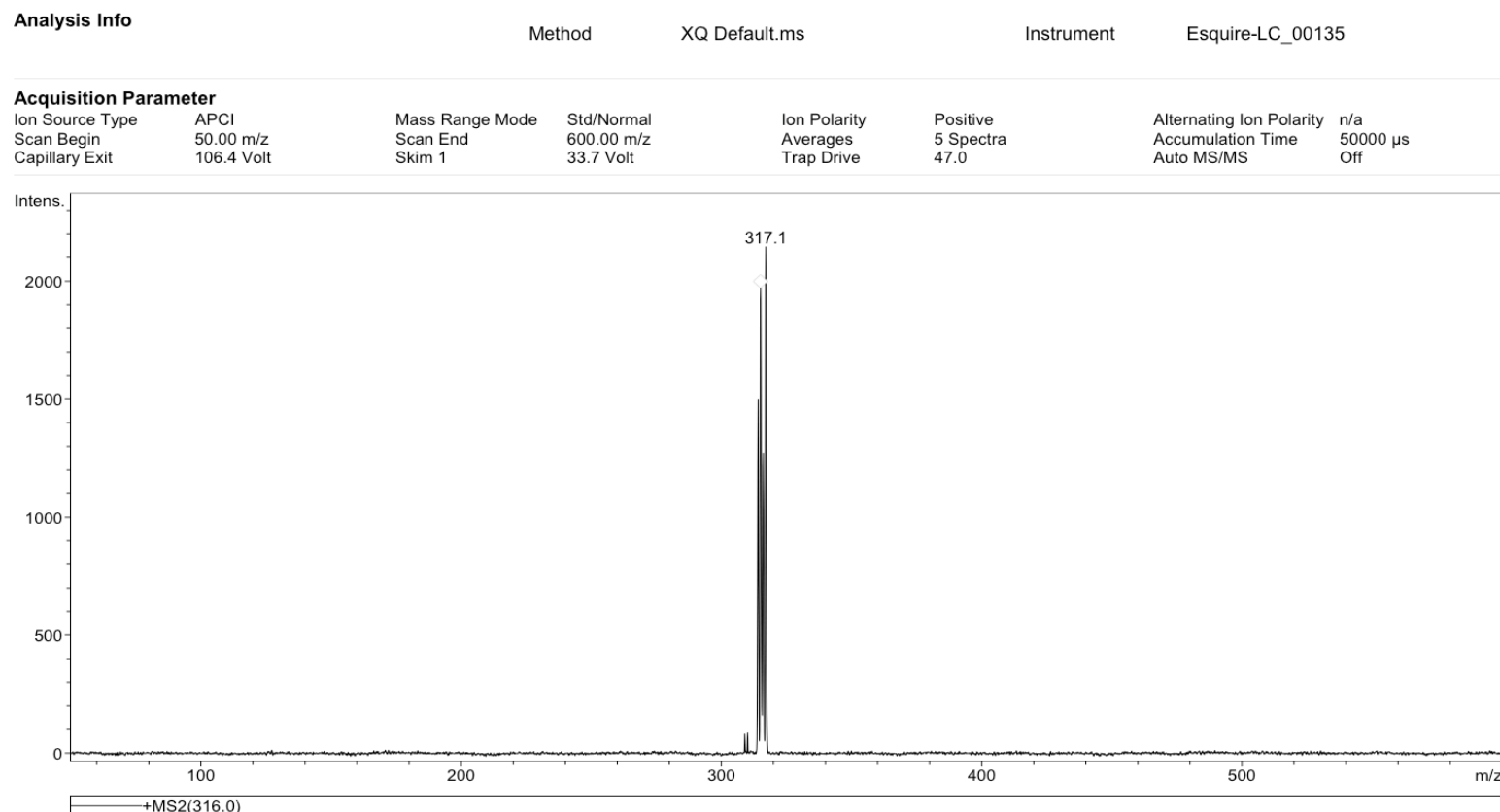


**Figure 35:** APCI mass spectrum of methyl 2,3,4-tri-*O*-acetyl-1,5-anhydro-D-*arabino*-hex-1-enopyranuronate (7).

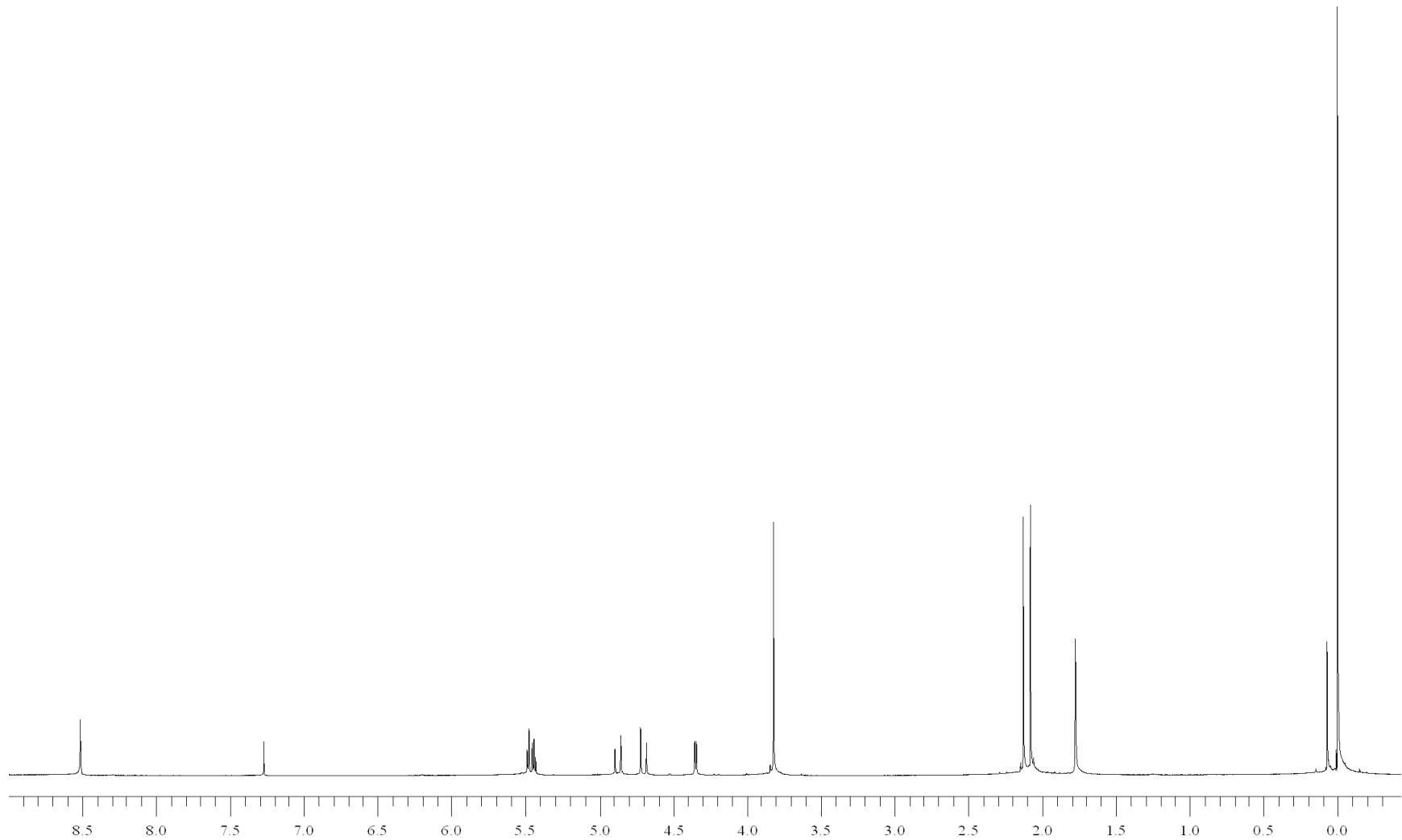


**Figure 36:** 400 MHz  $^1\text{H}$  NMR ( $\text{CDCl}_3$ ) spectrum of methyl 3,4-di-*O*-acetyl-2-deoxy-2-(hydroxyimino)-D-*arabino*-hex-2-enopyranuronate (**8**).

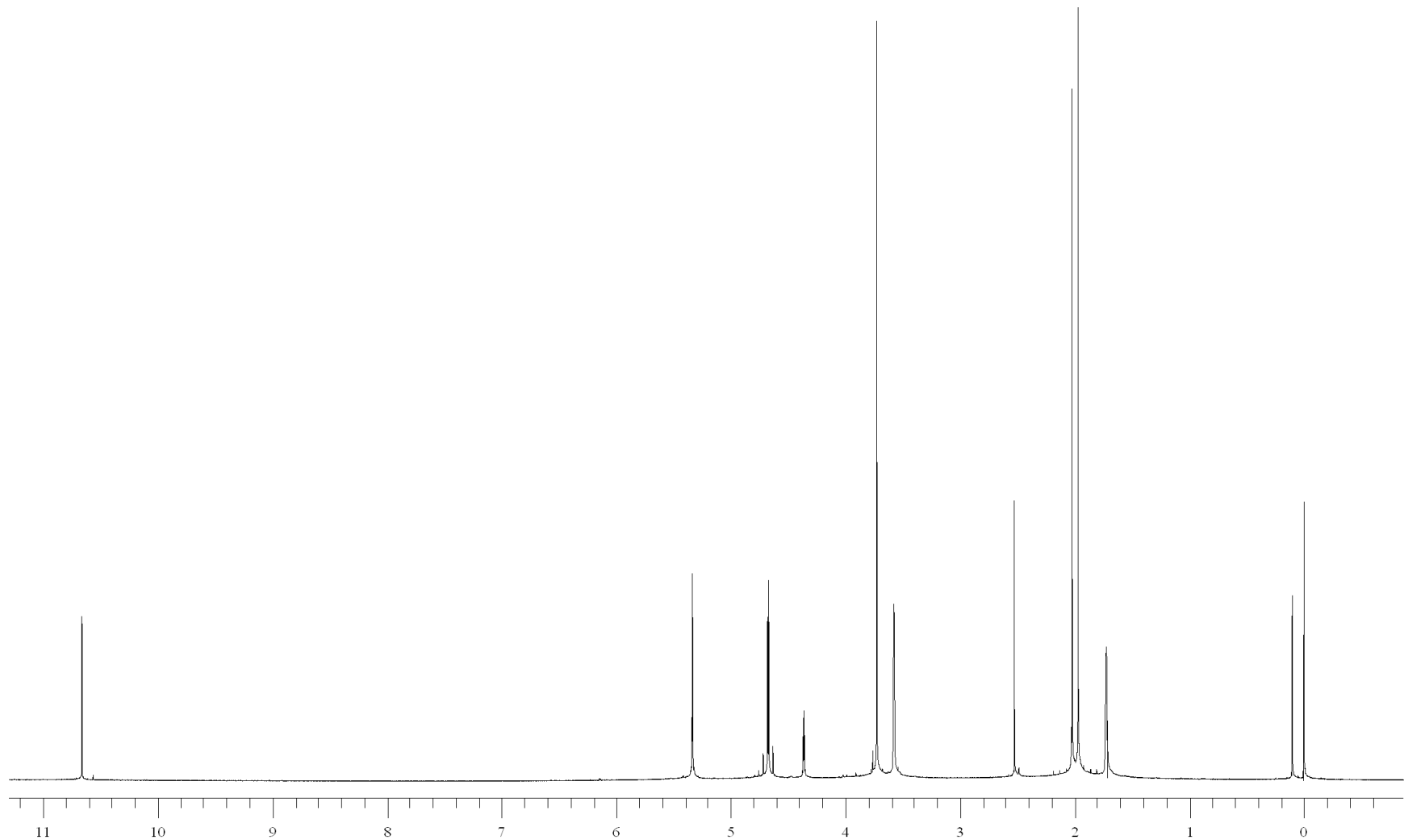


**Figure 37:** 400 MHz  $^1\text{H}$  NMR ( $\text{THF}-d_6$ ) spectrum of methyl 3,4-di-*O*-acetyl-2-deoxy-2-(hydroxyimino)-D-*arabino*-hex-2-enopyranuronate (**8**).

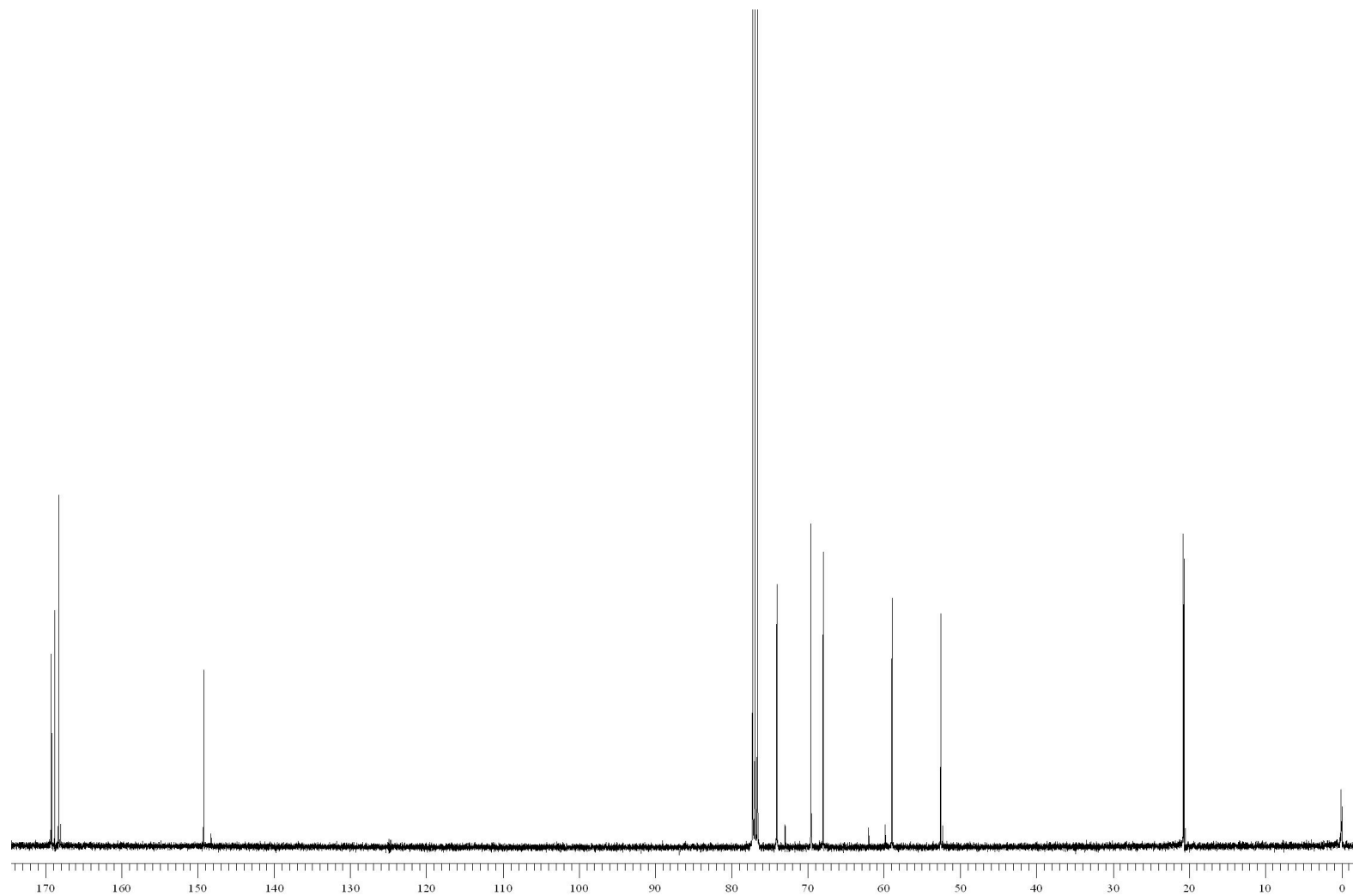


**Figure 38:** 100 MHz  $^{13}\text{C}$  NMR ( $\text{CDCl}_3$ ) spectrum of methyl 3,4-di-*O*-acetyl-2-deoxy-2-(hydroxyimino)-D-*arabino*-hex-2-enopyranuronate (**8**).

## Display Report

### Analysis Info

Method

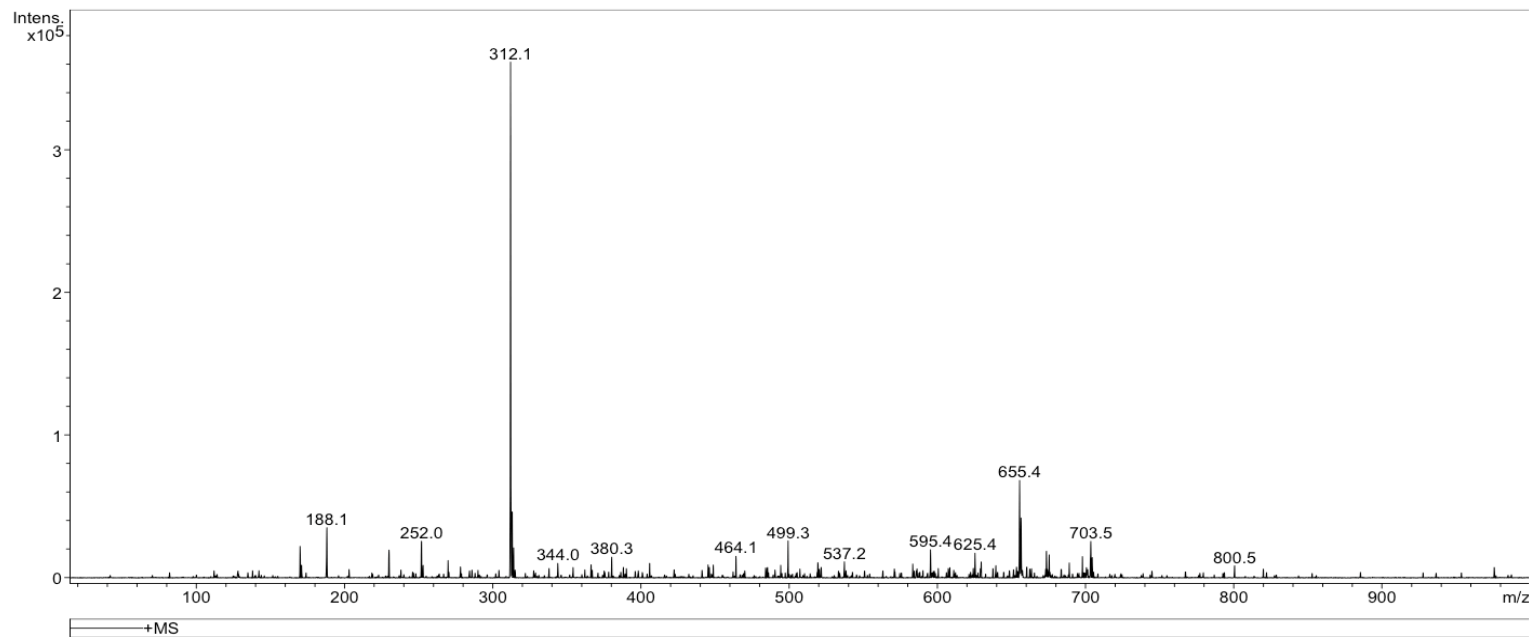
XQ Default.ms

Instrument

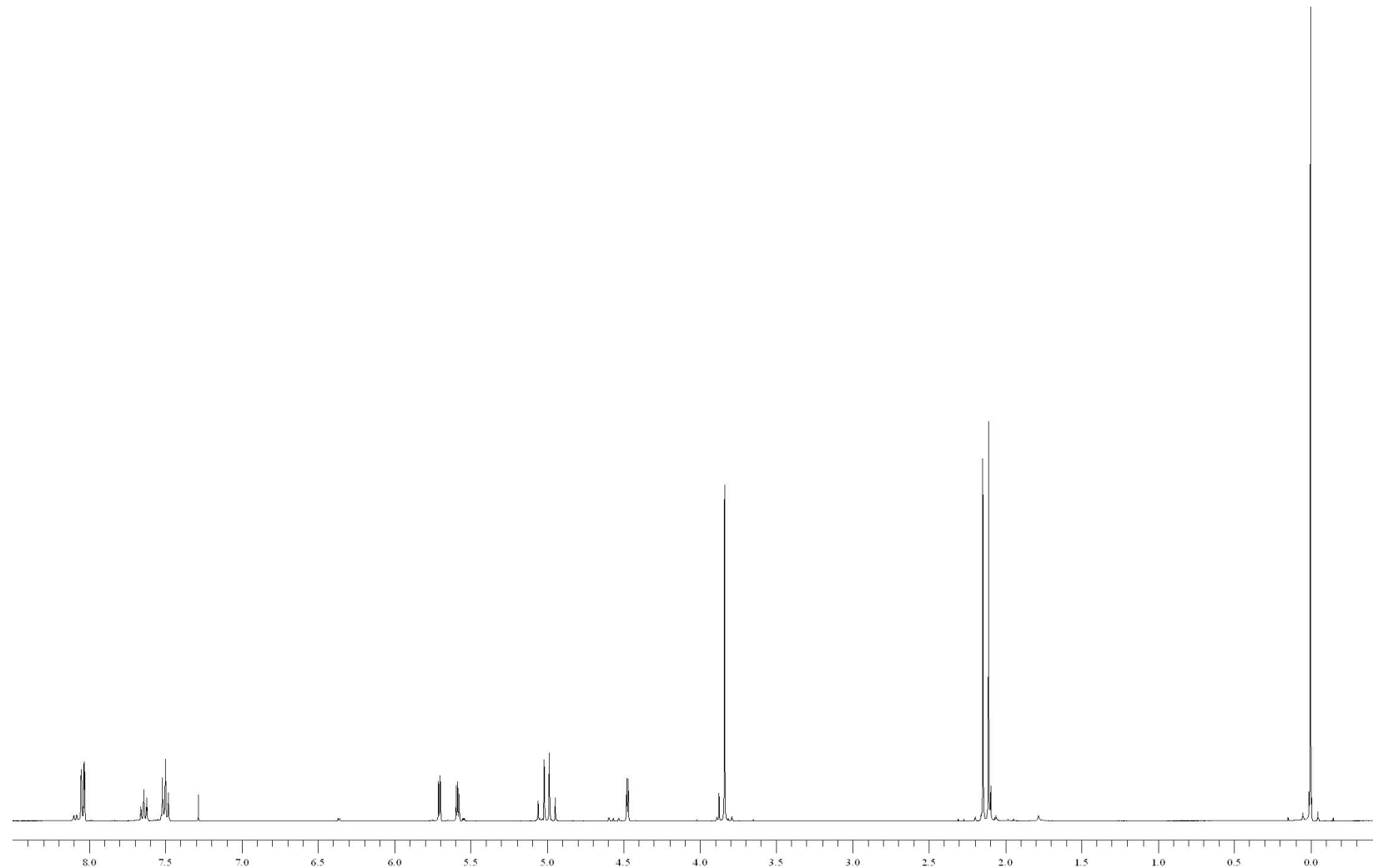
Esquire-LC\_00135

### Acquisition Parameter

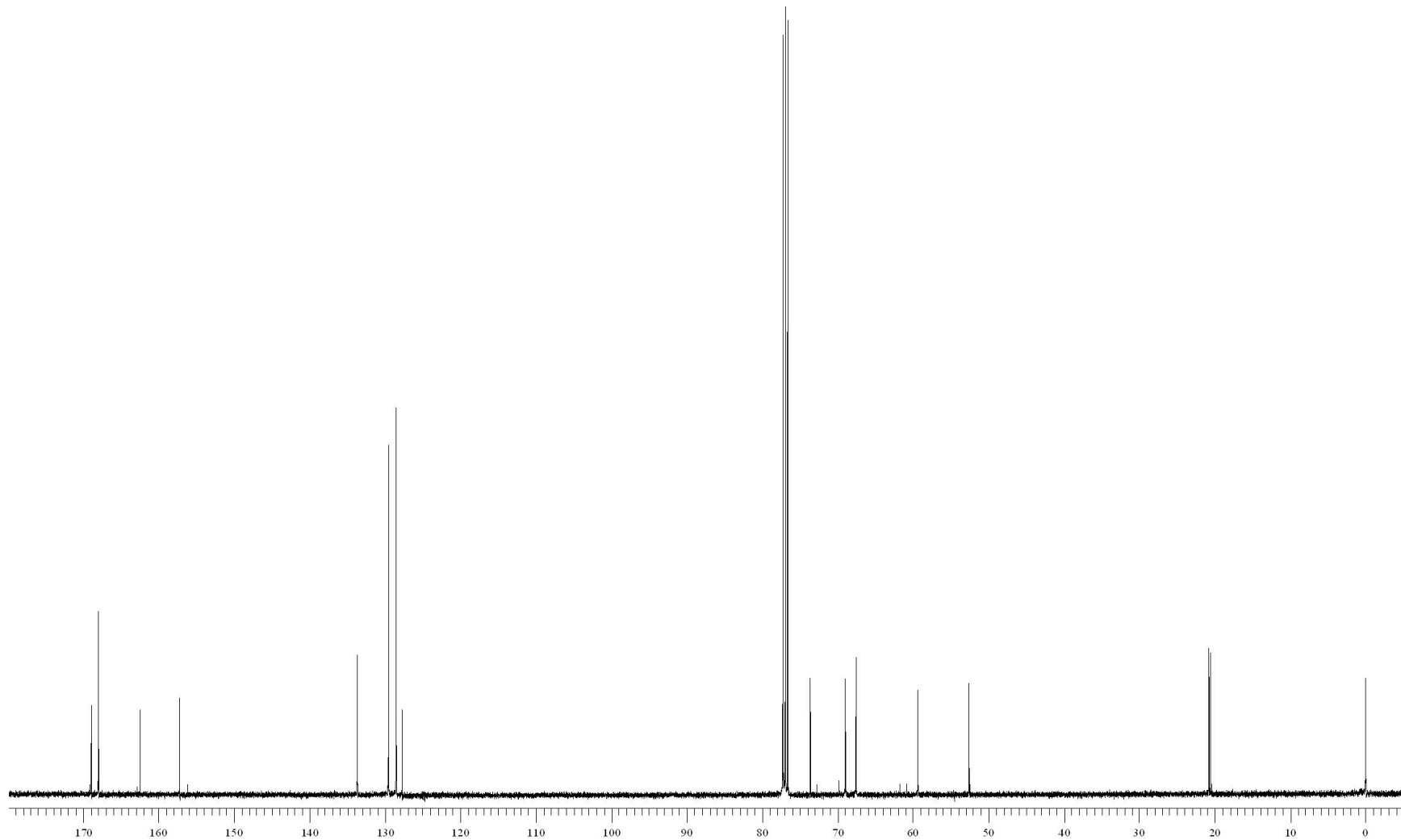
Ion Source Type	ESI	Mass Range Mode	Std/Normal	Ion Polarity	Positive	Alternating Ion Polarity	n/a
Scan Begin	15.00 m/z	Scan End	1000.00 m/z	Averages	5 Spectra	Accumulation Time	3280 $\mu$ s
Capillary Exit	104.1 Volt	Skim 1	32.0 Volt	Trap Drive	46.0	Auto MS/MS	Off



**Figure 39:** ESI mass spectrum of methyl 3,4-di-*O*-acetyl-2-deoxy-2-(hydroxyimino)-D-*arabino*-hex-2-enopyranuronate (**8**).

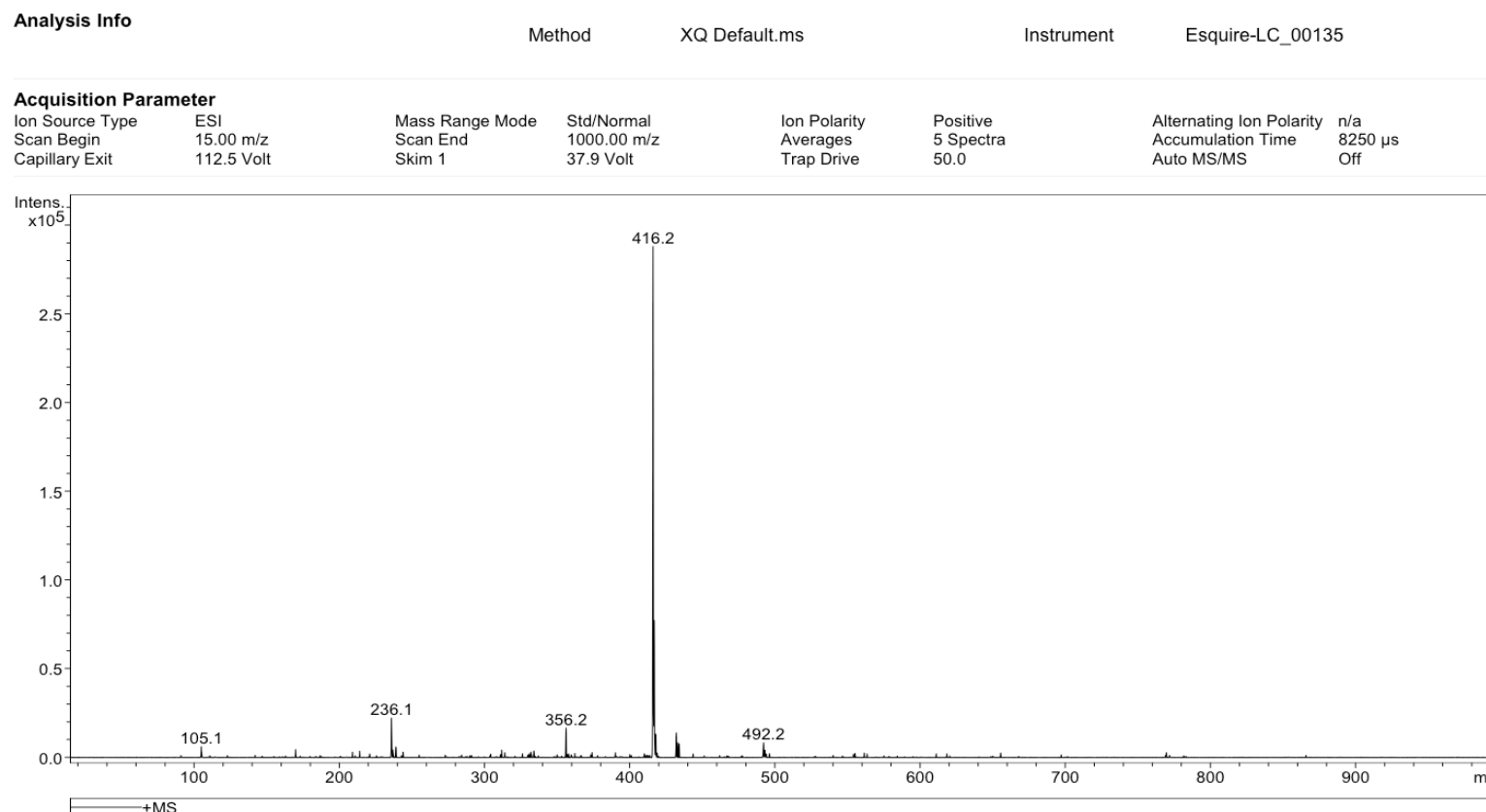


**Figure 40:** 400 MHz  $^1\text{H}$  NMR spectrum of methyl 3,4-di-*O*-acetyl-2-deoxy-2-(benzoyloxyimino)-D-*arabino*-hex-2-enopyranuronate (**9**).

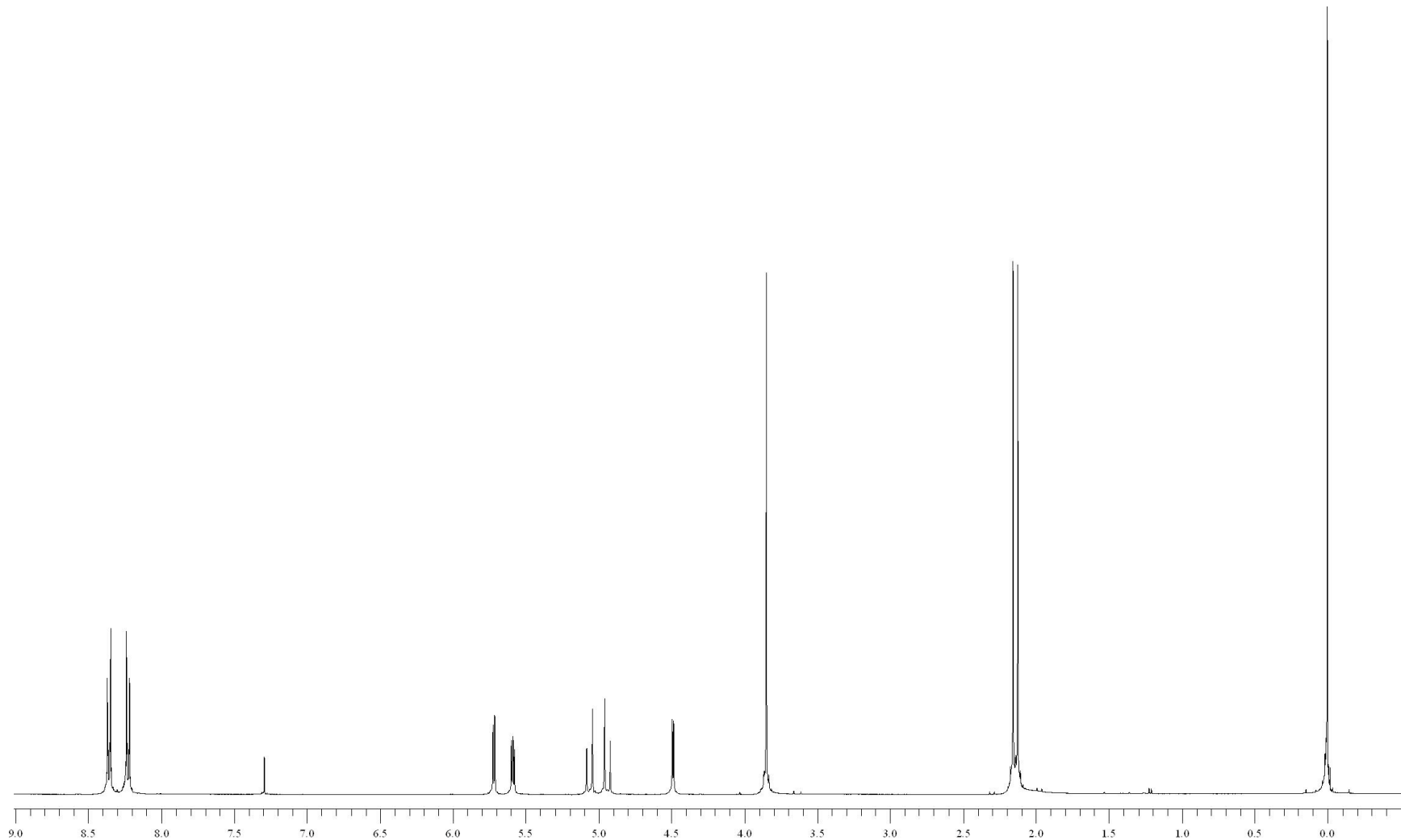


**Figure 41:** 100 MHz  $^{13}\text{C}$  NMR spectrum of methyl 3,4-di-*O*-acetyl-2-deoxy-2-(benzoyloxyimino)-D-*arabino*-hex-2-enopyranuronate (**9**).

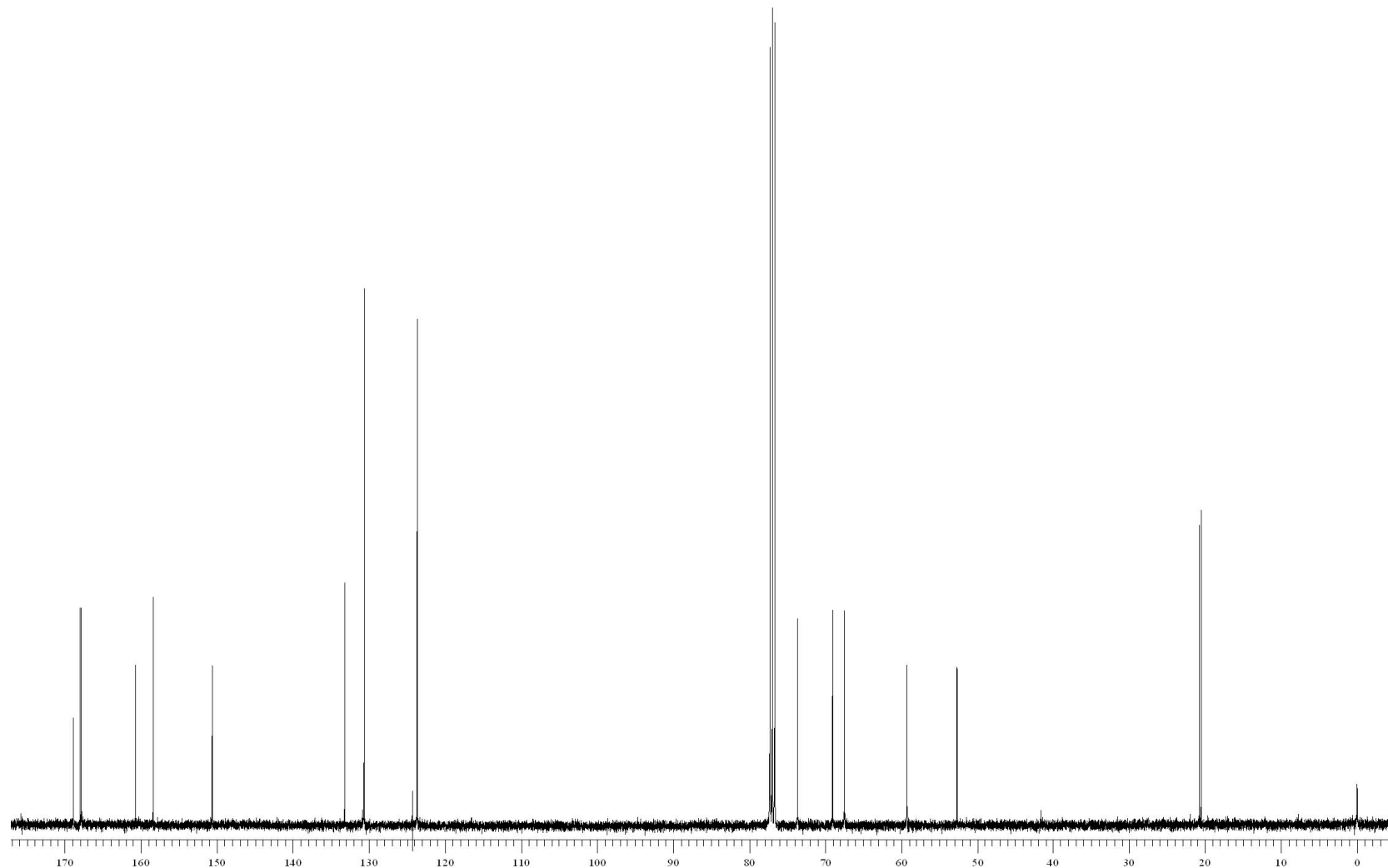
## Display Report



**Figure 42:** ESI mass spectrum of methyl 3,4-di-*O*-acetyl-2-deoxy-2-(benzoyloxyimino)-D-*arabino*-hex-2-enopyranuronate (**9**).

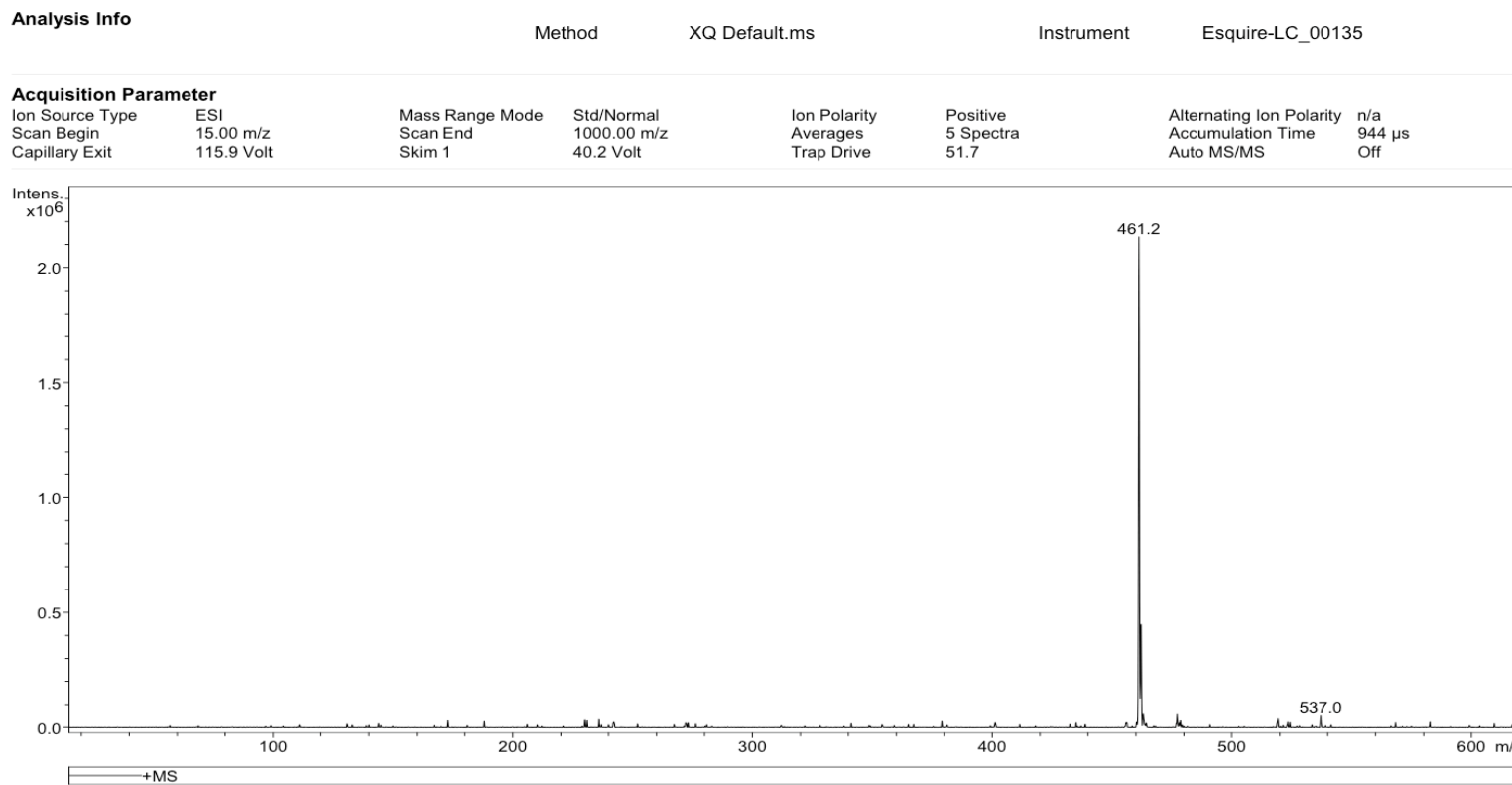


**Figure 43:** 400 MHz  $^1\text{H}$  NMR spectrum of methyl 3,4-di-*O*-acetyl-2-deoxy-2-(4-nitrobenzoyloxyimino)-D-*arabino*-hex-2-enopyranuronate (**10**).

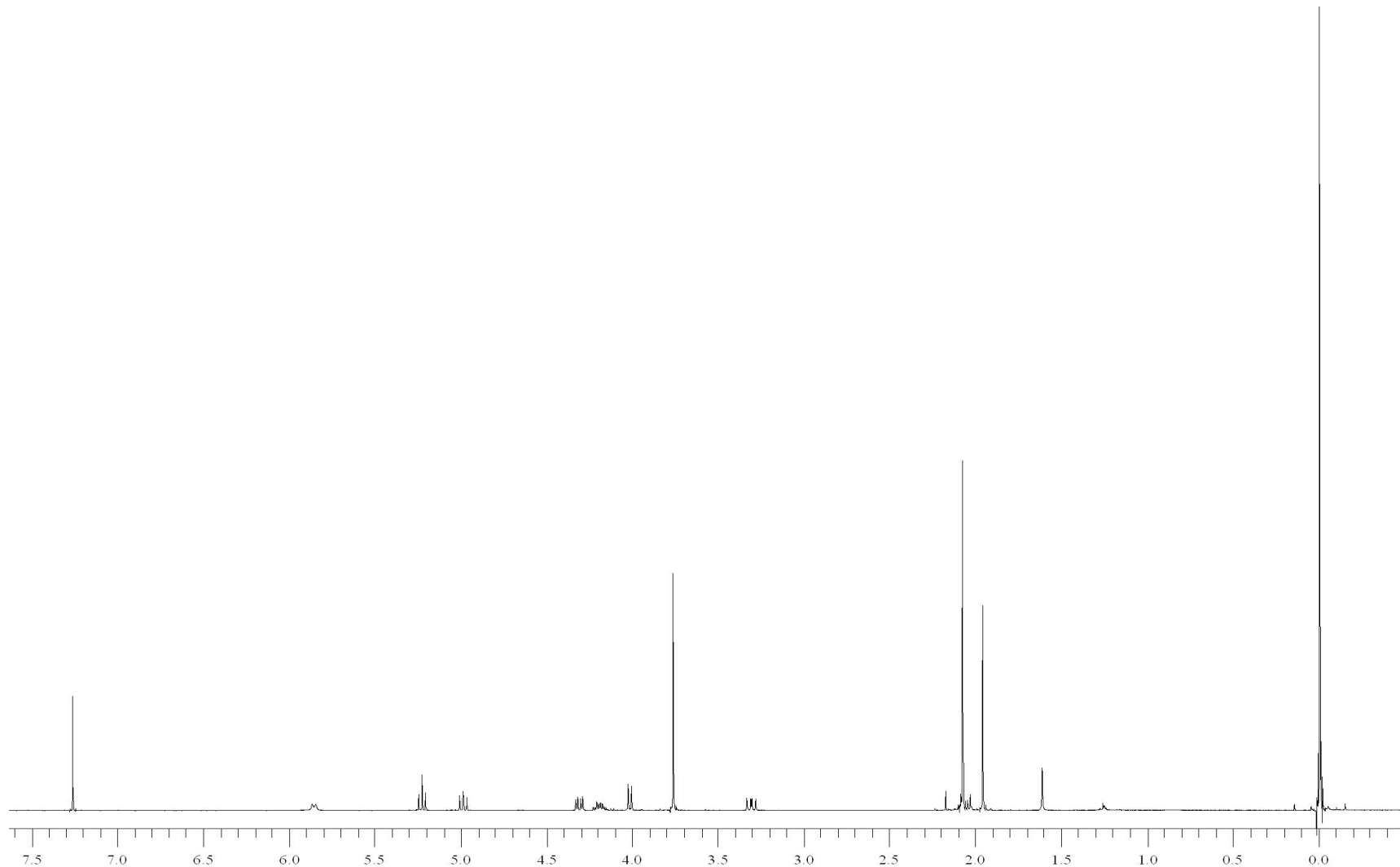


**Figure 44:** 100 MHZ  $^{13}\text{C}$  NMR spectrum of methyl 3,4-di-*O*-acetyl-2-deoxy-2-(4-nitrobenzoyloxyimino)-D-*arabino*-hex-2-enopyranuronate (**10**).

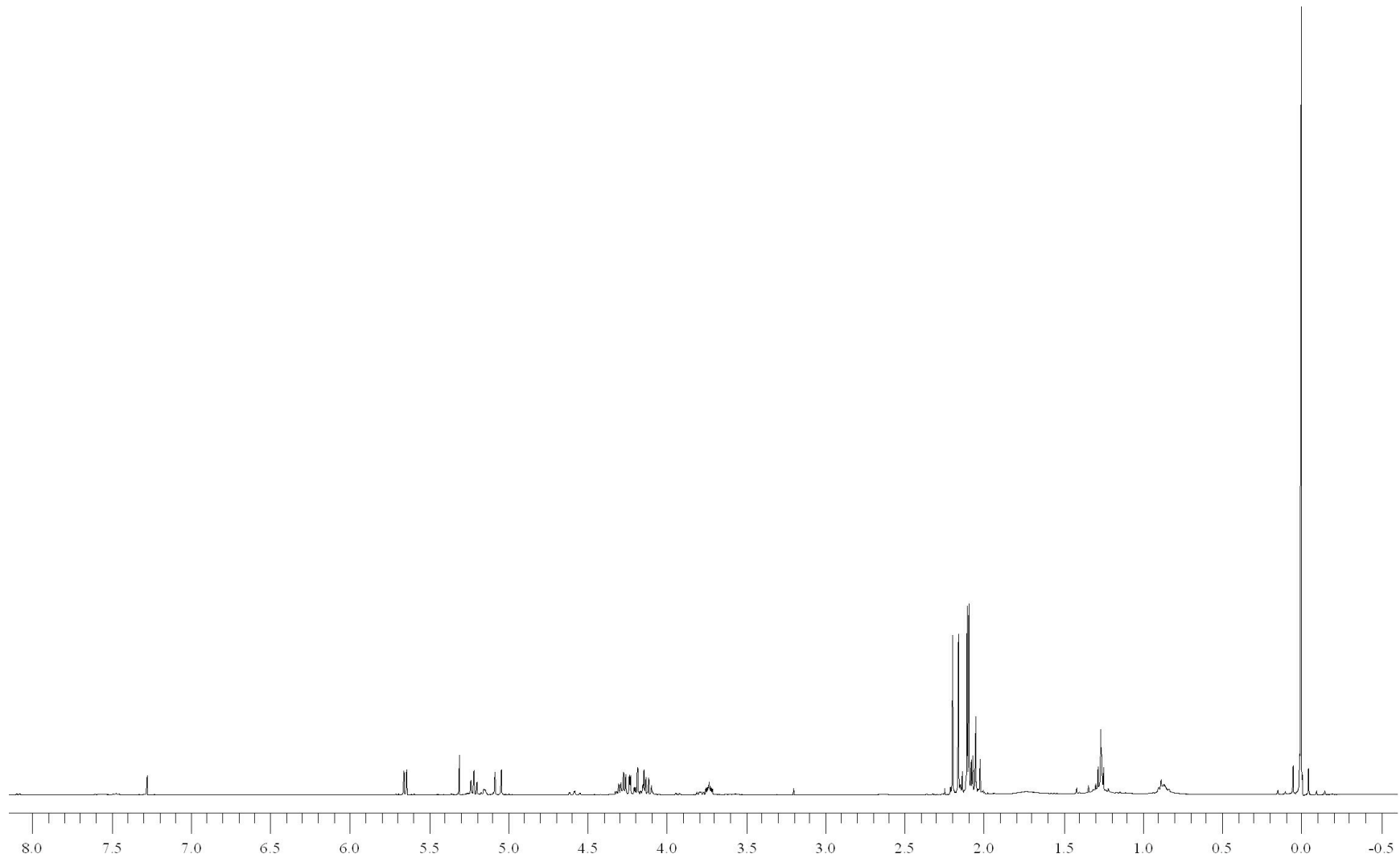
## Display Report



**Figure 45:** ESI mass spectrum of methyl 3,4-di-*O*-acetyl-1,2-dideoxy-2-(4-nitrobenzoyloxyimino)-D-*arabino*-hex-2-enopyranuronate (**10**).

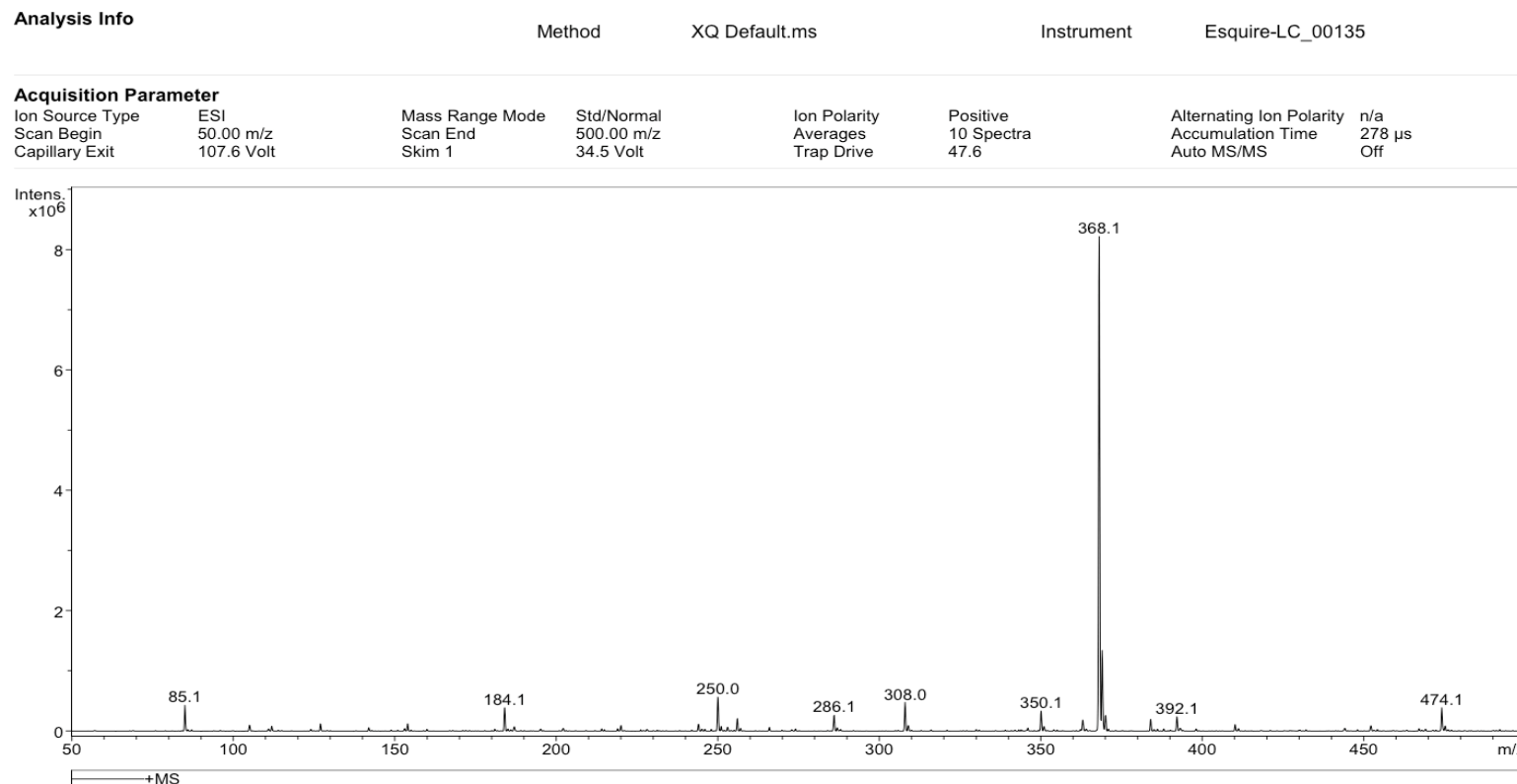


**Figure 46:** 400 MHz  $^1\text{H}$  NMR spectrum of methyl 3,4-di-*O*-acetyl-1,2-dideoxy-2-acetamido-D-glucopyranuronate (**13**).

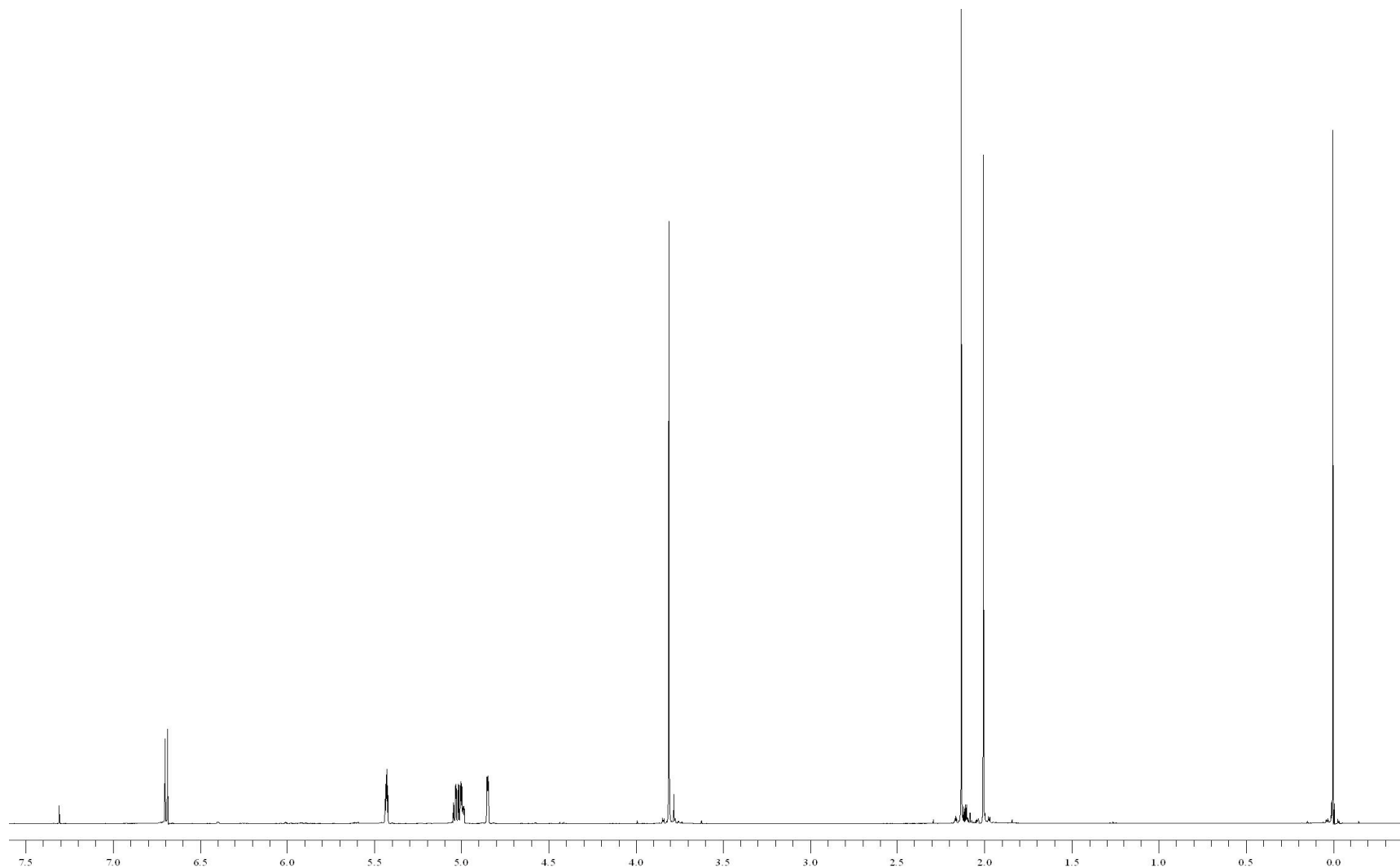


**Figure 47:** 400 MHz  $^1\text{H}$  NMR of methyl 3,4,6-tri-*O*-acetyl-2-deoxy-2-(acetyloxyimino)-D-*arabino*-hex-2-enopyranuronate (**14**).

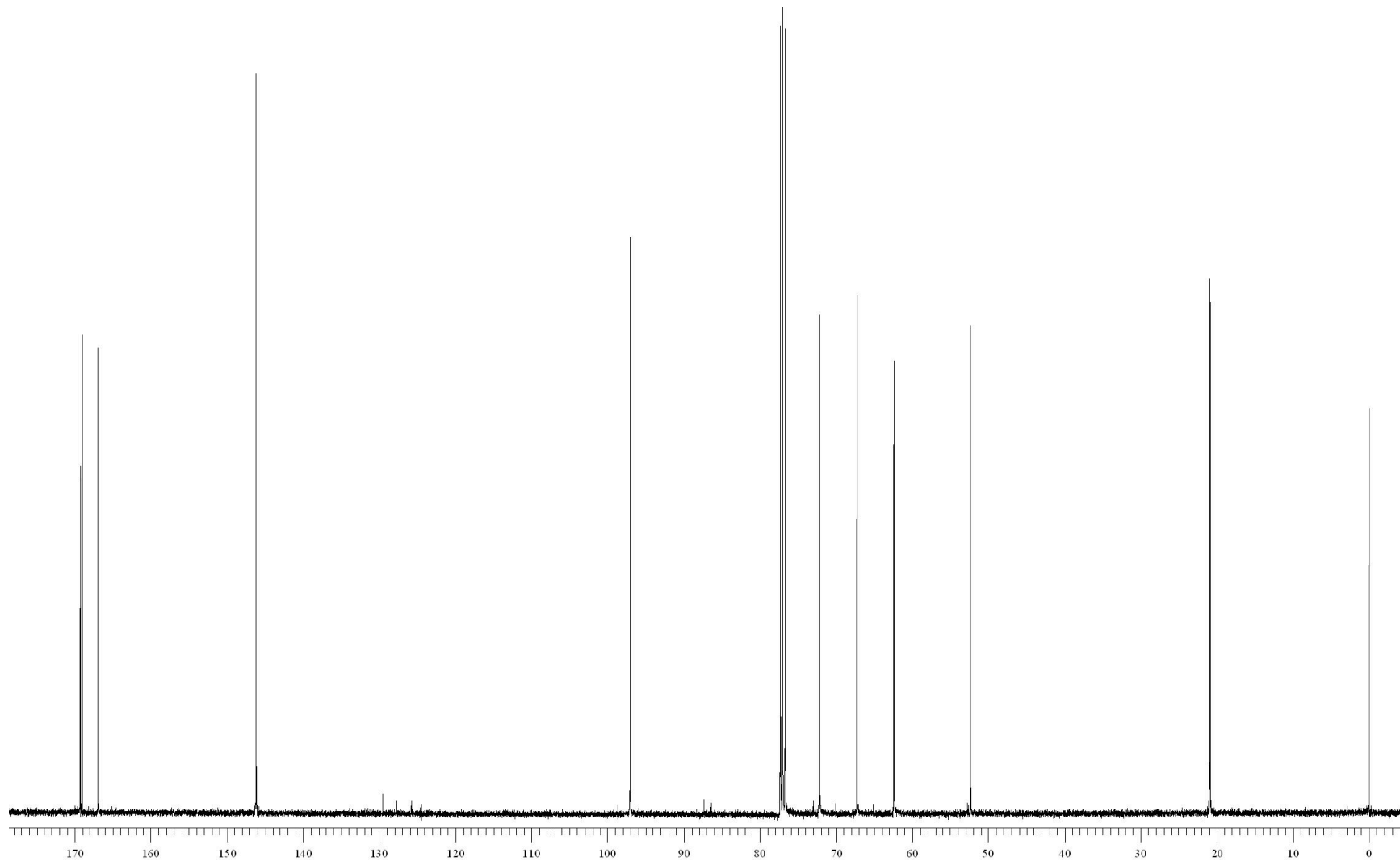
## Display Report



**Figure 48:** ESI mass spectrum of methyl 3,4,6-tri-O-acetyl-2-deoxy-2-(acetyloxyimino)-D-arabino-hex-2-enopyranuronate (**14**).

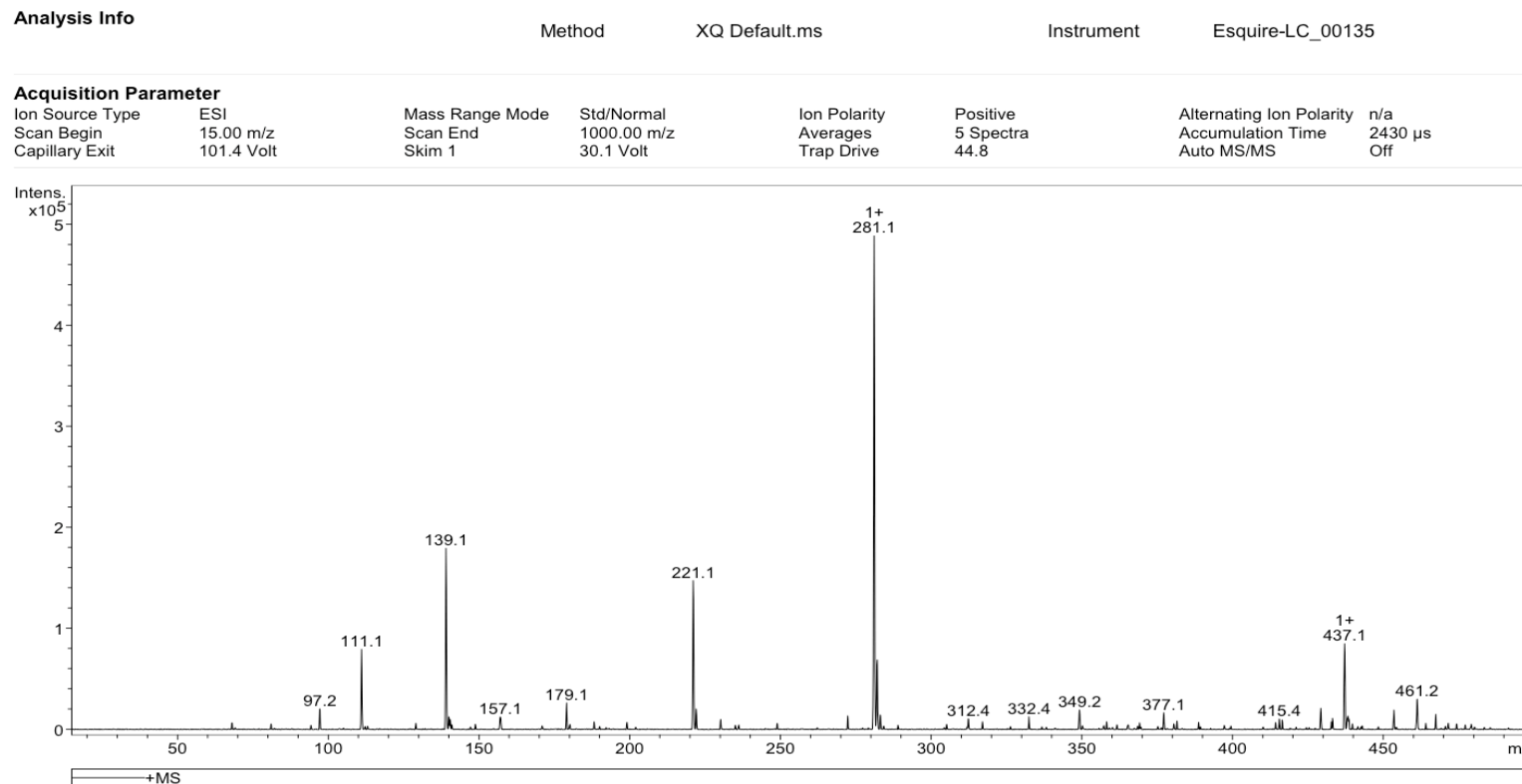


**Figure 49:** 400 MHz  $^1\text{H}$  NMR spectrum of methyl 3,4-di-*O*-acetyl-1,5-anhydro-2-deoxy-D-*arabino*-hex-1-enopyranuronate (**15**). 105

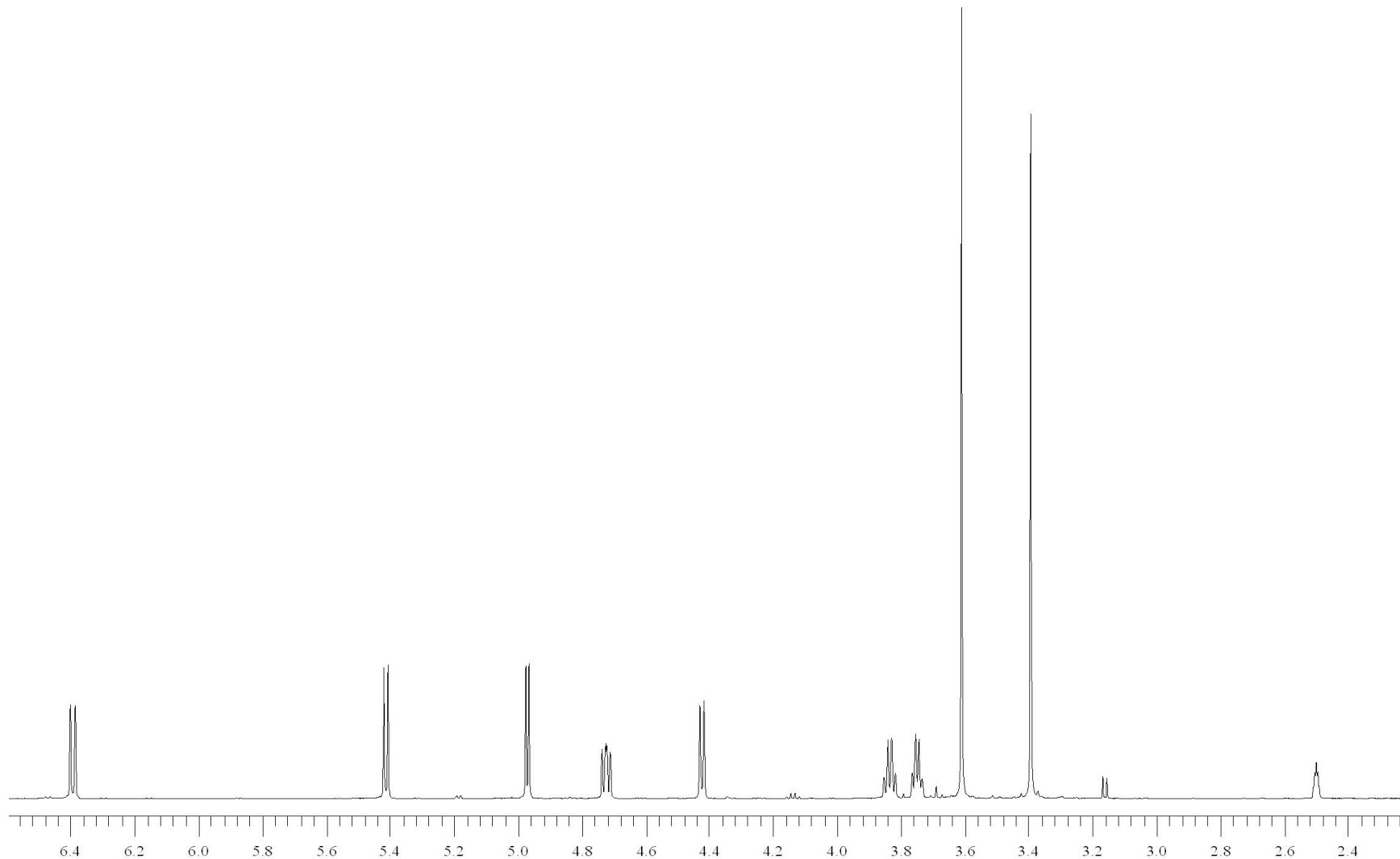


**Figure 50:** 100 MHz  $^{13}\text{C}$  NMR spectrum of methyl 3,4-di-*O*-acetyl-1,5-anhydro-2-deoxy-D-*arabino*-hex-1-enopyranuronate (**15**).

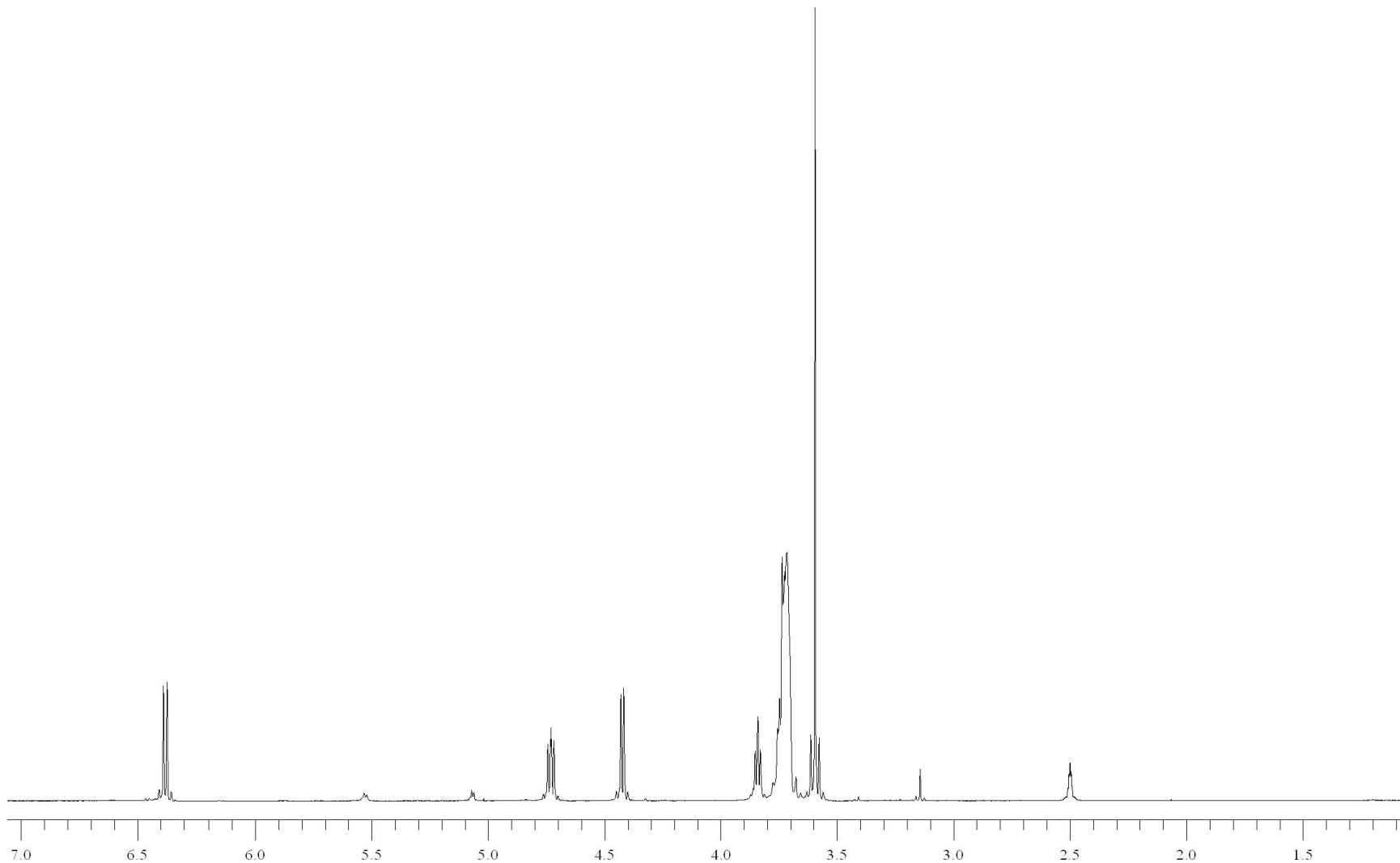
## Display Report



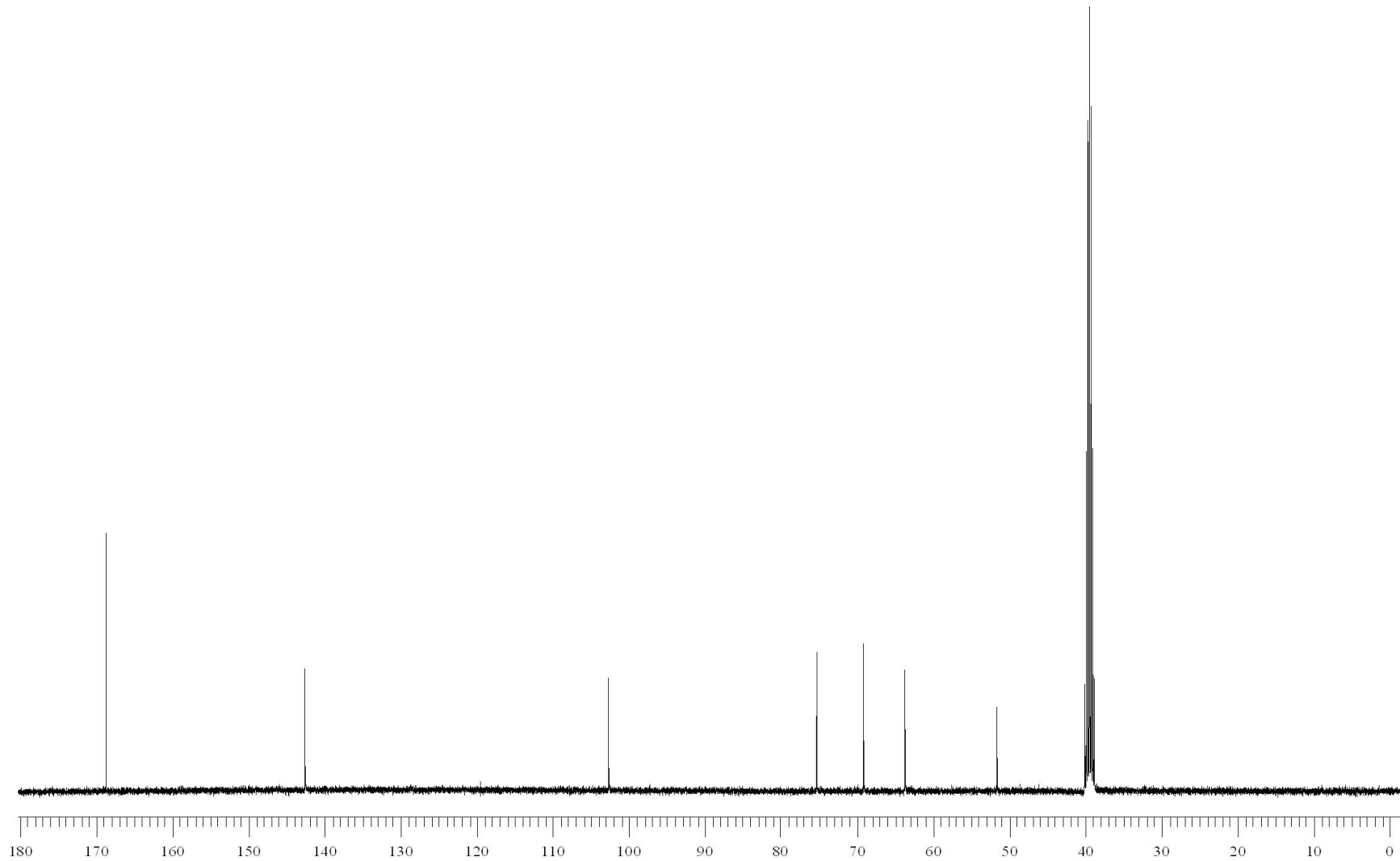
**Figure 51:** ESI mass spectrum of methyl 3,4-di-*O*-acetyl-1,5-anhydro-2-deoxy-D-*arabino*-hex-1-enopyranuronate (**15**).



**Figure 52:** 400 MHz  $^1\text{H}$  NMR spectrum of methyl 1,5-anhydro-2-deoxy-D-*arabino*-hex-1-enopyranuronate (**16**).

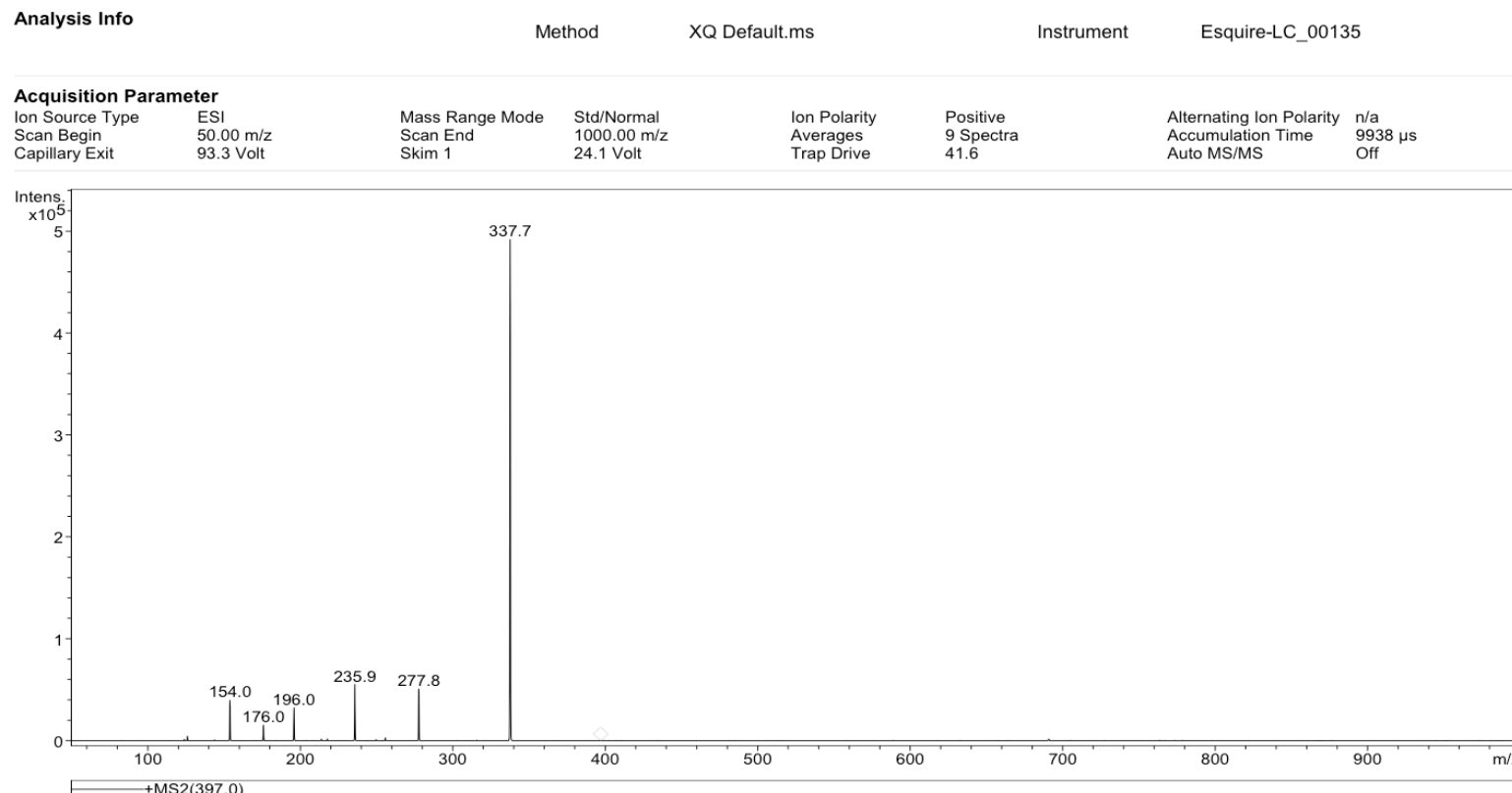


**Figure 53:** 400 MHz  $^1\text{H}$  NMR spectrum of methyl 1,5-anhydro-2-deoxy-D-arabino-hex-1-enopyranuronate (**16**) treated with  $\text{D}_2\text{O}$ .



**Figure 54:** 100 MHz  $^{13}\text{C}$  NMR spectrum of methyl 1,5-anhydro-2-deoxy-D-*arabino*-hex-1-enopyranuronate (**16**).

## Display Report



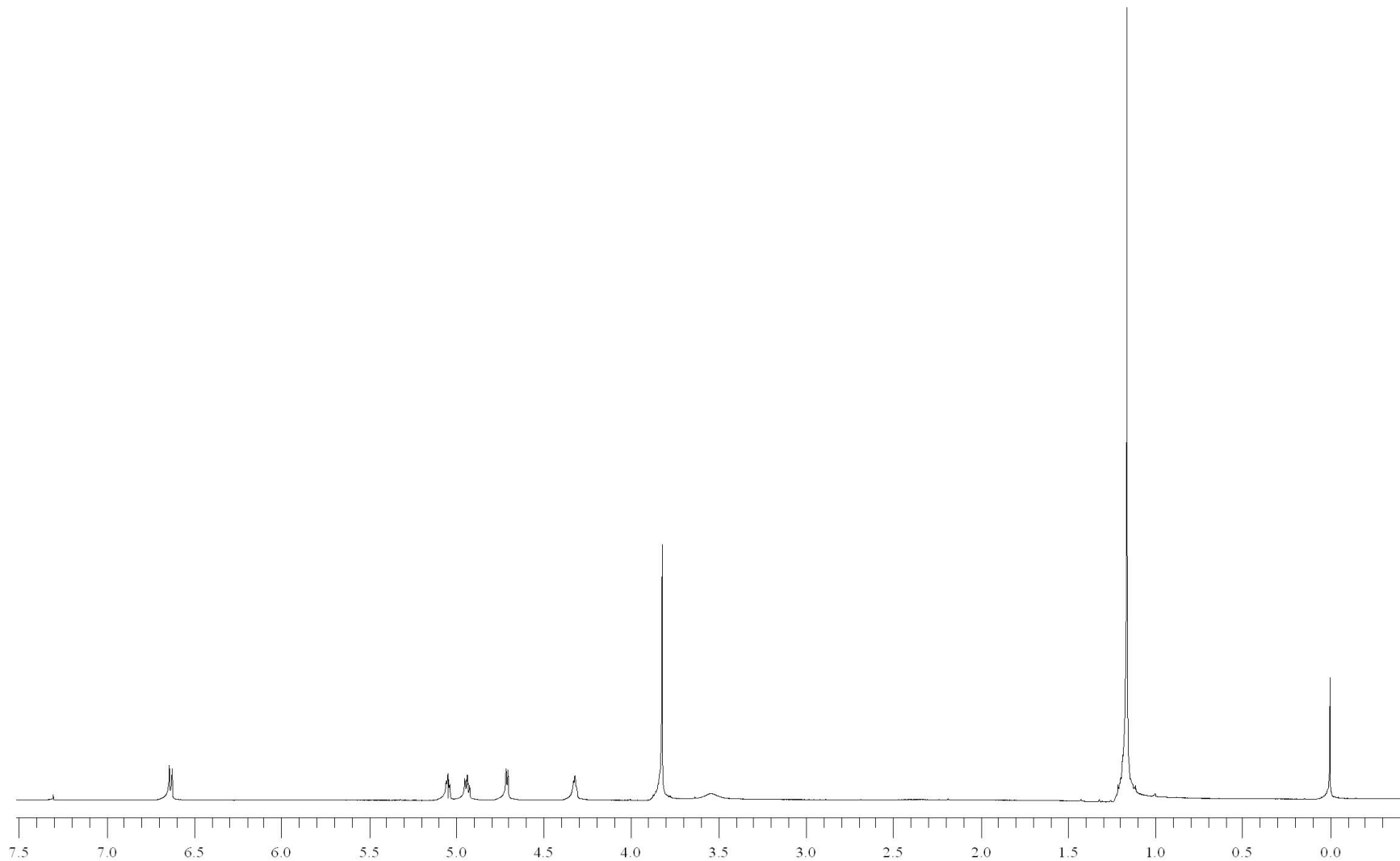


**Figure 56:** 400 MHz  $^1\text{H}$  NMR spectrum of methyl 1,5-anhydro-2-deoxy-3-*O*-pivaloyl-D-*arabino*-hex-1-enopyranuronate (**17**).

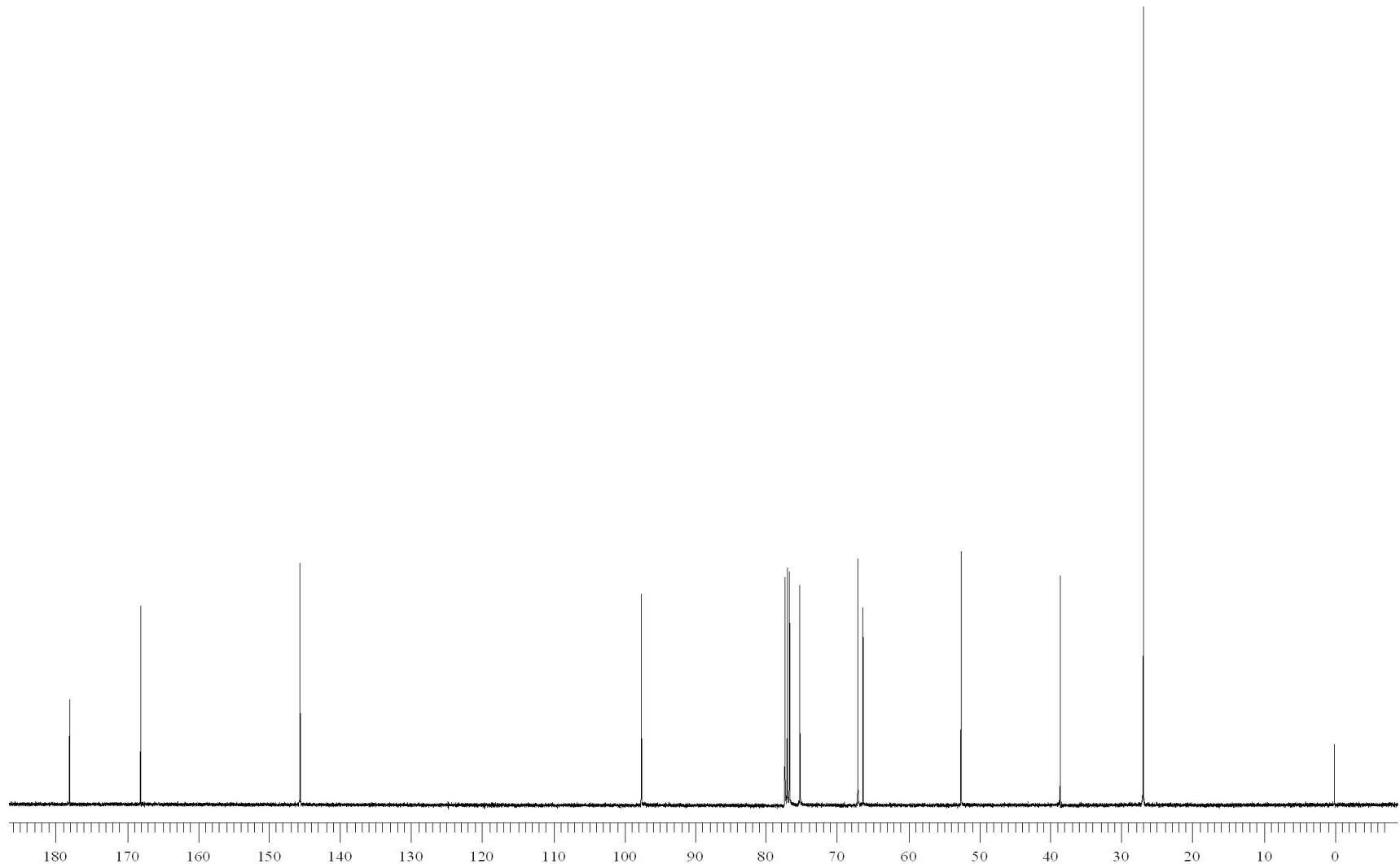


**Figure 57:** 100 MHz  $^{13}\text{C}$  NMR spectrum of methyl 1,5-anhydro-2-deoxy-3-*O*-pivaloyl-D-*arabino*-hex-1-enopyranuronate (**17**).

## Display Report

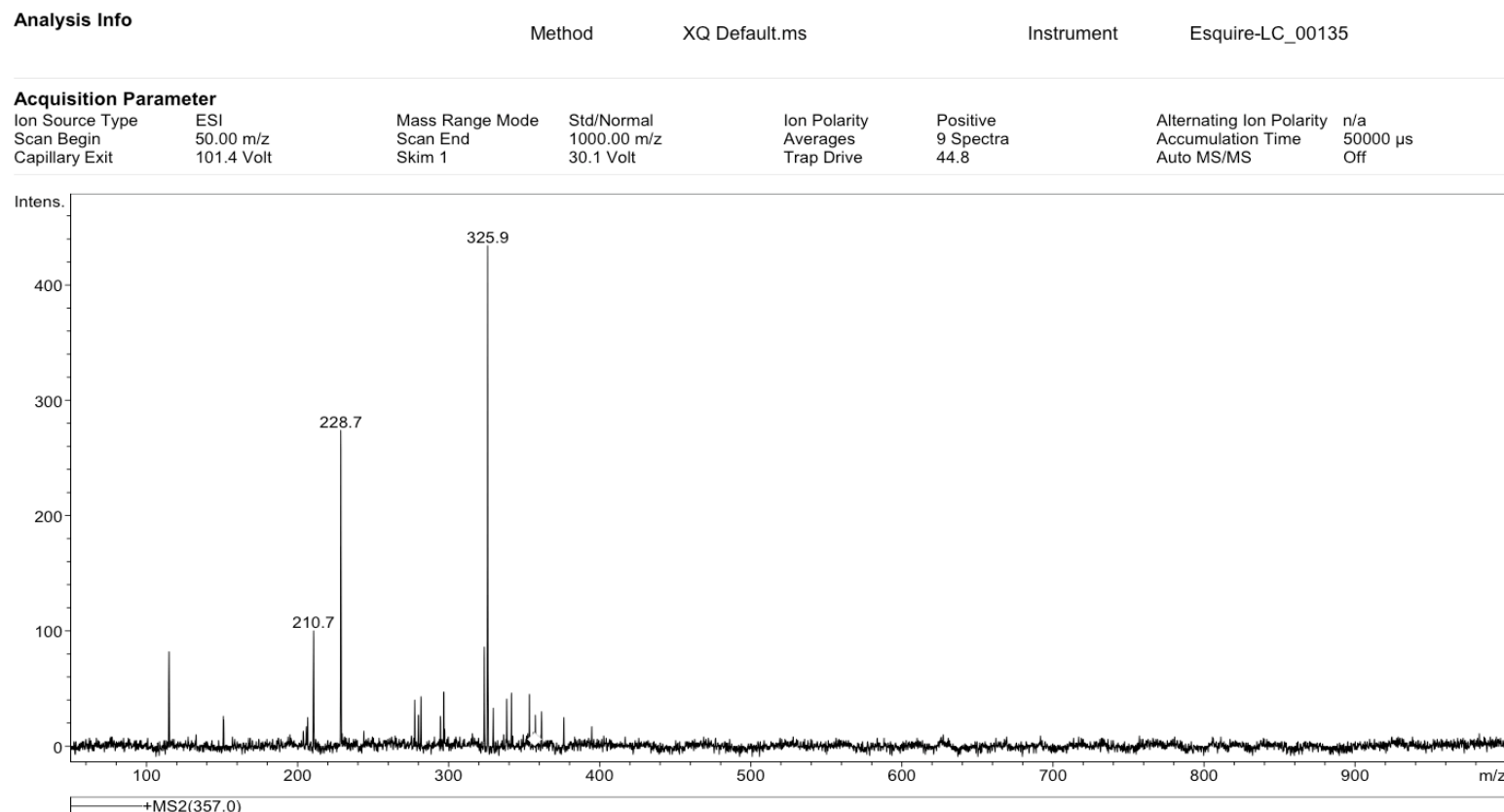


**Figure 58:** ESI mass spectrum of methyl 1,5-anhydro-2-deoxy-3-O-pivaloyl-D-arabino-hex-1-enopyranuronate (**17**).

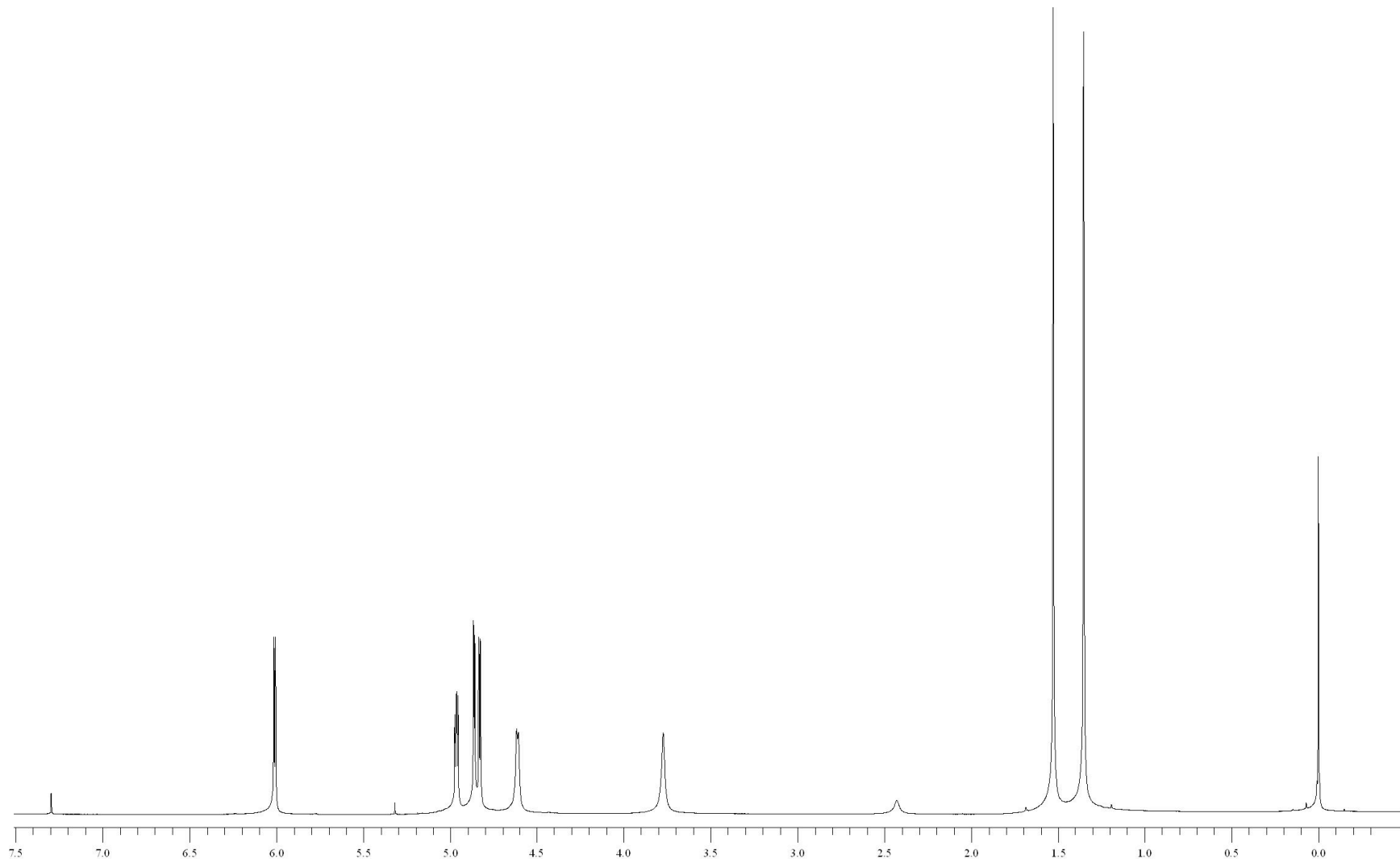


**Figure 59:** 400 MHz  $^1\text{H}$  NMR spectrum of 1,2-*O*-isopropylidene- $\alpha$ -D-glucofuranosidurono-6,3-lactone (**19**).

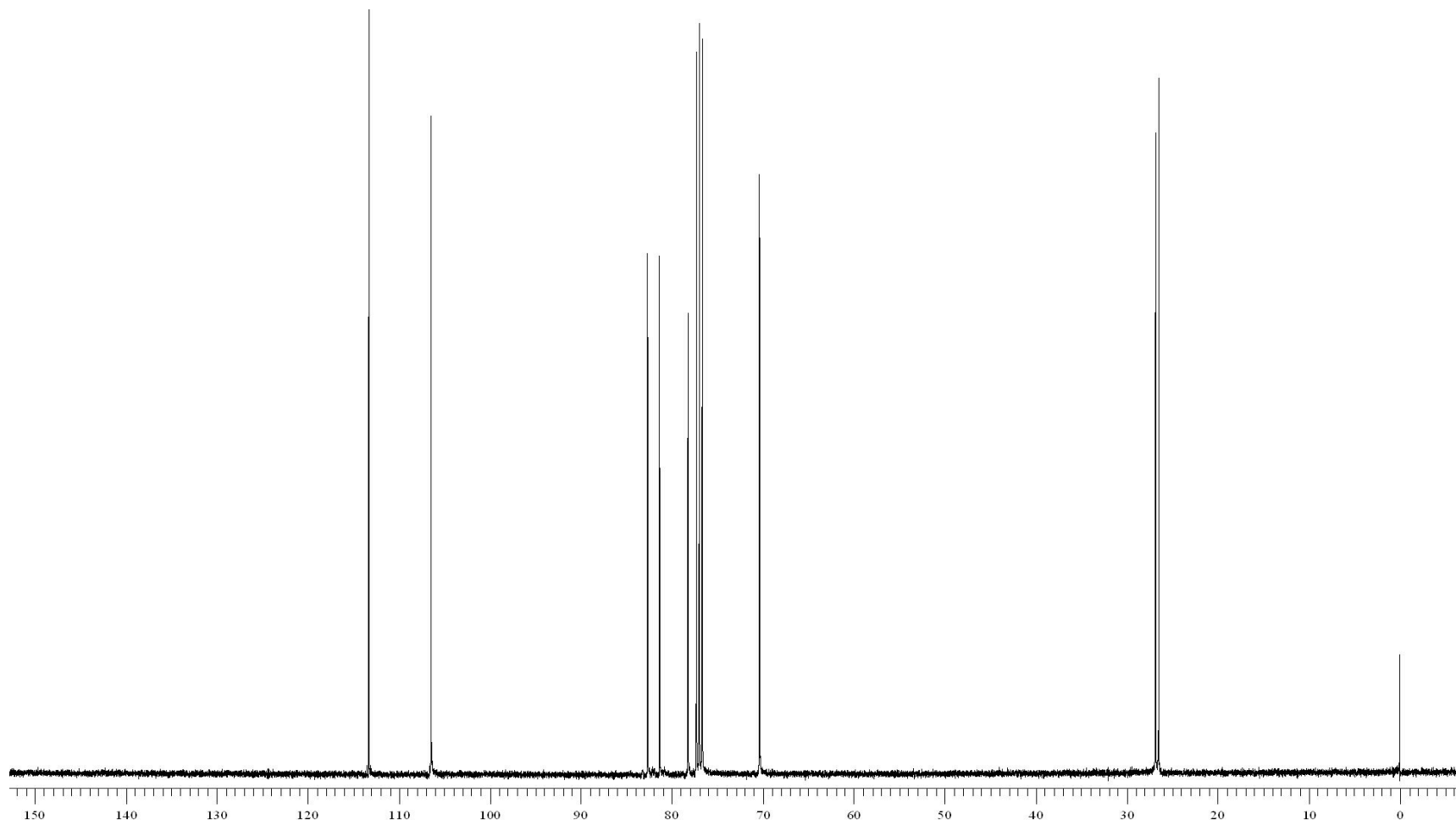


**Figure 60:** 100 MHz  $^{13}\text{C}$  NMR spectrum of 1,2-*O*-isopropylidene- $\alpha$ -D-glucofuranosidurono-6,3-lactone (**19**).

## Display Report

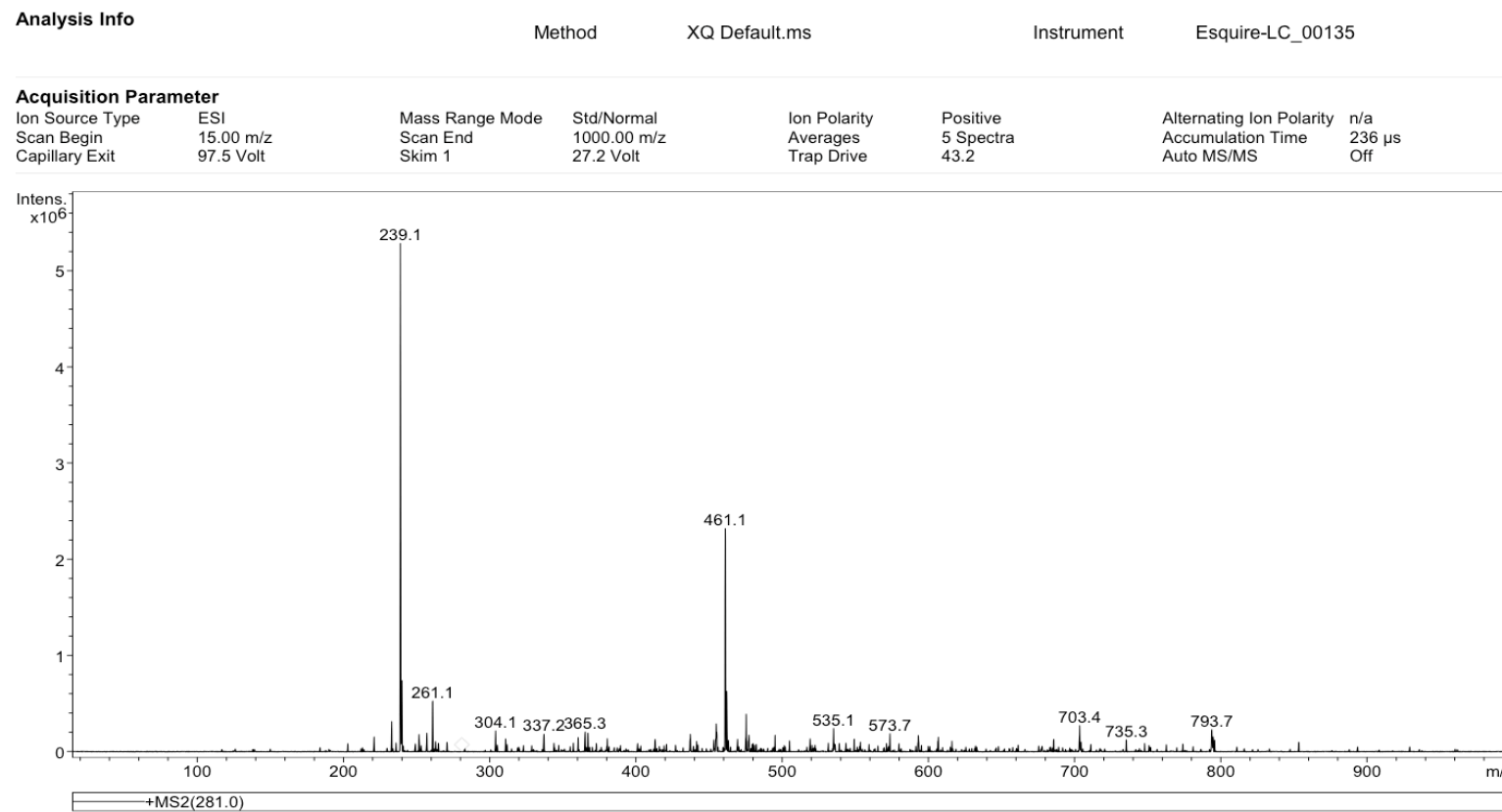


**Figure 61:** ESI mass spectrum of 1,2-*O*-isopropylidene- $\alpha$ -D-glucofuranosiduron-6,3-lactone (**19**).

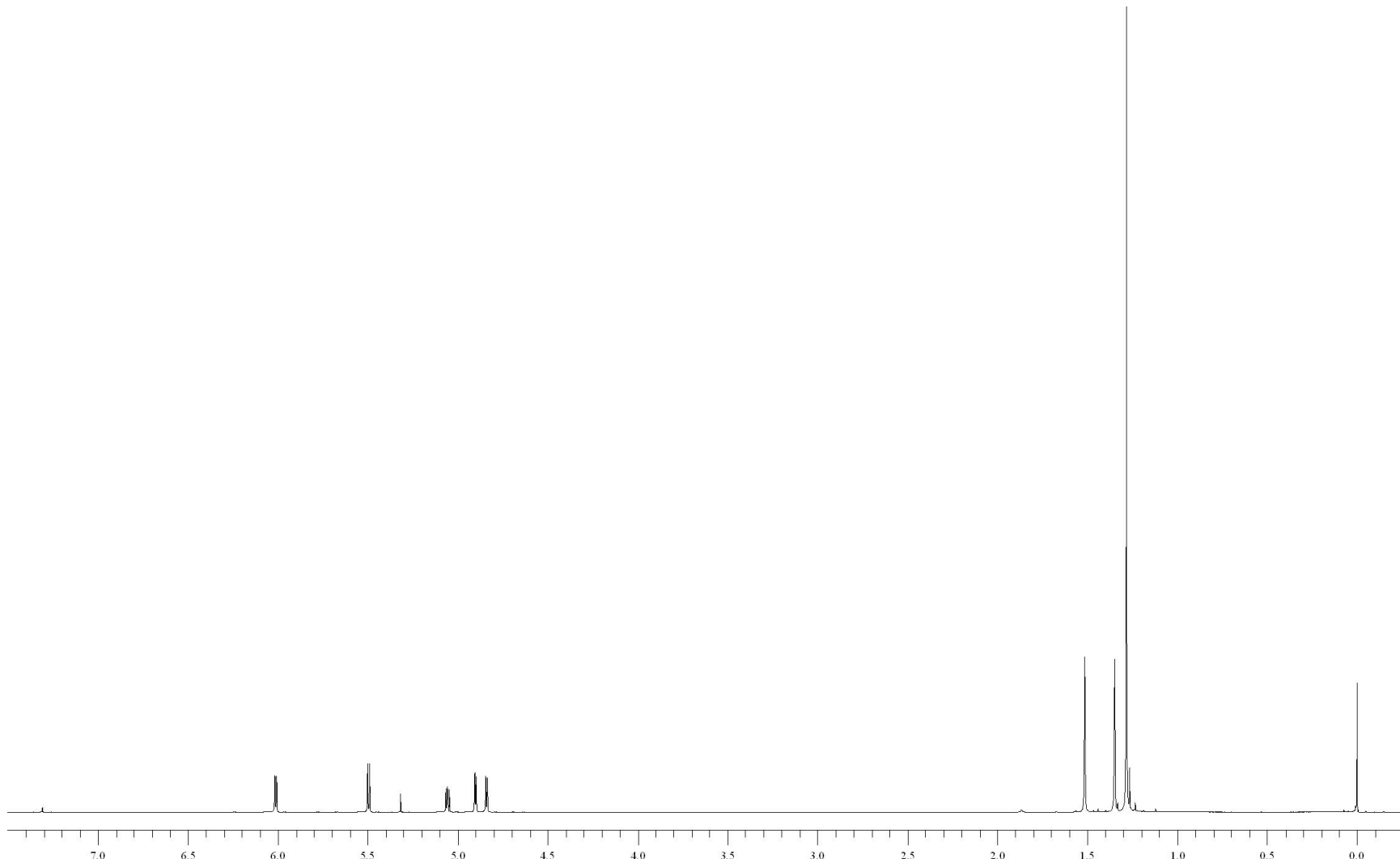


**Figure 62:** 400 MHz  $^1\text{H}$  NMR spectrum of 1,2-*O*-isopropylidene-6-*O*-pivaloyl- $\alpha$ -D-glucurono-6,3-lactone (**20**).

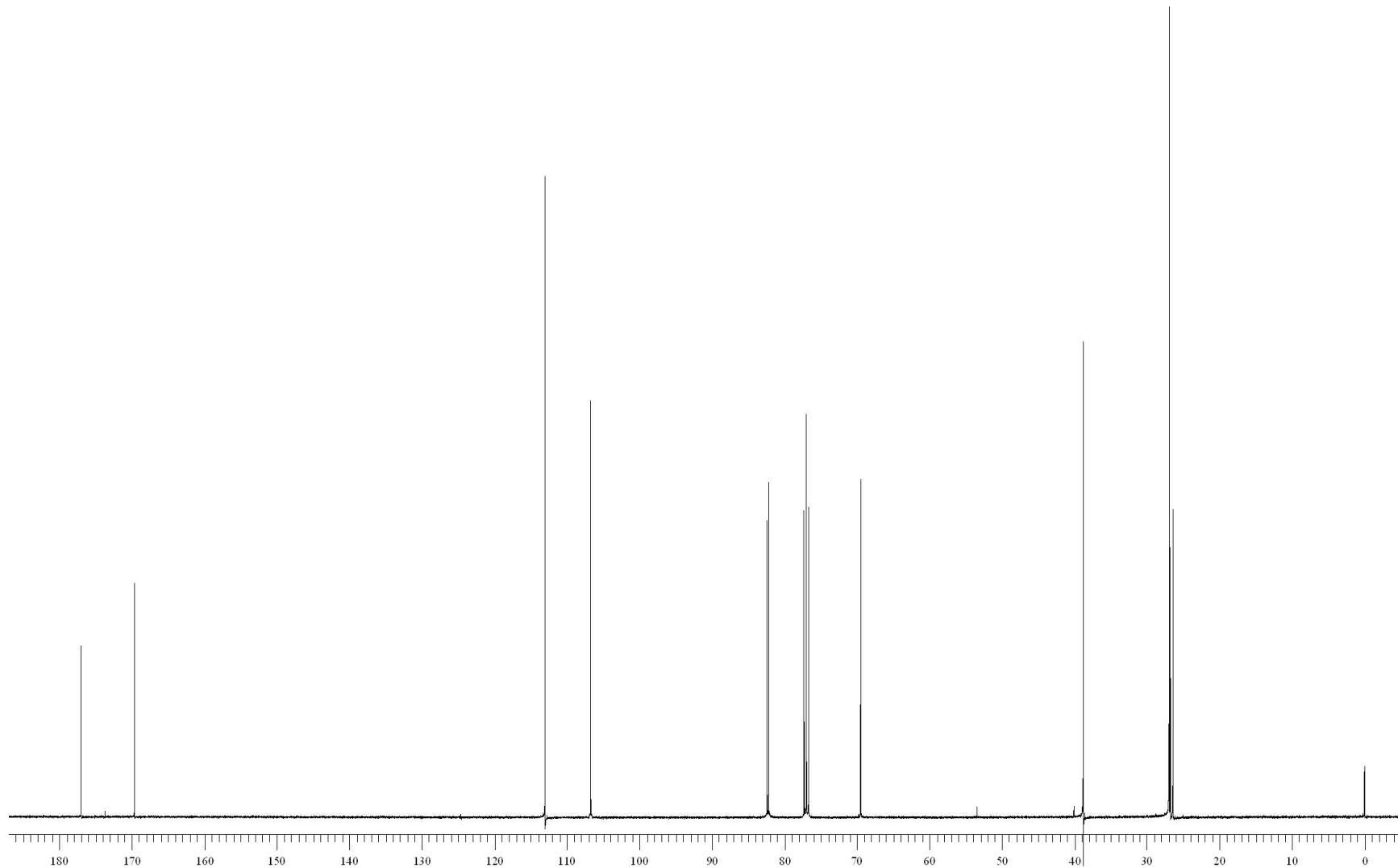


**Figure 63:** 100 MHz  $^{13}\text{C}$  NMR spectrum of 1,2-*O*-isopropylidene-6-*O*-pivaloyl- $\alpha$ -D-glucurono-6,3-lactone (**20**).

## Display Report

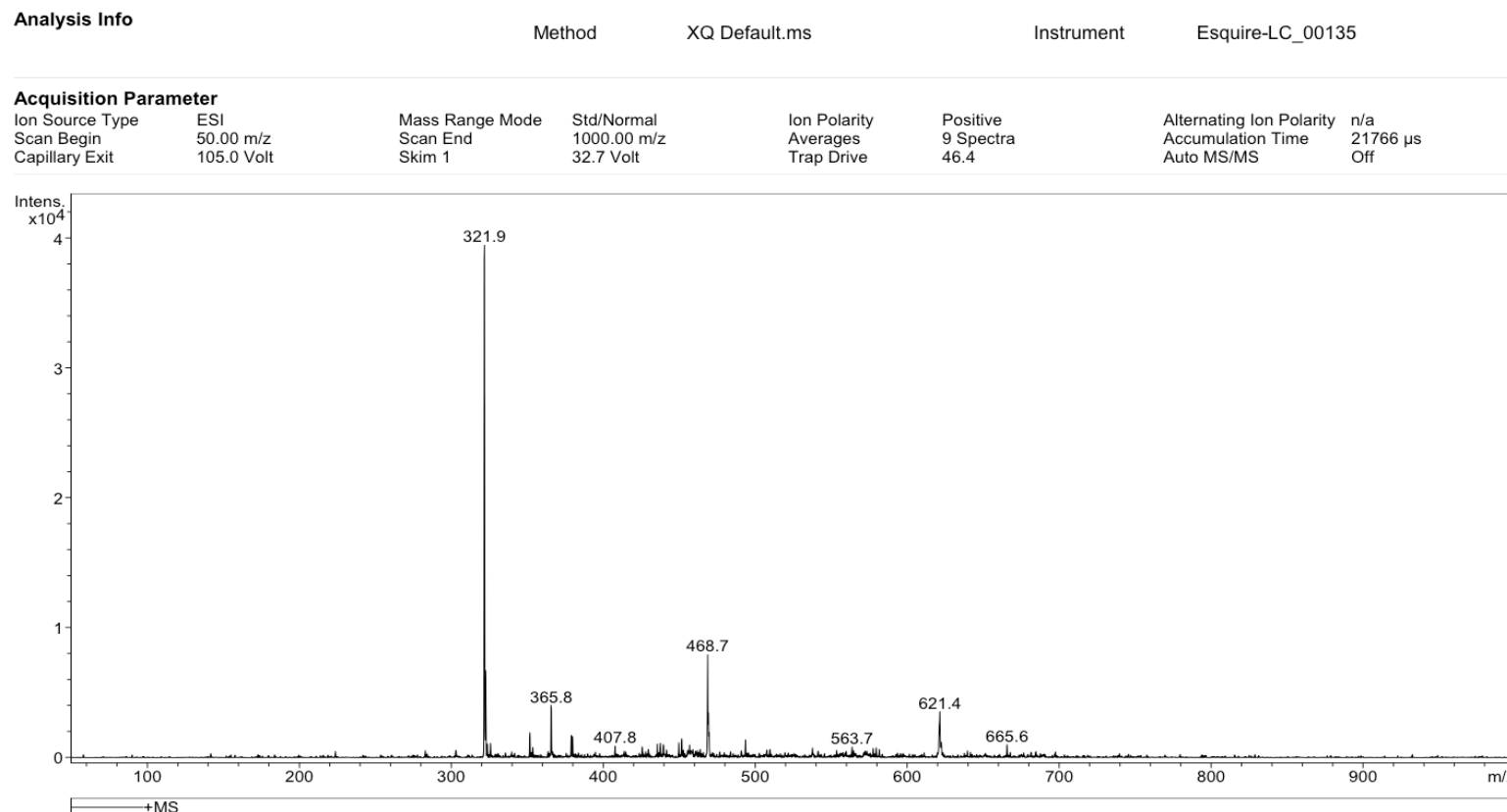


**Figure 64:** ESI mass spectrum of 1,2-*O*-isopropylidene-6-*O*-pivaloyl- $\alpha$ -D-glucurono-6,3-lactone (**20**).

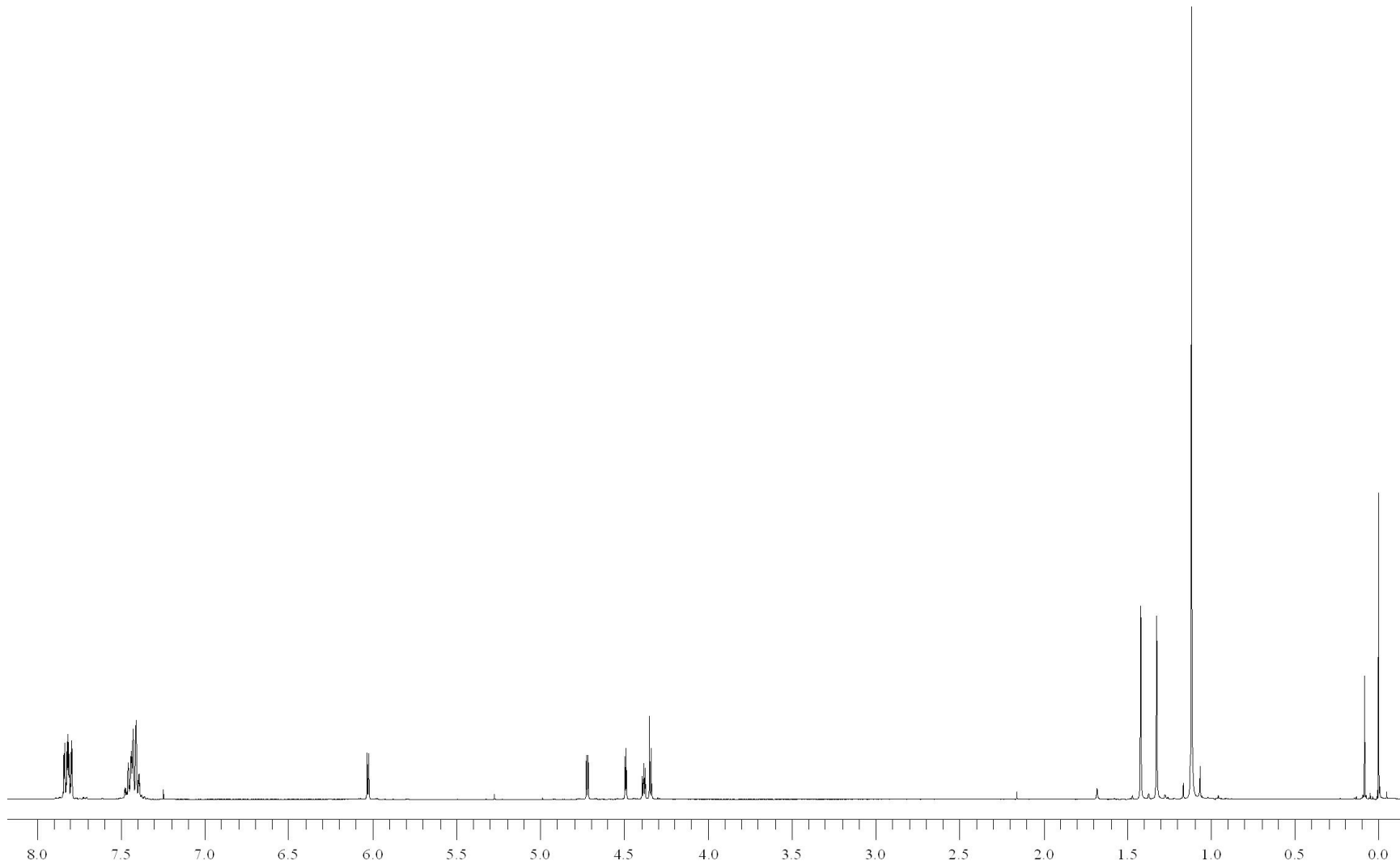


**Figure 65:** 400 MHz  $^1\text{H}$  NMR spectrum of 1,2-*O*-isopropylidene-6-*O*-*tert*-butyldiphenylsilyl- $\alpha$ -D-glucurono-6,3-lactone (**21**).

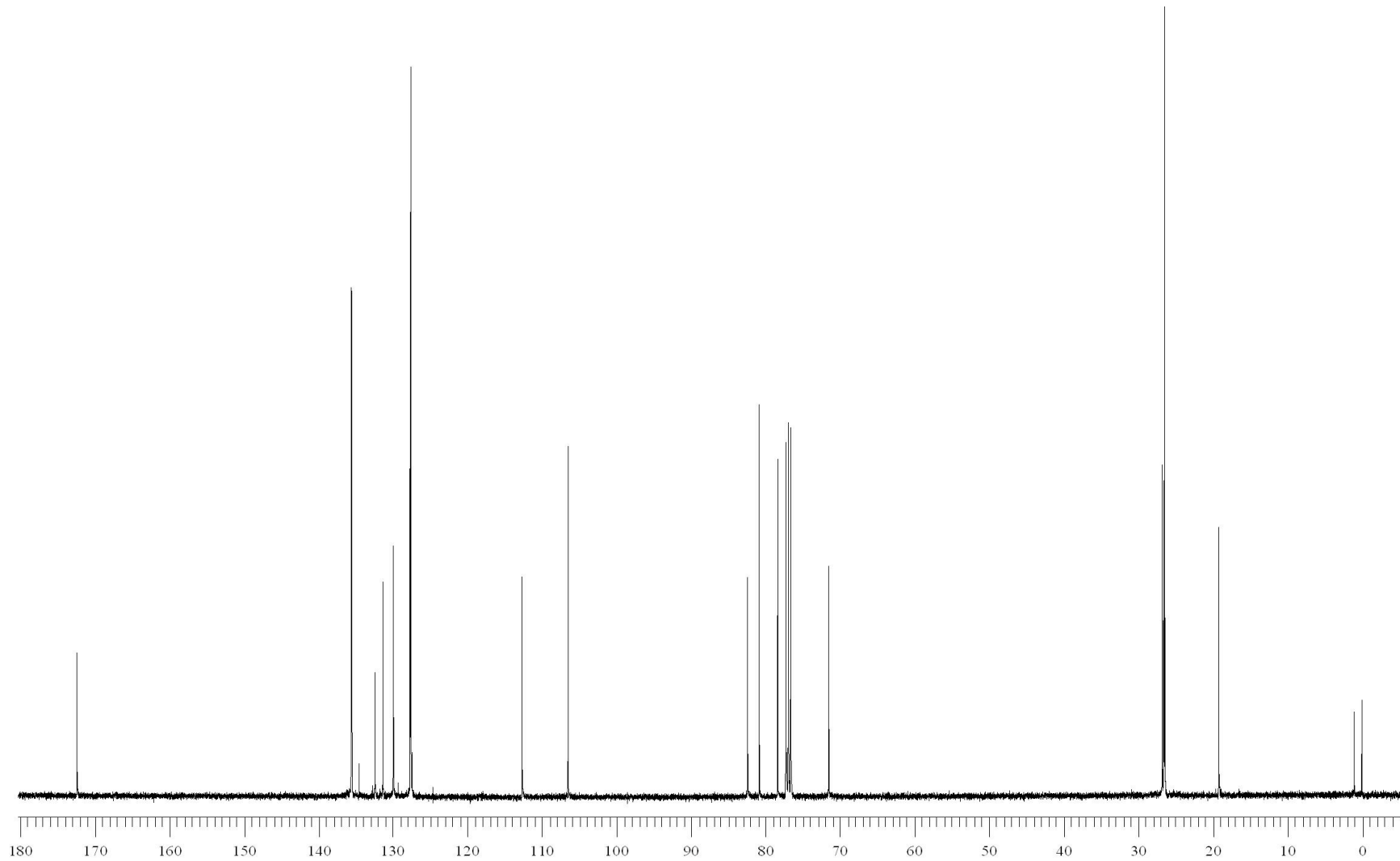


**Figure 66:** 100 MHz  $^{13}\text{C}$  NMR spectrum of 1,2-*O*-isopropylidene-6-*O*-*tert*-butyldiphenylsilyl- $\alpha$ -D-glucurono-6,3-lactone (**21**).

## Display Report

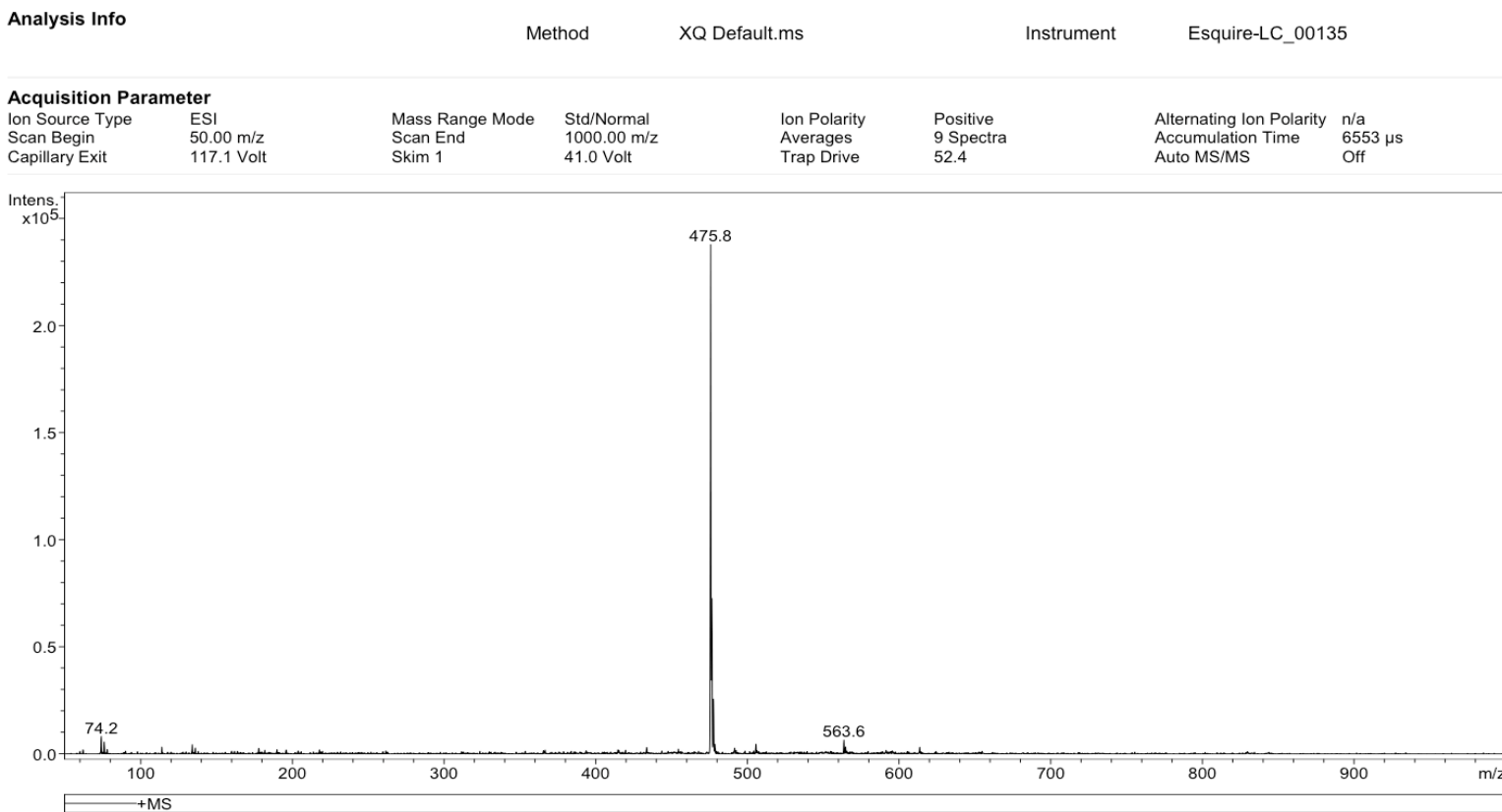


**Figure 67:** ESI mass spectrum of 1,2-*O*-isopropylidene-6-*O*-*tert*-butyldiphenylsilyl- $\alpha$ -D-glucurono-6,3-lactone (**21**).

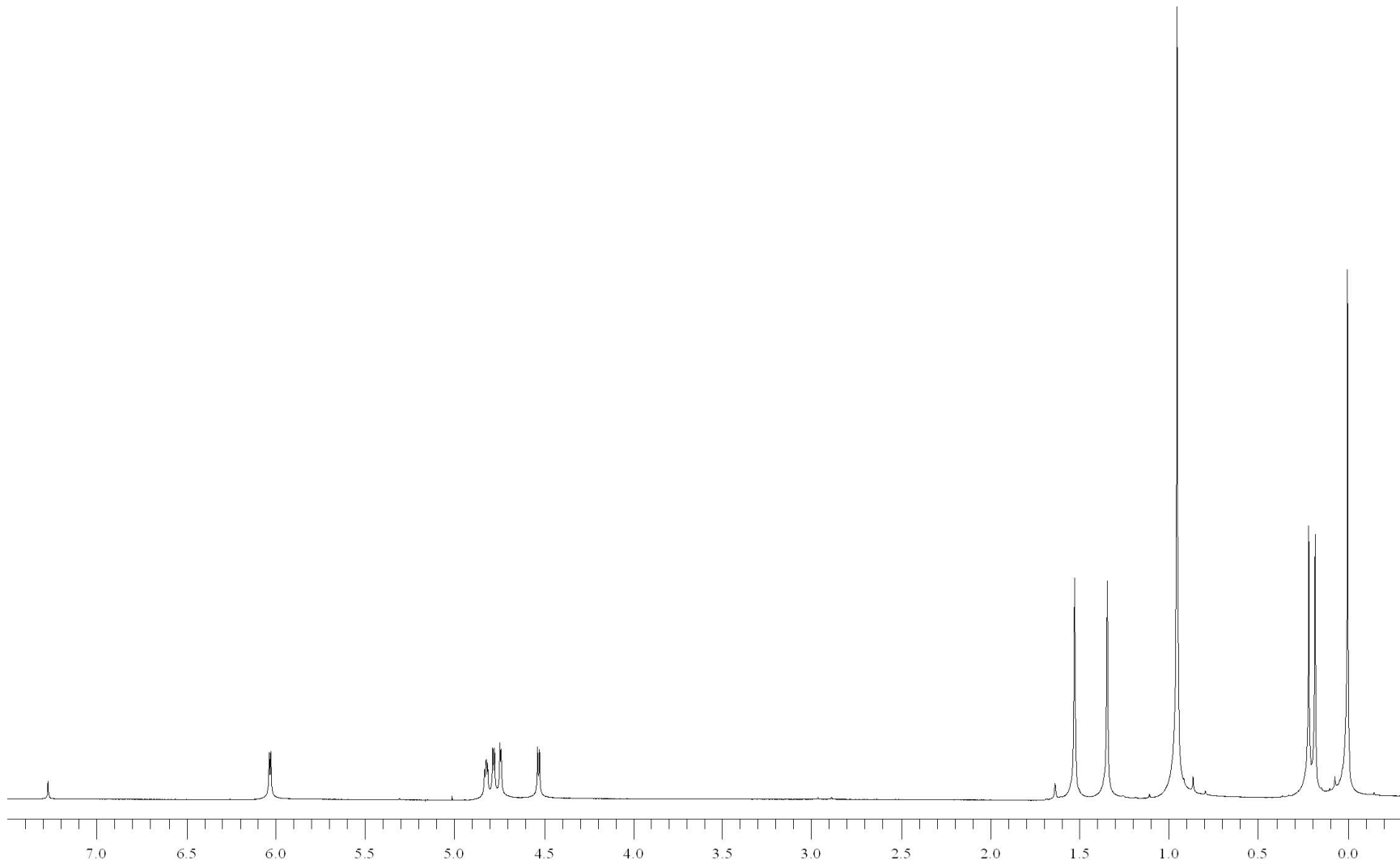


**Figure 68:** 400 MHz  $^1\text{H}$  NMR spectrum of 1,2-*O*-isopropylidene-6-*O*-*tert*-butyldimethylsilyl- $\alpha$ -D-glucurono-6,3-lactone (**22**).

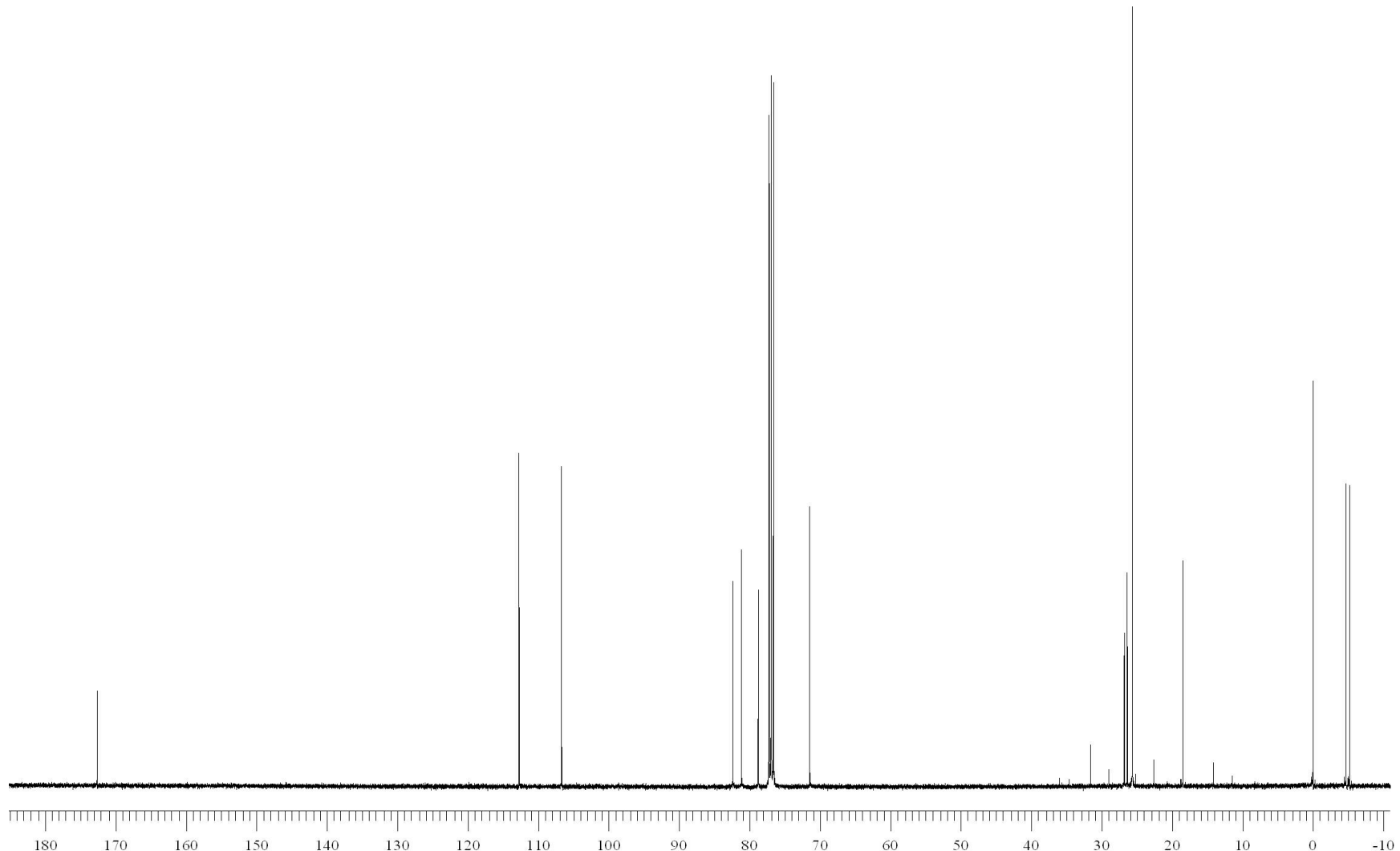


**Figure 69:** 100 MHz  $^{13}\text{C}$  NMR spectrum of 1,2-*O*-isopropylidene-6-*O*-*tert*-butyldimethylsilyl- $\alpha$ -D-glucurono-6,3-lactone (**22**).

## Display Report

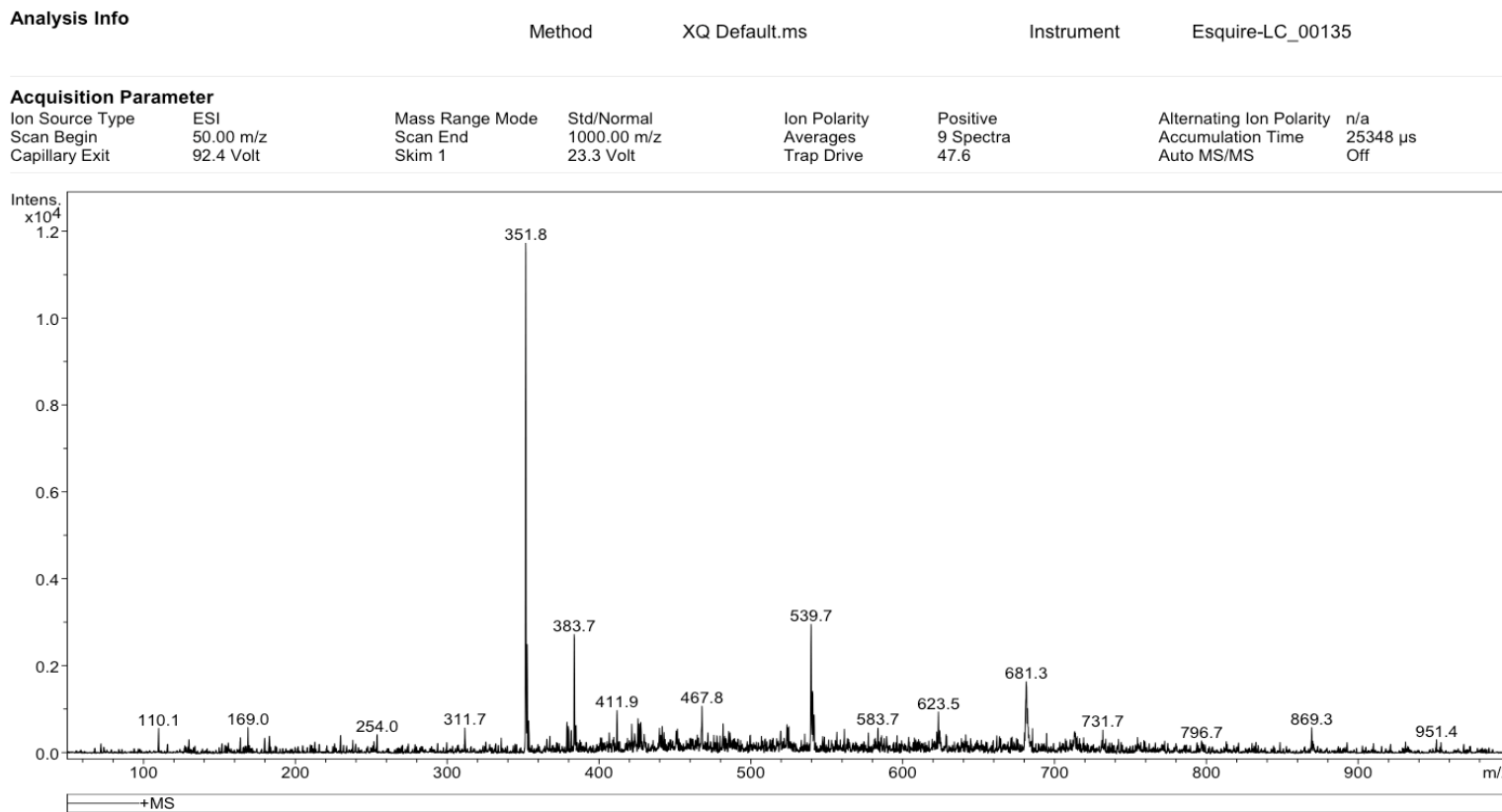


**Figure 70:** ESI mass spectrum of 1,2-*O*-isopropylidene-6-*O*-*tert*-butyldimethylsilyl- $\alpha$ -D-glucurono-6,3-lactone (**22**).

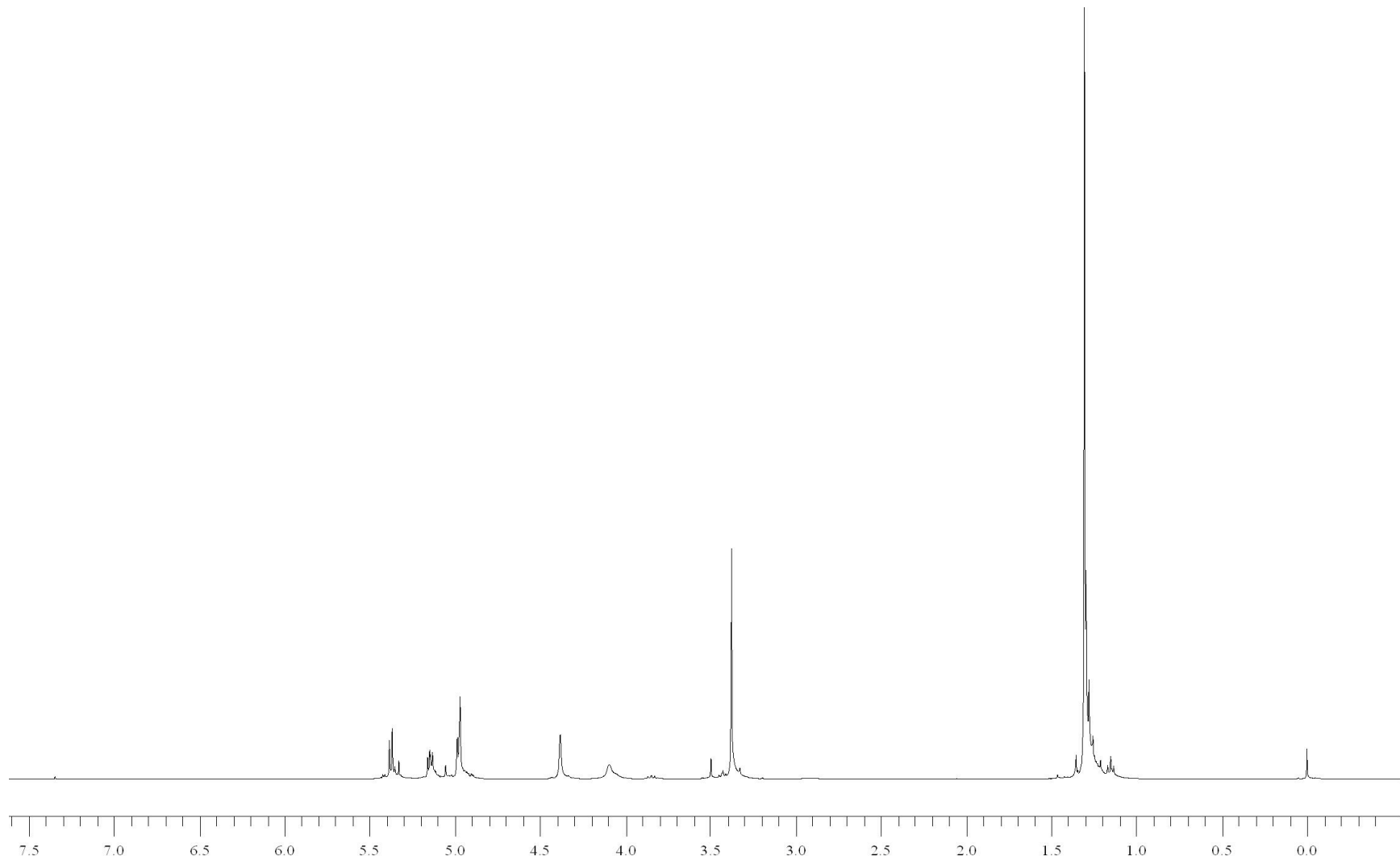


**Figure 71:** 400 MHz  $^1\text{H}$  NMR spectrum of methyl 6-*O*-pivaloyl- $\beta$ -D-glucurono-6,3-lactone (**23**).

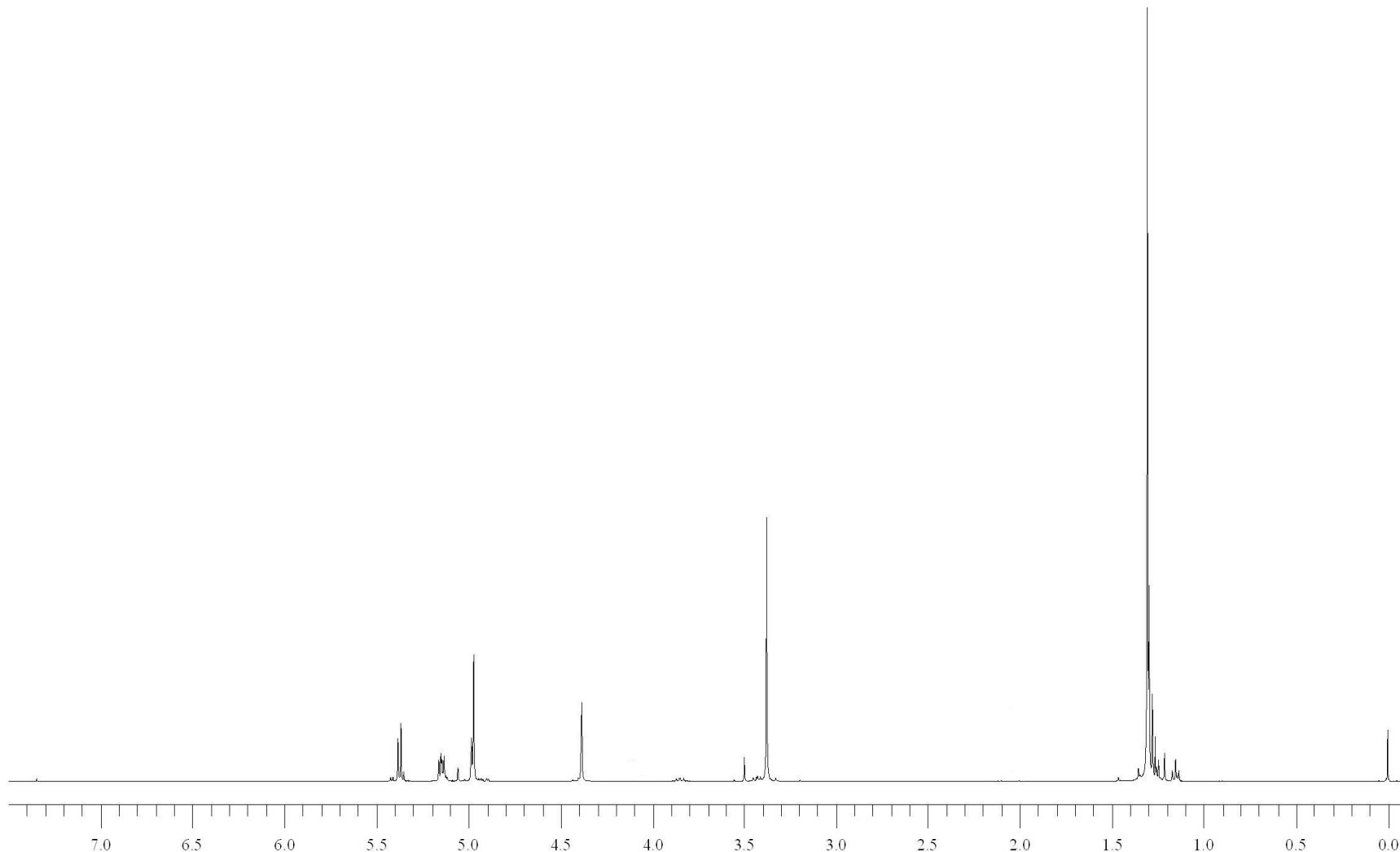


**Figure 72:** 400 MHz  $^1\text{H}$  NMR spectrum of methyl 6-*O*-pivaloyl- $\beta$ -D-glucurono-6,3-lactone (**23**) treated with  $\text{D}_2\text{O}$ .

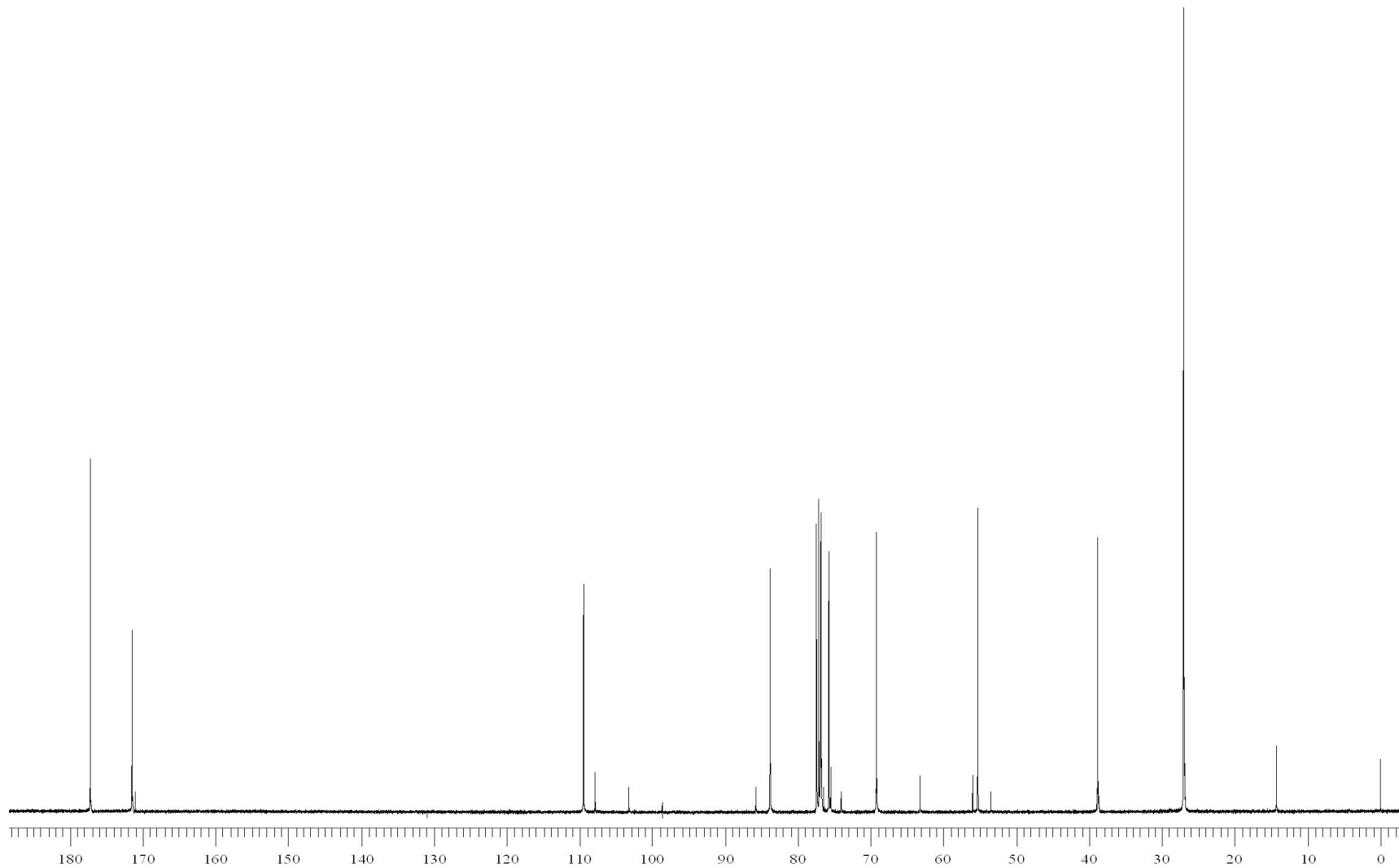


**Figure 73:** 100 MHz  $^{13}\text{C}$  NMR spectrum of methyl 6-*O*-pivaloyl- $\beta$ -D-glucurono-6,3-lactone (**23**).

## Display Report

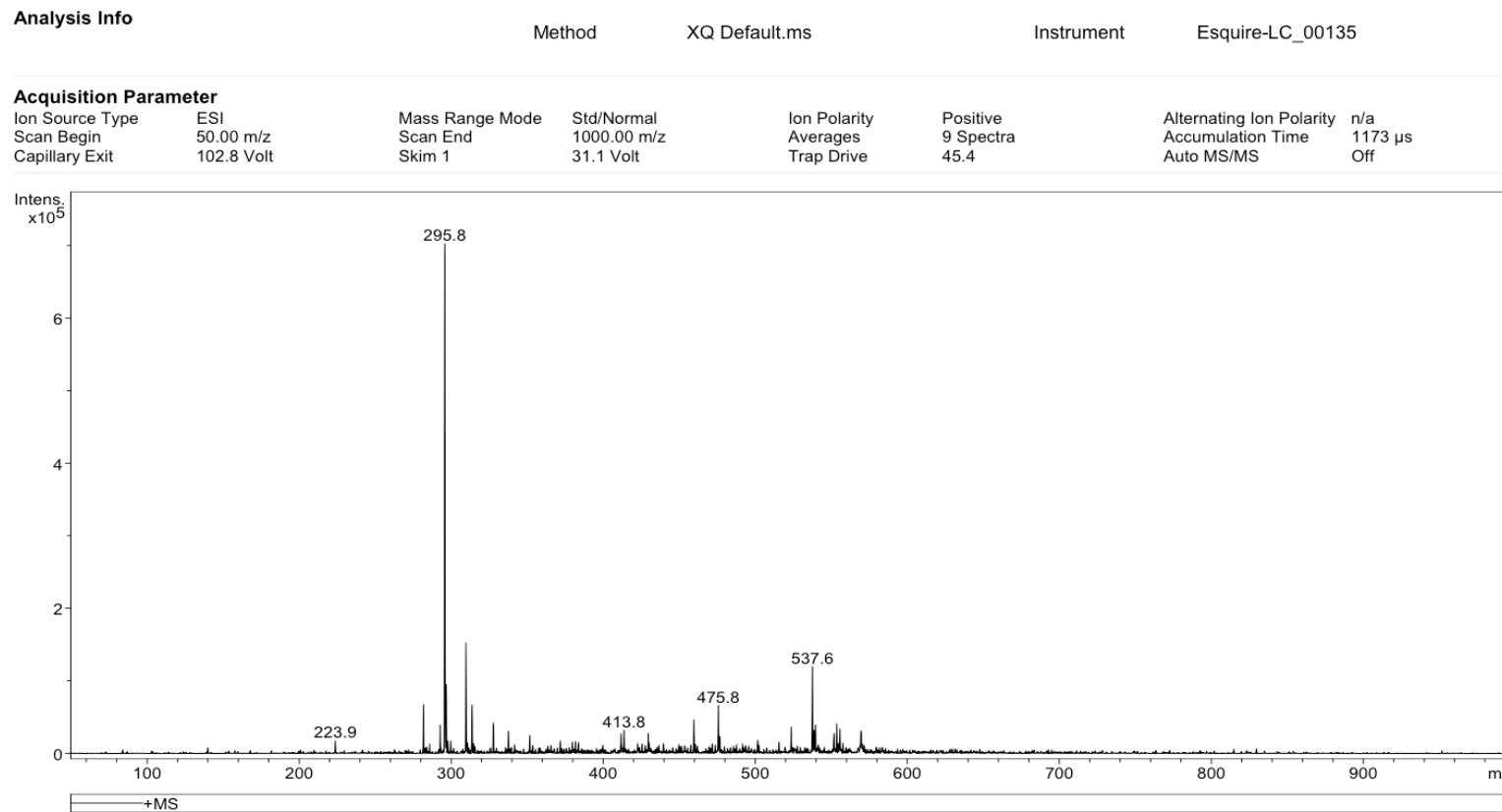


**Figure 74:** ESI mass spectrum of methyl 6-*O*-pivaloyl- $\beta$ -D-glucurono-6,3-lactone (**23**).

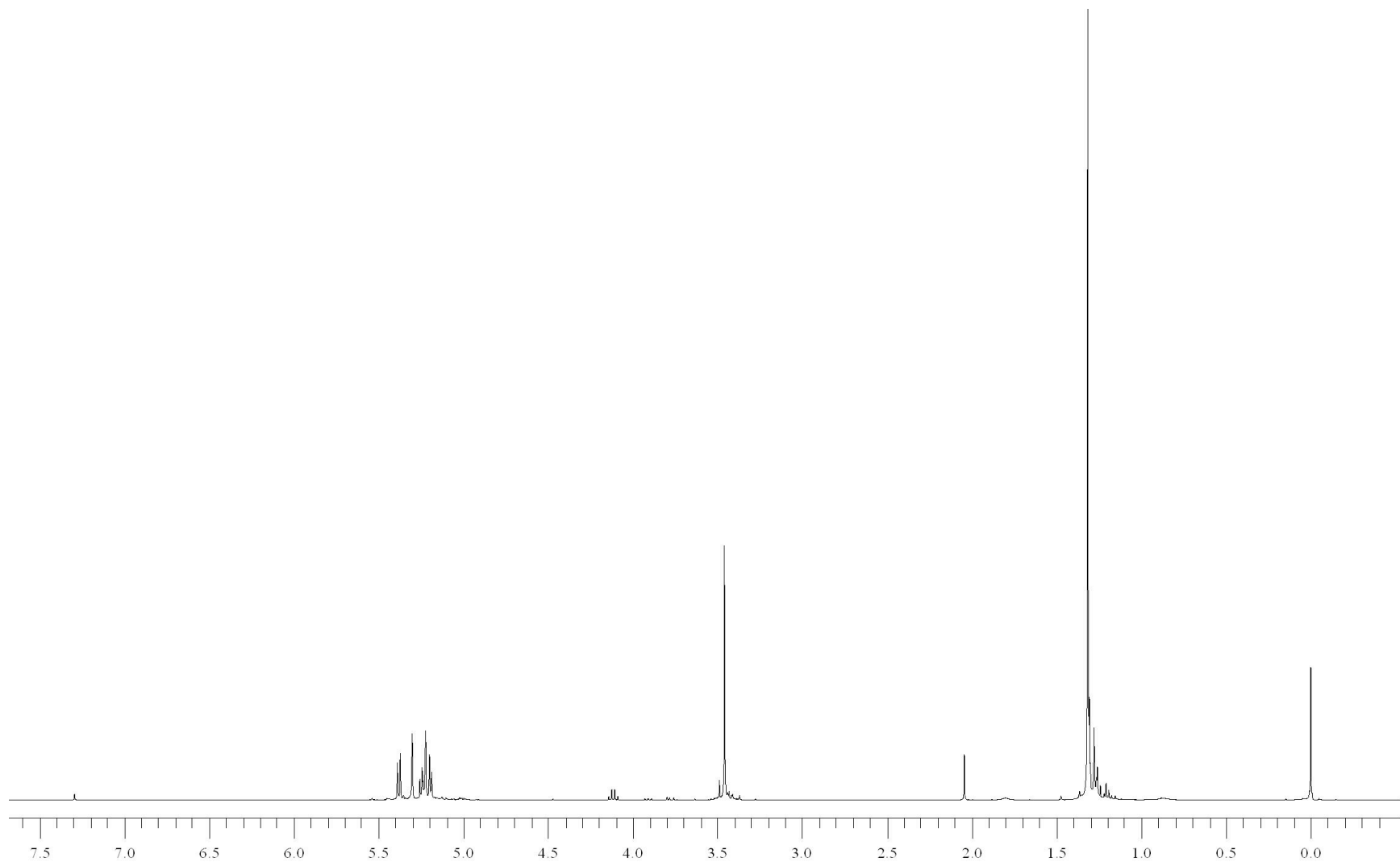


**Figure 75:** 400 MHz  $^1\text{H}$  NMR spectrum of methyl 6-*O*-pivaloyl-2-*O*-trifluoromethylsulfonyl- $\beta$ -D-glucurono-6,3-lactone (**24**).

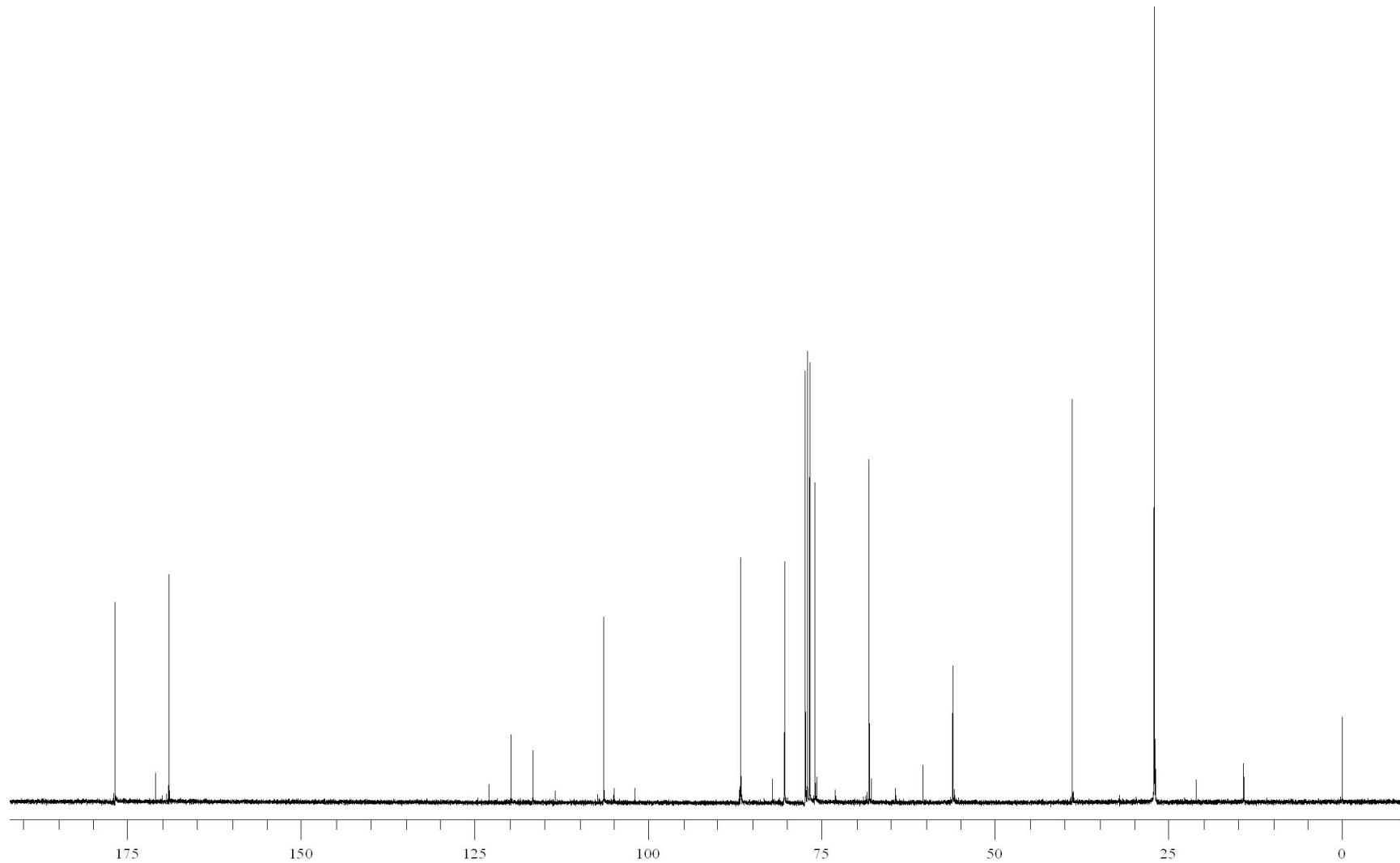


**Figure 76:** 100 MHz  $^{13}\text{C}$  NMR spectrum of methyl 6-*O*-pivaloyl-2-*O*-trifluoromethylsulfonyl- $\beta$ -D-glucurono-6,3-lactone (**24**).

## Display Report

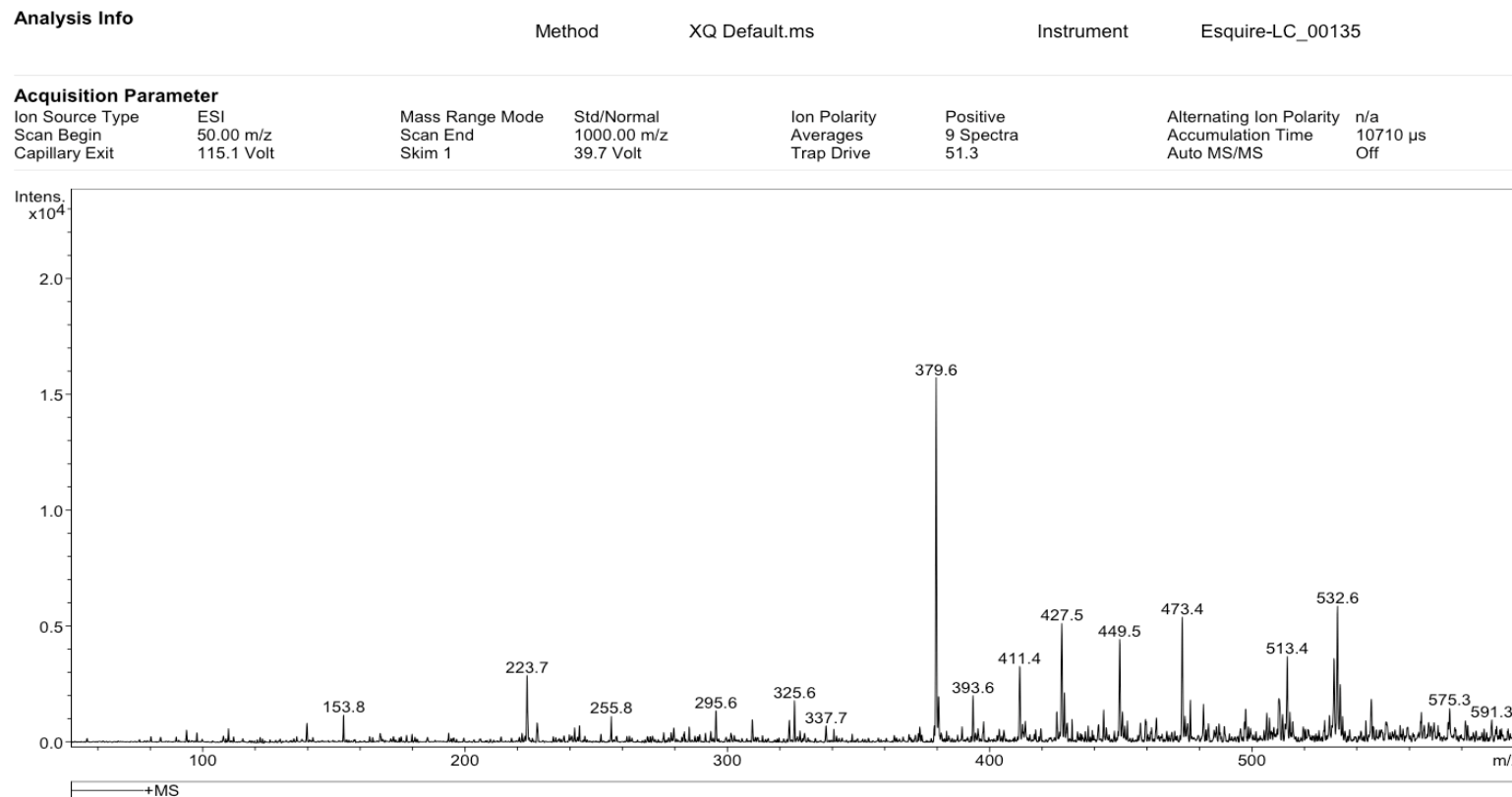


**Figure 77:** ESI mass spectrum of methyl 6-*O*-pivaloyl-2-*O*-trifluoromethylsulfonyl- $\beta$ -D-glucurono-6,3-lactone (**24**).

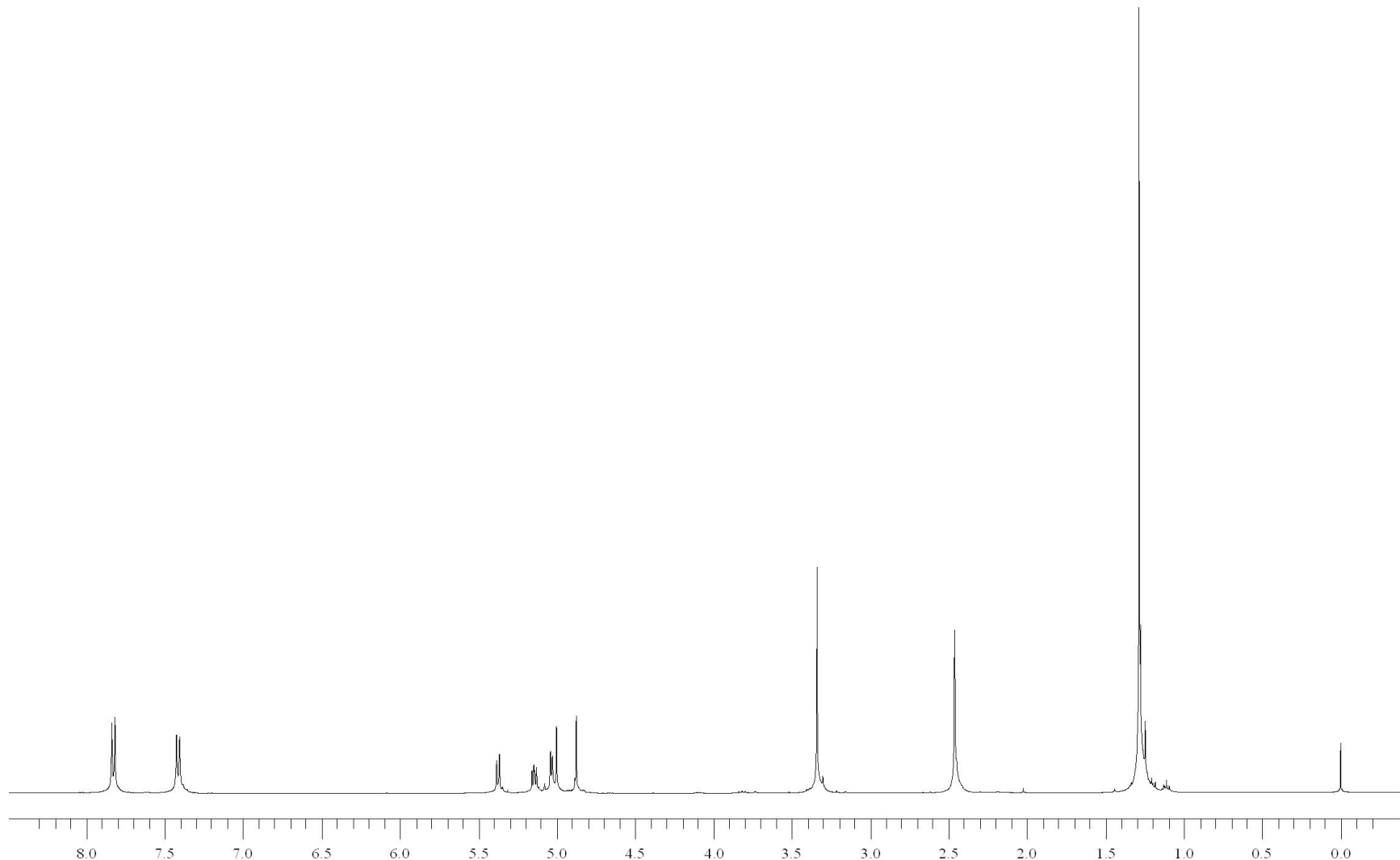


**Figure 78:** 400 MHz  $^1\text{H}$  NMR spectrum of methyl 6-*O*-pivaloyl-2-*O*-(*p*-methylphenylsulfonyl)- $\beta$ -D-glucurono-6,3-lactone (**26**).

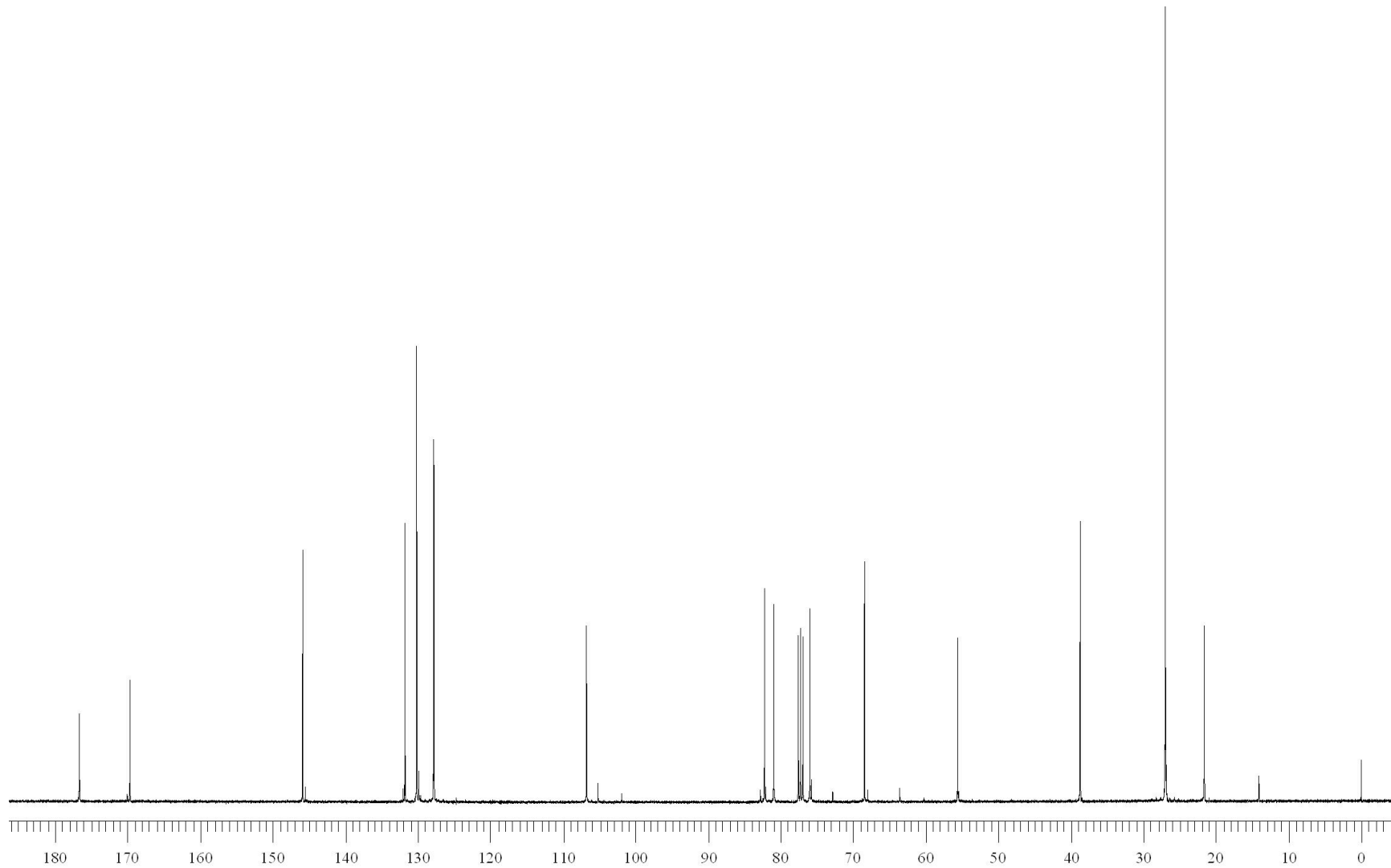


**Figure 79:** 100 MHz  $^{13}\text{C}$  NMR spectrum of methyl 6-*O*-pivaloyl-2-*O*-(*p*-methylphenylsulfonyl)- $\beta$ -D-glucurono-6,3-lactone (**26**).

## Display Report

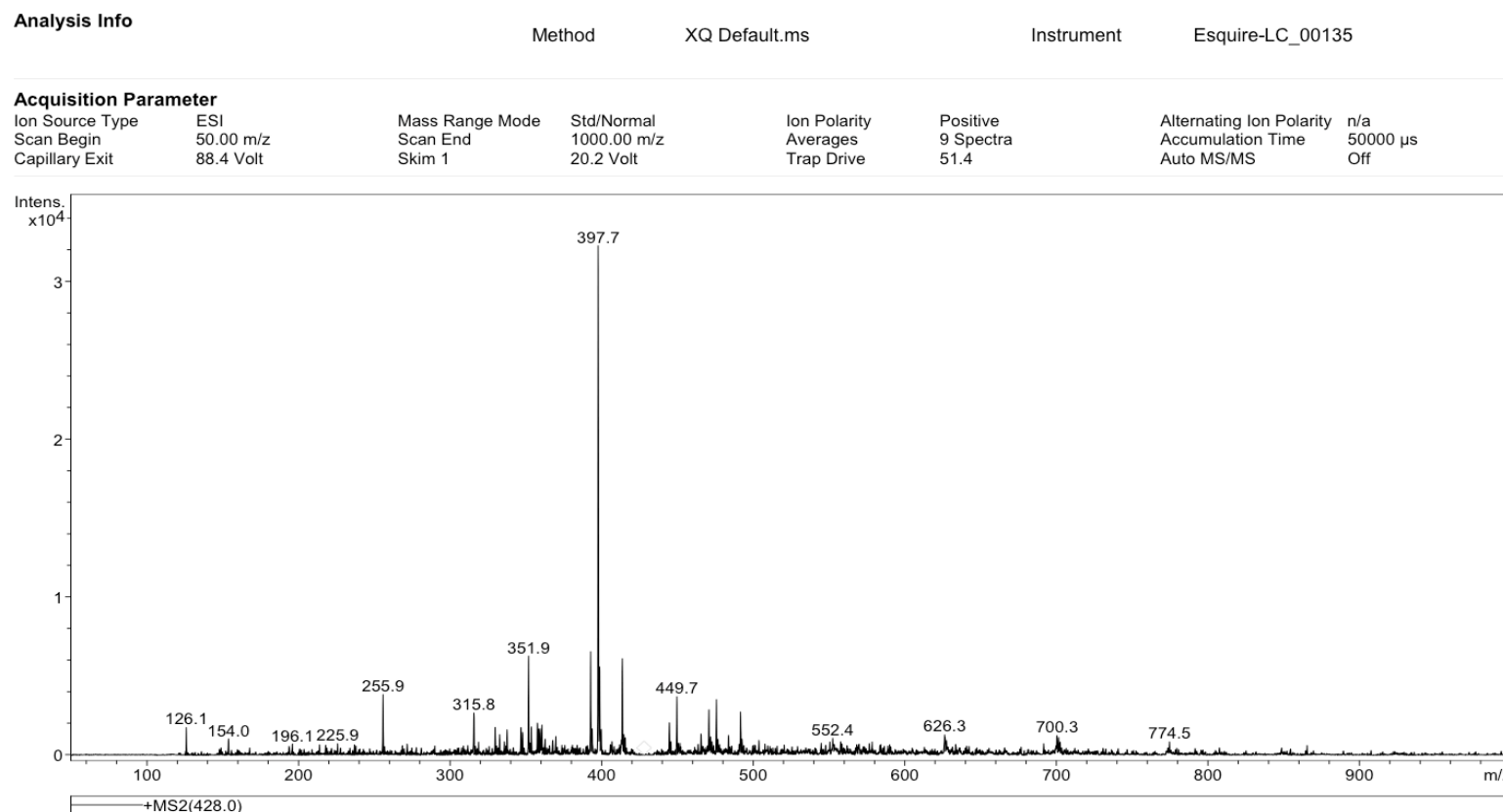


**Figure 80:** ESI mass spectrum of methyl 6-*O*-pivaloyl-2-*O*-(*p*-methylphenylsulfonyl)- $\beta$ -D-glucurono-6,3-lactone (**26**).

## **Appendix B**

### **X-ray Crystallography**

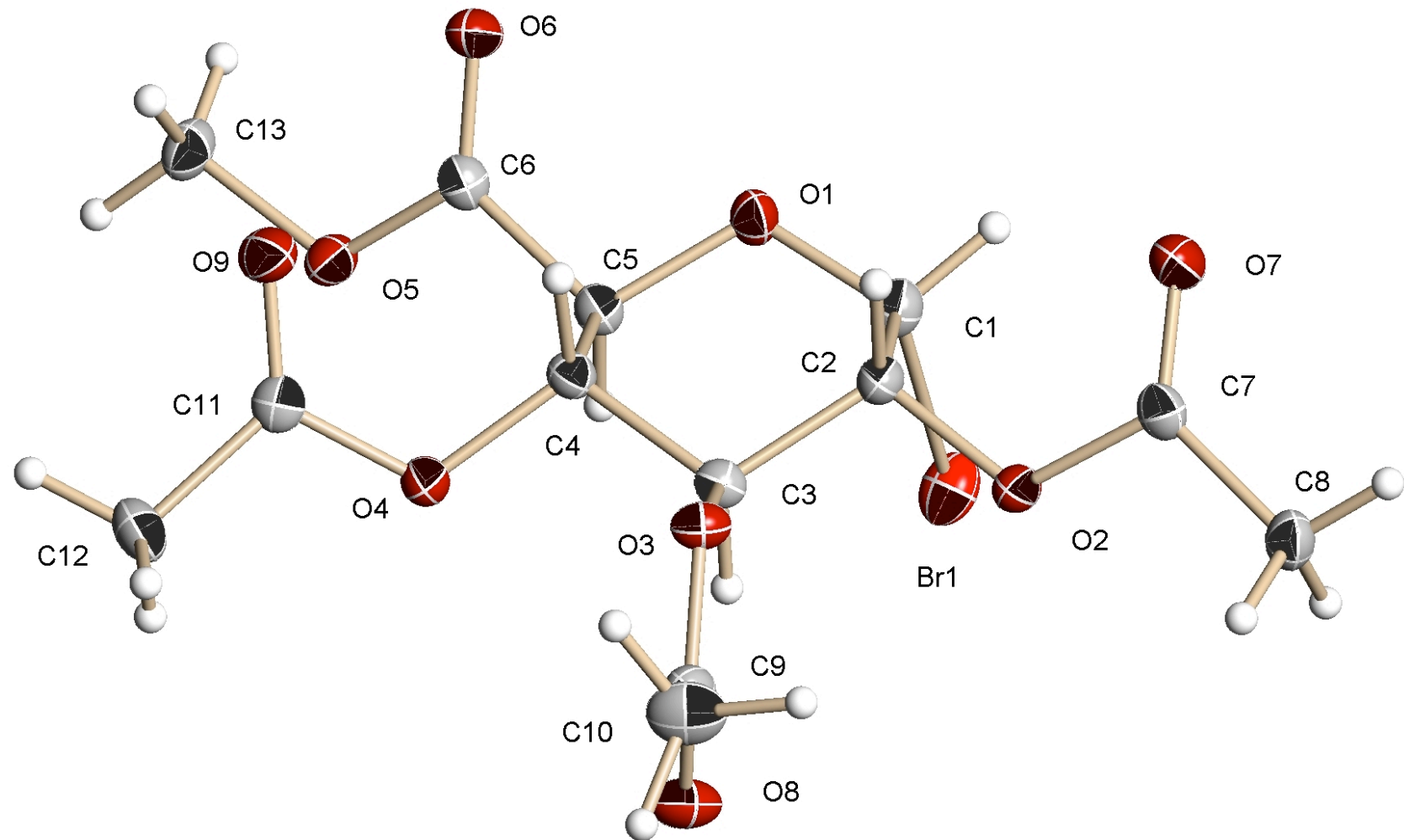


**Figure 81:** X-Ray crystal structure of methyl 2,3,4-tri-O-acetyl- $\alpha$ -D-glucopyranuronosyl bromide (**6**).

Table 1. Crystal data and structure refinement for 07mz173m:

Identification code: 07mz173m  
 Empirical formula: C13 H17 Br1 O9  
 Formula weight: 397.18  
 Temperature: 100(2) K  
 Wavelength: 0.71073 Å  
 Crystal system: Monoclinic  
 Space group: P2<sub>1</sub>  
 Unit cell dimensions:  
 a = 8.7834(7) Å, α = 90°  
 b = 10.7465(8) Å, β = 94.3320(10)°  
 c = 8.9976(7) Å, γ = 90°  
 Volume, Z: 846.86(11) Å<sup>3</sup>, 2  
 Density (calculated): 1.558 Mg/m<sup>3</sup>  
 Absorption coefficient: 2.469 mm<sup>-1</sup>  
 F(000): 404  
 Crystal size: 0.52 × 0.49 × 0.36 mm  
 Crystal shape, colour: block, colourless  
 θ range for data collection: 2.27 to 28.28°  
 Limiting indices: -11 ≤ h ≤ 11, -14 ≤ k ≤ 10, -11 ≤ l ≤ 11  
 Reflections collected: 7330  
 Independent reflections: 3741 (R(int) = 0.0145)  
 Completeness to θ = 28.28°: 100.0 %  
 Absorption correction: multi-scan  
 Max. and min. transmission: 0.411 and 0.322  
 Refinement method: Full-matrix least-squares on  $F^2$   
 Data / restraints / parameters: 3741 / 1 / 212  
 Goodness-of-fit on  $F^2$ : 1.068  
 Final R indices [ $I > 2\sigma(I)$ ]: R1 = 0.0239, wR2 = 0.0613  
 R indices (all data): R1 = 0.0247, wR2 = 0.0621  
 Absolute structure parameter: -0.023(5)  
 Largest diff. peak and hole: 0.435 and -0.440 e × Å<sup>-3</sup>

Refinement of  $F^2$  against ALL reflections. The weighted R-factor wR and goodness of fit are based on  $F^2$ , conventional R-factors R are based on  $F$ , with  $F$  set to zero for negative  $F^2$ . The threshold expression of  $F^2 > 2\sigma(F^2)$  is used only for calculating R-factors

## Treatment of hydrogen atoms:

All hydrogen atoms were placed in calculated positions and were refined with an isotropic displacement parameter 1.5 (methyl) or 1.2 times (all

others) that of the adjacent carbon atom.

Table 2. Atomic coordinates [ $\times 10^4$ ] and equivalent isotropic displacement parameters [ $\text{\AA}^2 \times 10^3$ ] for 07mz173m.  $U(\text{eq})$  is defined as one third of the trace of the orthogonalized  $U_{ij}$  tensor.

	x	y	z	$U(\text{eq})$
Br(1)	396(1)	1807(1)	1555(1)	27(1)
C(1)	912(2)	3544(2)	1027(2)	21(1)
C(2)	2219(2)	3573(2)	0(2)	18(1)
C(3)	3717(2)	3209(2)	839(2)	17(1)
C(4)	3984(2)	4048(2)	2195(2)	17(1)
C(5)	2621(2)	3950(2)	3165(2)	18(1)
C(6)	2751(2)	4902(2)	4420(2)	18(1)
C(7)	1047(2)	3135(2)	-2407(2)	19(1)
C(8)	965(2)	2189(2)	-3623(2)	22(1)
C(9)	5826(2)	2460(2)	-434(2)	21(1)
C(10)	6909(3)	2832(2)	-1576(3)	31(1)
C(11)	6231(2)	4505(2)	3734(2)	19(1)
C(12)	7688(2)	3957(2)	4414(2)	25(1)
C(13)	3862(3)	5329(2)	6813(2)	24(1)
O(1)	1241(2)	4271(2)	2292(2)	20(1)
O(2)	1991(2)	2736(1)	-1226(2)	19(1)
O(3)	4916(2)	3435(1)	-134(2)	18(1)
O(4)	5350(2)	3613(1)	3008(2)	18(1)
O(5)	3528(2)	4429(1)	5626(2)	20(1)
O(6)	2253(2)	5940(2)	4317(2)	23(1)
O(7)	388(2)	4105(2)	-2401(2)	26(1)
O(8)	5749(2)	1455(2)	117(2)	27(1)
O(9)	5849(2)	5572(2)	3789(2)	24(1)

All esds (except the esd in the dihedral angle between two l.s. planes) are estimated using the full covariance matrix. The cell esds are taken into account individually in the estimation of esds in distances, angles and torsion angles; correlations between esds in cell parameters are only used when they are defined by crystal symmetry. An approximate (isotropic) treatment of cell esds is used for estimating esds involving l.s. planes.

Table 3. Bond lengths [ $\text{\AA}$ ] and angles [deg] for 07mz173m.

Br(1)-C(1)	1.987(2)	C(1)-O(1)	1.392(2)
------------	----------	-----------	----------

C (1) -C (2)	1.527 (3)	O (2) -C (2) -H (2)	108.8
C (1) -H (1)	1.0000	C (3) -C (2) -H (2)	108.8
C (2) -O (2)	1.426 (2)	C (1) -C (2) -H (2)	108.8
C (2) -C (3)	1.518 (2)	O (3) -C (3) -C (2)	107.51 (15)
C (2) -H (2)	1.0000	O (3) -C (3) -C (4)	108.13 (15)
C (3) -O (3)	1.441 (2)	C (2) -C (3) -C (4)	108.75 (16)
C (3) -C (4)	1.521 (3)	O (3) -C (3) -H (3)	110.8
C (3) -H (3)	1.0000	C (2) -C (3) -H (3)	110.8
C (4) -O (4)	1.435 (2)	C (4) -C (3) -H (3)	110.8
C (4) -C (5)	1.538 (3)	O (4) -C (4) -C (3)	106.78 (15)
C (4) -H (4)	1.0000	O (4) -C (4) -C (5)	110.16 (15)
C (5) -O (1)	1.435 (2)	C (3) -C (4) -C (5)	109.58 (16)
C (5) -C (6)	1.521 (3)	O (4) -C (4) -H (4)	110.1
C (5) -H (5)	1.0000	C (3) -C (4) -H (4)	110.1
C (6) -O (6)	1.199 (3)	C (5) -C (4) -H (4)	110.1
C (6) -O (5)	1.338 (2)	O (1) -C (5) -C (6)	104.98 (16)
C (7) -O (7)	1.193 (3)	O (1) -C (5) -C (4)	109.52 (15)
C (7) -O (2)	1.367 (2)	C (6) -C (5) -C (4)	110.94 (16)
C (7) -C (8)	1.491 (3)	O (1) -C (5) -H (5)	110.4
C (8) -H (8A)	0.9800	C (6) -C (5) -H (5)	110.4
C (8) -H (8B)	0.9800	C (4) -C (5) -H (5)	110.4
C (8) -H (8C)	0.9800	O (6) -C (6) -O (5)	125.25 (19)
C (9) -O (8)	1.193 (3)	O (6) -C (6) -C (5)	124.13 (17)
C (9) -O (3)	1.357 (3)	O (5) -C (6) -C (5)	110.60 (18)
C (9) -C (10)	1.506 (3)	O (7) -C (7) -O (2)	122.45 (19)
C (10) -H (10A)	0.9800	O (7) -C (7) -C (8)	127.10 (18)
C (10) -H (10B)	0.9800	O (2) -C (7) -C (8)	110.44 (18)
C (10) -H (10C)	0.9800	C (7) -C (8) -H (8A)	109.5
C (11) -O (9)	1.196 (3)	C (7) -C (8) -H (8B)	109.5
C (11) -O (4)	1.367 (2)	H (8A) -C (8) -H (8B)	109.5
C (11) -C (12)	1.498 (3)	C (7) -C (8) -H (8C)	109.5
C (12) -H (12A)	0.9800	H (8A) -C (8) -H (8C)	109.5
C (12) -H (12B)	0.9800	H (8B) -C (8) -H (8C)	109.5
C (12) -H (12C)	0.9800	O (8) -C (9) -O (3)	124.37 (19)
C (13) -O (5)	1.454 (3)	O (8) -C (9) -C (10)	125.6 (2)
C (13) -H (13A)	0.9800	O (3) -C (9) -C (10)	110.06 (19)
C (13) -H (13B)	0.9800	C (9) -C (10) -H (10A)	109.5
C (13) -H (13C)	0.9800	C (9) -C (10) -H (10B)	109.5
		H (10A) -C (10) -H (10B)	109.5
O (1) -C (1) -C (2)		C (9) -C (10) -H (10C)	109.5
111.32 (16)		H (10A) -C (10) -H (10C)	109.5
O (1) -C (1) -Br (1)		H (10B) -C (10) -H (10C)	109.5
111.61 (13)		O (9) -C (11) -O (4)	122.79 (19)
C (2) -C (1) -Br (1)		O (9) -C (11) -C (12)	126.4 (2)
111.03 (15)		O (4) -C (11) -C (12)	110.78 (19)
O (1) -C (1) -H (1)		C (11) -C (12) -H (12A)	109.5
107.6		C (11) -C (12) -H (12B)	109.5
C (2) -C (1) -H (1)		H (12A) -C (12) -H (12B)	109.5
107.6		C (11) -C (12) -H (12C)	109.5
Br (1) -C (1) -H (1)		H (12A) -C (12) -H (12C)	109.5
107.6		H (12B) -C (12) -H (12C)	109.5
O (2) -C (2) -C (3)		O (5) -C (13) -H (13A)	109.5
106.70 (16)		O (5) -C (13) -H (13B)	109.5
O (2) -C (2) -C (1)		H (13A) -C (13) -H (13B)	109.5
112.78 (16)		O (5) -C (13) -H (13C)	109.5
C (3) -C (2) -C (1)		H (13A) -C (13) -H (13C)	109.5
110.93 (15)		H (13B) -C (13) -H (13C)	109.5

C(1)-O(1)-C(5)  
115.34(16)  
C(7)-O(2)-C(2)  
116.42(16)  
C(9)-O(3)-C(3)  
117.32(16)  
C(11)-O(4)-C(4)  
115.88(16)  
C(6)-O(5)-C(13)  
113.89(17)

Table 4. Anisotropic displacement parameters [ $\text{\AA}^2 \times 10^3$ ] for 07mz173m. The anisotropic displacement factor exponent takes the form:  $-2 \pi^2 [(h a*)^2 U_{11} + \dots + 2 h k a^* b^* U_{12}]$

	U11	U22	U33	U23	U13	U12
Br(1)	28(1)	28(1)	26(1)	-1(1)	4(1)	-11(1)
C(1)	20(1)	23(1)	20(1)	-2(1)	1(1)	-2(1)
C(2)	19(1)	16(1)	18(1)	-2(1)	-2(1)	0(1)
C(3)	17(1)	17(1)	16(1)	1(1)	3(1)	1(1)
C(4)	17(1)	16(1)	16(1)	1(1)	1(1)	1(1)
C(5)	17(1)	19(1)	17(1)	1(1)	1(1)	1(1)
C(6)	17(1)	23(1)	16(1)	1(1)	2(1)	0(1)
C(7)	14(1)	23(1)	19(1)	1(1)	1(1)	0(1)
C(8)	18(1)	27(1)	23(1)	-5(1)	-1(1)	-1(1)
C(9)	22(1)	23(1)	17(1)	-3(1)	1(1)	3(1)
C(10)	29(1)	32(2)	33(1)	0(1)	15(1)	4(1)
C(11)	18(1)	21(1)	18(1)	1(1)	4(1)	-3(1)
C(12)	20(1)	28(1)	27(1)	6(1)	-5(1)	0(1)
C(13)	32(1)	23(1)	17(1)	-3(1)	-2(1)	-2(1)
O(1)	16(1)	25(1)	19(1)	-4(1)	0(1)	2(1)
O(2)	23(1)	17(1)	17(1)	-3(1)	-2(1)	3(1)
O(3)	21(1)	16(1)	18(1)	1(1)	7(1)	1(1)
O(4)	18(1)	17(1)	18(1)	0(1)	-1(1)	0(1)
O(5)	25(1)	17(1)	17(1)	-1(1)	0(1)	0(1)
O(6)	26(1)	21(1)	23(1)	-3(1)	-1(1)	6(1)
O(7)	26(1)	26(1)	26(1)	-4(1)	-4(1)	7(1)
O(8)	34(1)	20(1)	27(1)	2(1)	7(1)	8(1)
O(9)	22(1)	19(1)	30(1)	-2(1)	1(1)	-2(1)

Table 5. Hydrogen coordinates ( $\times 10^4$ ) and isotropic displacement parameters ( $\text{\AA}^2 \times 10^3$ ) for 07mz173m.

	x	y	z	U(eq)
H(1)	-7	3911	466	25
H(2)	2316	4437	-394	21
H(3)	3701	2314	1143	20
H(4)	4119	4929	1872	20
H(5)	2547	3090	3578	21
H(8A)	453	1440	-3289	34

H (8B)	2000	1975	-3872	34
H (8C)	387	2529	-4505	34
H (10A)	7762	2242	-1550	46
H (10B)	7301	3670	-1352	46
H (10C)	6369	2824	-2570	46
H (12A)	8428	3892	3655	38
H (12B)	7487	3127	4805	38
H (12C)	8104	4492	5228	38
H (13A)	4479	6008	6445	37
H (13B)	4429	4921	7657	37
H (13C)	2904	5667	7135	37

---

Table 6. Torsion angles [deg] for 07mz173m.

O(1)-C(1)-C(2)-O(2)	173.70(16)
Br(1)-C(1)-C(2)-O(2)	48.70(19)
O(1)-C(1)-C(2)-C(3)	54.1(2)
Br(1)-C(1)-C(2)-C(3)	-70.93(18)
O(2)-C(2)-C(3)-O(3)	65.17(19)
C(1)-C(2)-C(3)-O(3)	-171.63(16)
O(2)-C(2)-C(3)-C(4)	-177.98(15)
C(1)-C(2)-C(3)-C(4)	-54.8(2)
O(3)-C(3)-C(4)-O(4)	-67.63(18)
C(2)-C(3)-C(4)-O(4)	175.92(15)
O(3)-C(3)-C(4)-C(5)	173.08(15)
C(2)-C(3)-C(4)-C(5)	56.6(2)
O(4)-C(4)-C(5)-O(1)	-174.33(16)
C(3)-C(4)-C(5)-O(1)	-57.1(2)
O(4)-C(4)-C(5)-C(6)	70.3(2)
C(3)-C(4)-C(5)-C(6)	-172.55(16)
O(1)-C(5)-C(6)-O(6)	-29.1(2)
C(4)-C(5)-C(6)-O(6)	89.1(2)
O(1)-C(5)-C(6)-O(5)	152.50(15)
C(4)-C(5)-C(6)-O(5)	-89.3(2)
C(2)-C(1)-O(1)-C(5)	-56.7(2)
Br(1)-C(1)-O(1)-C(5)	67.94(18)
C(6)-C(5)-O(1)-C(1)	177.58(16)
C(4)-C(5)-O(1)-C(1)	58.4(2)
O(7)-C(7)-O(2)-C(2)	-3.2(3)
C(8)-C(7)-O(2)-C(2)	177.84(16)
C(3)-C(2)-O(2)-C(7)	-157.40(16)
C(1)-C(2)-O(2)-C(7)	80.6(2)
O(8)-C(9)-O(3)-C(3)	-4.3(3)
C(10)-C(9)-O(3)-C(3)	174.56(17)
C(2)-C(3)-O(3)-C(9)	-123.16(18)
C(4)-C(3)-O(3)-C(9)	119.59(18)
O(9)-C(11)-O(4)-C(4)	5.3(3)
C(12)-C(11)-O(4)-C(4)	-174.54(16)
C(3)-C(4)-O(4)-C(11)	146.79(16)
C(5)-C(4)-O(4)-C(11)	-94.29(19)
O(6)-C(6)-O(5)-C(13)	-5.4(3)

C(5)-C(6)-O(5)-C(13)

172.94(16)

---

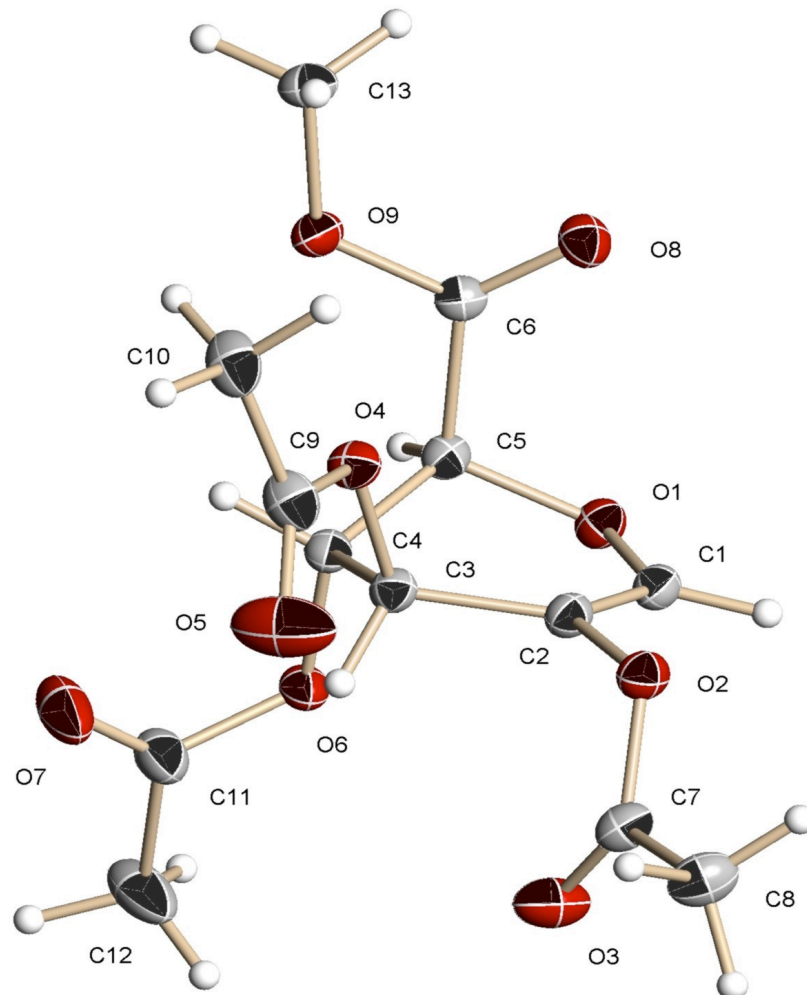


**Figure 82:** X-Ray crystal structure of methyl 2,3,4-tri-*O*-acetyl-1,5-anhydro-D-*arabino*-hex-1-enopyranuronate (7).

Table 1. Crystal data and structure refinement for 06mz040m:

Identification code: 06mz040m  
 Empirical formula: C13 H16 O9  
 Formula weight: 316.26  
 Temperature: 100(2) K  
 Wavelength: 0.71073 Å  
 Crystal system: Orthorhombic  
 Space group: P2<sub>1</sub>2<sub>1</sub>2<sub>1</sub>  
 Unit cell dimensions:  
 a = 9.4229(5) Å, α = 90°  
 b = 12.3082(7) Å, β = 90°  
 c = 12.8889(7) Å, γ = 90°  
 Volume, Z: 1494.84(14) Å<sup>3</sup>, 4  
 Density (calculated): 1.405 Mg/m<sup>3</sup>  
 Absorption coefficient: 0.121 mm<sup>-1</sup>  
 F(000): 664  
 Crystal size: 0.75 × 0.64 × 0.55 mm  
 Crystal shape, colour: block, colourless  
 θ range for data collection: 2.29 to 28.28°  
 Limiting indices: -12 ≤ h ≤ 12, -15 ≤ k ≤ 16, -17 ≤ l ≤ 17  
 Reflections collected: 15454  
 Independent reflections: 2115 (R(int) = 0.0193)  
 Completeness to θ = 28.28°: 100.0 %  
 Absorption correction: multi-scan  
 Max. and min. transmission: 0.936 and 0.870  
 Refinement method: Full-matrix least-squares on  $F^2$   
 Data / restraints / parameters: 2115 / 0 / 203  
 Goodness-of-fit on  $F^2$ : 1.030  
 Final R indices [I>2σ(I)]: R1 = 0.0327, wR2 = 0.0913  
 R indices (all data): R1 = 0.0333, wR2 = 0.0922  
 Largest diff. peak and hole: 0.316 and -0.182 e × Å<sup>-3</sup>

Refinement of  $F^2$  against ALL reflections. The weighted R-factor wR and goodness of fit are based on  $F^2$ , conventional R-factors R are based on  $F$ , with  $F$  set to zero for negative  $F^2$ . The threshold expression of  $F^2 > 2\sigma(F^2)$  is used only for calculating R-factors

Treatment of hydrogen atoms:

All hydrogen atoms were placed in calculated positions and were isotropically refined with a displacement parameter of 1.5 times (methyl) or 1.2 times (all others) that of the adjacent carbon atom.

Table 2. Atomic coordinates [ $\times 10^4$ ] and equivalent isotropic displacement parameters [ $\text{\AA}^2 \times 10^3$ ] for 06mz040m.  $U(\text{eq})$  is defined as one third of the trace of the orthogonalized  $U_{ij}$  tensor.

	X	Y	Z	$U(\text{eq})$
C(1)	7571(2)	3783(1)	8237(1)	19(1)
C(2)	6870(2)	4449(1)	8862(1)	18(1)
C(3)	7330(2)	4720(1)	9933(1)	17(1)
C(4)	8815(2)	4262(1)	10131(1)	17(1)
C(5)	9039(2)	3175(1)	9592(1)	18(1)
C(6)	8154(2)	2279(1)	10101(1)	18(1)
C(7)	5805(2)	6008(1)	8182(1)	22(1)
C(8)	4422(2)	6483(2)	7842(1)	28(1)
C(9)	5494(2)	4932(1)	11194(1)	25(1)
C(10)	4754(2)	4377(2)	12072(1)	29(1)
C(11)	10242(2)	5822(1)	10339(1)	27(1)
C(12)	11386(2)	6502(2)	9861(2)	41(1)
C(13)	7702(2)	1437(1)	11716(1)	24(1)
O(1)	8751(1)	3212(1)	8509(1)	20(1)
O(2)	5631(1)	4954(1)	8499(1)	21(1)
O(3)	6929(1)	6458(1)	8202(1)	31(1)
O(4)	6397(1)	4240(1)	10704(1)	20(1)
O(5)	5343(2)	5858(1)	10943(1)	48(1)
O(6)	9859(1)	4994(1)	9703(1)	20(1)
O(7)	9717(2)	5958(1)	11176(1)	40(1)
O(8)	7308(1)	1714(1)	9654(1)	23(1)
O(9)	8498(1)	2211(1)	11098(1)	23(1)

All esds (except the esd in the dihedral angle between two l.s. planes)

are estimated using the full covariance matrix. The cell esds are taken

into account individually in the estimation of esds in distances, angles

and torsion angles; correlations between esds in cell parameters are only

used when they are defined by crystal symmetry. An approximate (isotropic)

treatment of cell esds is used for estimating esds involving l.s. planes.

Table 3. Bond lengths [Å] and angles [deg] for 06mz040m.

C(1)-C(2)	1.326 (2)	C(2)-C(1)-O(1)	124.76 (13)
C(1)-O(1)		C(2)-C(1)-H(1)	117.6
1.3612 (18)		O(1)-C(1)-H(1)	117.6
C(1)-H(1)	0.9500	C(1)-C(2)-O(2)	119.14 (13)
C(2)-O(2)		C(1)-C(2)-C(3)	123.88 (13)
1.4026 (17)		O(2)-C(2)-C(3)	116.97 (12)
C(2)-C(3)		O(4)-C(3)-C(2)	111.56 (11)
1.4847 (19)		O(4)-C(3)-C(4)	106.82 (11)
C(3)-O(4)		C(2)-C(3)-C(4)	109.89 (12)
1.4526 (17)		O(4)-C(3)-H(3)	109.5
C(3)-C(4)	1.530 (2)	C(2)-C(3)-H(3)	109.5
C(3)-H(3)	1.0000	C(4)-C(3)-H(3)	109.5
C(4)-O(6)		O(6)-C(4)-C(5)	106.29 (11)
1.4431 (17)		O(6)-C(4)-C(3)	109.20 (11)
C(4)-C(5)	1.522 (2)	C(5)-C(4)-C(3)	111.98 (11)
C(4)-H(4)	1.0000	O(6)-C(4)-H(4)	109.8
C(5)-O(1)		C(5)-C(4)-H(4)	109.8
1.4235 (17)		C(3)-C(4)-H(4)	109.8
C(5)-C(6)		O(1)-C(5)-C(4)	113.14 (12)
1.5292 (19)		O(1)-C(5)-C(6)	109.84 (11)
C(5)-H(5)	1.0000	C(4)-C(5)-C(6)	111.26 (11)
C(6)-O(8)		O(1)-C(5)-H(5)	107.4
1.2038 (18)		C(4)-C(5)-H(5)	107.4
C(6)-O(9)		C(6)-C(5)-H(5)	107.4
1.3290 (18)		O(8)-C(6)-O(9)	125.98 (13)
C(7)-O(3)	1.196 (2)	O(8)-C(6)-C(5)	124.93 (13)
C(7)-O(2)		O(9)-C(6)-C(5)	109.06 (12)
1.3697 (18)		O(3)-C(7)-O(2)	122.56 (14)
C(7)-C(8)	1.494 (2)	O(3)-C(7)-C(8)	126.71 (14)
C(8)-H(8A)	0.9800	O(2)-C(7)-C(8)	110.72 (14)
C(8)-H(8B)	0.9800	C(7)-C(8)-H(8A)	109.5
C(8)-H(8C)	0.9800	C(7)-C(8)-H(8B)	109.5
C(9)-O(5)	1.194 (2)	H(8A)-C(8)-H(8B)	109.5
C(9)-O(4)		C(7)-C(8)-H(8C)	109.5
1.3597 (18)		H(8A)-C(8)-H(8C)	109.5
C(9)-C(10)	1.494 (2)	H(8B)-C(8)-H(8C)	109.5
C(10)-H(10A)	0.9800	O(5)-C(9)-O(4)	123.15 (16)
C(10)-H(10B)	0.9800	O(5)-C(9)-C(10)	125.88 (16)
C(10)-H(10C)	0.9800	O(4)-C(9)-C(10)	110.96 (14)
C(11)-O(7)	1.198 (2)	C(9)-C(10)-H(10A)	109.5
C(11)-O(6)		C(9)-C(10)-H(10B)	109.5
1.3560 (19)		H(10A)-C(10)-H(10B)	109.5
C(11)-C(12)	1.498 (2)	C(9)-C(10)-H(10C)	109.5
C(12)-H(12A)	0.9800	H(10A)-C(10)-H(10C)	109.5
C(12)-H(12B)	0.9800	H(10B)-C(10)-H(10C)	109.5
C(12)-H(12C)	0.9800	O(7)-C(11)-O(6)	122.64 (15)
C(13)-O(9)		O(7)-C(11)-C(12)	126.07 (16)
1.4506 (18)		O(6)-C(11)-C(12)	111.29 (14)
C(13)-H(13A)	0.9800	C(11)-C(12)-H(12A)	109.5
C(13)-H(13B)	0.9800	C(11)-C(12)-H(12B)	109.5
C(13)-H(13C)	0.9800	H(12A)-C(12)-H(12B)	109.5
		C(11)-C(12)-H(12C)	109.5
		H(12A)-C(12)-H(12C)	109.5

H(12B)-C(12)-H(12C)  
109.5  
O(9)-C(13)-H(13A)  
109.5  
O(9)-C(13)-H(13B)  
109.5  
H(13A)-C(13)-H(13B)  
109.5  
O(9)-C(13)-H(13C)  
109.5  
H(13A)-C(13)-H(13C)  
109.5  
H(13B)-C(13)-H(13C)  
109.5  
C(1)-O(1)-C(5)  
115.15(11)  
C(7)-O(2)-C(2)  
114.83(12)  
C(9)-O(4)-C(3)  
116.24(12)  
C(11)-O(6)-C(4)  
114.81(12)  
C(6)-O(9)-C(13)  
116.48(12)

Table 4. Anisotropic displacement parameters [ $\text{\AA}^2 \times 10^3$ ] for 06mz040m.  
The anisotropic displacement factor exponent takes the form:  $-2 \pi^2 [(h a^*)^2 U11 + \dots + 2 h k a^* b^* U12]$

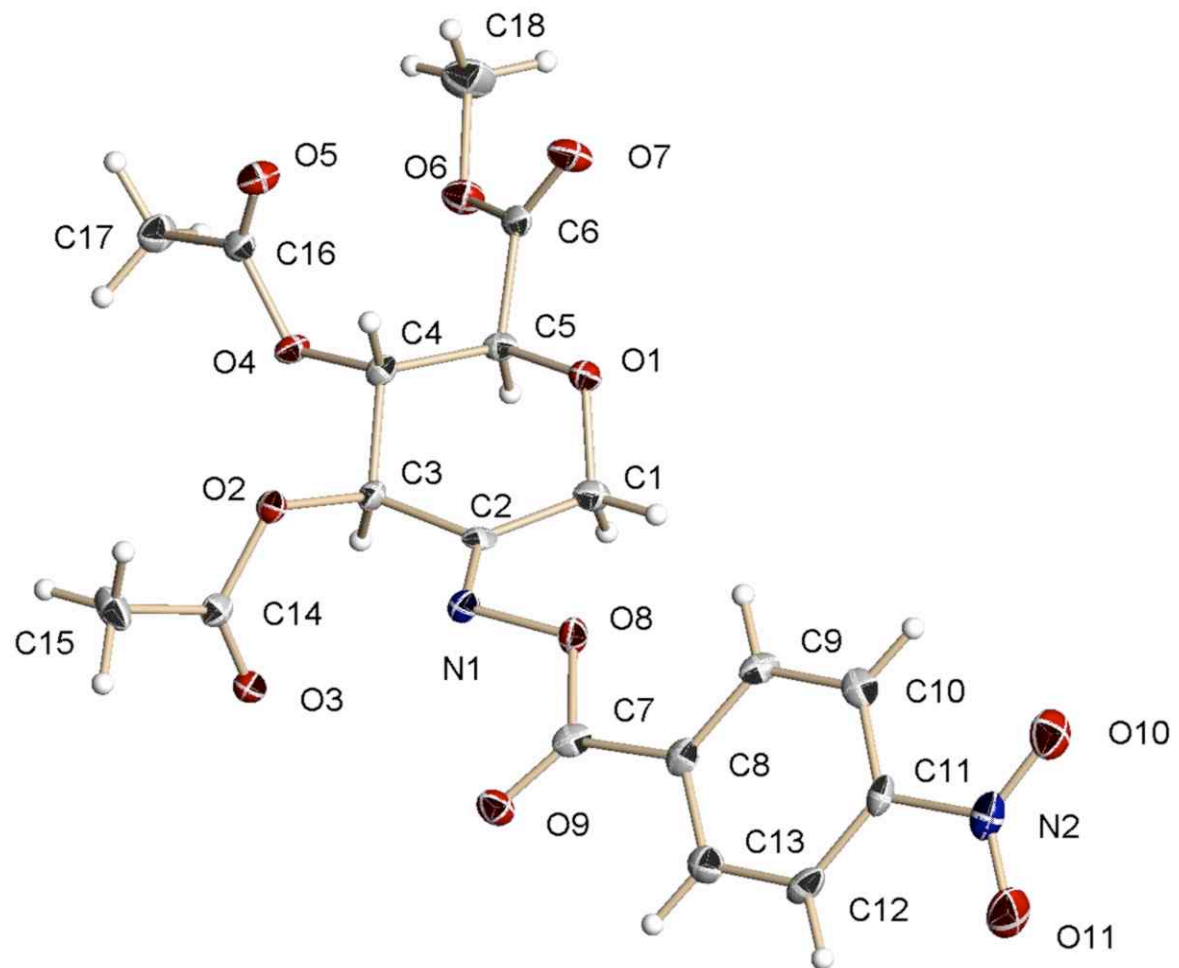
	U11	U22	U33	U23	U13	U12
C(1)	20(1)	21(1)	17(1)	2(1)	-1(1)	-2(1)
C(2)	18(1)	20(1)	17(1)	2(1)	-2(1)	0(1)
C(3)	19(1)	18(1)	16(1)	0(1)	1(1)	1(1)
C(4)	17(1)	19(1)	17(1)	1(1)	1(1)	-3(1)
C(5)	16(1)	19(1)	18(1)	1(1)	0(1)	0(1)
C(6)	15(1)	18(1)	20(1)	1(1)	1(1)	2(1)
C(7)	23(1)	23(1)	20(1)	4(1)	2(1)	4(1)
C(8)	24(1)	30(1)	31(1)	8(1)	2(1)	7(1)
C(9)	23(1)	27(1)	26(1)	-7(1)	4(1)	1(1)
C(10)	25(1)	37(1)	24(1)	-10(1)	8(1)	-5(1)
C(11)	29(1)	28(1)	24(1)	-4(1)	3(1)	-9(1)
C(12)	48(1)	37(1)	38(1)	-11(1)	15(1)	-23(1)
C(13)	28(1)	22(1)	24(1)	6(1)	1(1)	-3(1)
O(1)	21(1)	22(1)	17(1)	-1(1)	2(1)	2(1)
O(2)	19(1)	22(1)	22(1)	2(1)	-3(1)	1(1)
O(3)	24(1)	27(1)	42(1)	11(1)	1(1)	0(1)
O(4)	20(1)	21(1)	18(1)	0(1)	5(1)	1(1)
O(5)	53(1)	29(1)	63(1)	4(1)	30(1)	11(1)
O(6)	20(1)	20(1)	19(1)	0(1)	2(1)	-5(1)
O(7)	50(1)	43(1)	26(1)	-12(1)	10(1)	-22(1)
O(8)	21(1)	25(1)	23(1)	-2(1)	1(1)	-4(1)
O(9)	24(1)	24(1)	21(1)	5(1)	-4(1)	-5(1)

Table 5. Hydrogen coordinates ( $\times 10^4$ ) and isotropic displacement parameters ( $\text{\AA}^2 \times 10^3$ ) for 06mz040m.

	x	y	z	U(eq)
H(1)	7226	3698	7549	23
H(3)	7345	5527	10022	21
H(4)	8973	4179	10894	21
H(5)	10061	2974	9678	21
H(8A)	3918	6775	8445	42
H(8B)	3844	5917	7514	42
H(8C)	4598	7068	7343	42
H(10A)	4343	4923	12536	43
H(10B)	5437	3932	12457	43
H(10C)	3998	3912	11798	43
H(12A)	10969	6987	9341	61
H(12B)	12088	6028	9529	61
H(12C)	11850	6935	10401	61

H (13A)	6749	1724	11849	37
H (13B)	8191	1317	12377	37
H (13C)	7628	748	11339	37

---



**Figure 83:** X-Ray crystal structure of methyl 3,4-di-*O*-acetyl-2-deoxy-2-(4-nitrobenzoyloxyimino)-D-*arabino*-hex-2-enopyranuronate (**10**).

Table 1. Crystal data and structure refinement for 06mz333m:

Identification code: 06mz333m

Empirical formula: C<sub>18</sub> H<sub>18</sub> N<sub>2</sub> O<sub>11</sub>

Formula weight: 438.34

Temperature: 100(2) K

Wavelength: 0.71073 Å

Crystal system: Orthorhombic

Space group: P<sub>2</sub><sub>1</sub>2<sub>1</sub>2<sub>1</sub>

Unit cell dimensions:

a = 7.6879(10) Å, α = 90°

b = 9.9406(13) Å, β = 90°

c = 25.416(3) Å, γ = 90°

Volume, Z: 1942.3(4) Å<sup>3</sup>, 4

Density (calculated): 1.499 Mg/m<sup>3</sup>

Absorption coefficient: 0.127 mm<sup>-1</sup>

F(000): 912

Crystal size: 0.54 × 0.16 × 0.16 mm

Crystal shape, colour: rod, colourless

θ range for data collection: 1.60 to 28.28°

Limiting indices: -10 ≤ h ≤ 9, -13 ≤ k ≤ 12, -33 ≤ l ≤ 33

Reflections collected: 18200

Independent reflections: 2747 (R(int) = 0.0410)

Completeness to θ = 28.28°: 99.3 %

Absorption correction: multi-scan

Max. and min. transmission: 0.980 and 0.687

Refinement method: Full-matrix least-squares on F<sup>2</sup>

Data / restraints / parameters: 2747 / 0 / 283

Goodness-of-fit on F<sup>2</sup>: 1.404

Final R indices [I>2σ(I)]: R1 = 0.0660, wR2 = 0.1363

R indices (all data): R1 = 0.0667, wR2 = 0.1365

Largest diff. peak and hole: 0.407 and -0.293 e × Å<sup>-3</sup>

Refinement of F<sup>2</sup> against ALL reflections. The weighted R-factor wR and goodness of fit are based on F<sup>2</sup>, conventional R-factors R are based on F, with F set to zero for negative F<sup>2</sup>. The threshold expression of F<sup>2</sup> > 2σ(F<sup>2</sup>) is used only for calculating R-factors

Treatment of hydrogen atoms:

All other hydrogen atoms were placed in calculated positions and were refined with an isotropic displacement parameter 1.5 (methyl) or 1.2 times (all others) that of the adjacent carbon atom.

Table 2. Atomic coordinates [ $\times 10^4$ ] and equivalent isotropic displacement parameters [ $\text{\AA}^2 \times 10^3$ ] for 06mz333m.  $U(\text{eq})$  is defined as one third of the trace of the orthogonalized  $U_{ij}$  tensor.

	x	y	z	$U(\text{eq})$
C (1)	1100 (5)	7769 (4)	9441 (2)	18 (1)
C (2)	2790 (5)	7048 (4)	9320 (1)	13 (1)
C (3)	4005 (5)	7786 (4)	8948 (1)	14 (1)
C (4)	3013 (5)	8441 (4)	8494 (1)	14 (1)
C (5)	1390 (5)	9156 (4)	8707 (1)	14 (1)
C (6)	304 (5)	9786 (4)	8268 (2)	16 (1)
C (7)	2702 (6)	4526 (4)	10204 (2)	16 (1)
C (8)	1253 (6)	3792 (4)	10477 (2)	16 (1)
C (9)	-446 (6)	3815 (4)	10287 (2)	16 (1)
C (10)	-1743 (6)	3108 (4)	10549 (2)	18 (1)
C (11)	-1297 (6)	2400 (4)	10996 (2)	17 (1)
C (12)	378 (6)	2350 (4)	11193 (2)	20 (1)
C (13)	1653 (6)	3053 (4)	10926 (2)	20 (1)
C (14)	6746 (5)	6682 (4)	9002 (2)	16 (1)
C (15)	7941 (6)	5771 (5)	8709 (2)	24 (1)
C (16)	4104 (5)	9542 (4)	7730 (2)	16 (1)
C (17)	5291 (6)	10659 (4)	7564 (2)	22 (1)
C (18)	158 (7)	11647 (5)	7686 (2)	32 (1)
N (1)	3332 (5)	5925 (3)	9495 (1)	16 (1)
N (2)	-2681 (5)	1649 (4)	11273 (2)	24 (1)
O (1)	335 (4)	8209 (3)	8960 (1)	17 (1)
O (2)	5261 (4)	6911 (3)	8715 (1)	15 (1)
O (3)	6999 (4)	7184 (3)	9422 (1)	21 (1)
O (4)	4192 (4)	9393 (3)	8264 (1)	16 (1)
O (5)	3208 (4)	8867 (3)	7454 (1)	21 (1)
O (6)	1026 (4)	10957 (3)	8120 (1)	21 (1)
O (7)	-991 (4)	9306 (3)	8088 (1)	23 (1)
O (8)	2020 (4)	5339 (3)	9827 (1)	18 (1)
O (9)	4214 (4)	4398 (3)	10301 (1)	20 (1)
O (10)	-4140 (5)	1650 (4)	11079 (1)	30 (1)
O (11)	-2299 (5)	1081 (4)	11683 (1)	37 (1)

All esds (except the esd in the dihedral angle between two l.s. planes)

are estimated using the full covariance matrix. The cell esds are taken

into account individually in the estimation of esds in distances, angles

and torsion angles; correlations between esds in cell parameters are only used when they are defined by crystal symmetry. An approximate (isotropic) treatment of cell esds is used for estimating esds involving l.s. planes.

Table 3. Bond lengths [Å] and angles [deg] for 06mz333m.

C(1)-O(1)	1.423 (5)	C(18)-H(18B)	0.9800
C(1)-C(2)	1.515 (6)	C(18)-H(18C)	0.9800
C(1)-H(1A)	0.9900	N(1)-O(8)	1.438 (4)
C(1)-H(1B)	0.9900	N(2)-O(11)	1.221 (5)
C(2)-N(1)	1.272 (5)	N(2)-O(10)	1.225 (5)
C(2)-C(3)	1.518 (5)		
C(3)-O(2)	1.428 (5)	O(1)-C(1)-C(2)	109.0 (3)
C(3)-C(4)	1.529 (5)	O(1)-C(1)-H(1A)	109.9
C(3)-H(3)	1.0000	C(2)-C(1)-H(1A)	109.9
C(4)-O(4)	1.434 (5)	O(1)-C(1)-H(1B)	109.9
C(4)-C(5)	1.535 (5)	C(2)-C(1)-H(1B)	109.9
C(4)-H(4)	1.0000	H(1A)-C(1)-H(1B)	108.3
C(5)-O(1)	1.400 (5)	N(1)-C(2)-C(1)	128.7 (4)
C(5)-C(6)	1.529 (5)	N(1)-C(2)-C(3)	116.2 (4)
C(5)-H(5)	1.0000	C(1)-C(2)-C(3)	115.1 (3)
C(6)-O(7)	1.195 (5)	O(2)-C(3)-C(2)	112.3 (3)
C(6)-O(6)	1.343 (5)	O(2)-C(3)-C(4)	106.5 (3)
C(7)-O(9)	1.195 (5)	C(2)-C(3)-C(4)	111.7 (3)
C(7)-O(8)	1.358 (5)	O(2)-C(3)-H(3)	108.8
C(7)-C(8)	1.502 (6)	C(2)-C(3)-H(3)	108.8
C(8)-C(13)	1.392 (6)	C(4)-C(3)-H(3)	108.8
C(8)-C(9)	1.393 (6)	O(4)-C(4)-C(3)	105.8 (3)
C(9)-C(10)	1.390 (6)	O(4)-C(4)-C(5)	110.6 (3)
C(9)-H(9)	0.9500	C(3)-C(4)-C(5)	109.6 (3)
C(10)-C(11)	1.378 (6)	O(4)-C(4)-H(4)	110.3
C(10)-H(10)	0.9500	C(3)-C(4)-H(4)	110.3
C(11)-C(12)	1.383 (6)	C(5)-C(4)-H(4)	110.3
C(11)-N(2)	1.478 (5)	O(1)-C(5)-C(6)	107.2 (3)
C(12)-C(13)	1.383 (6)	O(1)-C(5)-C(4)	108.8 (3)
C(12)-H(12)	0.9500	C(6)-C(5)-C(4)	112.1 (3)
C(13)-H(13)	0.9500	O(1)-C(5)-H(5)	109.6
C(14)-O(3)	1.195 (5)	C(6)-C(5)-H(5)	109.6
C(14)-O(2)	1.373 (5)	C(4)-C(5)-H(5)	109.6
C(14)-C(15)	1.490 (6)	O(7)-C(6)-O(6)	125.7 (4)
C(15)-H(15A)	0.9800	O(7)-C(6)-C(5)	124.8 (4)
C(15)-H(15B)	0.9800	O(6)-C(6)-C(5)	109.5 (3)
C(15)-H(15C)	0.9800	O(9)-C(7)-O(8)	125.8 (4)
C(16)-O(5)	1.190 (5)	O(9)-C(7)-C(8)	125.0 (4)
C(16)-O(4)	1.367 (4)	O(8)-C(7)-C(8)	109.2 (3)
C(16)-C(17)	1.498 (6)	C(13)-C(8)-C(9)	120.0 (4)
C(17)-H(17A)	0.9800	C(13)-C(8)-C(7)	118.1 (4)
C(17)-H(17B)	0.9800	C(9)-C(8)-C(7)	121.8 (4)
C(17)-H(17C)	0.9800	C(10)-C(9)-C(8)	119.9 (4)
C(18)-O(6)	1.459 (5)	C(10)-C(9)-H(9)	120.1
C(18)-H(18A)	0.9800	C(8)-C(9)-H(9)	120.1

C(11)-C(10)-C(9)	109.3(3)
118.4(4)	C(16)-C(17)-H(17A)
C(11)-C(10)-H(10)	109.5
120.8	C(16)-C(17)-H(17B)
C(9)-C(10)-H(10)	109.5
120.8	H(17A)-C(17)-H(17B)
C(10)-C(11)-C(12)	109.5
123.3(4)	C(16)-C(17)-H(17C)
C(10)-C(11)-N(2)	109.5
118.1(4)	H(17A)-C(17)-H(17C)
C(12)-C(11)-N(2)	109.5
118.6(4)	H(17B)-C(17)-H(17C)
C(13)-C(12)-C(11)	109.5
117.6(4)	O(6)-C(18)-H(18A)
C(13)-C(12)-H(12)	109.5
121.2	O(6)-C(18)-H(18B)
C(11)-C(12)-H(12)	109.5
121.2	H(18A)-C(18)-H(18B)
C(12)-C(13)-C(8)	109.5
120.9(4)	O(6)-C(18)-H(18C)
C(12)-C(13)-H(13)	109.5
119.6	H(18A)-C(18)-H(18C)
C(8)-C(13)-H(13)	109.5
119.6	C(2)-N(1)-O(8)
O(3)-C(14)-O(2)	109.3(3)
122.7(4)	O(11)-N(2)-O(10)
O(3)-C(14)-C(15)	124.3(4)
126.9(4)	O(11)-N(2)-C(11)
O(2)-C(14)-C(15)	117.8(4)
110.3(3)	O(10)-N(2)-C(11)
C(14)-C(15)-H(15A)	117.8(4)
109.5	C(5)-O(1)-C(1)
C(14)-C(15)-H(15B)	111.2(3)
109.5	C(14)-O(2)-C(3)
H(15A)-C(15)-H(15B)	116.3(3)
109.5	C(16)-O(4)-C(4)
C(14)-C(15)-H(15C)	116.3(3)
109.5	C(6)-O(6)-C(18)
H(15A)-C(15)-H(15C)	115.5(4)
109.5	C(7)-O(8)-N(1)
H(15B)-C(15)-H(15C)	112.6(3)
109.5	
O(5)-C(16)-O(4)	
123.6(4)	
O(5)-C(16)-C(17)	
127.1(4)	
O(4)-C(16)-C(17)	

Table 4. Anisotropic displacement parameters [ $\text{\AA}^2 \times 10^3$ ] for 06mz333m.  
The anisotropic displacement factor exponent takes the form:  $-2 \pi^2 [(h a*)^2 U_{11} + \dots + 2 h k a^* b^* U_{12}]$

	U11	U22	U33	U23	U13	U12
C(1)	18 (2)	18 (2)	17 (2)	2 (2)	-3 (2)	-1 (2)
C(2)	14 (2)	15 (2)	10 (2)	-3 (1)	-6 (1)	-3 (2)
C(3)	14 (2)	15 (2)	11 (2)	-1 (1)	2 (1)	-2 (2)
C(4)	17 (2)	12 (2)	12 (2)	-2 (1)	2 (2)	0 (2)
C(5)	17 (2)	12 (2)	12 (2)	-2 (1)	-2 (2)	2 (2)
C(6)	16 (2)	17 (2)	14 (2)	0 (2)	2 (2)	6 (2)
C(7)	24 (2)	8 (2)	15 (2)	-3 (1)	-1 (2)	-1 (2)
C(8)	21 (2)	12 (2)	16 (2)	-5 (2)	4 (2)	2 (2)
C(9)	25 (2)	11 (2)	13 (2)	-2 (2)	-2 (2)	-3 (2)
C(10)	20 (2)	12 (2)	22 (2)	-7 (2)	0 (2)	0 (2)
C(11)	20 (2)	16 (2)	16 (2)	-2 (2)	9 (2)	0 (2)
C(12)	30 (2)	17 (2)	14 (2)	5 (2)	5 (2)	4 (2)
C(13)	20 (2)	18 (2)	21 (2)	-2 (2)	0 (2)	2 (2)
C(14)	17 (2)	14 (2)	16 (2)	2 (1)	2 (2)	-3 (2)
C(15)	15 (2)	25 (2)	31 (2)	-10 (2)	-2 (2)	5 (2)
C(16)	16 (2)	16 (2)	15 (2)	1 (1)	1 (2)	4 (2)
C(17)	24 (2)	21 (2)	21 (2)	6 (2)	1 (2)	-6 (2)
C(18)	38 (3)	26 (2)	33 (2)	12 (2)	-7 (2)	4 (2)
N(1)	16 (2)	17 (2)	14 (1)	2 (1)	2 (1)	-1 (1)
N(2)	28 (2)	19 (2)	26 (2)	-1 (2)	11 (2)	0 (2)
O(1)	14 (1)	19 (1)	16 (1)	3 (1)	-1 (1)	0 (1)
O(2)	15 (1)	16 (1)	14 (1)	-3 (1)	2 (1)	3 (1)
O(3)	15 (1)	30 (2)	16 (1)	1 (1)	-1 (1)	-1 (1)
O(4)	19 (1)	17 (1)	12 (1)	3 (1)	-1 (1)	-3 (1)
O(5)	27 (2)	19 (1)	16 (1)	1 (1)	-2 (1)	-3 (1)
O(6)	24 (2)	16 (1)	23 (1)	4 (1)	-4 (1)	2 (1)
O(7)	23 (2)	22 (2)	25 (2)	5 (1)	-8 (1)	0 (1)
O(8)	15 (1)	18 (1)	19 (1)	4 (1)	5 (1)	2 (1)
O(9)	17 (2)	19 (1)	24 (1)	4 (1)	-2 (1)	-1 (1)
O(10)	26 (2)	32 (2)	33 (2)	-2 (2)	5 (2)	-10 (2)
O(11)	35 (2)	38 (2)	37 (2)	21 (2)	11 (2)	4 (2)

Table 5. Hydrogen coordinates ( $\times 10^4$ ) and isotropic displacement parameters ( $\text{\AA}^2 \times 10^3$ ) for 06mz333m.

	x	y	z	U (eq)
--	---	---	---	--------

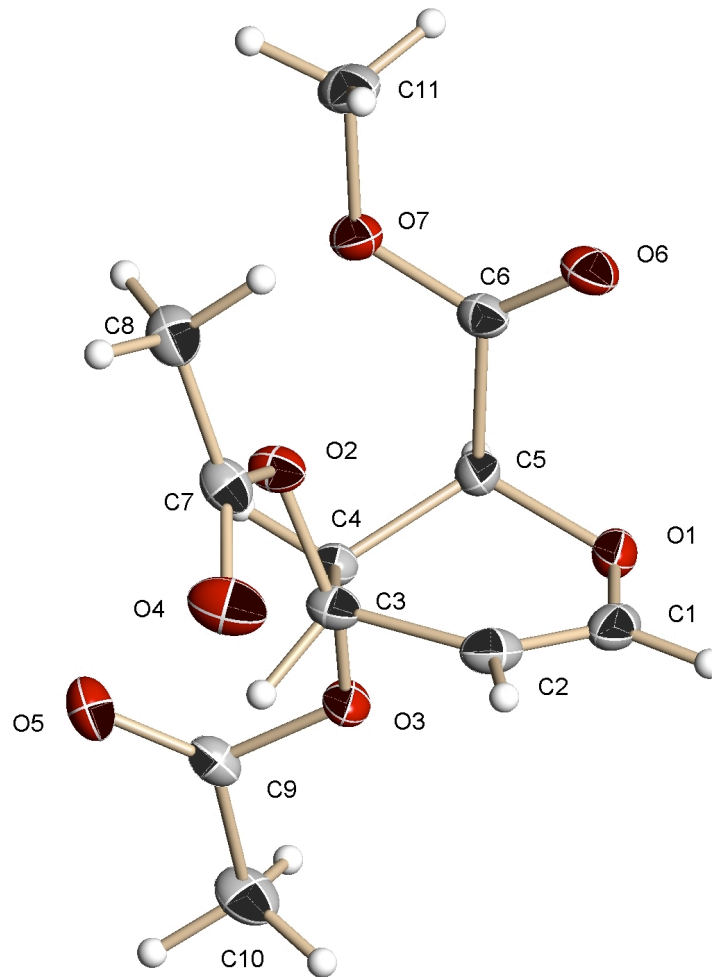
H (1A)	295	7153	9626	21
H (1B)	1328	8551	9671	21
H (3)	4628	8504	9149	16
H (4)	2673	7746	8228	16
H (5)	1747	9868	8963	17
H (9)	-718	4312	9979	20
H (10)	-2907	3113	10424	22
H (12)	643	1849	11502	24
H (13)	2818	3033	11051	24
H (15A)	8561	5192	8958	36
H (15B)	8783	6309	8510	36
H (15C)	7266	5213	8465	36
H (17A)	5299	10722	7179	33
H (17B)	6471	10475	7690	33
H (17C)	4878	11510	7713	33
H (18A)	-926	12051	7813	49
H (18B)	-103	11000	7406	49
H (18C)	921	12353	7548	49

Table 6. Torsion angles [deg] for 06mz333m.

O(1)-C(1)-C(2)-N(1)	-132.8(4)
O(1)-C(1)-C(2)-C(3)	48.5(4)
N(1)-C(2)-C(3)-O(2)	20.4(5)
C(1)-C(2)-C(3)-O(2)	-160.8(3)
N(1)-C(2)-C(3)-C(4)	139.9(3)
C(1)-C(2)-C(3)-C(4)	-41.2(4)
O(2)-C(3)-C(4)-O(4)	-72.9(4)
C(2)-C(3)-C(4)-O(4)	164.2(3)
O(2)-C(3)-C(4)-C(5)	167.8(3)
C(2)-C(3)-C(4)-C(5)	44.9(4)
O(4)-C(4)-C(5)-O(1)	-175.7(3)
C(3)-C(4)-C(5)-O(1)	-59.5(4)
O(4)-C(4)-C(5)-C(6)	65.9(4)
C(3)-C(4)-C(5)-C(6)	-177.8(3)
O(1)-C(5)-C(6)-O(7)	-18.5(5)
C(4)-C(5)-C(6)-O(7)	100.7(5)
O(1)-C(5)-C(6)-O(6)	161.2(3)
C(4)-C(5)-C(6)-O(6)	-79.5(4)
O(9)-C(7)-C(8)-C(13)	9.8(6)
O(8)-C(7)-C(8)-C(13)	-171.0(3)
O(9)-C(7)-C(8)-C(9)	-168.9(4)
O(8)-C(7)-C(8)-C(9)	10.3(5)
C(13)-C(8)-C(9)-C(10)	0.5(6)
C(7)-C(8)-C(9)-C(10)	179.3(3)
C(8)-C(9)-C(10)-C(11)	0.1(6)
C(9)-C(10)-C(11)-C(12)	-0.5(6)
C(9)-C(10)-C(11)-N(2)	-180.0(3)
C(10)-C(11)-C(12)-C(13)	0.2(6)
N(2)-C(11)-C(12)-C(13)	179.7(4)
C(11)-C(12)-C(13)-C(8)	0.5(6)

C (9) -C (8) -C (13) -C (12)	-0.8 (6)
C (7) -C (8) -C (13) -C (12)	-179.6 (4)
C (1) -C (2) -N (1) -O (8)	3.0 (5)
C (3) -C (2) -N (1) -O (8)	-178.3 (3)
C (10) -C (11) -N (2) -O (11)	-176.3 (4)
C (12) -C (11) -N (2) -O (11)	4.2 (6)
C (10) -C (11) -N (2) -O (10)	3.0 (6)
C (12) -C (11) -N (2) -O (10)	-176.5 (4)
C (6) -C (5) -O (1) -C (1)	-167.9 (3)
C (4) -C (5) -O (1) -C (1)	70.7 (4)
C (2) -C (1) -O (1) -C (5)	-63.8 (4)
O (3) -C (14) -O (2) -C (3)	-0.3 (5)
C (15) -C (14) -O (2) -C (3)	-179.2 (3)
C (2) -C (3) -O (2) -C (14)	-85.4 (4)
C (4) -C (3) -O (2) -C (14)	152.1 (3)
O (5) -C (16) -O (4) -C (4)	-5.5 (6)
C (17) -C (16) -O (4) -C (4)	174.6 (3)
C (3) -C (4) -O (4) -C (16)	144.2 (3)
C (5) -C (4) -O (4) -C (16)	-97.2 (4)
O (7) -C (6) -O (6) -C (18)	-2.6 (6)
C (5) -C (6) -O (6) -C (18)	177.7 (4)
O (9) -C (7) -O (8) -N (1)	7.9 (5)
C (8) -C (7) -O (8) -N (1)	-171.3 (3)
C (2) -N (1) -O (8) -C (7)	-151.9 (3)

---



**Figure 84:** X-Ray crystal structure of methyl 3,4-di-*O*-acetyl-1,5-anhydro-2-deoxy-D-*arabino*-hex-1-enopyranuronate (**15**).

Table 1. Crystal data and structure refinement for 07mz145m:

Identification code: 07mz145m

Empirical formula: C11 H14 O7

Formula weight: 258.22

Temperature: 100(2) K

Wavelength: 0.71073 Å

Crystal system: Triclinic

Space group: P1

Unit cell dimensions:

$a = 7.1472(10)$  Å,  $\alpha = 106.238(2)^\circ$

$b = 7.2811(10)$  Å,  $\beta = 114.827(2)^\circ$

$c = 7.4841(10)$  Å,  $\gamma = 105.335(2)^\circ$

Volume,  $Z$ : 305.05(7) Å<sup>3</sup>, 1

Density (calculated): 1.406 Mg/m<sup>3</sup>

Absorption coefficient: 0.119 mm<sup>-1</sup>

$F(000)$ : 136

Crystal size: 0.53 × 0.45 × 0.20 mm

Crystal shape, colour: block, colourless

$\theta$  range for data collection: 1.39 to 28.28°

Limiting indices: -9 ≤  $h$  ≤ 9, 9 ≤  $k$  ≤ 9, 9 ≤  $l$  ≤ 9

Reflections collected: 3174

Independent reflections: 1506 ( $R(\text{int}) = 0.0265$ )

Completeness to  $\theta = 28.27^\circ$ : 99.4 %

Absorption correction: multi-scan

Max. and min. transmission: 0.976 and 0.873

Refinement method: Full-matrix least-squares on  $F^2$

Data / restraints / parameters: 1506 / 3 / 166

Goodness-of-fit on  $F^2$ : 1.053

Final  $R$  indices [ $I > 2\sigma(I)$ ]:  $R1 = 0.0313$ ,  $wR2 = 0.0842$

$R$  indices (all data):  $R1 = 0.0316$ ,  $wR2 = 0.0848$

Largest diff. peak and hole: 0.257 and -0.220 e × Å<sup>-3</sup>

Refinement of  $F^2$  against ALL reflections. The weighted  $R$ -factor  $wR$  and goodness of fit are based on  $F^2$ , conventional  $R$ -factors  $R$  are based on  $F$ , with  $F$  set to zero for negative  $F^2$ . The threshold expression of  $F^2 > 2\sigma(F^2)$  is used only for calculating  $R$ -factors

Treatment of hydrogen atoms:

All hydrogen atoms were placed in calculated positions and were refined with an isotropic displacement parameter 1.5 (methyl) or 1.2 times (all others) that of the adjacent carbon atom.

Table 2. Atomic coordinates [ $\times 10^4$ ] and equivalent isotropic displacement parameters [ $\text{\AA}^2 \times 10^3$ ] for 07mz145m.  $U(\text{eq})$  is defined as one third of the trace of the orthogonalized  $U_{ij}$  tensor.

	x	y	z	$U(\text{eq})$
C(1)	9094 (3)	6207 (3)	10385 (3)	26 (1)
C(2)	7413 (3)	6577 (3)	9124 (3)	25 (1)
C(3)	5381 (3)	4882 (3)	6938 (3)	20 (1)
C(4)	5339 (3)	2704 (3)	6650 (3)	17 (1)
C(5)	7751 (3)	2843 (3)	7562 (3)	19 (1)
C(6)	8823 (3)	3420 (3)	6280 (3)	19 (1)
C(7)	4946 (3)	6598 (3)	4579 (3)	23 (1)
C(8)	5148 (3)	6666 (3)	2679 (3)	26 (1)
C(9)	2345 (3)	707 (3)	6948 (3)	20 (1)
C(10)	1878 (3)	23 (3)	8495 (4)	30 (1)
C(11)	8291 (4)	2539 (4)	2793 (3)	29 (1)
O(1)	9267 (2)	4328 (2)	9827 (2)	23 (1)
O(2)	5487 (2)	5095 (2)	5085 (2)	22 (1)
O(3)	4587 (2)	2060 (2)	7984 (2)	21 (1)
O(4)	4414 (3)	7740 (2)	5579 (3)	34 (1)
O(5)	960 (2)	146 (2)	5051 (2)	27 (1)
O(6)	10676 (2)	4850 (2)	7120 (2)	26 (1)
O(7)	7446 (2)	2070 (2)	4148 (2)	22 (1)

All esds (except the esd in the dihedral angle between two l.s. planes) are estimated using the full covariance matrix. The cell esds are taken into account individually in the estimation of esds in distances, angles and torsion angles; correlations between esds in cell parameters are only used when they are defined by crystal symmetry. An approximate (isotropic) treatment of cell esds is used for estimating esds involving l.s. planes.

Table 3. Bond lengths [Å] and angles [deg] for 07mz145m.

C(1)-C(2)	1.330 (3)	C(2)-C(3)-H(3)	110.1
C(1)-O(1)	1.369 (3)	C(4)-C(3)-H(3)	110.1
C(1)-H(1)	0.9500	O(3)-C(4)-C(5)	105.06 (12)
C(2)-C(3)	1.496 (3)	O(3)-C(4)-C(3)	108.31 (13)
C(2)-H(2)	0.9500	C(5)-C(4)-C(3)	111.04 (13)
C(3)-O(2)	1.468 (2)	O(3)-C(4)-H(4)	110.8
C(3)-C(4)	1.530 (2)	C(5)-C(4)-H(4)	110.8
C(3)-H(3)	1.0000	C(3)-C(4)-H(4)	110.8
C(4)-O(3)		O(1)-C(5)-C(4)	112.16 (13)
1.4435 (18)		O(1)-C(5)-C(6)	108.67 (14)
C(4)-C(5)	1.526 (2)	C(4)-C(5)-C(6)	113.07 (13)
C(4)-H(4)	1.0000	O(1)-C(5)-H(5)	107.6
C(5)-O(1)	1.425 (2)	C(4)-C(5)-H(5)	107.6
C(5)-C(6)	1.535 (2)	C(6)-C(5)-H(5)	107.6
C(5)-H(5)	1.0000	O(6)-C(6)-O(7)	125.66 (17)
C(6)-O(6)	1.199 (2)	O(6)-C(6)-C(5)	123.90 (16)
C(6)-O(7)	1.332 (2)	O(7)-C(6)-C(5)	110.40 (14)
C(7)-O(4)	1.205 (2)	O(4)-C(7)-O(2)	123.11 (17)
C(7)-O(2)	1.350 (2)	O(4)-C(7)-C(8)	125.70 (16)
C(7)-C(8)	1.501 (3)	O(2)-C(7)-C(8)	111.18 (15)
C(8)-H(8A)	0.9800	C(7)-C(8)-H(8A)	109.5
C(8)-H(8B)	0.9800	C(7)-C(8)-H(8B)	109.5
C(8)-H(8C)	0.9800	H(8A)-C(8)-H(8B)	109.5
C(9)-O(5)	1.202 (2)	C(7)-C(8)-H(8C)	109.5
C(9)-O(3)	1.355 (2)	H(8A)-C(8)-H(8C)	109.5
C(9)-C(10)	1.502 (3)	H(8B)-C(8)-H(8C)	109.5
C(10)-H(10A)	0.9800	O(5)-C(9)-O(3)	123.57 (16)
C(10)-H(10B)	0.9800	O(5)-C(9)-C(10)	125.96 (16)
C(10)-H(10C)	0.9800	O(3)-C(9)-C(10)	110.47 (15)
C(11)-O(7)	1.453 (2)	C(9)-C(10)-H(10A)	109.5
C(11)-H(11A)	0.9800	C(9)-C(10)-H(10B)	109.5
C(11)-H(11B)	0.9800	H(10A)-C(10)-H(10B)	109.5
C(11)-H(11C)	0.9800	C(9)-C(10)-H(10C)	109.5
		H(10A)-C(10)-H(10C)	109.5
C(2)-C(1)-O(1)		H(10B)-C(10)-H(10C)	109.5
125.51 (16)		O(7)-C(11)-H(11A)	109.5
C(2)-C(1)-H(1)		O(7)-C(11)-H(11B)	109.5
117.2		H(11A)-C(11)-H(11B)	109.5
O(1)-C(1)-H(1)		O(7)-C(11)-H(11C)	109.5
117.2		H(11A)-C(11)-H(11C)	109.5
C(1)-C(2)-C(3)		H(11B)-C(11)-H(11C)	109.5
122.37 (17)		C(1)-O(1)-C(5)	114.85 (13)
C(1)-C(2)-H(2)		C(7)-O(2)-C(3)	116.57 (14)
118.8		C(9)-O(3)-C(4)	116.81 (13)
C(3)-C(2)-H(2)		C(6)-O(7)-C(11)	114.19 (15)
118.8			
O(2)-C(3)-C(2)			
112.78 (14)			
O(2)-C(3)-C(4)			
103.73 (13)			
C(2)-C(3)-C(4)			
109.99 (15)			
O(2)-C(3)-H(3)			
110.1			

Table 4. Anisotropic displacement parameters [ $\text{\AA}^2 \times 10^3$ ] for 07mz145m.  
The anisotropic displacement factor exponent takes the form:  $-2 \pi^2 [(h a*)^2 U_{11} + \dots + 2 h k a^* b^* U_{12}]$

	U11	U22	U33	U23	U13	U12
C(1)	22(1)	26(1)	20(1)	5(1)	13(1)	2(1)
C(2)	29(1)	21(1)	27(1)	8(1)	20(1)	8(1)
C(3)	22(1)	23(1)	24(1)	13(1)	16(1)	11(1)
C(4)	16(1)	19(1)	17(1)	9(1)	10(1)	6(1)
C(5)	17(1)	23(1)	17(1)	10(1)	9(1)	8(1)
C(6)	21(1)	23(1)	22(1)	13(1)	14(1)	13(1)
C(7)	20(1)	21(1)	29(1)	13(1)	13(1)	8(1)
C(8)	24(1)	28(1)	29(1)	18(1)	13(1)	11(1)
C(9)	18(1)	17(1)	28(1)	11(1)	14(1)	9(1)
C(10)	26(1)	30(1)	39(1)	20(1)	22(1)	9(1)
C(11)	35(1)	41(1)	24(1)	20(1)	20(1)	22(1)
O(1)	18(1)	31(1)	17(1)	10(1)	8(1)	7(1)
O(2)	26(1)	25(1)	26(1)	16(1)	17(1)	15(1)
O(3)	17(1)	24(1)	20(1)	11(1)	11(1)	5(1)
O(4)	44(1)	31(1)	50(1)	24(1)	34(1)	24(1)
O(5)	17(1)	27(1)	30(1)	13(1)	9(1)	7(1)
O(6)	23(1)	29(1)	29(1)	12(1)	18(1)	9(1)
O(7)	24(1)	27(1)	20(1)	12(1)	13(1)	13(1)

Table 5. Hydrogen coordinates ( $\times 10^4$ ) and isotropic displacement parameters ( $\text{\AA}^2 \times 10^3$ ) for 07mz145m.

	x	y	z	U(eq)
H(1)	10275	7342	11793	31
H(2)	7506	7968	9630	30
H(3)	3935	4888	6817	24
H(4)	4299	1633	5069	21
H(5)	7636	1408	7436	23
H(8A)	4160	7262	1940	39
H(8B)	4671	5221	1635	39
H(8C)	6744	7560	3220	39
H(10A)	221	-625	7871	45
H(10B)	2635	1266	9914	45
H(10C)	2474	-1016	8708	45

H (11A)	8584	4000	3006	43
H (11B)	7142	1547	1242	43
H (11C)	9718	2387	3216	43

---

Table 6. Torsion angles [deg] for 07mz145m.

O(1)-C(1)-C(2)-C(3)	4.0(3)
C(1)-C(2)-C(3)-O(2)	-104.27(19)
C(1)-C(2)-C(3)-C(4)	11.0(2)
O(2)-C(3)-C(4)-O(3)	-163.92(12)
C(2)-C(3)-C(4)-O(3)	75.22(16)
O(2)-C(3)-C(4)-C(5)	81.22(16)
C(2)-C(3)-C(4)-C(5)	-39.65(18)
O(3)-C(4)-C(5)-O(1)	-59.20(16)
C(3)-C(4)-C(5)-O(1)	57.67(18)
O(3)-C(4)-C(5)-C(6)	177.49(13)
C(3)-C(4)-C(5)-C(6)	-65.64(18)
O(1)-C(5)-C(6)-O(6)	2.6(2)
C(4)-C(5)-C(6)-O(6)	127.80(18)
O(1)-C(5)-C(6)-O(7)	-179.71(14)
C(4)-C(5)-C(6)-O(7)	-54.50(18)
C(2)-C(1)-O(1)-C(5)	12.8(2)
C(4)-C(5)-O(1)-C(1)	-43.16(19)
C(6)-C(5)-O(1)-C(1)	82.58(16)
O(4)-C(7)-O(2)-C(3)	0.6(3)
C(8)-C(7)-O(2)-C(3)	179.37(14)
C(2)-C(3)-O(2)-C(7)	-77.81(19)
C(4)-C(3)-O(2)-C(7)	163.23(14)
O(5)-C(9)-O(3)-C(4)	-5.0(2)
C(10)-C(9)-O(3)-C(4)	174.55(14)
C(5)-C(4)-O(3)-C(9)	-143.20(14)
C(3)-C(4)-O(3)-C(9)	98.07(17)
O(6)-C(6)-O(7)-C(11)	-4.3(2)
C(5)-C(6)-O(7)-C(11)	178.06(14)

---

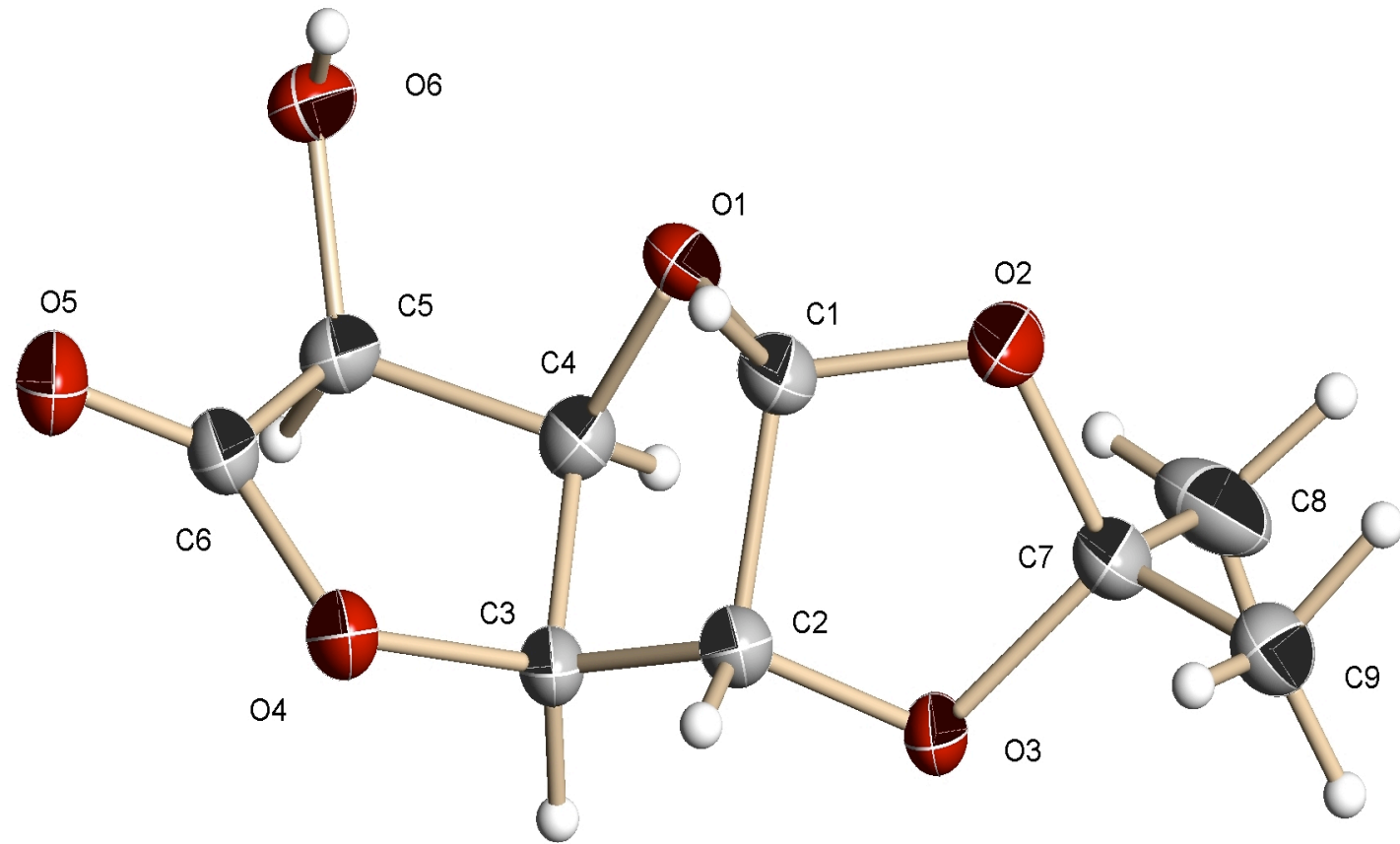


**Figure 85:** X-Ray crystal structure of 1,2-O-isopropylidene- $\alpha$ -D-glucurono-6,3-lactone (**19**).

Table 1. Crystal data and structure refinement for 06mz412m:

Identification code: 06mz412m  
 Empirical formula: C9 H12 O6  
 Formula weight: 216.19  
 Temperature: 100(2) K  
 Wavelength: 0.71073 Å  
 Crystal system: Monoclinic  
 Space group: P2<sub>1</sub>  
 Unit cell dimensions:  
 a = 7.777(3) Å, α = 90°  
 b = 6.104(3) Å, β = 106.277(8)°  
 c = 11.169(5) Å, γ = 90°  
 Volume, Z: 508.9(4) Å<sup>3</sup>, 2  
 Density (calculated): 1.411 Mg/m<sup>3</sup>  
 Absorption coefficient: 0.120 mm<sup>-1</sup>  
 F(000): 228  
 Crystal size: 0.70 x 0.15 x 0.10 mm  
 Crystal shape, colour: needle, colourless  
 θ range for data collection: 1.90 to 28.27°  
 Limiting indices: -9 ≤ h ≤ 10, -8 ≤ k ≤ 8, -14 ≤ l ≤ 12  
 Reflections collected: 3561  
 Independent reflections: 1354 (R(int) = 0.0521)  
 Completeness to θ = 28.27°: 98.3 %  
 Absorption correction: multi-scan  
 Max. and min. transmission: 1 and 0.506685  
 Refinement method: Full-matrix least-squares on  $F^2$   
 Data / restraints / parameters: 1354 / 1 / 139  
 Goodness-of-fit on  $F^2$ : 1.132  
 Final R indices [ $I > 2\sigma(I)$ ]: R1 = 0.0637, wR2 = 0.1491  
 R indices (all data): R1 = 0.0729, wR2 = 0.1541  
 Largest diff. peak and hole: 0.528 and -0.318 e × Å<sup>-3</sup>

Refinement of  $F^2$  against ALL reflections. The weighted R-factor wR and goodness of fit are based on  $F^2$ , conventional R-factors R are based on  $F$ , with  $F$  set to zero for negative  $F^2$ . The threshold expression of  $F^2 > 2\sigma(F^2)$  is used only for calculating R-factors

**Comments:**

The crystals under investigation are extremely flexible long intergrown needles and are easily bent when attempting to be cut to size. As no

crystals in the appropriate size range had been available attempts have been made to dissolve the crystals to size. One of the better crystals made this way was used for the data collection, but even crystals prepared this way showed severely odd shaped peak patterns.

Treatment of hydrogen atoms:

All hydrogen atoms were placed in calculated positions and were refined with an isotropic displacement parameter 1.5 (methyl, hydroxyl) or 1.2 times (all others) that of the adjacent carbon or oxygen atom.

Table 2. Atomic coordinates [ $\times 10^4$ ] and equivalent isotropic displacement parameters [ $\text{\AA}^2 \times 10^3$ ] for 06rk001m.  $U(\text{eq})$  is defined as one third of the trace of the orthogonalized  $U_{ij}$  tensor.

	x	y	z	$U(\text{eq})$
C(1)	6030 (5)	4620 (6)	7383 (3)	32 (1)
C(2)	6361 (5)	2751 (6)	6542 (3)	30 (1)
C(3)	8104 (5)	3422 (6)	6244 (3)	28 (1)
C(4)	9107 (5)	4856 (6)	7371 (3)	30 (1)
C(5)	9882 (5)	6746 (6)	6764 (3)	30 (1)
C(6)	8532 (5)	6875 (6)	5450 (3)	30 (1)
C(7)	6055 (5)	1298 (6)	8458 (4)	34 (1)
C(8)	7569 (6)	892 (10)	9628 (4)	48 (1)
C(9)	4376 (5)	-76 (8)	8353 (4)	40 (1)
O(1)	7699 (4)	5775 (5)	7852 (2)	37 (1)
O(2)	5493 (4)	3596 (5)	8353 (3)	40 (1)
O(3)	6742 (4)	892 (5)	7379 (2)	33 (1)
O(4)	7614 (3)	4932 (5)	5165 (2)	32 (1)
O(5)	8236 (4)	8413 (5)	4726 (3)	38 (1)
O(6)	10099 (3)	8774 (4)	7419 (3)	34 (1)

All esds (except the esd in the dihedral angle between two l.s. planes) are estimated using the full covariance matrix. The cell esds are taken into account individually in the estimation of esds in distances, angles and torsion angles; correlations between esds in cell parameters are only used when they are defined by crystal symmetry. An approximate (isotropic) treatment of cell esds is used for estimating esds involving l.s. planes.

Table 3. Bond lengths [Å] and angles [deg] for 06mz412m.

C(1)-O(2)	1.412 (5)	O(4)-C(3)-C(2)	107.5 (3)
C(1)-O(1)	1.440 (5)	O(4)-C(3)-C(4)	105.4 (3)
C(1)-C(2)	1.545 (5)	C(2)-C(3)-C(4)	104.4 (3)
C(1)-H(1)	1.0000	O(4)-C(3)-H(3)	113.0
C(2)-O(3)	1.447 (4)	C(2)-C(3)-H(3)	113.0
C(2)-C(3)	1.539 (5)	C(4)-C(3)-H(3)	113.0
C(2)-H(2)	1.0000	O(1)-C(4)-C(5)	107.4 (3)
C(3)-O(4)	1.480 (4)	O(1)-C(4)-C(3)	104.9 (3)
C(3)-C(4)	1.551 (5)	C(5)-C(4)-C(3)	103.6 (3)
C(3)-H(3)	1.0000	O(1)-C(4)-H(4)	113.4
C(4)-O(1)	1.460 (4)	C(5)-C(4)-H(4)	113.4
C(4)-C(5)	1.543 (5)	C(3)-C(4)-H(4)	113.4
C(4)-H(4)	1.0000	O(6)-C(5)-C(4)	115.4 (3)
C(5)-O(6)	1.424 (4)	O(6)-C(5)-C(6)	113.2 (3)
C(5)-C(6)	1.549 (5)	C(4)-C(5)-C(6)	102.1 (3)
C(5)-H(5)	1.0000	O(6)-C(5)-H(5)	108.6
C(6)-O(5)	1.218 (5)	C(4)-C(5)-H(5)	108.6
C(6)-O(4)	1.375 (5)	C(6)-C(5)-H(5)	108.6
C(7)-O(2)	1.464 (5)	O(5)-C(6)-O(4)	121.5 (3)
C(7)-O(3)	1.469 (4)	O(5)-C(6)-C(5)	128.3 (3)
C(7)-C(8)	1.514 (6)	O(4)-C(6)-C(5)	110.2 (3)
C(7)-C(9)	1.528 (6)	O(2)-C(7)-O(3)	105.4 (3)
C(8)-H(8A)	0.9800	O(2)-C(7)-C(8)	111.6 (4)
C(8)-H(8B)	0.9800	O(3)-C(7)-C(8)	107.9 (3)
C(8)-H(8C)	0.9800	O(2)-C(7)-C(9)	106.9 (3)
C(9)-H(9A)	0.9800	O(3)-C(7)-C(9)	110.1 (3)
C(9)-H(9B)	0.9800	C(8)-C(7)-C(9)	114.7 (4)
C(9)-H(9C)	0.9800	C(7)-C(8)-H(8A)	109.5
O(6)-H(6)	0.8400	C(7)-C(8)-H(8B)	109.5
		H(8A)-C(8)-H(8B)	109.5
O(2)-C(1)-O(1)		C(7)-C(8)-H(8C)	109.5
111.6 (3)		H(8A)-C(8)-H(8C)	109.5
O(2)-C(1)-C(2)		H(8B)-C(8)-H(8C)	109.5
106.0 (3)		C(7)-C(9)-H(9A)	109.5
O(1)-C(1)-C(2)		C(7)-C(9)-H(9B)	109.5
107.2 (3)		H(9A)-C(9)-H(9B)	109.5
O(2)-C(1)-H(1)		C(7)-C(9)-H(9C)	109.5
110.6		H(9A)-C(9)-H(9C)	109.5
O(1)-C(1)-H(1)		H(9B)-C(9)-H(9C)	109.5
110.6		C(1)-O(1)-C(4)	111.8 (3)
C(2)-C(1)-H(1)		C(1)-O(2)-C(7)	109.8 (3)
110.6		C(2)-O(3)-C(7)	110.0 (3)
O(3)-C(2)-C(3)		C(6)-O(4)-C(3)	110.5 (3)
108.3 (3)		C(5)-O(6)-H(6)	109.5
O(3)-C(2)-C(1)			
103.0 (3)			
C(3)-C(2)-C(1)			
104.0 (3)			
O(3)-C(2)-H(2)			
113.5			
C(3)-C(2)-H(2)			
113.5			
C(1)-C(2)-H(2)			
113.5			

Table 4. Anisotropic displacement parameters [ $\text{\AA}^2 \times 10^3$ ] for 06mz412m.  
The anisotropic displacement factor exponent takes the form:  $-2 \pi^2 [ (h a*)^2 U_{11} + \dots + 2 h k a^* b^* U_{12} ]$

	U11	U22	U33	U23	U13	U12
C(1)	46 (2)	25 (2)	30 (2)	0 (2)	20 (2)	4 (2)
C(2)	44 (2)	23 (2)	27 (2)	0 (1)	17 (1)	-1 (1)
C(3)	43 (2)	20 (2)	26 (2)	2 (1)	19 (1)	0 (1)
C(4)	43 (2)	22 (2)	30 (2)	1 (2)	16 (1)	-1 (2)
C(5)	41 (2)	21 (2)	32 (2)	-3 (1)	17 (2)	-2 (1)
C(6)	43 (2)	25 (2)	29 (2)	2 (1)	20 (1)	1 (2)
C(7)	49 (2)	26 (2)	33 (2)	-2 (1)	24 (2)	0 (2)
C(8)	60 (2)	53 (3)	34 (2)	-10 (2)	18 (2)	13 (2)
C(9)	56 (2)	33 (2)	41 (2)	-6 (2)	30 (2)	-7 (2)
O(1)	59 (2)	27 (1)	35 (1)	-8 (1)	31 (1)	-6 (1)
O(2)	63 (2)	23 (1)	47 (2)	-1 (1)	38 (1)	0 (1)
O(3)	54 (1)	21 (1)	35 (1)	2 (1)	30 (1)	0 (1)
O(4)	49 (1)	26 (1)	26 (1)	2 (1)	18 (1)	-2 (1)
O(5)	54 (2)	31 (1)	36 (1)	7 (1)	24 (1)	-1 (1)
O(6)	46 (1)	23 (1)	40 (1)	-7 (1)	21 (1)	-5 (1)

Table 5. Hydrogen coordinates ( $\times 10^4$ ) and isotropic displacement parameters ( $\text{\AA}^2 \times 10^3$ ) for 06mz412m.

	x	y	z	U (eq)
H(1)	5074	5631	6900	38
H(2)	5334	2502	5782	35
H(3)	8825	2138	6107	33
H(4)	10039	4033	8013	36
H(5)	11071	6281	6673	36
H(8A)	8540	1935	9664	72
H(8B)	8017	-606	9615	72
H(8C)	7129	1084	10362	72
H(9A)	4691	-1634	8400	60
H(9B)	3491	227	7554	60
H(9C)	3870	299	9037	60
H(6)	9092	9359	7325	51

Table 6. Torsion angles [deg] for 06mz412m.

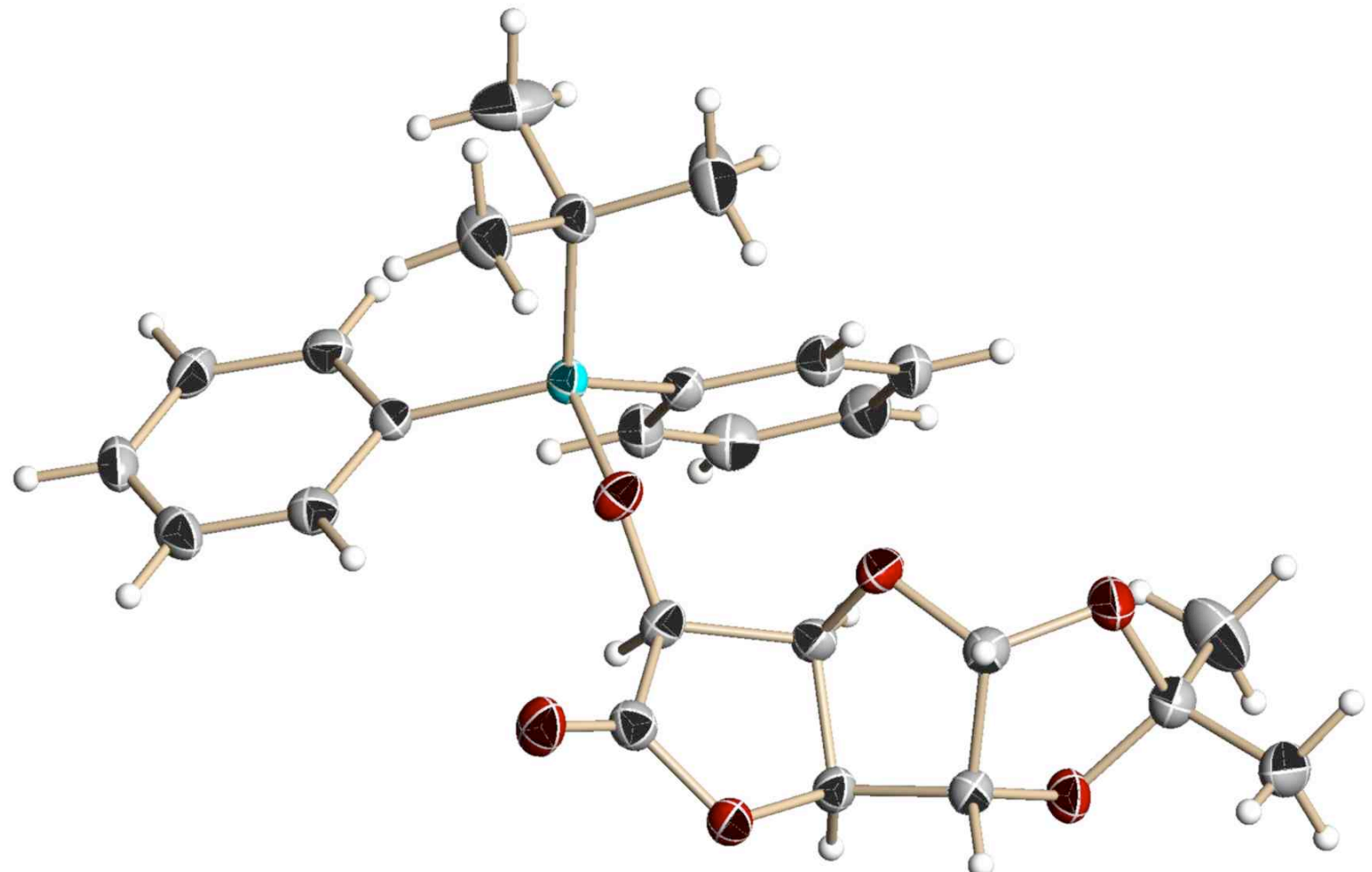
O(2)-C(1)-C(2)-O(3)	-24.3(4)
O(1)-C(1)-C(2)-O(3)	95.0(3)
O(2)-C(1)-C(2)-C(3)	-137.3(3)
O(1)-C(1)-C(2)-C(3)	-17.9(4)
O(3)-C(2)-C(3)-O(4)	166.3(3)
C(1)-C(2)-C(3)-O(4)	-84.7(3)
O(3)-C(2)-C(3)-C(4)	-82.2(3)
C(1)-C(2)-C(3)-C(4)	26.9(4)
O(4)-C(3)-C(4)-O(1)	86.5(3)
C(2)-C(3)-C(4)-O(1)	-26.5(4)
O(4)-C(3)-C(4)-C(5)	-26.0(3)
C(2)-C(3)-C(4)-C(5)	-139.0(3)
O(1)-C(4)-C(5)-O(6)	40.2(4)
C(3)-C(4)-C(5)-O(6)	150.8(3)
O(1)-C(4)-C(5)-C(6)	-83.0(3)
C(3)-C(4)-C(5)-C(6)	27.6(3)
O(6)-C(5)-C(6)-O(5)	33.6(5)
C(4)-C(5)-C(6)-O(5)	158.4(4)
O(6)-C(5)-C(6)-O(4)	-145.7(3)
C(4)-C(5)-C(6)-O(4)	-20.9(4)
O(2)-C(1)-O(1)-C(4)	116.8(3)
C(2)-C(1)-O(1)-C(4)	1.2(4)
C(5)-C(4)-O(1)-C(1)	125.8(3)
C(3)-C(4)-O(1)-C(1)	16.0(4)
O(1)-C(1)-O(2)-C(7)	-96.3(4)
C(2)-C(1)-O(2)-C(7)	20.1(4)
O(3)-C(7)-O(2)-C(1)	-7.9(4)
C(8)-C(7)-O(2)-C(1)	109.0(4)
C(9)-C(7)-O(2)-C(1)	-125.0(3)
C(3)-C(2)-O(3)-C(7)	129.7(3)
C(1)-C(2)-O(3)-C(7)	19.9(4)
O(2)-C(7)-O(3)-C(2)	-8.6(4)
C(8)-C(7)-O(3)-C(2)	-127.9(4)
C(9)-C(7)-O(3)-C(2)	106.3(4)
O(5)-C(6)-O(4)-C(3)	-174.6(3)
C(5)-C(6)-O(4)-C(3)	4.7(4)
C(2)-C(3)-O(4)-C(6)	124.5(3)
C(4)-C(3)-O(4)-C(6)	13.6(3)

Table 7. Hydrogen bonds for 06mz412m [ $\text{\AA}$  and deg].

D-H...A	d(D-H)	d(H...A)	d(D...A)	$\angle$ (DHA)
O(6)-H(6)...O(3) #1	0.84	2.07	2.903(4)	171.4

---

```
Symmetry transformations used to generate equivalent atoms: #1 x,y+1,z
```



**Figure 86:** X-Ray crystal structure of 1,2-O-isopropylidene-6-O-tert-butyldiphenylsilyl- $\alpha$ -D-glucurono-6,3-lactone (**21**).

Table 1. Crystal data and structure refinement for 06mz341m:

Identification code: 06mz341m  
 Empirical formula: C<sub>25</sub> H<sub>30</sub> O<sub>6</sub> Si<sub>1</sub>  
 Formula weight: 454.58  
 Temperature: 100(2) K  
 Wavelength: 0.71073 Å  
 Crystal system: Monoclinic  
 Space group: P<sub>2</sub><sub>1</sub>  
 Unit cell dimensions:  
 a = 9.8494(12) Å, α = 90°  
 b = 9.3400(11) Å, β = 105.318(2)°  
 c = 13.4557(16) Å, γ = 90°  
 Volume, Z: 1193.9(2) Å<sup>3</sup>, 2  
 Density (calculated): 1.265 Mg/m<sup>3</sup>  
 Absorption coefficient: 0.136 mm<sup>-1</sup>  
 F(000): 484  
 Crystal size: 0.57 × 0.36 × 0.31 mm  
 Crystal shape, colour: block, colourless  
 θ range for data collection: 1.57 to 28.28°  
 Limiting indices: -12 ≤ h ≤ 13, -12 ≤ k ≤ 12, -17 ≤ l ≤ 17  
 Reflections collected: 8315  
 Independent reflections: 5334 (R(int) = 0.0256)  
 Completeness to θ = 28.28°: 98.1 %  
 Absorption correction: multi-scan  
 Max. and min. transmission: 0.959 and 0.848  
 Refinement method: Full-matrix least-squares on  $F^2$   
 Data / restraints / parameters: 5334 / 1 / 294  
 Goodness-of-fit on  $F^2$ : 1.182  
 Final R indices [ $I > 2\sigma(I)$ ]: R1 = 0.0537, wR2 = 0.1353  
 R indices (all data): R1 = 0.0578, wR2 = 0.1374  
 Largest diff. peak and hole: 0.492 and -0.246 e × Å<sup>-3</sup>

Refinement of  $F^2$  against ALL reflections. The weighted R-factor wR and goodness of fit are based on  $F^2$ , conventional R-factors R are based on  $F$ , with  $F$  set to zero for negative  $F^2$ . The threshold expression of  $F^2 > 2\sigma(F^2)$  is used only for calculating R-factors

## Treatment of hydrogen atoms:

All other hydrogen atoms were placed in calculated positions and were refined with an isotropic displacement parameter 1.5 (methyl) or 1.2 times (all others) that of the adjacent carbon atom.

Table 2. Atomic coordinates [ $\times 10^4$ ] and equivalent isotropic displacement parameters [ $\text{\AA}^2 \times 10^3$ ] for 06mz341m.  $U(\text{eq})$  is defined as one third of the trace of the orthogonalized  $U_{ij}$  tensor.

	x	y	z	$U(\text{eq})$
C(1)	2519(3)	4153(3)	1272(2)	25(1)
C(2)	2404(3)	3381(3)	2261(2)	24(1)
C(3)	3390(3)	4219(3)	3137(2)	22(1)
C(4)	3433(3)	5712(3)	2659(2)	23(1)
C(5)	4949(3)	6195(3)	3167(2)	24(1)
C(6)	5747(3)	4759(3)	3283(2)	27(1)
C(7)	-849(4)	5177(5)	1330(3)	51(1)
C(8)	154(3)	3969(4)	1281(2)	30(1)
C(9)	-564(4)	2614(4)	781(3)	46(1)
C(10)	3729(3)	9451(3)	2946(2)	22(1)
C(11)	3547(3)	10002(3)	3870(2)	28(1)
C(12)	2204(3)	10290(4)	3997(2)	31(1)
C(13)	1013(3)	10036(3)	3190(3)	29(1)
C(14)	1154(3)	9472(3)	2267(2)	28(1)
C(15)	2494(3)	9178(3)	2147(2)	26(1)
C(16)	6949(3)	9472(3)	3929(2)	21(1)
C(17)	8031(3)	8493(3)	4375(2)	25(1)
C(18)	9171(3)	8894(4)	5195(2)	29(1)
C(19)	9269(3)	10279(4)	5581(2)	29(1)
C(20)	8218(3)	11272(3)	5158(2)	28(1)
C(21)	7065(3)	10871(3)	4340(2)	26(1)
C(22)	5881(3)	9706(3)	1559(2)	25(1)
C(23)	7295(3)	9061(5)	1489(2)	38(1)
C(24)	6065(5)	11353(4)	1662(3)	50(1)
C(25)	4748(4)	9353(5)	577(3)	47(1)
O(1)	3293(2)	5449(2)	1586(2)	30(1)
O(2)	1123(2)	4447(3)	710(2)	36(1)
O(3)	1004(2)	3690(2)	2307(2)	29(1)
O(4)	4831(2)	3673(2)	3321(2)	25(1)
O(5)	6969(2)	4562(3)	3362(2)	34(1)
O(6)	5526(2)	7178(2)	2607(2)	25(1)
Si(1)	5501(1)	8959(1)	2765(1)	20(1)

All esds (except the esd in the dihedral angle between two l.s. planes) are estimated using the full covariance matrix. The cell esds are taken

into account individually in the estimation of esds in distances, angles and torsion angles; correlations between esds in cell parameters are only used when they are defined by crystal symmetry. An approximate (isotropic) treatment of cell esds is used for estimating esds involving l.s. planes.

Table 3. Bond lengths [Å] and angles [deg] for 06mz341m.

C(1)-O(2)	1.410 (3)	C(13)-H(13)	0.9500
C(1)-O(1)	1.433 (3)	C(14)-C(15)	1.399 (4)
C(1)-C(2)	1.544 (4)	C(14)-H(14)	0.9500
C(1)-H(1)	1.0000	C(15)-H(15)	0.9500
C(2)-O(3)	1.426 (4)	C(16)-C(21)	1.411 (4)
C(2)-C(3)	1.530 (4)	C(16)-C(17)	1.412 (4)
C(2)-H(2)	1.0000	C(16)-Si(1)	1.881 (3)
C(3)-O(4)	1.466 (3)	C(17)-C(18)	1.401 (4)
C(3)-C(4)	1.540 (4)	C(17)-H(17)	0.9500
C(3)-H(3)	1.0000	C(18)-C(19)	1.387 (5)
C(4)-O(1)	1.435 (3)	C(18)-H(18)	0.9500
C(4)-C(5)	1.536 (4)	C(19)-C(20)	1.395 (5)
C(4)-H(4)	1.0000	C(19)-H(19)	0.9500
C(5)-O(6)	1.400 (3)	C(20)-C(21)	1.407 (4)
C(5)-C(6)	1.542 (4)	C(20)-H(20)	0.9500
C(5)-H(5)	1.0000	C(21)-H(21)	0.9500
C(6)-O(5)	1.195 (4)	C(22)-C(25)	1.524 (4)
C(6)-O(4)	1.367 (4)	C(22)-C(23)	1.544 (4)
C(7)-C(8)	1.512 (5)	C(22)-C(24)	1.551 (5)
C(7)-H(7A)	0.9800	C(22)-Si(1)	1.893 (3)
C(7)-H(7B)	0.9800	C(23)-H(23A)	0.9800
C(7)-H(7C)	0.9800	C(23)-H(23B)	0.9800
C(8)-O(3)	1.437 (3)	C(23)-H(23C)	0.9800
C(8)-O(2)	1.445 (4)	C(24)-H(24A)	0.9800
C(8)-C(9)	1.517 (5)	C(24)-H(24B)	0.9800
C(9)-H(9A)	0.9800	C(24)-H(24C)	0.9800
C(9)-H(9B)	0.9800	C(25)-H(25A)	0.9800
C(9)-H(9C)	0.9800	C(25)-H(25B)	0.9800
C(10)-C(11)	1.401 (4)	C(25)-H(25C)	0.9800
C(10)-C(15)	1.418 (4)	O(6)-Si(1)	1.677 (2)
C(10)-Si(1)	1.881 (3)		
C(11)-C(12)	1.403 (4)	O(2)-C(1)-O(1)	111.2 (2)
C(11)-H(11)	0.9500	O(2)-C(1)-C(2)	105.7 (2)
C(12)-C(13)	1.392 (4)	O(1)-C(1)-C(2)	107.2 (2)
C(12)-H(12)	0.9500	O(2)-C(1)-H(1)	110.9
C(13)-C(14)	1.390 (4)	O(1)-C(1)-H(1)	110.9

C (2)-C (1)-H (1)	109.4
110.9	
O (3)-C (2)-C (3)	109.4
106.7 (2)	122.8 (3)
O (3)-C (2)-C (1)	128.2 (3)
103.6 (2)	109.0 (2)
C (3)-C (2)-C (1)	109.5
104.3 (2)	109.5
O (3)-C (2)-H (2)	109.5
113.7	109.5
C (3)-C (2)-H (2)	109.5
113.7	105.5 (2)
C (1)-C (2)-H (2)	108.4 (3)
113.7	108.9 (3)
O (4)-C (3)-C (2)	111.1 (3)
110.0 (2)	108.5 (3)
O (4)-C (3)-C (4)	114.1 (3)
104.7 (2)	109.5
C (2)-C (3)-C (4)	109.5
103.0 (2)	109.5
O (4)-C (3)-H (3)	109.5
112.8	109.5
C (2)-C (3)-H (3)	109.5
112.8	117.0 (3)
C (4)-C (3)-H (3)	123.0 (2)
112.8	119.8 (2)
O (1)-C (4)-C (5)	121.6 (3)
108.8 (2)	119.2
O (1)-C (4)-C (3)	119.2
105.0 (2)	120.0 (3)
C (5)-C (4)-C (3)	120.0
102.2 (2)	120.0
O (1)-C (4)-H (4)	119.9 (3)
113.3	120.0
C (5)-C (4)-H (4)	120.0
113.3	119.9 (3)
C (3)-C (4)-H (4)	120.1
113.3	120.1
O (6)-C (5)-C (4)	121.6 (3)
116.0 (2)	119.2
O (6)-C (5)-C (6)	119.2
110.9 (2)	117.3 (3)
C (4)-C (5)-C (6)	121.8 (2)
101.5 (2)	120.7 (2)
O (6)-C (5)-H (5)	121.3 (3)
109.4	119.3
C (4)-C (5)-H (5)	119.3

C(19)-C(18)-C(17)	109.5
120.4 (3)	
C(19)-C(18)-H(18)	109.5
119.8	
C(17)-C(18)-H(18)	109.5
119.8	
C(18)-C(19)-C(20)	109.5
119.8 (3)	
C(18)-C(19)-H(19)	109.5
120.1	
C(20)-C(19)-H(19)	109.5
120.1	
C(19)-C(20)-C(21)	109.5
120.0 (3)	
C(19)-C(20)-H(20)	109.5
120.0	
C(21)-C(20)-H(20)	109.5
120.0	
C(20)-C(21)-C(16)	108.96 (12)
121.2 (3)	
C(20)-C(21)-H(21)	107.70 (12)
119.4	
C(16)-C(21)-H(21)	104.11 (12)
119.4	
C(25)-C(22)-C(23)	110.00 (13)
109.2 (3)	
C(25)-C(22)-C(24)	114.91 (13)
109.5 (3)	
C(23)-C(22)-C(24)	124.05 (18)
107.8 (3)	
C(25)-C(22)-Si(1)	108.70 (12)
113.5 (2)	
C(23)-C(22)-Si(1)	107.70 (12)
107.1 (2)	
C(24)-C(22)-Si(1)	109.5 (2)
109.5	
C(22)-C(23)-H(23A)	109.5
109.5	
C(22)-C(23)-H(23B)	109.5
109.5	
H(23A)-C(23)-H(23B)	109.5
109.5	
C(22)-C(23)-H(23C)	109.5
109.5	
H(23A)-C(23)-H(23C)	109.5
109.5	
H(23B)-C(23)-H(23C)	109.5

Table 4. Anisotropic displacement parameters [ $\text{\AA}^2 \times 10^3$ ] for 06mz341m.  
The anisotropic displacement factor exponent takes the form:  $-2 \pi^2 [(h a*)^2 U_{11} + \dots + 2 h k a^* b^* U_{12}]$

	U11	U22	U33	U23	U13	U12
C(1)	25(1)	24(2)	26(1)	1(1)	6(1)	-1(1)
C(2)	22(1)	23(1)	25(1)	1(1)	6(1)	-1(1)
C(3)	20(1)	20(1)	26(1)	0(1)	6(1)	0(1)
C(4)	20(1)	20(1)	27(1)	2(1)	6(1)	2(1)
C(5)	22(1)	21(1)	28(1)	-2(1)	8(1)	-2(1)
C(6)	29(1)	25(2)	25(1)	-2(1)	2(1)	0(1)
C(7)	39(2)	63(3)	46(2)	6(2)	3(2)	22(2)
C(8)	26(1)	31(1)	30(1)	1(1)	5(1)	-4(1)
C(9)	51(2)	45(2)	33(2)	6(2)	-7(2)	-20(2)
C(10)	20(1)	20(1)	26(1)	1(1)	6(1)	0(1)
C(11)	23(1)	29(2)	30(2)	-2(1)	3(1)	-1(1)
C(12)	32(2)	32(2)	32(2)	-2(1)	14(1)	4(1)
C(13)	21(1)	28(2)	41(2)	2(1)	12(1)	4(1)
C(14)	21(1)	30(2)	32(2)	1(1)	3(1)	-1(1)
C(15)	25(1)	24(2)	28(1)	-2(1)	6(1)	0(1)
C(16)	19(1)	24(1)	21(1)	3(1)	6(1)	-2(1)
C(17)	25(1)	27(1)	26(1)	1(1)	11(1)	1(1)
C(18)	20(1)	39(2)	28(1)	5(1)	6(1)	4(1)
C(19)	21(1)	44(2)	22(1)	1(1)	2(1)	-7(1)
C(20)	32(2)	25(1)	29(2)	-5(1)	10(1)	-10(1)
C(21)	24(1)	23(1)	30(2)	5(1)	8(1)	1(1)
C(22)	22(1)	30(2)	24(1)	2(1)	6(1)	0(1)
C(23)	25(1)	57(2)	34(2)	3(2)	11(1)	4(2)
C(24)	74(3)	37(2)	46(2)	8(2)	30(2)	-1(2)
C(25)	28(2)	83(3)	29(2)	1(2)	4(1)	-11(2)
O(1)	32(1)	30(1)	27(1)	4(1)	5(1)	-10(1)
O(2)	25(1)	50(2)	31(1)	10(1)	2(1)	-6(1)
O(3)	20(1)	37(1)	28(1)	1(1)	5(1)	-2(1)
O(4)	21(1)	21(1)	32(1)	2(1)	4(1)	2(1)
O(5)	22(1)	31(1)	49(1)	1(1)	6(1)	2(1)
O(6)	25(1)	20(1)	33(1)	-3(1)	11(1)	-2(1)
Si(1)	18(1)	20(1)	23(1)	-1(1)	5(1)	0(1)

Table 5. Hydrogen coordinates ( $\times 10^4$ ) and isotropic displacement parameters ( $\text{\AA}^2 \times 10^3$ ) for 06mz341m.

	x	y	z	U (eq)
H (1)	3003	3534	865	30
H (2)	2619	2334	2270	28
H (3)	3054	4246	3776	27
H (4)	2706	6383	2786	27
H (5)	5002	6596	3866	28
H (7A)	-1481	4879	1745	76
H (7B)	-1405	5415	631	76
H (7C)	-312	6020	1644	76
H (9A)	148	1879	786	69
H (9B)	-1087	2820	69	69
H (9C)	-1215	2269	1167	69
H (11)	4352	10186	4425	34
H (12)	2108	10658	4633	37
H (13)	105	10248	3271	35
H (14)	342	9288	1718	34
H (15)	2579	8785	1514	31
H (17)	7985	7544	4115	30
H (18)	9881	8214	5488	35
H (19)	10050	10549	6132	35
H (20)	8281	12221	5421	34
H (21)	6352	11553	4060	31
H (23A)	7182	8030	1357	57
H (23B)	8011	9222	2139	57
H (23C)	7591	9521	925	57
H (24A)	6838	11577	2269	74
H (24B)	5193	11785	1740	74
H (24C)	6282	11737	1044	74
H (25A)	5058	9667	-23	71
H (25B)	3873	9847	584	71
H (25C)	4584	8317	537	71

Table 6. Torsion angles [deg] for 06mz341m.

O(2)-C(1)-C(2)-O(3)	-16.7(3)
O(1)-C(1)-C(2)-O(3)	101.9(2)
O(2)-C(1)-C(2)-C(3)	-128.2(2)
O(1)-C(1)-C(2)-C(3)	-9.6(3)
O(3)-C(2)-C(3)-O(4)	164.8(2)
C(1)-C(2)-C(3)-O(4)	-85.9(3)
O(3)-C(2)-C(3)-C(4)	-84.1(3)
C(1)-C(2)-C(3)-C(4)	25.2(3)
O(4)-C(3)-C(4)-O(1)	82.5(2)
C(2)-C(3)-C(4)-O(1)	-32.6(3)
O(4)-C(3)-C(4)-C(5)	-31.1(3)
C(2)-C(3)-C(4)-C(5)	-146.1(2)
O(1)-C(4)-C(5)-O(6)	42.7(3)
C(3)-C(4)-C(5)-O(6)	153.4(2)
O(1)-C(4)-C(5)-C(6)	-77.5(3)
C(3)-C(4)-C(5)-C(6)	33.1(3)

O(6)-C(5)-C(6)-O(5)	33.2(4)
C(4)-C(5)-C(6)-O(5)	157.0(3)
O(6)-C(5)-C(6)-O(4)	-148.9(2)
C(4)-C(5)-C(6)-O(4)	-25.1(3)
C(15)-C(10)-C(11)-C(12)	-0.8(4)
Si(1)-C(10)-C(11)-C(12)	-176.7(2)
C(10)-C(11)-C(12)-C(13)	-0.4(5)
C(11)-C(12)-C(13)-C(14)	1.2(5)
C(12)-C(13)-C(14)-C(15)	-0.7(5)
C(13)-C(14)-C(15)-C(10)	-0.5(5)
C(11)-C(10)-C(15)-C(14)	1.2(4)
Si(1)-C(10)-C(15)-C(14)	177.3(2)
C(21)-C(16)-C(17)-C(18)	0.2(4)
Si(1)-C(16)-C(17)-C(18)	175.3(2)
C(16)-C(17)-C(18)-C(19)	-0.8(4)
C(17)-C(18)-C(19)-C(20)	0.7(4)
C(18)-C(19)-C(20)-C(21)	-0.2(4)
C(19)-C(20)-C(21)-C(16)	-0.4(4)
C(17)-C(16)-C(21)-C(20)	0.3(4)
Si(1)-C(16)-C(21)-C(20)	-174.7(2)
O(2)-C(1)-O(1)-C(4)	103.4(3)
C(2)-C(1)-O(1)-C(4)	-11.5(3)
C(5)-C(4)-O(1)-C(1)	136.7(2)
C(3)-C(4)-O(1)-C(1)	27.9(3)
O(1)-C(1)-O(2)-C(8)	-113.9(3)
C(2)-C(1)-O(2)-C(8)	2.0(3)
O(3)-C(8)-O(2)-C(1)	13.4(3)
C(7)-C(8)-O(2)-C(1)	129.6(3)
C(9)-C(8)-O(2)-C(1)	-105.7(3)
C(3)-C(2)-O(3)-C(8)	135.3(2)
C(1)-C(2)-O(3)-C(8)	25.5(3)
O(2)-C(8)-O(3)-C(2)	-24.8(3)
C(7)-C(8)-O(3)-C(2)	-141.4(3)
C(9)-C(8)-O(3)-C(2)	92.5(3)
O(5)-C(6)-O(4)-C(3)	-176.3(3)
C(5)-C(6)-O(4)-C(3)	5.6(3)
C(2)-C(3)-O(4)-C(6)	126.4(2)
C(4)-C(3)-O(4)-C(6)	16.4(3)
C(4)-C(5)-O(6)-Si(1)	94.4(3)
C(6)-C(5)-O(6)-Si(1)	-150.60(19)
C(5)-O(6)-Si(1)-C(16)	80.0(2)
C(5)-O(6)-Si(1)-C(10)	-40.3(2)
C(5)-O(6)-Si(1)-C(22)	-162.7(2)
C(21)-C(16)-Si(1)-O(6)	-171.0(2)
C(17)-C(16)-Si(1)-O(6)	14.2(3)
C(21)-C(16)-Si(1)-C(10)	-52.6(3)
C(17)-C(16)-Si(1)-C(10)	132.5(2)
C(21)-C(16)-Si(1)-C(22)	75.5(3)
C(17)-C(16)-Si(1)-C(22)	-99.3(2)
C(11)-C(10)-Si(1)-O(6)	113.7(2)
C(15)-C(10)-Si(1)-O(6)	-62.1(2)
C(11)-C(10)-Si(1)-C(16)	-5.4(3)
C(15)-C(10)-Si(1)-C(16)	178.8(2)
C(11)-C(10)-Si(1)-C(22)	-130.8(2)
C(15)-C(10)-Si(1)-C(22)	53.4(3)
C(25)-C(22)-Si(1)-O(6)	64.0(3)
C(23)-C(22)-Si(1)-O(6)	-56.6(2)

C(24)-C(22)-Si(1)-O(6)	-173.3 (2)
C(25)-C(22)-Si(1)-C(16)	-179.4 (3)
C(23)-C(22)-Si(1)-C(16)	60.0 (3)
C(24)-C(22)-Si(1)-C(16)	-56.6 (3)
C(25)-C(22)-Si(1)-C(10)	-53.5 (3)
C(23)-C(22)-Si(1)-C(10)	-174.1 (2)
C(24)-C(22)-Si(1)-C(10)	69.2 (3)

---

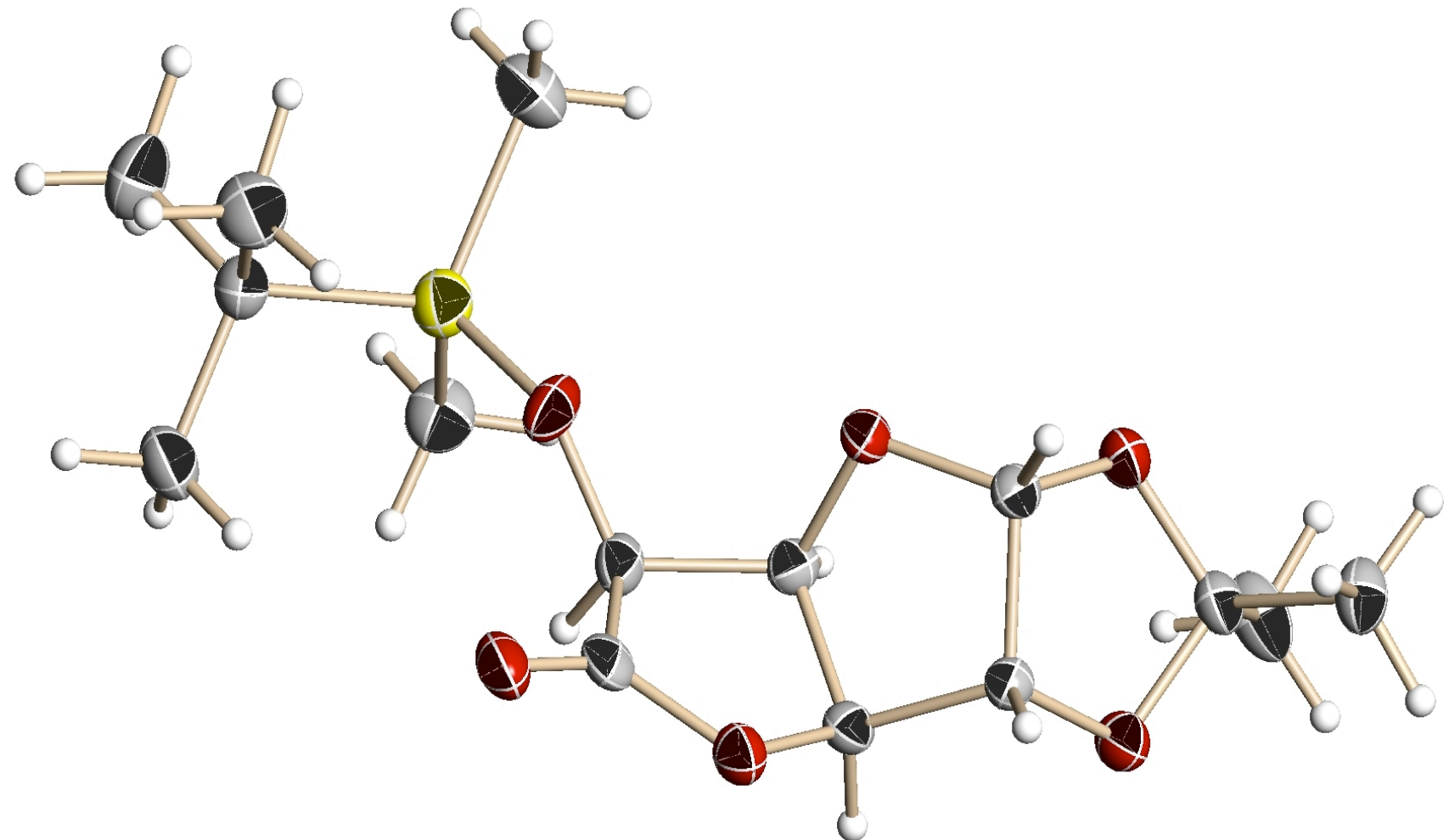


**Figure 87:** X-Ray crystal structure of 1,2-*O*-isopropylidene-6-*O*-*tert*-butyldimethylsilyl- $\alpha$ -D-glucurono-6,3-lactone (**22**).

Table 1. Crystal data and structure refinement for 07mz240m:

Identification code: 07mz240m  
 Empirical formula: C15 H26 O6 S  
 Formula weight: 334.43  
 Temperature: 100(2) K  
 Wavelength: 0.71073 Å  
 Crystal system: Hexagonal  
 Space group: P6<sub>1</sub>  
 Unit cell dimensions:  
 a = 21.718(2) Å, α = 90°  
 b = 21.718(2) Å, β = 90°  
 c = 7.0065(13) Å, γ = 90°  
 Volume, Z: 2862.1(7) Å<sup>3</sup>, 6  
 Density (calculated): 1.164 Mg/m<sup>3</sup>  
 Absorption coefficient: 0.192 mm<sup>-1</sup>  
 F(000): 1080  
 Crystal size: 0.45 × 0.21 × 0.20 mm  
 Crystal shape, colour: block, colourless  
 θ range for data collection: 1.08 to 28.27°  
 Limiting indices: -19 ≤ h ≤ 28, -28 ≤ k ≤ 27, -9 ≤ l ≤ 9  
 Reflections collected: 17664  
 Independent reflections: 4719 (R(int) = 0.0542)  
 Completeness to θ = 28.27°: 100.0 %  
 Absorption correction: multi-scan  
 Max. and min. transmission: 0.962 and 0.750  
 Refinement method: Full-matrix least-squares on  $F^2$   
 Data / restraints / parameters: 4719 / 1 / 206  
 Goodness-of-fit on  $F^2$ : 1.129  
 Final R indices [ $I > 2\sigma(I)$ ]: R1 = 0.0635, wR2 = 0.1857  
 R indices (all data): R1 = 0.0761, wR2 = 0.1990  
 Largest diff. peak and hole: 1.089 and -0.441 e × Å<sup>-3</sup>  
  
 Refinement of  $F^2$  against ALL reflections. The weighted R-factor wR and  
 goodness of fit are based on  $F^2$ , conventional R-factors R are based  
 on  $F$ , with  $F$  set to zero for negative  $F^2$ . The threshold expression of  
 $F^2 > 2\sigma(F^2)$  is used only for calculating R-factors

## Comments:

The structure contains solvent accessible voids of The 329.00 Å<sup>3</sup> (12% of  
 the structure). The voids are located around the six fold screw axis  
 along the c-axis of the unit cell. The two largest remaining electron

density peaks are 1.09 and 0.52 cubic electrons per square inch and thus all the remaining electron density was ignored.

Treatment of hydrogen atoms:

All hydrogen atoms were placed in calculated positions and all H atoms were refined with an isotropic displacement parameter 1.5 (methyl) or 1.2 times (all others) that of the adjacent carbon atom.

Table 2. Atomic coordinates [ $\times 10^4$ ] and equivalent isotropic displacement parameters [ $\text{\AA}^2 \times 10^3$ ] for 07mz240m.  $U(\text{eq})$  is defined as one third of the trace of the orthogonalized  $U_{ij}$  tensor.

	x	y	z	$U(\text{eq})$
C(1)	7698(2)	4051(2)	1326(5)	21(1)
C(2)	8209(1)	4833(2)	1824(4)	20(1)
C(3)	8938(2)	4888(2)	1902(5)	22(1)
C(4)	8823(2)	4202(2)	958(5)	22(1)
C(5)	9295(2)	4013(2)	2105(5)	26(1)
C(6)	9322(2)	4344(2)	4061(5)	27(1)
C(7)	7612(2)	4761(2)	-962(5)	24(1)
C(8)	7818(2)	4927(2)	-3028(5)	38(1)
C(9)	6963(2)	4826(2)	-410(6)	31(1)
C(10)	9989(2)	3347(2)	-771(6)	36(1)
C(11)	8556(2)	2032(2)	92(6)	41(1)
C(12)	9780(2)	2520(2)	2998(6)	29(1)
C(13)	9255(2)	2145(2)	4667(6)	40(1)
C(14)	9986(2)	2004(2)	2127(7)	46(1)
C(15)	10444(2)	3170(2)	3804(6)	36(1)
O(1)	8096(1)	3698(1)	1392(3)	23(1)
O(2)	7482(1)	4066(1)	-568(4)	26(1)
O(3)	8205(1)	5224(1)	192(3)	26(1)
O(4)	9121(1)	4842(1)	3876(3)	26(1)
O(5)	9494(1)	4222(1)	5583(4)	33(1)
O(6)	9067(1)	3299(1)	2282(4)	31(1)
S(1)	9352(1)	2812(1)	1155(1)	32(1)

All esds (except the esd in the dihedral angle between two l.s. planes) are estimated using the full covariance matrix. The cell esds are taken into account individually in the estimation of esds in distances, angles and torsion angles; correlations between esds in cell parameters are only used when they are defined by crystal symmetry. An approximate (isotropic) treatment of cell esds is used for estimating esds involving l.s. planes.

Table 3. Bond lengths [Å] and angles [deg] for 07mz240m.

C(1)-O(2)	1.413 (4)	O(2)-C(1)-C(2)	104.6 (2)
C(1)-O(1)	1.414 (3)	O(1)-C(1)-C(2)	107.0 (2)
C(1)-C(2)	1.535 (4)	O(2)-C(1)-H(1)	111.6
C(1)-H(1)	1.0000	O(1)-C(1)-H(1)	111.6
C(2)-O(3)	1.427 (4)	C(2)-C(1)-H(1)	111.6
C(2)-C(3)	1.527 (4)	O(3)-C(2)-C(3)	107.3 (2)
C(2)-H(2)	1.0000	O(3)-C(2)-C(1)	105.1 (2)
C(3)-O(4)	1.456 (4)	C(3)-C(2)-C(1)	104.1 (2)
C(3)-C(4)	1.532 (4)	O(3)-C(2)-H(2)	113.2
C(3)-H(3)	1.0000	C(3)-C(2)-H(2)	113.2
C(4)-O(1)	1.433 (3)	C(1)-C(2)-H(2)	113.2
C(4)-C(5)	1.513 (4)	O(4)-C(3)-C(2)	109.7 (2)
C(4)-H(4)	1.0000	O(4)-C(3)-C(4)	105.1 (2)
C(5)-O(6)	1.376 (4)	C(2)-C(3)-C(4)	104.4 (2)
C(5)-C(6)	1.536 (5)	O(4)-C(3)-H(3)	112.4
C(5)-H(5)	1.0000	C(2)-C(3)-H(3)	112.4
C(6)-O(5)	1.203 (4)	C(4)-C(3)-H(3)	112.4
C(6)-O(4)	1.359 (4)	O(1)-C(4)-C(5)	108.5 (2)
C(7)-O(2)	1.417 (4)	O(1)-C(4)-C(3)	103.5 (2)
C(7)-O(3)	1.425 (4)	C(5)-C(4)-C(3)	103.4 (3)
C(7)-C(8)	1.505 (5)	O(1)-C(4)-H(4)	113.5
C(7)-C(9)	1.532 (4)	C(5)-C(4)-H(4)	113.5
C(8)-H(8A)	0.9800	C(3)-C(4)-H(4)	113.5
C(8)-H(8B)	0.9800	O(6)-C(5)-C(4)	116.3 (3)
C(8)-H(8C)	0.9800	O(6)-C(5)-C(6)	110.8 (3)
C(9)-H(9A)	0.9800	C(4)-C(5)-C(6)	102.6 (2)
C(9)-H(9B)	0.9800	O(6)-C(5)-H(5)	108.9
C(9)-H(9C)	0.9800	C(4)-C(5)-H(5)	108.9
C(10)-S(1)	1.865 (4)	C(6)-C(5)-H(5)	108.9
C(10)-H(10A)	0.9800	O(5)-C(6)-O(4)	121.3 (3)
C(10)-H(10B)	0.9800	O(5)-C(6)-C(5)	129.1 (3)
C(10)-H(10C)	0.9800	O(4)-C(6)-C(5)	109.7 (3)
C(11)-S(1)	1.866 (4)	O(2)-C(7)-O(3)	105.6 (2)
C(11)-H(11A)	0.9800	O(2)-C(7)-C(8)	108.6 (3)
C(11)-H(11B)	0.9800	O(3)-C(7)-C(8)	108.7 (3)
C(11)-H(11C)	0.9800	O(2)-C(7)-C(9)	110.2 (2)
C(12)-C(14)	1.527 (5)	O(3)-C(7)-C(9)	109.9 (3)
C(12)-C(15)	1.535 (5)	C(8)-C(7)-C(9)	113.5 (3)
C(12)-C(13)	1.550 (5)	C(7)-C(8)-H(8A)	109.5
C(12)-S(1)	1.877 (4)	C(7)-C(8)-H(8B)	109.5
C(13)-H(13A)	0.9800	H(8A)-C(8)-H(8B)	109.5
C(13)-H(13B)	0.9800	C(7)-C(8)-H(8C)	109.5
C(13)-H(13C)	0.9800	H(8A)-C(8)-H(8C)	109.5
C(14)-H(14A)	0.9800	H(8B)-C(8)-H(8C)	109.5
C(14)-H(14B)	0.9800	C(7)-C(9)-H(9A)	109.5
C(14)-H(14C)	0.9800	C(7)-C(9)-H(9B)	109.5
C(15)-H(15A)	0.9800	H(9A)-C(9)-H(9B)	109.5
C(15)-H(15B)	0.9800	C(7)-C(9)-H(9C)	109.5
C(15)-H(15C)	0.9800	H(9A)-C(9)-H(9C)	109.5
O(6)-S(1)	1.666 (2)	H(9B)-C(9)-H(9C)	109.5
O(2)-C(1)-O(1)		S(1)-C(10)-H(10A)	109.5
110.1 (2)		S(1)-C(10)-H(10B)	109.5
		H(10A)-C(10)-H(10B)	109.5

S(1)-C(10)-H(10C)	C(12)-C(15)-H(15B)	109.5
109.5	H(15A)-C(15)-H(15B)	109.5
H(10A)-C(10)-H(10C)	C(12)-C(15)-H(15C)	109.5
109.5	H(15A)-C(15)-H(15C)	109.5
H(10B)-C(10)-H(10C)	H(15B)-C(15)-H(15C)	109.5
109.5	C(1)-O(1)-C(4)	108.5(2)
S(1)-C(11)-H(11A)	C(1)-O(2)-C(7)	108.4(2)
109.5	C(7)-O(3)-C(2)	107.9(2)
S(1)-C(11)-H(11B)	C(6)-O(4)-C(3)	110.6(3)
109.5	C(5)-O(6)-S(1)	129.3(2)
H(11A)-C(11)-H(11B)	O(6)-S(1)-C(10)	110.03(15)
109.5	O(6)-S(1)-C(11)	107.29(16)
S(1)-C(11)-H(11C)	C(10)-S(1)-C(11)	109.78(19)
109.5	O(6)-S(1)-C(12)	107.00(15)
H(11A)-C(11)-H(11C)	C(10)-S(1)-C(12)	111.69(16)
109.5	C(11)-S(1)-C(12)	110.91(17)
H(11B)-C(11)-H(11C)		
109.5		
C(14)-C(12)-C(15)		
109.6(3)		
C(14)-C(12)-C(13)		
109.0(3)		
C(15)-C(12)-C(13)		
108.1(3)		
C(14)-C(12)-S(1)		
110.5(3)		
C(15)-C(12)-S(1)		
109.8(2)		
C(13)-C(12)-S(1)		
109.7(2)		
C(12)-C(13)-H(13A)		
109.5		
C(12)-C(13)-H(13B)		
109.5		
H(13A)-C(13)-H(13B)		
109.5		
C(12)-C(13)-H(13C)		
109.5		
H(13A)-C(13)-H(13C)		
109.5		
H(13B)-C(13)-H(13C)		
109.5		
C(12)-C(14)-H(14A)		
109.5		
C(12)-C(14)-H(14B)		
109.5		
H(14A)-C(14)-H(14B)		
109.5		
C(12)-C(14)-H(14C)		
109.5		
H(14A)-C(14)-H(14C)		
109.5		
H(14B)-C(14)-H(14C)		
109.5		
C(12)-C(15)-H(15A)		
109.5		

Table 4. Anisotropic displacement parameters [ $\text{\AA}^2 \times 10^3$ ] for 07mz240m. The anisotropic displacement factor exponent takes the form:  $-2 \pi^2 [ (h a^*)^2 U_{11} + \dots + 2 h k a^* b^* U_{12}]$

	U11	U22	U33	U23	U13	U12
C(1)	18(1)	21(1)	26(2)	1(1)	2(1)	10(1)
C(2)	18(1)	19(1)	22(1)	2(1)	1(1)	9(1)
C(3)	18(1)	20(1)	25(2)	-1(1)	0(1)	8(1)
C(4)	20(1)	22(1)	25(2)	1(1)	3(1)	11(1)
C(5)	17(1)	25(1)	37(2)	6(1)	3(1)	12(1)
C(6)	13(1)	24(1)	37(2)	4(1)	0(1)	5(1)
C(7)	19(1)	29(1)	25(2)	2(1)	-1(1)	12(1)
C(8)	27(2)	59(2)	25(2)	5(2)	1(1)	19(2)
C(9)	27(2)	39(2)	33(2)	6(1)	3(1)	21(1)
C(10)	36(2)	37(2)	34(2)	6(2)	7(1)	18(2)
C(11)	31(2)	43(2)	43(2)	-7(2)	-8(2)	14(2)
C(12)	27(2)	28(2)	34(2)	1(1)	-3(1)	15(1)
C(13)	38(2)	39(2)	39(2)	11(2)	3(2)	16(2)
C(14)	50(2)	46(2)	58(3)	0(2)	0(2)	36(2)
C(15)	27(2)	41(2)	40(2)	-1(2)	-6(1)	17(1)
O(1)	17(1)	20(1)	30(1)	3(1)	0(1)	8(1)
O(2)	25(1)	27(1)	29(1)	-4(1)	-8(1)	14(1)
O(3)	25(1)	25(1)	26(1)	4(1)	-3(1)	10(1)
O(4)	25(1)	27(1)	25(1)	1(1)	-3(1)	12(1)
O(5)	23(1)	33(1)	38(2)	6(1)	-7(1)	11(1)
O(6)	27(1)	26(1)	46(2)	10(1)	11(1)	17(1)
S(1)	29(1)	32(1)	36(1)	3(1)	1(1)	16(1)

Table 5. Hydrogen coordinates ( $\times 10^4$ ) and isotropic displacement parameters ( $\text{\AA}^2 \times 10^3$ ) for 07mz240m.

	x	y	z	U(eq)
H(1)	7283	3830	2218	26
H(2)	8081	4987	3033	24
H(3)	9313	5324	1245	26
H(4)	8930	4253	-440	26
H(5)	9783	4258	1536	31
H(8A)	7911	5407	-3320	57
H(8B)	7430	4582	-3836	57
H(8C)	8248	4899	-3273	57
H(9A)	6841	4687	928	46
H(9B)	6560	4512	-1224	46
H(9C)	7074	5318	-582	46

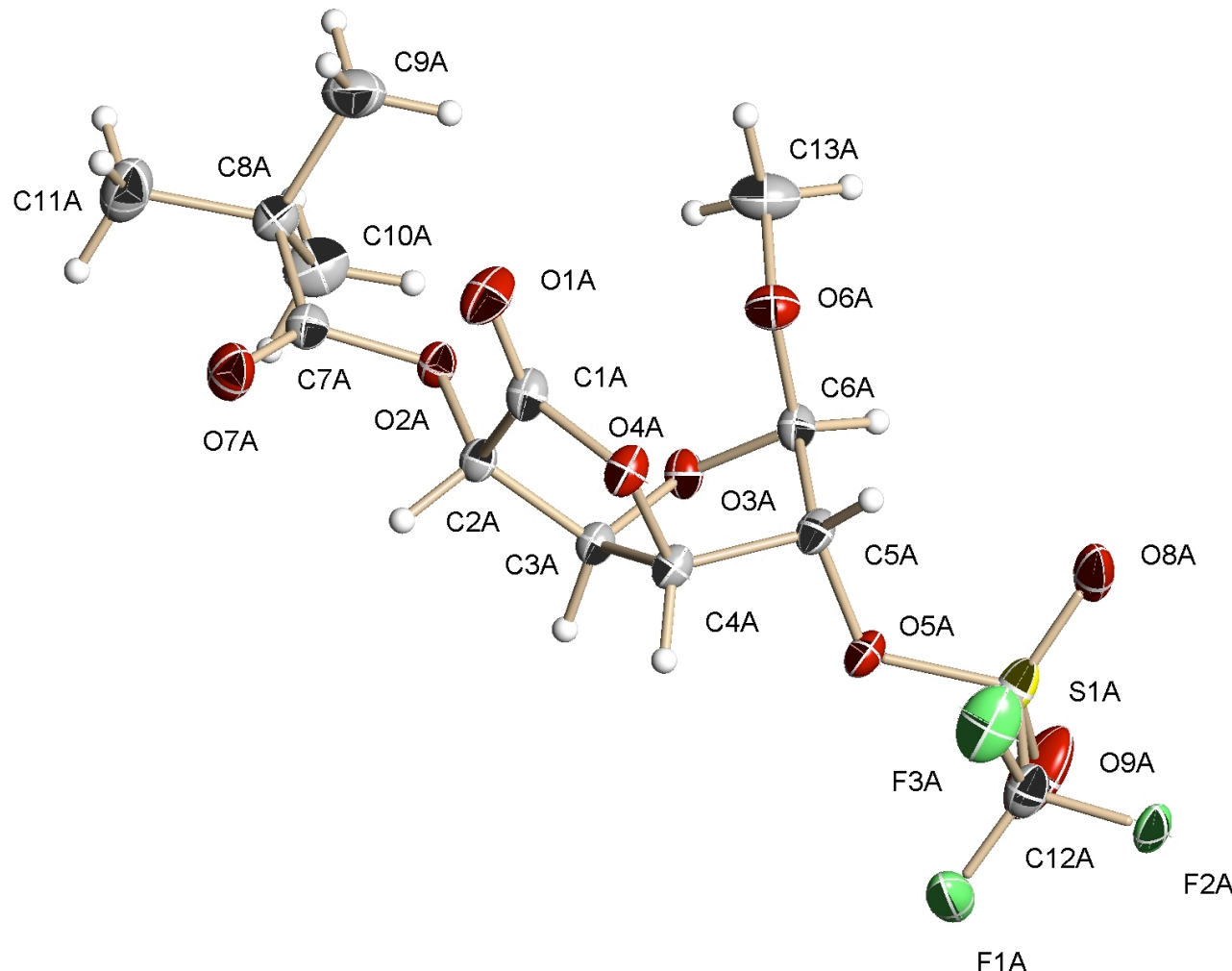
H (10A)	9761	3526	-1642	54
H (10B)	10129	3048	-1480	54
H (10C)	10411	3749	-203	54
H (11A)	8210	1769	1100	62
H (11B)	8701	1719	-526	62
H (11C)	8340	2197	-856	62
H (13A)	9496	2039	5686	61
H (13B)	8848	1702	4208	61
H (13C)	9088	2459	5162	61
H (14A)	10284	2222	999	69
H (14B)	9556	1565	1754	69
H (14C)	10252	1895	3067	69
H (15A)	10655	3016	4800	54
H (15B)	10311	3502	4350	54
H (15C)	10790	3405	2777	54

Table 6. Torsion angles [deg] for 07mz240m.

O(2)-C(1)-C(2)-O(3)	3.1(3)
O(1)-C(1)-C(2)-O(3)	119.9(3)
O(2)-C(1)-C(2)-C(3)	-109.5(2)
O(1)-C(1)-C(2)-C(3)	7.3(3)
O(3)-C(2)-C(3)-O(4)	150.8(2)
C(1)-C(2)-C(3)-O(4)	-98.1(3)
O(3)-C(2)-C(3)-C(4)	-97.0(3)
C(1)-C(2)-C(3)-C(4)	14.0(3)
O(4)-C(3)-C(4)-O(1)	85.1(3)
C(2)-C(3)-C(4)-O(1)	-30.3(3)
O(4)-C(3)-C(4)-C(5)	-28.0(3)
C(2)-C(3)-C(4)-C(5)	-143.5(2)
O(1)-C(4)-C(5)-O(6)	39.3(4)
C(3)-C(4)-C(5)-O(6)	148.7(3)
O(1)-C(4)-C(5)-C(6)	-81.8(3)
C(3)-C(4)-C(5)-C(6)	27.6(3)
O(6)-C(5)-C(6)-O(5)	37.4(4)
C(4)-C(5)-C(6)-O(5)	162.2(3)
O(6)-C(5)-C(6)-O(4)	-143.4(2)
C(4)-C(5)-C(6)-O(4)	-18.6(3)
O(2)-C(1)-O(1)-C(4)	85.2(3)
C(2)-C(1)-O(1)-C(4)	-28.0(3)
C(5)-C(4)-O(1)-C(1)	146.0(3)
C(3)-C(4)-O(1)-C(1)	36.6(3)
O(1)-C(1)-O(2)-C(7)	-134.5(2)
C(2)-C(1)-O(2)-C(7)	-19.9(3)
O(3)-C(7)-O(2)-C(1)	29.5(3)
C(8)-C(7)-O(2)-C(1)	145.9(2)
C(9)-C(7)-O(2)-C(1)	-89.2(3)
O(2)-C(7)-O(3)-C(2)	-27.1(3)
C(8)-C(7)-O(3)-C(2)	-143.5(3)
C(9)-C(7)-O(3)-C(2)	91.8(3)
C(3)-C(2)-O(3)-C(7)	125.0(2)
C(1)-C(2)-O(3)-C(7)	14.6(3)
O(5)-C(6)-O(4)-C(3)	-179.9(3)
C(5)-C(6)-O(4)-C(3)	0.9(3)

C (2) -C (3) -O (4) -C (6)	129.0 (2)
C (4) -C (3) -O (4) -C (6)	17.2 (3)
C (4) -C (5) -O (6) -S (1)	103.1 (3)
C (6) -C (5) -O (6) -S (1)	-140.3 (3)
C (5) -O (6) -S (1) -C (10)	-7.8 (3)
C (5) -O (6) -S (1) -C (11)	-127.2 (3)
C (5) -O (6) -S (1) -C (12)	113.7 (3)
C (14) -C (12) -S (1) -O (6)	174.0 (2)
C (15) -C (12) -S (1) -O (6)	-65.0 (3)
C (13) -C (12) -S (1) -O (6)	53.7 (3)
C (14) -C (12) -S (1) -C (10)	-65.5 (3)
C (15) -C (12) -S (1) -C (10)	55.5 (3)
C (13) -C (12) -S (1) -C (10)	174.2 (3)
C (14) -C (12) -S (1) -C (11)	57.3 (3)
C (15) -C (12) -S (1) -C (11)	178.3 (3)
C (13) -C (12) -S (1) -C (11)	-63.0 (3)

---



**Figure 88:** X-Ray crystal structure of methyl 6-O-pivaloyl-2-O-trifluoromethylsulfonyl- $\beta$ -D-glucurono-6,3-lactone (**24**).

Table 1. Crystal data and structure refinement for 06mz359m:

Identification code: 06mz359m  
 Empirical formula: C13 H17 F3 O9 S  
 Formula weight: 406.33  
 Temperature: 100(2) K  
 Wavelength: 0.71073 Å  
 Crystal system: Monoclinic  
 Space group: P2<sub>1</sub>  
 Unit cell dimensions:  
 a = 12.1829(8) Å, α = 90°  
 b = 19.5940(13) Å, β = 105.7570(10)°  
 c = 15.2989(10) Å, γ = 90°  
 Volume, Z: 3514.8(4) Å<sup>3</sup>, 8  
 Density (calculated): 1.536 Mg/m<sup>3</sup>  
 Absorption coefficient: 0.259 mm<sup>-1</sup>  
 F(000): 1680  
 Crystal size: 0.60 × 0.37 × 0.23 mm  
 Crystal shape, colour: block, orange  
 θ range for data collection: 1.38 to 28.28°  
 Limiting indices: -16 ≤ h ≤ 16, -26 ≤ k ≤ 26, -20 ≤ l ≤ 20  
 Reflections collected: 36808  
 Independent reflections: 17351 (R(int) = 0.0180)  
 Completeness to θ = 28.28°: 100.0 %  
 Absorption correction: multi-scan  
 Max. and min. transmission: 0.942 and 0.857  
 Refinement method: Full-matrix least-squares on  $F^2$   
 Data / restraints / parameters: 17351 / 19 / 984  
 Goodness-of-fit on  $F^2$ : 1.044  
 Final R indices [ $I > 2\sigma(I)$ ]: R1 = 0.0336, wR2 = 0.0856  
 R indices (all data): R1 = 0.0355, wR2 = 0.0870  
 Absolute structure parameter: 0.00(3)  
 Largest diff. peak and hole: 0.545 and -0.292 e × Å<sup>-3</sup>

Refinement of  $F^2$  against ALL reflections. The weighted R-factor wR and goodness of fit are based on  $F^2$ , conventional R-factors R are based on  $F$ , with  $F$  set to zero for negative  $F^2$ . The threshold expression of  $F^2 > 2\sigma(F^2)$  is used only for calculating R-factors

## Comments:

One of the tert-butyl groups of one of the four independent molecules shows rotational disorder, the occupancy ratio refined to 0.682(8) to

0.318(8).

The C-C distances were refined to be the same within a standard deviation of 0.02, and all methyl-methyl distances within the minor component were restrained to be the same.

Treatment of hydrogen atoms:

All hydrogen atoms were placed in calculated positions and were refined with an isotropic displacement parameter 1.5 (methyl) or 1.2 times (all others) that of the adjacent carbon atom.

Table 2. Atomic coordinates [ $\times 10^4$ ] and equivalent isotropic displacement parameters [ $\text{\AA}^2 \times 10^3$ ] for 06mz359m. U(eq) is defined as one third of the trace of the orthogonalized  $U_{ij}$  tensor.

	x	y	z	U(eq)
C(1A)	2101(1)	371(1)	8099(1)	23(1)
C(2A)	870(1)	406(1)	7530(1)	18(1)
C(3A)	288(1)	870(1)	8063(1)	17(1)
C(4A)	1303(1)	1297(1)	8629(1)	20(1)
C(5A)	1157(1)	1257(1)	9587(1)	22(1)
C(6A)	574(1)	565(1)	9585(1)	21(1)
C(7A)	508(1)	-586(1)	6635(1)	18(1)
C(8A)	-3(1)	-1299(1)	6569(1)	20(1)
C(9A)	702(2)	-1718(1)	7373(1)	29(1)
C(10A)	-1248(2)	-1249(1)	6602(1)	27(1)
C(11A)	71(2)	-1619(1)	5676(1)	31(1)
C(12A)	1147(2)	2885(1)	10471(1)	28(1)
C(13A)	1040(2)	-594(1)	9850(2)	35(1)
C(1B)	7775(1)	50(1)	9167(1)	20(1)
C(2B)	7015(1)	139(1)	8206(1)	19(1)
C(3B)	6265(1)	759(1)	8261(1)	18(1)
C(4B)	6947(1)	1119(1)	9145(1)	18(1)
C(5B)	6097(1)	1159(1)	9716(1)	18(1)
C(6B)	5265(1)	583(1)	9332(1)	19(1)
C(7B)	6026(1)	-567(1)	7011(1)	17(1)
C(8B)	5345(1)	-1230(1)	6770(1)	18(1)
C(9B)	5854(2)	-1793(1)	7454(1)	24(1)
C(10B)	5364(2)	-1442(1)	5813(1)	28(1)
C(11B)	4110(1)	-1074(1)	6784(1)	23(1)
C(12B)	6392(2)	2682(1)	10779(1)	25(1)
C(13B)	5121(2)	-611(1)	9533(1)	28(1)
C(1C)	2792(1)	339(1)	5036(1)	19(1)
C(2C)	2206(1)	850(1)	5503(1)	18(1)
C(3C)	1000(1)	928(1)	4865(1)	18(1)

C (4C)	876 (1)	274 (1)	4279 (1)	19 (1)
C (5C)	601 (1)	540 (1)	3308 (1)	20 (1)
C (6C)	1081 (1)	1262 (1)	3429 (1)	21 (1)
C (7C)	2652 (1)	1842 (1)	6376 (1)	22 (1)
C (8C)	3412 (2)	2471 (1)	6589 (1)	25 (1)
C (9C)	3595 (5)	2678 (2)	7553 (2)	46 (1)
C (10C)	4576 (2)	2364 (2)	6353 (3)	39 (1)
C (11C)	2762 (3)	3041 (2)	5948 (3)	29 (1)
C (9E)	3044 (8)	2846 (5)	7390 (7)	43 (2)
C (10E)	4619 (5)	2193 (4)	7004 (6)	40 (2)
C (11E)	3292 (12)	2907 (5)	5802 (6)	69 (4)
C (12C)	-1647 (2)	-485 (1)	2161 (1)	31 (1)
C (13C)	2794 (2)	1837 (1)	3477 (1)	28 (1)
C (1D)	7760 (1)	660 (1)	5517 (1)	22 (1)
C (2D)	6901 (1)	1159 (1)	5702 (1)	21 (1)
C (3D)	5841 (1)	1078 (1)	4908 (1)	19 (1)
C (4D)	6021 (1)	360 (1)	4556 (1)	18 (1)
C (5D)	5836 (1)	474 (1)	3540 (1)	19 (1)
C (6D)	6172 (1)	1220 (1)	3494 (1)	20 (1)
C (7D)	7734 (1)	2060 (1)	6682 (1)	18 (1)
C (8D)	8249 (1)	2770 (1)	6710 (1)	22 (1)
C (9D)	9404 (2)	2681 (1)	6493 (2)	33 (1)
C (10D)	8409 (2)	3060 (1)	7661 (1)	37 (1)
C (11D)	7475 (2)	3235 (1)	5997 (2)	33 (1)
C (12D)	4258 (2)	-275 (1)	1610 (1)	38 (1)
C (13D)	7813 (2)	1892 (1)	3624 (1)	29 (1)
F (10)	5364 (1)	-286 (1)	1674 (1)	57 (1)
F (11)	3787 (1)	-840 (1)	1203 (1)	61 (1)
F (12)	3793 (1)	247 (1)	1125 (1)	61 (1)
F (1A)	691 (1)	3254 (1)	9743 (1)	49 (1)
F (2A)	1207 (1)	3250 (1)	11214 (1)	36 (1)
F (3A)	2177 (1)	2696 (1)	10464 (1)	47 (1)
F (1B)	7247 (1)	2260 (1)	11132 (1)	31 (1)
F (2B)	6203 (1)	3063 (1)	11437 (1)	41 (1)
F (3B)	6673 (1)	3079 (1)	10179 (1)	42 (1)
F (1C)	-700 (1)	-842 (1)	2476 (1)	57 (1)
F (2C)	-2256 (1)	-743 (1)	1390 (1)	50 (1)
F (3C)	-2240 (1)	-523 (1)	2770 (1)	46 (1)
O (1A)	2795 (1)	-56 (1)	8100 (1)	34 (1)
O (2A)	371 (1)	-253 (1)	7379 (1)	17 (1)
O (3A)	-180 (1)	516 (1)	8698 (1)	19 (1)
O (4A)	2338 (1)	945 (1)	8623 (1)	24 (1)
O (5A)	307 (1)	1789 (1)	9586 (1)	26 (1)
O (6A)	1440 (1)	80 (1)	9745 (1)	27 (1)
O (7A)	990 (1)	-342 (1)	6122 (1)	24 (1)
O (8A)	825 (2)	1750 (1)	11253 (1)	47 (1)
O (9A)	-870 (1)	2386 (1)	10352 (1)	58 (1)

O (1B)	8288 (1)	-442 (1)	9508 (1)	26 (1)
O (2B)	6412 (1)	-476 (1)	7924 (1)	21 (1)
O (3B)	5180 (1)	584 (1)	8385 (1)	20 (1)
O (4B)	7847 (1)	659 (1)	9605 (1)	20 (1)
O (5B)	5502 (1)	1814 (1)	9493 (1)	22 (1)
O (6B)	5792 (1)	-3 (1)	9772 (1)	21 (1)
O (7B)	6210 (1)	-162 (1)	6481 (1)	28 (1)
O (8B)	4932 (1)	1741 (1)	10917 (1)	34 (1)
O (9B)	4266 (1)	2676 (1)	9805 (1)	36 (1)
O (1C)	3788 (1)	231 (1)	5168 (1)	27 (1)
O (2C)	2866 (1)	1458 (1)	5701 (1)	22 (1)
O (3C)	877 (1)	1494 (1)	4248 (1)	21 (1)
O (4C)	1984 (1)	-45 (1)	4465 (1)	20 (1)
O (5C)	-649 (1)	598 (1)	2998 (1)	25 (1)
O (6C)	2242 (1)	1195 (1)	3496 (1)	23 (1)
O (7C)	1917 (1)	1690 (1)	6736 (1)	30 (1)
O (8C)	-2328 (1)	768 (1)	1772 (1)	34 (1)
O (9C)	-518 (1)	390 (1)	1452 (1)	36 (1)
O (1D)	8773 (1)	656 (1)	5838 (1)	31 (1)
O (2D)	7333 (1)	1836 (1)	5814 (1)	24 (1)
O (3D)	5775 (1)	1546 (1)	4176 (1)	20 (1)
O (4D)	7363 (1)	1227 (1)	3697 (1)	23 (1)
O (5D)	4606 (1)	451 (1)	3094 (1)	23 (1)
O (6D)	7205 (1)	176 (1)	4933 (1)	20 (1)
O (7D)	7694 (1)	1719 (1)	7326 (1)	25 (1)
O (8D)	4677 (1)	-798 (1)	3226 (1)	34 (1)
O (9D)	2851 (1)	-181 (1)	2625 (1)	33 (1)
S (1A)	259 (1)	2141 (1)	10490 (1)	28 (1)
S (1B)	5101 (1)	2196 (1)	10246 (1)	22 (1)
S (1C)	-1285 (1)	403 (1)	1998 (1)	22 (1)
S (1D)	4035 (1)	-248 (1)	2743 (1)	22 (1)

All esds (except the esd in the dihedral angle between two l.s. planes) are estimated using the full covariance matrix. The cell esds are taken into account individually in the estimation of esds in distances, angles and torsion angles; correlations between esds in cell parameters are only used when they are defined by crystal symmetry. An approximate (isotropic) treatment of cell esds is used for estimating esds involving l.s. planes.

Table 3. Bond lengths [Å] and angles [deg] for 06mz359m.

C(1A)-O(1A)	1.191 (2)	C(1B)-O(1B)	1.189 (2)
C(1A)-O(4A)	1.365 (2)	C(1B)-O(4B)	1.360 (2)
C(1A)-C(2A)	1.517 (2)	C(1B)-C(2B)	1.519 (2)
C(2A)-O(2A)		C(2B)-O(2B)	1.4167 (19)
1.4177 (19)		C(2B)-C(3B)	1.537 (2)
C(2A)-C(3A)	1.519 (2)	C(2B)-H(2B)	1.0000
C(2A)-H(2A)	1.0000	C(3B)-O(3B)	1.4279 (18)
C(3A)-O(3A)		C(3B)-C(4B)	1.552 (2)
1.4322 (19)		C(3B)-H(3B)	1.0000
C(3A)-C(4A)	1.549 (2)	C(4B)-O(4B)	1.4461 (19)
C(3A)-H(3A)	1.0000	C(4B)-C(5B)	1.528 (2)
C(4A)-O(4A)		C(4B)-H(4B)	1.0000
1.4396 (19)		C(5B)-O(5B)	1.4666 (18)
C(4A)-C(5A)	1.526 (2)	C(5B)-C(6B)	1.524 (2)
C(4A)-H(4A)	1.0000	C(5B)-H(5B)	1.0000
C(5A)-O(5A)	1.469 (2)	C(6B)-O(6B)	1.3954 (19)
C(5A)-C(6A)	1.531 (2)	C(6B)-O(3B)	1.4237 (18)
C(5A)-H(5A)	1.0000	C(6B)-H(6B)	1.0000
C(6A)-O(6A)	1.391 (2)	C(7B)-O(7B)	1.198 (2)
C(6A)-O(3A)		C(7B)-O(2B)	1.3586 (19)
1.4203 (19)		C(7B)-C(8B)	1.532 (2)
C(6A)-H(6A)	1.0000	C(8B)-C(10B)	1.528 (2)
C(7A)-O(7A)	1.201 (2)	C(8B)-C(9B)	1.531 (2)
C(7A)-O(2A)		C(8B)-C(11B)	1.541 (2)
1.3608 (18)		C(9B)-H(9B1)	0.9800
C(7A)-C(8A)	1.521 (2)	C(9B)-H(9B2)	0.9800
C(8A)-C(11A)	1.529 (2)	C(9B)-H(9B3)	0.9800
C(8A)-C(9A)	1.533 (2)	C(10B)-H(10D)	0.9800
C(8A)-C(10A)	1.535 (2)	C(10B)-H(10E)	0.9800
C(9A)-H(9A1)	0.9800	C(10B)-H(10F)	0.9800
C(9A)-H(9A2)	0.9800	C(11B)-H(11D)	0.9800
C(9A)-H(9A3)	0.9800	C(11B)-H(11E)	0.9800
C(10A)-H(10A)	0.9800	C(11B)-H(11F)	0.9800
C(10A)-H(10B)	0.9800	C(12B)-F(3B)	1.318 (2)
C(10A)-H(10C)	0.9800	C(12B)-F(2B)	1.324 (2)
C(11A)-H(11A)	0.9800	C(12B)-F(1B)	1.325 (2)
C(11A)-H(11B)	0.9800	C(12B)-S(1B)	1.8289 (18)
C(11A)-H(11C)	0.9800	C(13B)-O(6B)	1.435 (2)
C(12A)-F(3A)	1.311 (2)	C(13B)-H(13D)	0.9800
C(12A)-F(1A)	1.318 (2)	C(13B)-H(13E)	0.9800
C(12A)-F(2A)	1.328 (2)	C(13B)-H(13F)	0.9800
C(12A)-S(1A)		C(1C)-O(1C)	1.193 (2)
1.8204 (19)		C(1C)-O(4C)	1.354 (2)
C(13A)-O(6A)	1.431 (2)	C(1C)-C(2C)	1.517 (2)
C(13A)-H(13A)	0.9800	C(2C)-O(2C)	1.4229 (19)
C(13A)-H(13B)	0.9800	C(2C)-C(3C)	1.534 (2)
C(13A)-H(13C)	0.9800	C(2C)-H(2C)	1.0000

C(3C)-O(3C)		C(13C)-O(6C)	1.430 (2)
1.4377 (19)		C(13C)-H(13G)	0.9800
C(3C)-C(4C)	1.549 (2)	C(13C)-H(13H)	0.9800
C(3C)-H(3C)	1.0000	C(13C)-H(13I)	0.9800
C(4C)-O(4C)		C(1D)-O(1D)	1.198 (2)
1.4432 (18)		C(1D)-O(6D)	1.352 (2)
C(4C)-C(5C)	1.524 (2)	C(1D)-C(2D)	1.515 (2)
C(4C)-H(4C)	1.0000	C(2D)-O(2D)	1.4189 (19)
C(5C)-O(5C)		C(2D)-C(3D)	1.522 (2)
1.4715 (18)		C(2D)-H(2D)	1.0000
C(5C)-C(6C)	1.523 (2)	C(3D)-O(3D)	1.433 (2)
C(5C)-H(5C)	1.0000	C(3D)-C(4D)	1.543 (2)
C(6C)-O(6C)		C(3D)-H(3D)	1.0000
1.3963 (19)		C(4D)-O(6D)	1.4459 (18)
C(6C)-O(3C)	1.418 (2)	C(4D)-C(5D)	1.526 (2)
C(6C)-H(6C)	1.0000	C(4D)-H(4D)	1.0000
C(7C)-O(7C)	1.209 (2)	C(5D)-O(5D)	1.4684 (18)
C(7C)-O(2C)	1.357 (2)	C(5D)-C(6D)	1.526 (2)
C(7C)-C(8C)	1.523 (2)	C(5D)-H(5D)	1.0000
C(8C)-C(11E)	1.451 (7)	C(6D)-O(4D)	1.3988 (19)
C(8C)-C(9C)	1.486 (4)	C(6D)-O(3D)	1.416 (2)
C(8C)-C(10E)	1.534 (6)	C(6D)-H(6D)	1.0000
C(8C)-C(11C)	1.554 (4)	C(7D)-O(7D)	1.202 (2)
C(8C)-C(10C)	1.569 (4)	C(7D)-O(2D)	1.359 (2)
C(8C)-C(9E)	1.594 (7)	C(7D)-C(8D)	1.521 (2)
C(9C)-H(9C1)	0.9800	C(8D)-C(10D)	1.524 (2)
C(9C)-H(9C2)	0.9800	C(8D)-C(11D)	1.533 (3)
C(9C)-H(9C3)	0.9800	C(8D)-C(9D)	1.541 (2)
C(10C)-H(10G)	0.9800	C(9D)-H(9D1)	0.9800
C(10C)-H(10H)	0.9800	C(9D)-H(9D2)	0.9800
C(10C)-H(10I)	0.9800	C(9D)-H(9D3)	0.9800
C(11C)-H(11G)	0.9800	C(10D)-H(10M)	0.9800
C(11C)-H(11H)	0.9800	C(10D)-H(10N)	0.9800
C(11C)-H(11I)	0.9800	C(10D)-H(10O)	0.9800
C(9E)-H(9E1)	0.9800	C(11D)-H(11M)	0.9800
C(9E)-H(9E2)	0.9800	C(11D)-H(11N)	0.9800
C(9E)-H(9E3)	0.9800	C(11D)-H(11O)	0.9800
C(10E)-H(10J)	0.9800	C(12D)-F(12)	1.300 (3)
C(10E)-H(10K)	0.9800	C(12D)-F(11)	1.321 (3)
C(10E)-H(10L)	0.9800	C(12D)-F(10)	1.325 (2)
C(11E)-H(11J)	0.9800	C(12D)-S(1D)	1.8267 (19)
C(11E)-H(11K)	0.9800	C(13D)-O(4D)	1.430 (2)
C(11E)-H(11L)	0.9800	C(13D)-H(13M)	0.9800
C(12C)-F(2C)	1.312 (2)	C(13D)-H(13N)	0.9800
C(12C)-F(1C)	1.324 (2)	C(13D)-H(13O)	0.9800
C(12C)-F(3C)	1.327 (2)	O(5A)-S(1A)	1.5594 (13)
C(12C)-S(1C)	1.828 (2)	O(8A)-S(1A)	1.4103 (18)

O (9A) -S (1A)	C (2A) -C (3A) -H (3A)	111.3
1.4170 (17)	C (4A) -C (3A) -H (3A)	111.3
O (5B) -S (1B)	O (4A) -C (4A) -C (5A)	108.18 (13)
1.5601 (12)	O (4A) -C (4A) -C (3A)	107.76 (12)
O (8B) -S (1B)	C (5A) -C (4A) -C (3A)	103.03 (12)
1.4163 (15)	O (4A) -C (4A) -H (4A)	112.4
O (9B) -S (1B)	C (5A) -C (4A) -H (4A)	112.4
1.4147 (14)	C (3A) -C (4A) -H (4A)	112.4
O (5C) -S (1C)	O (5A) -C (5A) -C (4A)	103.25 (13)
1.5627 (12)	O (5A) -C (5A) -C (6A)	107.56 (13)
O (8C) -S (1C)	C (4A) -C (5A) -C (6A)	102.68 (13)
1.4176 (14)	O (5A) -C (5A) -H (5A)	114.1
O (9C) -S (1C)	C (4A) -C (5A) -H (5A)	114.1
1.4119 (14)	C (6A) -C (5A) -H (5A)	114.1
O (5D) -S (1D)	O (6A) -C (6A) -O (3A)	112.61 (13)
1.5645 (12)	O (6A) -C (6A) -C (5A)	105.98 (13)
O (8D) -S (1D)	O (3A) -C (6A) -C (5A)	103.93 (13)
1.4172 (15)	O (6A) -C (6A) -H (6A)	111.3
O (9D) -S (1D)	O (3A) -C (6A) -H (6A)	111.3
1.4106 (13)	C (5A) -C (6A) -H (6A)	111.3
O (1A) -C (1A) -O (4A)	O (7A) -C (7A) -O (2A)	123.24 (14)
122.81 (15)	O (7A) -C (7A) -C (8A)	125.85 (14)
O (1A) -C (1A) -C (2A)	O (2A) -C (7A) -C (8A)	110.90 (13)
128.51 (16)	C (7A) -C (8A) -C (11A)	108.28 (14)
O (4A) -C (1A) -C (2A)	C (7A) -C (8A) -C (9A)	107.94 (13)
108.64 (14)	C (11A) -C (8A) -C (9A)	110.01 (15)
O (2A) -C (2A) -C (1A)	C (7A) -C (8A) -C (10A)	109.17 (13)
111.49 (13)	C (11A) -C (8A) -C (10A)	110.73 (15)
O (2A) -C (2A) -C (3A)	C (9A) -C (8A) -C (10A)	110.62 (14)
112.92 (12)	C (8A) -C (9A) -H (9A1)	109.5
C (1A) -C (2A) -C (3A)	C (8A) -C (9A) -H (9A2)	109.5
104.53 (12)	H (9A1) -C (9A) -H (9A2)	109.5
O (2A) -C (2A) -H (2A)	C (8A) -C (9A) -H (9A3)	109.5
109.3	H (9A1) -C (9A) -H (9A3)	109.5
C (1A) -C (2A) -H (2A)	H (9A2) -C (9A) -H (9A3)	109.5
109.3	C (8A) -C (10A) -H (10A)	109.5
C (3A) -C (2A) -H (2A)	C (8A) -C (10A) -H (10B)	109.5
109.3	H (10A) -C (10A) -H (10B)	109.5
O (3A) -C (3A) -C (2A)	C (8A) -C (10A) -H (10C)	109.5
113.88 (13)	H (10A) -C (10A) -H (10C)	109.5
O (3A) -C (3A) -C (4A)	H (10B) -C (10A) -H (10C)	109.5
106.66 (12)	C (8A) -C (11A) -H (11A)	109.5
C (2A) -C (3A) -C (4A)	C (8A) -C (11A) -H (11B)	109.5
101.86 (12)	H (11A) -C (11A) -H (11B)	109.5
O (3A) -C (3A) -H (3A)	C (8A) -C (11A) -H (11C)	109.5
111.3	H (11A) -C (11A) -H (11C)	109.5
	H (11B) -C (11A) -H (11C)	109.5

F (3A) -C (12A) -F (1A)	102.77 (12)
109.44 (17)	O (3B) -C (3B) -H (3B)
F (3A) -C (12A) -F (2A)	C (2B) -C (3B) -H (3B)
109.12 (16)	C (4B) -C (3B) -H (3B)
F (1A) -C (12A) -F (2A)	O (4B) -C (4B) -C (5B)
109.92 (15)	O (4B) -C (4B) -C (3B)
F (3A) -C (12A) -S (1A)	C (5B) -C (4B) -C (3B)
110.41 (13)	O (4B) -C (4B) -H (4B)
F (1A) -C (12A) -S (1A)	C (5B) -C (4B) -H (4B)
109.73 (13)	C (3B) -C (4B) -H (4B)
F (2A) -C (12A) -S (1A)	O (5B) -C (5B) -C (6B)
108.22 (13)	O (5B) -C (5B) -C (4B)
O (6A) -C (13A) -H (13A)	C (6B) -C (5B) -C (4B)
109.5	O (5B) -C (5B) -H (5B)
O (6A) -C (13A) -H (13B)	C (6B) -C (5B) -H (5B)
109.5	C (4B) -C (5B) -H (5B)
H (13A) -C (13A) -H (13B)	O (6B) -C (6B) -O (3B)
109.5	O (6B) -C (6B) -C (5B)
O (6A) -C (13A) -H (13C)	O (3B) -C (6B) -C (5B)
109.5	O (6B) -C (6B) -H (6B)
H (13A) -C (13A) -H (13C)	O (3B) -C (6B) -H (6B)
109.5	C (5B) -C (6B) -H (6B)
H (13B) -C (13A) -H (13C)	O (7B) -C (7B) -O (2B)
109.5	O (7B) -C (7B) -C (8B)
O (1B) -C (1B) -O (4B)	O (2B) -C (7B) -C (8B)
122.58 (15)	C (10B) -C (8B) -C (9B)
O (1B) -C (1B) -C (2B)	C (10B) -C (8B) -C (7B)
128.83 (15)	C (9B) -C (8B) -C (7B)
O (4B) -C (1B) -C (2B)	C (10B) -C (8B) -C (11B)
108.50 (13)	C (9B) -C (8B) -C (11B)
O (2B) -C (2B) -C (1B)	C (7B) -C (8B) -C (11B)
109.04 (13)	C (8B) -C (9B) -H (9B1)
O (2B) -C (2B) -C (3B)	C (8B) -C (9B) -H (9B2)
115.03 (13)	H (9B1) -C (9B) -H (9B2)
C (1B) -C (2B) -C (3B)	C (8B) -C (9B) -H (9B3)
104.68 (12)	H (9B1) -C (9B) -H (9B3)
O (2B) -C (2B) -H (2B)	H (9B2) -C (9B) -H (9B3)
109.3	C (8B) -C (10B) -H (10D)
C (1B) -C (2B) -H (2B)	C (8B) -C (10B) -H (10E)
109.3	H (10D) -C (10B) -H (10E)
C (3B) -C (2B) -H (2B)	C (8B) -C (10B) -H (10F)
109.3	H (10D) -C (10B) -H (10F)
O (3B) -C (3B) -C (2B)	H (10E) -C (10B) -H (10F)
113.73 (13)	C (8B) -C (11B) -H (11D)
O (3B) -C (3B) -C (4B)	C (8B) -C (11B) -H (11E)
106.82 (12)	H (11D) -C (11B) -H (11E)
C (2B) -C (3B) -C (4B)	C (8B) -C (11B) -H (11F)

H (11D) -C (11B) -H (11F)	113.92 (12)
109.5	O (3C) -C (3C) -C (4C) 106.40 (12)
H (11E) -C (11B) -H (11F)	C (2C) -C (3C) -C (4C) 102.18 (12)
109.5	O (3C) -C (3C) -H (3C) 111.3
F (3B) -C (12B) -F (2B)	C (2C) -C (3C) -H (3C) 111.3
109.12 (15)	C (4C) -C (3C) -H (3C) 111.3
F (3B) -C (12B) -F (1B)	O (4C) -C (4C) -C (5C) 106.67 (12)
109.22 (15)	O (4C) -C (4C) -C (3C) 107.81 (12)
F (2B) -C (12B) -F (1B)	C (5C) -C (4C) -C (3C) 103.97 (13)
108.80 (15)	O (4C) -C (4C) -H (4C) 112.6
F (3B) -C (12B) -S (1B)	C (5C) -C (4C) -H (4C) 112.6
110.62 (13)	C (3C) -C (4C) -H (4C) 112.6
F (2B) -C (12B) -S (1B)	O (5C) -C (5C) -C (6C) 107.33 (13)
109.02 (12)	O (5C) -C (5C) -C (4C) 105.92 (12)
F (1B) -C (12B) -S (1B)	C (6C) -C (5C) -C (4C) 102.97 (13)
110.04 (12)	O (5C) -C (5C) -H (5C) 113.3
O (6B) -C (13B) -H (13D)	C (6C) -C (5C) -H (5C) 113.3
109.5	C (4C) -C (5C) -H (5C) 113.3
O (6B) -C (13B) -H (13E)	O (6C) -C (6C) -O (3C) 112.50 (13)
109.5	O (6C) -C (6C) -C (5C) 105.60 (13)
H (13D) -C (13B) -H (13E)	O (3C) -C (6C) -C (5C) 104.59 (12)
109.5	O (6C) -C (6C) -H (6C) 111.3
O (6B) -C (13B) -H (13F)	O (3C) -C (6C) -H (6C) 111.3
109.5	C (5C) -C (6C) -H (6C) 111.3
H (13D) -C (13B) -H (13F)	O (7C) -C (7C) -O (2C) 121.93 (15)
109.5	O (7C) -C (7C) -C (8C) 125.68 (16)
H (13E) -C (13B) -H (13F)	O (2C) -C (7C) -C (8C) 112.37 (14)
109.5	C (11E) -C (8C) -C (7C) 112.3 (4)
O (1C) -C (1C) -O (4C)	C (9C) -C (8C) -C (7C) 110.6 (2)
122.66 (15)	C (11E) -C (8C) -C (10E) 114.9 (6)
O (1C) -C (1C) -C (2C)	C (7C) -C (8C) -C (10E) 105.1 (3)
128.56 (15)	C (9C) -C (8C) -C (11C) 110.1 (3)
O (4C) -C (1C) -C (2C)	C (7C) -C (8C) -C (11C) 105.69 (18)
108.54 (13)	C (9C) -C (8C) -C (10C) 111.3 (3)
O (2C) -C (2C) -C (1C)	C (7C) -C (8C) -C (10C) 112.13 (17)
110.06 (12)	C (11C) -C (8C) -C (10C) 106.7 (2)
O (2C) -C (2C) -C (3C)	C (11E) -C (8C) -C (9E) 112.4 (6)
116.10 (13)	C (7C) -C (8C) -C (9E) 104.9 (3)
C (1C) -C (2C) -C (3C)	C (10E) -C (8C) -C (9E) 106.5 (4)
105.00 (12)	C (8C) -C (9C) -H (9C1) 109.5
O (2C) -C (2C) -H (2C)	C (8C) -C (9C) -H (9C2) 109.5
108.5	C (8C) -C (9C) -H (9C3) 109.5
C (1C) -C (2C) -H (2C)	C (8C) -C (10C) -H (10G) 109.5
108.5	C (8C) -C (10C) -H (10H) 109.5
C (3C) -C (2C) -H (2C)	C (8C) -C (10C) -H (10I) 109.5
108.5	C (8C) -C (11C) -H (11G) 109.5
O (3C) -C (3C) -C (2C)	C (8C) -C (11C) -H (11H) 109.5

C (8C) -C (11C) -H (11I)	109.44 (14)
109.5	F (3C) -C (12C) -S (1C) 110.26 (14)
C (8C) -C (9E) -H (9E1)	O (6C) -C (13C) -H (13G) 109.5
109.5	O (6C) -C (13C) -H (13H) 109.5
C (8C) -C (9E) -H (9E2)	H (13G) -C (13C) -H (13H) 109.5
109.5	O (6C) -C (13C) -H (13I) 109.5
H (9E1) -C (9E) -H (9E2)	H (13G) -C (13C) -H (13I) 109.5
109.5	H (13H) -C (13C) -H (13I) 109.5
C (8C) -C (9E) -H (9E3)	O (1D) -C (1D) -O (6D) 122.76 (17)
109.5	O (1D) -C (1D) -C (2D) 127.96 (17)
H (9E1) -C (9E) -H (9E3)	O (6D) -C (1D) -C (2D) 109.25 (13)
109.5	O (2D) -C (2D) -C (1D) 111.92 (13)
H (9E2) -C (9E) -H (9E3)	O (2D) -C (2D) -C (3D) 113.63 (14)
109.5	C (1D) -C (2D) -C (3D) 105.23 (13)
C (8C) -C (10E) -H (10J)	O (2D) -C (2D) -H (2D) 108.6
109.5	C (1D) -C (2D) -H (2D) 108.6
C (8C) -C (10E) -H (10K)	C (3D) -C (2D) -H (2D) 108.6
109.5	O (3D) -C (3D) -C (2D) 114.33 (12)
H (10J) -C (10E) -H (10K)	O (3D) -C (3D) -C (4D) 107.12 (12)
109.5	C (2D) -C (3D) -C (4D) 101.77 (13)
C (8C) -C (10E) -H (10L)	O (3D) -C (3D) -H (3D) 111.1
109.5	C (2D) -C (3D) -H (3D) 111.1
H (10J) -C (10E) -H (10L)	C (4D) -C (3D) -H (3D) 111.1
109.5	O (6D) -C (4D) -C (5D) 107.32 (12)
H (10K) -C (10E) -H (10L)	O (6D) -C (4D) -C (3D) 108.05 (12)
109.5	C (5D) -C (4D) -C (3D) 103.11 (13)
C (8C) -C (11E) -H (11J)	O (6D) -C (4D) -H (4D) 112.6
109.5	C (5D) -C (4D) -H (4D) 112.6
C (8C) -C (11E) -H (11K)	C (3D) -C (4D) -H (4D) 112.6
109.5	O (5D) -C (5D) -C (6D) 105.08 (13)
H (11J) -C (11E) -H (11K)	O (5D) -C (5D) -C (4D) 108.61 (12)
109.5	C (6D) -C (5D) -C (4D) 102.65 (13)
C (8C) -C (11E) -H (11L)	O (5D) -C (5D) -H (5D) 113.2
109.5	C (6D) -C (5D) -H (5D) 113.2
H (11J) -C (11E) -H (11L)	C (4D) -C (5D) -H (5D) 113.2
109.5	O (4D) -C (6D) -O (3D) 111.97 (13)
H (11K) -C (11E) -H (11L)	O (4D) -C (6D) -C (5D) 105.89 (13)
109.5	O (3D) -C (6D) -C (5D) 104.41 (12)
F (2C) -C (12C) -F (1C)	O (4D) -C (6D) -H (6D) 111.4
110.38 (18)	O (3D) -C (6D) -H (6D) 111.4
F (2C) -C (12C) -F (3C)	C (5D) -C (6D) -H (6D) 111.4
109.09 (17)	O (7D) -C (7D) -O (2D) 122.51 (14)
F (1C) -C (12C) -F (3C)	O (7D) -C (7D) -C (8D) 126.37 (15)
107.57 (17)	O (2D) -C (7D) -C (8D) 111.09 (13)
F (2C) -C (12C) -S (1C)	C (7D) -C (8D) -C (10D) 108.19 (14)
110.06 (15)	C (7D) -C (8D) -C (11D) 110.72 (14)
F (1C) -C (12C) -S (1C)	C (10D) -C (8D) -C (11D) 110.66 (16)

C (7D) -C (8D) -C (9D)	108.9 (2)
106.52 (14)	F (12) -C (12D) -S (1D)
C (10D) -C (8D) -C (9D)	111.36 (17)
111.13 (16)	F (11) -C (12D) -S (1D)
C (11D) -C (8D) -C (9D)	108.26 (15)
109.54 (16)	F (10) -C (12D) -S (1D)
C (8D) -C (9D) -H (9D1)	109.93 (13)
109.5	O (4D) -C (13D) -H (13M)
C (8D) -C (9D) -H (9D2)	109.5
109.5	O (4D) -C (13D) -H (13N)
H (9D1) -C (9D) -H (9D2)	109.5
109.5	H (13M) -C (13D) -H (13N)
C (8D) -C (9D) -H (9D3)	109.5
109.5	H (13M) -C (13D) -H (13O)
H (9D1) -C (9D) -H (9D3)	109.5
109.5	H (13N) -C (13D) -H (13O)
H (9D2) -C (9D) -H (9D3)	109.5
109.5	C (7A) -O (2A) -C (2A)
C (8D) -C (10D) -H (10M)	115.41 (12)
109.5	C (6A) -O (3A) -C (3A)
C (8D) -C (10D) -H (10N)	110.05 (12)
109.5	C (1A) -O (4A) -C (4A)
H (10M) -C (10D) -H (10N)	110.59 (12)
109.5	C (5A) -O (5A) -S (1A)
C (8D) -C (10D) -H (10O)	120.63 (11)
109.5	C (6A) -O (6A) -C (13A)
H (10M) -C (10D) -H (10O)	112.64 (13)
109.5	C (7B) -O (2B) -C (2B)
C (8D) -C (11D) -H (11M)	115.49 (12)
109.5	C (6B) -O (3B) -C (3B)
H (11M) -C (11D) -H (11N)	108.74 (11)
109.5	C (1B) -O (4B) -C (4B)
C (8D) -C (11D) -H (11N)	111.58 (12)
109.5	C (5B) -O (5B) -S (1B)
H (11M) -C (11D) -H (11O)	118.85 (10)
109.5	C (6B) -O (6B) -C (13B)
C (8D) -C (11D) -H (11O)	113.83 (13)
109.5	C (7C) -O (2C) -C (2C)
H (11N) -C (11D) -H (11O)	114.37 (12)
109.5	C (6C) -O (3C) -C (3C)
C (8D) -C (11D) -H (11O)	108.72 (12)
109.5	C (1C) -O (4C) -C (4C)
H (11M) -C (11D) -H (11O)	111.33 (12)
109.5	C (5C) -O (5C) -S (1C)
C (8D) -C (11D) -H (11O)	119.38 (10)
109.5	C (6C) -O (6C) -C (13C)
H (11M) -C (11D) -H (11O)	112.81 (13)
109.5	C (7D) -O (2D) -C (2D)
C (8D) -C (11D) -H (11O)	116.33 (13)
109.5	C (6D) -O (3D) -C (3D)
H (11N) -C (11D) -H (11O)	109.21 (12)
109.5	C (6D) -O (4D) -C (13D)
C (8D) -C (11D) -H (11O)	112.78 (13)
109.5	C (5D) -O (5D) -S (1D)
H (11M) -C (11D) -H (11O)	119.24 (10)
109.5	C (1D) -O (6D) -C (4D)
C (8D) -C (11D) -H (11O)	110.73 (12)
109.5	O (8A) -S (1A) -O (9A)
H (11M) -C (11D) -H (11O)	122.98 (12)
109.5	O (8A) -S (1A) -O (5A)
C (8D) -C (11D) -H (11O)	111.45 (9)
109.5	O (9A) -S (1A) -O (5A)
H (11M) -C (11D) -H (11O)	106.67 (9)
109.5	O (8A) -S (1A) -C (12A)
C (8D) -C (11D) -H (11O)	106.79 (10)
109.5	O (9A) -S (1A) -C (12A)
H (11M) -C (11D) -H (11O)	106.41 (11)
109.5	O (5A) -S (1A) -C (12A)
C (8D) -C (11D) -H (11O)	100.03 (8)
109.5	O (9B) -S (1B) -O (8B)
H (11N) -C (11D) -H (11O)	122.52 (9)
109.5	O (9B) -S (1B) -O (5B)
C (8D) -C (11D) -H (11O)	107.16 (8)
109.5	O (8B) -S (1B) -O (5B)
H (11M) -C (11D) -H (11O)	111.58 (8)
109.5	O (9B) -S (1B) -C (12B)
C (8D) -C (11D) -H (11O)	106.69 (9)
109.5	O (8B) -S (1B) -C (12B)
H (11N) -C (11D) -H (11O)	106.38 (9)
109.5	O (5B) -S (1B) -C (12B)
F (12) -C (12D) -F (11)	100.08 (8)
108.92 (17)	O (9C) -S (1C) -O (8C)
F (12) -C (12D) -F (10)	123.88 (9)
109.41 (19)	O (9C) -S (1C) -O (5C)
F (11) -C (12D) -F (10)	110.60 (7)
	O (8C) -S (1C) -O (5C)
	106.76 (8)
	O (9C) -S (1C) -C (12C)
	106.70 (10)
	O (8C) -S (1C) -C (12C)
	106.26 (9)

O (5C) -S (1C) -C (12C)  
99.99 (9)  
O (9D) -S (1D) -O (8D)  
122.53 (9)  
O (9D) -S (1D) -O (5D)  
107.88 (8)  
O (8D) -S (1D) -O (5D)  
110.86 (7)  
O (9D) -S (1D) -C (12D)  
106.99 (9)  
O (8D) -S (1D) -C (12D)  
105.68 (11)  
O (5D) -S (1D) -C (12D)  
100.60 (9)

Table 4. Anisotropic displacement parameters [ $\text{\AA}^2 \times 10^3$ ] for 06mz359m.  
The anisotropic displacement factor exponent takes the form:  $-2 \pi^2 [ (h a^*)^2 U_{11} + \dots + 2 h k a^* b^* U_{12}]$

	U11	U22	U33	U23	U13	U12
C(1A)	18(1)	28(1)	25(1)	-6(1)	9(1)	-4(1)
C(2A)	17(1)	19(1)	19(1)	-3(1)	7(1)	-2(1)
C(3A)	15(1)	19(1)	19(1)	-3(1)	5(1)	-1(1)
C(4A)	16(1)	21(1)	25(1)	-5(1)	6(1)	-2(1)
C(5A)	19(1)	24(1)	24(1)	-6(1)	6(1)	1(1)
C(6A)	20(1)	25(1)	19(1)	-3(1)	5(1)	0(1)
C(7A)	15(1)	20(1)	18(1)	-2(1)	5(1)	0(1)
C(8A)	20(1)	19(1)	24(1)	-1(1)	8(1)	-2(1)
C(9A)	34(1)	21(1)	33(1)	4(1)	8(1)	2(1)
C(10A)	19(1)	25(1)	37(1)	-2(1)	9(1)	-6(1)
C(11A)	40(1)	27(1)	30(1)	-10(1)	13(1)	-6(1)
C(12A)	32(1)	26(1)	28(1)	-7(1)	11(1)	-6(1)
C(13A)	28(1)	26(1)	48(1)	7(1)	7(1)	2(1)
C(1B)	18(1)	23(1)	22(1)	-3(1)	9(1)	-2(1)
C(2B)	21(1)	20(1)	18(1)	-3(1)	8(1)	-3(1)
C(3B)	19(1)	18(1)	17(1)	-1(1)	5(1)	-4(1)
C(4B)	17(1)	18(1)	19(1)	-2(1)	4(1)	-1(1)
C(5B)	17(1)	17(1)	18(1)	-1(1)	3(1)	4(1)
C(6B)	17(1)	23(1)	18(1)	-1(1)	6(1)	1(1)
C(7B)	15(1)	19(1)	18(1)	-2(1)	6(1)	1(1)
C(8B)	18(1)	18(1)	19(1)	-2(1)	6(1)	-2(1)
C(9B)	23(1)	17(1)	31(1)	-1(1)	4(1)	1(1)
C(10B)	29(1)	34(1)	23(1)	-11(1)	9(1)	-7(1)
C(11B)	17(1)	26(1)	27(1)	3(1)	7(1)	1(1)
C(12B)	26(1)	19(1)	29(1)	-4(1)	7(1)	1(1)
C(13B)	38(1)	22(1)	26(1)	-1(1)	14(1)	-9(1)
C(1C)	18(1)	19(1)	21(1)	7(1)	7(1)	-1(1)
C(2C)	16(1)	21(1)	18(1)	3(1)	5(1)	-2(1)
C(3C)	16(1)	19(1)	20(1)	0(1)	6(1)	-1(1)
C(4C)	16(1)	20(1)	21(1)	1(1)	6(1)	0(1)
C(5C)	16(1)	27(1)	18(1)	1(1)	4(1)	1(1)
C(6C)	20(1)	24(1)	20(1)	5(1)	6(1)	4(1)
C(7C)	21(1)	22(1)	20(1)	3(1)	3(1)	0(1)
C(8C)	21(1)	22(1)	28(1)	-1(1)	0(1)	-3(1)
C(9C)	62(3)	47(2)	23(2)	-5(1)	-1(2)	-22(2)
C(10C)	18(1)	26(1)	68(3)	-5(1)	7(1)	-3(1)
C(11C)	31(2)	23(1)	32(2)	6(1)	8(1)	1(1)
C(9E)	33(4)	34(4)	61(6)	-27(4)	10(4)	-15(3)
C(10E)	19(3)	47(4)	51(5)	-18(4)	2(3)	-3(3)
C(11E)	109(11)	51(6)	35(4)	13(4)	-3(5)	-55(7)
C(12C)	27(1)	24(1)	41(1)	1(1)	9(1)	1(1)
C(13C)	24(1)	23(1)	39(1)	9(1)	13(1)	-1(1)
C(1D)	20(1)	25(1)	19(1)	5(1)	4(1)	-3(1)
C(2D)	24(1)	20(1)	18(1)	-2(1)	6(1)	-7(1)
C(3D)	16(1)	20(1)	24(1)	-3(1)	9(1)	-3(1)

C (4D)	15 (1)	21 (1)	20 (1)	-1 (1)	6 (1)	-2 (1)
C (5D)	14 (1)	23 (1)	19 (1)	-1 (1)	4 (1)	0 (1)
C (6D)	18 (1)	23 (1)	20 (1)	1 (1)	5 (1)	0 (1)
C (7D)	15 (1)	19 (1)	21 (1)	0 (1)	4 (1)	-1 (1)
C (8D)	22 (1)	19 (1)	25 (1)	-2 (1)	5 (1)	-4 (1)
C (9D)	23 (1)	32 (1)	47 (1)	-1 (1)	11 (1)	-9 (1)
C (10D)	51 (1)	28 (1)	32 (1)	-10 (1)	12 (1)	-13 (1)
C (11D)	36 (1)	21 (1)	40 (1)	4 (1)	5 (1)	0 (1)
C (12D)	34 (1)	60 (1)	20 (1)	-10 (1)	8 (1)	-18 (1)
C (13D)	26 (1)	28 (1)	35 (1)	4 (1)	12 (1)	-7 (1)
F (10)	33 (1)	108 (1)	34 (1)	-25 (1)	18 (1)	-20 (1)
F (11)	57 (1)	87 (1)	43 (1)	-41 (1)	22 (1)	-33 (1)
F (12)	59 (1)	84 (1)	31 (1)	14 (1)	-1 (1)	-18 (1)
F (1A)	81 (1)	29 (1)	31 (1)	0 (1)	7 (1)	-6 (1)
F (2A)	49 (1)	28 (1)	31 (1)	-13 (1)	11 (1)	-7 (1)
F (3A)	30 (1)	53 (1)	66 (1)	-18 (1)	24 (1)	-14 (1)
F (1B)	23 (1)	29 (1)	37 (1)	-3 (1)	2 (1)	4 (1)
F (2B)	41 (1)	39 (1)	41 (1)	-20 (1)	7 (1)	6 (1)
F (3B)	42 (1)	32 (1)	51 (1)	9 (1)	14 (1)	-10 (1)
F (1C)	37 (1)	33 (1)	98 (1)	12 (1)	15 (1)	15 (1)
F (2C)	50 (1)	41 (1)	56 (1)	-17 (1)	11 (1)	-16 (1)
F (3C)	44 (1)	44 (1)	55 (1)	10 (1)	24 (1)	-6 (1)
O (1A)	18 (1)	37 (1)	46 (1)	-13 (1)	7 (1)	5 (1)
O (2A)	17 (1)	19 (1)	19 (1)	-3 (1)	8 (1)	-3 (1)
O (3A)	16 (1)	26 (1)	17 (1)	-2 (1)	7 (1)	-3 (1)
O (4A)	14 (1)	27 (1)	31 (1)	-9 (1)	7 (1)	-4 (1)
O (5A)	26 (1)	25 (1)	27 (1)	-9 (1)	7 (1)	3 (1)
O (6A)	20 (1)	26 (1)	33 (1)	2 (1)	5 (1)	1 (1)
O (7A)	29 (1)	24 (1)	23 (1)	-2 (1)	14 (1)	-4 (1)
O (8A)	87 (1)	31 (1)	30 (1)	-3 (1)	27 (1)	-10 (1)
O (9A)	33 (1)	71 (1)	79 (1)	-38 (1)	31 (1)	-9 (1)
O (1B)	24 (1)	25 (1)	29 (1)	0 (1)	8 (1)	5 (1)
O (2B)	29 (1)	18 (1)	18 (1)	-3 (1)	10 (1)	-6 (1)
O (3B)	15 (1)	27 (1)	17 (1)	-2 (1)	4 (1)	-3 (1)
O (4B)	16 (1)	23 (1)	21 (1)	-5 (1)	3 (1)	1 (1)
O (5B)	26 (1)	20 (1)	20 (1)	-1 (1)	5 (1)	8 (1)
O (6B)	23 (1)	19 (1)	22 (1)	2 (1)	6 (1)	-1 (1)
O (7B)	31 (1)	31 (1)	20 (1)	2 (1)	4 (1)	-10 (1)
O (8B)	38 (1)	31 (1)	43 (1)	-2 (1)	27 (1)	-1 (1)
O (9B)	26 (1)	34 (1)	45 (1)	-5 (1)	5 (1)	13 (1)
O (1C)	16 (1)	29 (1)	39 (1)	7 (1)	11 (1)	3 (1)
O (2C)	21 (1)	23 (1)	23 (1)	0 (1)	7 (1)	-6 (1)
O (3C)	21 (1)	20 (1)	22 (1)	3 (1)	8 (1)	4 (1)
O (4C)	19 (1)	19 (1)	23 (1)	1 (1)	7 (1)	2 (1)
O (5C)	18 (1)	40 (1)	18 (1)	-3 (1)	3 (1)	2 (1)
O (6C)	20 (1)	22 (1)	30 (1)	5 (1)	12 (1)	1 (1)
O (7C)	34 (1)	27 (1)	35 (1)	-3 (1)	18 (1)	-4 (1)
O (8C)	32 (1)	34 (1)	27 (1)	0 (1)	-5 (1)	9 (1)
O (9C)	35 (1)	56 (1)	19 (1)	-2 (1)	9 (1)	-10 (1)
O (1D)	19 (1)	40 (1)	31 (1)	6 (1)	0 (1)	-3 (1)
O (2D)	31 (1)	20 (1)	20 (1)	-1 (1)	6 (1)	-10 (1)
O (3D)	18 (1)	20 (1)	23 (1)	-1 (1)	6 (1)	1 (1)
O (4D)	18 (1)	23 (1)	29 (1)	2 (1)	10 (1)	-2 (1)
O (5D)	16 (1)	23 (1)	27 (1)	-4 (1)	1 (1)	-3 (1)
O (6D)	16 (1)	22 (1)	23 (1)	2 (1)	6 (1)	2 (1)
O (7D)	30 (1)	25 (1)	19 (1)	0 (1)	6 (1)	-7 (1)
O (8D)	34 (1)	23 (1)	43 (1)	-2 (1)	8 (1)	-4 (1)

O (9D)	20 (1)	37 (1)	41 (1)	-12 (1)	9 (1)	-6 (1)
S (1A)	32 (1)	27 (1)	33 (1)	-11 (1)	20 (1)	-8 (1)
S (1B)	19 (1)	21 (1)	28 (1)	-3 (1)	9 (1)	3 (1)
S (1C)	22 (1)	25 (1)	17 (1)	2 (1)	2 (1)	-1 (1)
S (1D)	20 (1)	24 (1)	22 (1)	-5 (1)	7 (1)	-5 (1)

Table 5. Hydrogen coordinates ( $\times 10^4$ ) and isotropic displacement parameters ( $\text{\AA}^2 \times 10^3$ ) for 06mz359m.

	x	y	z	U (eq)
H (2A)	840	623	6932	21
H (3A)	-297	1165	7649	21
H (4A)	1290	1778	8405	24
H (5A)	1884	1309	10079	27
H (6A)	149	546	10060	25
H (9A1)	1498	-1734	7351	44
H (9A2)	397	-2183	7340	44
H (9A3)	662	-1505	7943	44
H (10A)	-1276	-1052	7184	40
H (10B)	-1589	-1705	6537	40
H (10C)	-1675	-957	6105	40
H (11A)	-380	-1347	5166	47
H (11B)	-229	-2086	5631	47
H (11C)	868	-1629	5657	47
H (13A)	727	-605	10376	52
H (13B)	1676	-917	9944	52
H (13C)	445	-720	9302	52
H (2B)	7499	246	7790	23
H (3B)	6178	1064	7722	22
H (4B)	7241	1577	9029	22
H (5B)	6468	1106	10381	22
H (6B)	4507	661	9449	23
H (9B1)	5422	-2216	7278	36
H (9B2)	5815	-1654	8061	36
H (9B3)	6652	-1868	7462	36
H (10D)	6156	-1495	5791	42
H (10E)	4987	-1092	5378	42
H (10F)	4961	-1877	5657	42
H (11D)	3776	-739	6311	35
H (11E)	4109	-889	7379	35
H (11F)	3659	-1495	6672	35
H (13D)	4370	-539	9636	42
H (13E)	5506	-991	9910	42
H (13F)	5029	-717	8892	42
H (2C)	2145	647	6087	22
H (3C)	415	944	5213	21
H (4C)	277	-42	4379	22
H (5C)	928	253	2900	25
H (6C)	694	1560	2905	25

H (9C1)	2857	2767	7671	70
H (9C2)	4062	3092	7672	70
H (9C3)	3987	2310	7952	70
H (10G)	5016	2789	6462	58
H (10H)	4428	2235	5713	58
H (10I)	5010	2001	6736	58
H (11G)	2027	3126	6074	43
H (11H)	2633	2896	5315	43
H (11I)	3217	3461	6050	43
H (9E1)	3604	3201	7653	65
H (9E2)	3011	2513	7860	65
H (9E3)	2292	3055	7149	65
H (10J)	4851	1914	6553	60
H (10K)	4626	1913	7537	60
H (10L)	5152	2575	7189	60
H (11J)	2488	3029	5551	104
H (11K)	3563	2663	5341	104
H (11L)	3745	3322	5982	104
H (13G)	2438	2071	2904	42
H (13H)	3604	1760	3527	42
H (13I)	2719	2118	3987	42
H (2D)	6710	1018	6272	25
H (3D)	5132	1095	5118	23
H (4D)	5486	14	4691	22
H (5D)	6288	155	3263	23
H (6D)	5816	1421	2882	24
H (9D1)	9896	2381	6946	50
H (9D2)	9772	3127	6506	50
H (9D3)	9280	2479	5888	50
H (10M)	7670	3081	7798	55
H (10N)	8734	3519	7692	55
H (10O)	8927	2765	8105	55
H (11M)	7421	3056	5389	50
H (11N)	7797	3696	6052	50
H (11O)	6713	3249	6095	50
H (13M)	7523	2058	2999	43
H (13N)	8648	1870	3785	43
H (13O)	7577	2205	4039	43

Table 6. Torsion angles [deg] for 06mz359m.

O (1A) -C (1A) -C (2A) -O (2A)	35.2 (2)
O (4A) -C (1A) -C (2A) -O (2A)	-147.17 (13)
O (1A) -C (1A) -C (2A) -C (3A)	157.48 (19)
O (4A) -C (1A) -C (2A) -C (3A)	-24.87 (17)
O (2A) -C (2A) -C (3A) -O (3A)	31.32 (17)
C (1A) -C (2A) -C (3A) -O (3A)	-90.04 (15)
O (2A) -C (2A) -C (3A) -C (4A)	145.74 (13)
C (1A) -C (2A) -C (3A) -C (4A)	24.38 (16)
O (3A) -C (3A) -C (4A) -O (4A)	102.39 (14)
C (2A) -C (3A) -C (4A) -O (4A)	-17.25 (16)
O (3A) -C (3A) -C (4A) -C (5A)	-11.84 (16)
C (2A) -C (3A) -C (4A) -C (5A)	-131.49 (13)

O (4A) -C (4A) -C (5A) -O (5A)	163.56 (12)
C (3A) -C (4A) -C (5A) -O (5A)	-82.52 (14)
O (4A) -C (4A) -C (5A) -C (6A)	-84.69 (14)
C (3A) -C (4A) -C (5A) -C (6A)	29.24 (15)
O (5A) -C (5A) -C (6A) -O (6A)	-169.87 (13)
C (4A) -C (5A) -C (6A) -O (6A)	81.62 (15)
O (5A) -C (5A) -C (6A) -O (3A)	71.25 (14)
C (4A) -C (5A) -C (6A) -O (3A)	-37.27 (15)
O (7A) -C (7A) -C (8A) -C (11A)	-6.9 (2)
O (2A) -C (7A) -C (8A) -C (11A)	174.44 (14)
O (7A) -C (7A) -C (8A) -C (9A)	112.14 (19)
O (2A) -C (7A) -C (8A) -C (9A)	-66.49 (16)
O (7A) -C (7A) -C (8A) -C (10A)	-127.56 (17)
O (2A) -C (7A) -C (8A) -C (10A)	53.80 (17)
O (1B) -C (1B) -C (2B) -O (2B)	36.3 (2)
O (4B) -C (1B) -C (2B) -O (2B)	-147.05 (12)
O (1B) -C (1B) -C (2B) -C (3B)	159.88 (16)
O (4B) -C (1B) -C (2B) -C (3B)	-23.48 (16)
O (2B) -C (2B) -C (3B) -O (3B)	24.16 (18)
C (1B) -C (2B) -C (3B) -O (3B)	-95.48 (14)
O (2B) -C (2B) -C (3B) -C (4B)	139.23 (13)
C (1B) -C (2B) -C (3B) -C (4B)	19.59 (15)
O (3B) -C (3B) -C (4B) -O (4B)	109.57 (13)
C (2B) -C (3B) -C (4B) -O (4B)	-10.39 (15)
O (3B) -C (3B) -C (4B) -C (5B)	-3.71 (16)
C (2B) -C (3B) -C (4B) -C (5B)	-123.68 (12)
O (4B) -C (4B) -C (5B) -O (5B)	155.83 (11)
C (3B) -C (4B) -C (5B) -O (5B)	-90.86 (14)
O (4B) -C (4B) -C (5B) -C (6B)	-89.76 (13)
C (3B) -C (4B) -C (5B) -C (6B)	23.55 (15)
O (5B) -C (5B) -C (6B) -O (6B)	-164.62 (12)
C (4B) -C (5B) -C (6B) -O (6B)	82.83 (13)
O (5B) -C (5B) -C (6B) -O (3B)	76.55 (14)
C (4B) -C (5B) -C (6B) -O (3B)	-36.00 (14)
O (7B) -C (7B) -C (8B) -C (10B)	23.2 (2)
O (2B) -C (7B) -C (8B) -C (10B)	-157.19 (14)
O (7B) -C (7B) -C (8B) -C (9B)	144.46 (17)
O (2B) -C (7B) -C (8B) -C (9B)	-35.92 (18)
O (7B) -C (7B) -C (8B) -C (11B)	-95.01 (19)
O (2B) -C (7B) -C (8B) -C (11B)	84.60 (15)
O (1C) -C (1C) -C (2C) -O (2C)	36.3 (2)
O (4C) -C (1C) -C (2C) -O (2C)	-149.09 (12)
O (1C) -C (1C) -C (2C) -C (3C)	161.98 (16)
O (4C) -C (1C) -C (2C) -C (3C)	-23.45 (16)
O (2C) -C (2C) -C (3C) -O (3C)	26.97 (18)
C (1C) -C (2C) -C (3C) -O (3C)	-94.81 (14)
O (2C) -C (2C) -C (3C) -C (4C)	141.28 (13)
C (1C) -C (2C) -C (3C) -C (4C)	19.50 (15)
O (3C) -C (3C) -C (4C) -O (4C)	109.32 (13)
C (2C) -C (3C) -C (4C) -O (4C)	-10.41 (15)
O (3C) -C (3C) -C (4C) -C (5C)	-3.65 (15)
C (2C) -C (3C) -C (4C) -C (5C)	-123.38 (12)
O (4C) -C (4C) -C (5C) -O (5C)	157.06 (12)
C (3C) -C (4C) -C (5C) -O (5C)	-89.14 (14)
O (4C) -C (4C) -C (5C) -C (6C)	-90.38 (14)
C (3C) -C (4C) -C (5C) -C (6C)	23.41 (15)
O (5C) -C (5C) -C (6C) -O (6C)	-165.53 (12)

C (4C) -C (5C) -C (6C) -O (6C)	82.95 (14)
O (5C) -C (5C) -C (6C) -O (3C)	75.58 (14)
C (4C) -C (5C) -C (6C) -O (3C)	-35.94 (15)
O (7C) -C (7C) -C (8C) -C (11E)	-120.5 (7)
O (2C) -C (7C) -C (8C) -C (11E)	58.0 (7)
O (7C) -C (7C) -C (8C) -C (9C)	29.7 (3)
O (2C) -C (7C) -C (8C) -C (9C)	-151.8 (3)
O (7C) -C (7C) -C (8C) -C (10E)	113.9 (4)
O (2C) -C (7C) -C (8C) -C (10E)	-67.6 (4)
O (7C) -C (7C) -C (8C) -C (11C)	-89.5 (2)
O (2C) -C (7C) -C (8C) -C (11C)	89.0 (2)
O (7C) -C (7C) -C (8C) -C (10C)	154.6 (2)
O (2C) -C (7C) -C (8C) -C (10C)	-26.9 (2)
O (7C) -C (7C) -C (8C) -C (9E)	1.9 (5)
O (2C) -C (7C) -C (8C) -C (9E)	-179.6 (5)
O (1D) -C (1D) -C (2D) -O (2D)	37.5 (2)
O (6D) -C (1D) -C (2D) -O (2D)	-144.63 (13)
O (1D) -C (1D) -C (2D) -C (3D)	161.40 (17)
O (6D) -C (1D) -C (2D) -C (3D)	-20.76 (17)
O (2D) -C (2D) -C (3D) -O (3D)	29.19 (18)
C (1D) -C (2D) -C (3D) -O (3D)	-93.58 (15)
O (2D) -C (2D) -C (3D) -C (4D)	144.29 (13)
C (1D) -C (2D) -C (3D) -C (4D)	21.52 (15)
O (3D) -C (3D) -C (4D) -O (6D)	103.90 (13)
C (2D) -C (3D) -C (4D) -O (6D)	-16.40 (15)
O (3D) -C (3D) -C (4D) -C (5D)	-9.52 (15)
C (2D) -C (3D) -C (4D) -C (5D)	-129.82 (12)
O (6D) -C (4D) -C (5D) -O (5D)	162.72 (12)
C (3D) -C (4D) -C (5D) -O (5D)	-83.34 (14)
O (6D) -C (4D) -C (5D) -C (6D)	-86.37 (14)
C (3D) -C (4D) -C (5D) -C (6D)	27.57 (14)
O (5D) -C (5D) -C (6D) -O (4D)	-165.20 (12)
C (4D) -C (5D) -C (6D) -O (4D)	81.26 (14)
O (5D) -C (5D) -C (6D) -O (3D)	76.46 (14)
C (4D) -C (5D) -C (6D) -O (3D)	-37.07 (14)
O (7D) -C (7D) -C (8D) -C (10D)	-15.5 (2)
O (2D) -C (7D) -C (8D) -C (10D)	166.18 (15)
O (7D) -C (7D) -C (8D) -C (11D)	-136.87 (18)
O (2D) -C (7D) -C (8D) -C (11D)	44.76 (19)
O (7D) -C (7D) -C (8D) -C (9D)	104.10 (19)
O (2D) -C (7D) -C (8D) -C (9D)	-74.27 (17)
O (7A) -C (7A) -O (2A) -C (2A)	-1.8 (2)
C (8A) -C (7A) -O (2A) -C (2A)	176.90 (12)
C (1A) -C (2A) -O (2A) -C (7A)	-88.36 (15)
C (3A) -C (2A) -O (2A) -C (7A)	154.31 (13)
O (6A) -C (6A) -O (3A) -C (3A)	-83.08 (16)
C (5A) -C (6A) -O (3A) -C (3A)	31.15 (15)
C (2A) -C (3A) -O (3A) -C (6A)	99.36 (15)
C (4A) -C (3A) -O (3A) -C (6A)	-12.18 (16)
O (1A) -C (1A) -O (4A) -C (4A)	-168.20 (17)
C (2A) -C (1A) -O (4A) -C (4A)	13.99 (18)
C (5A) -C (4A) -O (4A) -C (1A)	113.17 (15)
C (3A) -C (4A) -O (4A) -C (1A)	2.42 (18)
C (4A) -C (5A) -O (5A) -S (1A)	-154.20 (11)
C (6A) -C (5A) -O (5A) -S (1A)	97.68 (14)
O (3A) -C (6A) -O (6A) -C (13A)	-72.59 (19)
C (5A) -C (6A) -O (6A) -C (13A)	174.43 (15)

O (7B) -C (7B) -O (2B) -C (2B)	2.0 (2)
C (8B) -C (7B) -O (2B) -C (2B)	-177.68 (13)
C (1B) -C (2B) -O (2B) -C (7B)	-157.57 (13)
C (3B) -C (2B) -O (2B) -C (7B)	85.24 (16)
O (6B) -C (6B) -O (3B) -C (3B)	-77.83 (16)
C (5B) -C (6B) -O (3B) -C (3B)	35.22 (15)
C (2B) -C (3B) -O (3B) -C (6B)	92.97 (15)
C (4B) -C (3B) -O (3B) -C (6B)	-19.68 (16)
O (1B) -C (1B) -O (4B) -C (4B)	-165.67 (15)
C (2B) -C (1B) -O (4B) -C (4B)	17.43 (16)
C (5B) -C (4B) -O (4B) -C (1B)	106.70 (14)
C (3B) -C (4B) -O (4B) -C (1B)	-4.14 (16)
C (6B) -C (5B) -O (5B) -S (1B)	102.31 (13)
C (4B) -C (5B) -O (5B) -S (1B)	-147.41 (11)
O (3B) -C (6B) -O (6B) -C (13B)	-69.58 (16)
C (5B) -C (6B) -O (6B) -C (13B)	177.49 (12)
O (7C) -C (7C) -O (2C) -C (2C)	-3.8 (2)
C (8C) -C (7C) -O (2C) -C (2C)	177.67 (13)
C (1C) -C (2C) -O (2C) -C (7C)	-158.08 (13)
C (3C) -C (2C) -O (2C) -C (7C)	82.86 (16)
O (6C) -C (6C) -O (3C) -C (3C)	-78.96 (16)
C (5C) -C (6C) -O (3C) -C (3C)	35.15 (15)
C (2C) -C (3C) -O (3C) -C (6C)	92.11 (15)
C (4C) -C (3C) -O (3C) -C (6C)	-19.67 (15)
O (1C) -C (1C) -O (4C) -C (4C)	-167.79 (15)
C (2C) -C (1C) -O (4C) -C (4C)	17.25 (16)
C (5C) -C (4C) -O (4C) -C (1C)	107.14 (14)
C (3C) -C (4C) -O (4C) -C (1C)	-4.01 (16)
C (6C) -C (5C) -O (5C) -S (1C)	109.10 (13)
C (4C) -C (5C) -O (5C) -S (1C)	-141.42 (12)
O (3C) -C (6C) -O (6C) -C (13C)	-75.30 (17)
C (5C) -C (6C) -O (6C) -C (13C)	171.20 (13)
O (7D) -C (7D) -O (2D) -C (2D)	-2.6 (2)
C (8D) -C (7D) -O (2D) -C (2D)	175.88 (13)
C (1D) -C (2D) -O (2D) -C (7D)	-99.86 (16)
C (3D) -C (2D) -O (2D) -C (7D)	141.12 (14)
O (4D) -C (6D) -O (3D) -C (3D)	-81.73 (15)
C (5D) -C (6D) -O (3D) -C (3D)	32.37 (15)
C (2D) -C (3D) -O (3D) -C (6D)	97.61 (15)
C (4D) -C (3D) -O (3D) -C (6D)	-14.32 (15)
O (3D) -C (6D) -O (4D) -C (13D)	-70.67 (17)
C (5D) -C (6D) -O (4D) -C (13D)	176.15 (13)
C (6D) -C (5D) -O (5D) -S (1D)	161.09 (10)
C (4D) -C (5D) -O (5D) -S (1D)	-89.64 (14)
O (1D) -C (1D) -O (6D) -C (4D)	-171.76 (15)
C (2D) -C (1D) -O (6D) -C (4D)	10.26 (17)
C (5D) -C (4D) -O (6D) -C (1D)	114.86 (14)
C (3D) -C (4D) -O (6D) -C (1D)	4.28 (16)
C (5A) -O (5A) -S (1A) -O (8A)	-18.72 (16)
C (5A) -O (5A) -S (1A) -O (9A)	-155.46 (15)
C (5A) -O (5A) -S (1A) -C (12A)	93.90 (14)
F (3A) -C (12A) -S (1A) -O (8A)	55.98 (16)
F (1A) -C (12A) -S (1A) -O (8A)	176.69 (14)
F (2A) -C (12A) -S (1A) -O (8A)	-63.38 (15)
F (3A) -C (12A) -S (1A) -O (9A)	-171.05 (14)
F (1A) -C (12A) -S (1A) -O (9A)	-50.34 (16)
F (2A) -C (12A) -S (1A) -O (9A)	69.59 (16)

F (3A) -C (12A) -S (1A) -O (5A)	-60.20 (14)
F (1A) -C (12A) -S (1A) -O (5A)	60.50 (15)
F (2A) -C (12A) -S (1A) -O (5A)	-179.56 (13)
C (5B) -O (5B) -S (1B) -O (9B)	-161.82 (12)
C (5B) -O (5B) -S (1B) -O (8B)	-25.16 (14)
C (5B) -O (5B) -S (1B) -C (12B)	87.06 (12)
F (3B) -C (12B) -S (1B) -O (9B)	-53.17 (15)
F (2B) -C (12B) -S (1B) -O (9B)	66.83 (15)
F (1B) -C (12B) -S (1B) -O (9B)	-173.93 (12)
F (3B) -C (12B) -S (1B) -O (8B)	174.52 (12)
F (2B) -C (12B) -S (1B) -O (8B)	-65.49 (14)
F (1B) -C (12B) -S (1B) -O (8B)	53.75 (14)
F (3B) -C (12B) -S (1B) -O (5B)	58.31 (13)
F (2B) -C (12B) -S (1B) -O (5B)	178.30 (12)
F (1B) -C (12B) -S (1B) -O (5B)	-62.45 (13)
C (5C) -O (5C) -S (1C) -O (9C)	-17.81 (15)
C (5C) -O (5C) -S (1C) -O (8C)	-155.12 (13)
C (5C) -O (5C) -S (1C) -C (12C)	94.39 (13)
F (2C) -C (12C) -S (1C) -O (9C)	-68.24 (15)
F (1C) -C (12C) -S (1C) -O (9C)	53.23 (17)
F (3C) -C (12C) -S (1C) -O (9C)	171.37 (13)
F (2C) -C (12C) -S (1C) -O (8C)	65.69 (16)
F (1C) -C (12C) -S (1C) -O (8C)	-172.84 (15)
F (3C) -C (12C) -S (1C) -O (8C)	-54.70 (16)
F (2C) -C (12C) -S (1C) -O (5C)	176.56 (13)
F (1C) -C (12C) -S (1C) -O (5C)	-61.97 (16)
F (3C) -C (12C) -S (1C) -O (5C)	56.17 (15)
C (5D) -O (5D) -S (1D) -O (9D)	161.06 (12)
C (5D) -O (5D) -S (1D) -O (8D)	24.38 (14)
C (5D) -O (5D) -S (1D) -C (12D)	-87.06 (13)
F (12) -C (12D) -S (1D) -O (9D)	53.90 (17)
F (11) -C (12D) -S (1D) -O (9D)	-65.81 (19)
F (10) -C (12D) -S (1D) -O (9D)	175.33 (17)
F (12) -C (12D) -S (1D) -O (8D)	-174.05 (14)
F (11) -C (12D) -S (1D) -O (8D)	66.23 (18)
F (10) -C (12D) -S (1D) -O (8D)	-52.6 (2)
F (12) -C (12D) -S (1D) -O (5D)	-58.66 (15)
F (11) -C (12D) -S (1D) -O (5D)	-178.38 (16)
F (10) -C (12D) -S (1D) -O (5D)	62.77 (19)

---